2

CR-128539

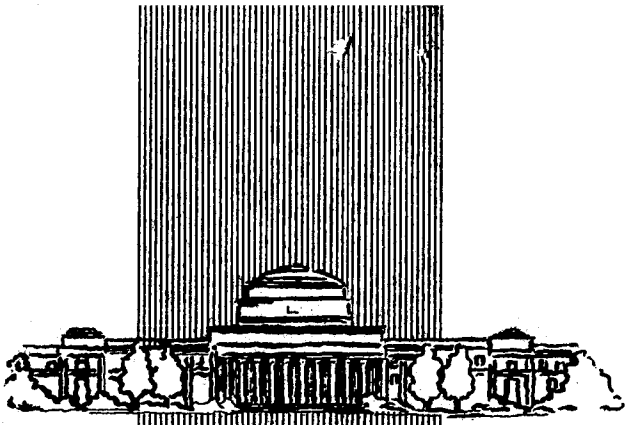

MASSACHUSETTS INSTITUTE OF TECHNOLOGY

INVESTIGATION OF THE EPOCH STATE FILTER

by

Joan Annette Edwards

February 1972

Degree of Master of Science

(NASA-CR-128539) INVESTIGATION OF THE EPOCH STATE FILTER M.S. Thesis J.A. Edwards (Massachusetts Inst. of Tech.) Feb. 1972 212 p CSCL 17G G3/21

N72-33639

Unclas 43884

T-569

PREPARED AT

CHARLES STARK DRAPER LABORATORY

CAMBRIDGE, MASSACHUSETTS, 02139

Reproduced by
NATIONAL TECHNICAL
INFORMATION SERVICE
US Department of Commerce
Springfield, VA. 22151

213P

INVESTIGATION OF THE EPOCH STATE FILTER

by

JOAN ANNETTE EDWARDS

B. S. A. E., PURDUE UNIVERSITY

(1970)

SUBMITTED IN PARTIAL FULFILLMENT

OF THE REQUIREMENTS FOR THE

DEGREE OF MASTER OF SCIENCE

at the

MASSACHUSETTS INSTITUTE OF TECHNOLOGY

February, 1972

Signature of Author Joan A. Edwards

Department of Aeronautics and Astronautics, January 21, 1972

Certified by Richard H. Battin

Thesis Supervisor

Accepted by Judson R. Baron

Chairman, Departmental Graduate Committee

ACKNOWLEDGMENT

I would like to express my appreciation to Dr. Richard H. Battin, my thesis supervisor, for suggesting that I develop as a thesis subject, The Epoch State Filter, which he initially conceived and for reviewing my final paper. I especially owe a debt of gratitude to Dr. Steven R. Croopnick for his continued assistance and encouragement through my thesis work.

I would further like to thank the Control and Flight Dynamics Division of the Charles Stark Draper Laboratory for providing this research opportunity and allowing me to use its research facilities.

A special note of appreciation is extended to the National Aeronautics and Space Administration and to ZONTA International for sponsoring my graduate study at M. I. T.

This report was prepared under DSR Project 55-41200, sponsored by the Manned Spacecraft Center of the National Aeronautics and Space Administration through contract NAS 9-10386.

The publication of this report does not constitute approval of the National Aeronautics and Space Administration or the Charles Stark Draper Laboratory of the findings or the conclusions contained herein. It is published only for the exchange and stimulation of ideas.

INVESTIGATION OF THE EPOCH STATE FILTER

by

Joan Annette Edwards

Submitted to the Department of Aeronautics and Astronautics on January 21, 1972 in partial fulfillment of the requirements for the degree of Master of Science.

ABSTRACT

A new navigation filtering technique has been formulated using as state variables the initial or epoch position and velocity of the spacecraft. The estimate of this initial state is then improved by filtering new measurements. The current state may be obtained by a conic extrapolation of the epoch state. Results of a digital computer simulation of the epoch state filter show that this formulation of the navigational problem results in less computer run time and less computer storage space than conventional techniques. The errors produced by this technique have been demonstrated to be comparable to those obtained by conventional maximum-likelihood filtering.

Thesis Supervisor: Richard H. Battin

Title: Asscciate Director, C. S. Draper Lab., M. I. T.

PRECEDING PAGE BLANK NOT FILMED

TABLE OF CONTENTS

Preceding page blank

LIST OF SYMBOLS

General Notation

An underlined symbol indicates a vector.

A prime to the upper right of a symbol indicates the quantity is that extrapolated from the previous measurement time.

A caret over a symbol indicates that the quantity is an estimate.

A bar over a symbol or group of symbols indicates the expected value of what is beneath.

A "o" subscript on a symbol denotes an epoch quantity.

A "k" subscript on a symbol denotes that quantity at the time of the k^{th} measurement.

Symbol	Definition
a	parameter of the weighting vector
a_o	parameter of the epoch weighting vector
$\underline{a}_d$	disturbing acceleration
α	reciprocal of the semimajor axis
$\overline{\alpha^2}$	apriori variance of measurement error
$\underline{b}$	geometry vector
$\underline{b}_o$	epoch geometry vector
$C(t)$	$R^{T-1}V^T$
c	variable defined in t_o equation
CSF	conventional or Apollo state filter

δ	variation in true anomaly difference θ
$\underline{\delta}$	position deviation from osculating orbit
$\underline{e}$	error vector $\begin{bmatrix} \underline{\epsilon} \\ \underline{\eta} \end{bmatrix}$
$\underline{e}_d$	error incurred using ESF
$\underline{\epsilon}$	error in position estimate
E'	extrapolated covariance matrix
E	covariance matrix of estimation errors
E'_o	extrapolated epoch covariance matrix
E_o	epoch covariance matrix
E^*_o	conic epoch covariance matrix
ESF	epoch state filter
ξ	variation in generalized anomaly x
f	true anomaly
F	scalar quantity in Ψ equation
F_t	scalar quantity in Ψ equation
F(t)	matrix in $\dot{\Phi}$ equation
$F_c(t)$	conic F(t)
$\underline{g}$	gravitational force per unit mass
G	scalar quantity in Ψ equation
G_t	scalar quantity in Ψ equation
G(t)	gradient of gravity vector
$G_c(t)$	conic G(t)
$G_{ad}(t)$	$G(t) - G_c(t)$
$\underline{h}$	angular momentum
$\underline{i}_r$	unit vector in radial direction
$\underline{i}_\theta$	unit vector normal to $\underline{i}_r$ in orbital plane

$\underline{i}_z$	$\underline{i}_r \times \underline{i}_\theta$
I	identity matrix
J_2	second zonal harmonic
$\underline{\eta}$	error in velocity estimate
p	orbital parameter
q	Encke integration variable
$\delta\tilde{q}$	measured quantity
$\delta\hat{q}'$	extrapolated estimate of measured quantity
$\underline{r}$	position vector
r	position
r_E	equatorial radius of earth
$\underline{r}_o$	epoch position vector
r_o	epoch position
$\underline{r}_{osc}$	osculating position vector
R	$\partial\underline{r}/\partial\underline{v}_o$
R^*	$\partial\underline{r}_o/\partial\underline{v}$
t_o	epoch time
u	gravitational parameter
U_n	n^{th} transcendental function
$\underline{\nu}$	velocity deviation from osculating orbit
$\underline{v}$	velocity vector
v	velocity
$\underline{v}_o$	epoch velocity vector
v_o	epoch velocity
$\underline{v}_{osc}$	osculating velocity
V	$\partial\underline{v}/\partial\underline{v}_o$

V^*	$\partial \underline{v}_o / \partial \underline{v}$
$\underline{\omega}$	weighting vector
$\underline{\omega}_o$	epoch weighting vector
x	generalized anomaly
$\underline{x}$	state vector $\begin{bmatrix} \underline{r} \\ \underline{v} \end{bmatrix}$
$\delta\hat{\underline{x}}$	estimated state deviation vector
$\delta\hat{\underline{x}}_o$	estimated epoch state deviation vector
Ψ	epoch to current state transformation matrix
σ	variational orbital element
σ_o	variational epoch orbital element
θ	true anomaly difference
$\delta\theta$	deviation in true anomaly difference
$\delta\theta_o$	epoch θ deviation
$\Delta\theta$	total change in θ
$\cos \phi$	$\underline{i}_r \cdot \underline{i}_z$
Φ	state transition matrix
Φ_c	conic state transition matrix
Φ_t	$\Phi_c^{-1}\Phi$

CHAPTER I

INTRODUCTION

One of the processes of coasting flight navigation involves improving the estimate of the spacecraft's position and velocity vectors. In the Apollo navigation system this is accomplished with a recursive formulation of the maximum-likelihood estimator in which state or process noise is neglected. Measurement data, regarded as scalar information, is incorporated as it is obtained to update the estimate of the state. This data handling technique is termed recursive processing as opposed to batch processing wherein measurement data is incorporated all at once.

The process of determining the estimate of the state vector as stored in the on-board digital computer involves integrating the equations of motion which govern the spacecraft. During both coasting flight and under the influence of a vector disturbing acceleration, $\underline{a}_d$, these equations are:

$$\frac{d^2\underline{r}(t)}{dt^2} + \frac{\mu \underline{r}(t)}{r^3(t)} = \underline{a}_d(\underline{r}(t))$$

$$\underline{v}(t) = \frac{d\underline{r}(t)}{dt}$$

where $\underline{r}(t)$ and $\underline{v}(t)$ are the current position and velocity vectors of the vehicle with respect to the primary body and μ is the

gravitational constant of the primary body. Integration of these equations involves selecting an appropriate set of state variables. For Apollo, current position and velocity are used to define the state. Intuitively, this is a proper choice of state variables since current position and velocity are ultimately the quantities which are estimated by the navigation filter. Another related set of variational parameters is the spacecraft's position and velocity at some initial time or epoch.

The formulation of the space navigation problem using the epoch state as state variables requires a variation of parameters solution which is discussed in this thesis. It is shown that this latter formulation has certain computational advantages over the conventional one, namely, less computer run time and computer storage space. The disadvantage, a slight decrease in accuracy, is introduced because of a simplifying assumption used to integrate the time derivatives of the epoch state error covariance matrix. However, in many cases this error is small so that the epoch formulation of the navigational problem may replace a formulation such as the one used in Apollo. Various examples are given as cases where the implementation error is negligible. Also, statistical equations were developed to predict the filtering approximations of the epoch state filter.

In Chapter II the conventional formulation of the navigational problem is discussed in detail. Its design philosophy is explained as well as how error is propogated and measurement date is recursively incorporated to improve the estimate of the

state vector. Also discussed in this chapter is the design philosophy and choice of state variables for the epoch formulation of the navigational problem. The equations for the epoch filter used to estimate the state vector are derived in Chapter III. Explanation is given for the assumption made to simplify this formulation. A comparison between the basic equations of the conventional and epoch filter formulations is also given. Finally, statistical equations for the error incurred using the epoch rather than the conventional state filter are derived. Computer simulation results of the epoch formulation of the navigational problem are presented and discussed in Chapter IV. Conclusions regarding the epoch state filter, its advantages and areas of application are explained in Chapter V.

CHAPTER II

NAVIGATION FILTER FORMULATIONS

2.1 Design Philosophy for the Apollo Navigation Filter

Position and velocity as maintained in the Apollo Guidance Computer (AGC) are estimates of the true state of the spacecraft. These estimates are propagated from measurement to measurement by integrating the equations of motion of the vehicle with respect to time. Integration of the spacecraft's motion involves the selection of an appropriate set of state variables. Current position and velocity of the spacecraft are used in the Apollo navigation system. Intuitively, this is a proper choice of state variables since these are the quantities to be estimated.

The vector equations governing the motion of the spacecraft during coasting flight are:

$$\frac{d^2\underline{r}(t)}{dt^2} + \frac{\mu}{r^3(t)}\,\underline{r}(t) = \underline{a}_d(\underline{r}(t)) \qquad (2.1.1)$$

$$\frac{d\,\underline{r}(t)}{dt} = \underline{v}(t) \qquad (2.1.2)$$

where $\underline{r}(t)$ and $\underline{v}(t)$ are the vector position and velocity of the vehicle in non-rotating rectangular coordinates with respect to the primary body and μ is the gravitational parameter of this body. The

quantity $\underline{a}_d$ is the vector disturbing acceleration which prevents the motion of the spacecraft from being precisely a conic orbit. The disturbing acceleration is a function solely of the position vector. For earth orbit, only gravitational perturbations due to the non-spherical gravity field of the earth need be considered in $\underline{a}_d$. The equation for the disturbing acceleration used in this study is given by:

$$\underline{a}_d = -\frac{\mu}{r^2}\,\frac{3}{2}\,J_2\left(\frac{r_E}{r}\right)^2\left[(1 - 5\cos\phi)\underline{i}_r + 2\cos\phi\,\underline{i}_z\right] \qquad (2.1.3)$$

where ϕ is the angle between $\underline{i}_r$ the unit vector in the $\underline{r}$ direction, and $\underline{i}_z$, the unit vector in the direction of the spin axis; r_E is the equatorial radius of the earth and J_2 is the coefficient of the second harmonic of the earth's potential function.

When $\underline{a}_d$ is small compared with the central field of the primary body, direct integration of Eqs. 2.1.1 and 2.1.2 in rectangular coordinates is inefficient. An alternate procedure suggested by Encke[1], is used to perform this integration. For the Encke method of integration, the actual position and velocity of the spacecraft, defined by the current values of $\underline{r}(t)$ and $\underline{v}(t)$, are viewed as deviations from a conic or osculating orbit

$$\underline{r}(t) = \underline{r}_{osc}(t) + \underline{\delta}(t) \qquad (2.1.4)$$

$$\underline{v}(t) = \underline{v}_{osc}(t) + \underline{\nu}(t) \qquad (2.1.5)$$

In practice, the osculating orbit and the deviations from this orbit onboard a spacecraft are only estimates of their true values and are represented with a superscript "^". Hence, the current position and

velocity estimates are given by

$$\hat{\underline{r}}(t) = \underline{r}_{osc}(t) + \hat{\underline{\delta}} \tag{2.1.6}$$

$$\hat{\underline{v}}(t) = \underline{v}_{osc}(t) + \hat{\underline{\nu}}(t) \tag{2.1.7}$$

The osculating orbit at any particular time is determined from ideal two-body motion by solving Kepler's equation for θ. This is accomplished by using the following equations for two-body motion:

$$\underline{r}_{osc} = F\,\underline{r}_o + G\,\underline{v}_o \tag{2.1.8}$$

$$\underline{v}_{osc} = F_t\,\underline{r}_o + G_t\,\underline{v}_o \tag{2.1.9}$$

where

$$F = 1 - \frac{r}{p}(1 - \cos\theta) \tag{2.1.10}$$

$$G = r\,\frac{r_o}{h}\sin\theta \tag{2.1.11}$$

$$F_t = \frac{\sqrt{\mu}}{r_o}\,\frac{\sigma_o}{p}(1 - \cos\theta) - \frac{\mu}{r_o h}\sin\theta \tag{2.1.12}$$

$$G_t = 1 - \frac{r_o}{p}(1 - \cos\theta) \tag{2.1.13}$$

and

$$r = \frac{p}{1 + (\frac{p}{r_o} - 1)\cos\theta - \frac{h}{\sqrt{\mu}}\,\frac{\sigma_o}{r_o}\sin\theta} \tag{2.1.14}$$

The parameters in 2.1.14 are determined according to the following equations:

$$\sigma_o = \frac{\underline{r}_o \cdot \underline{v}_o}{\sqrt{\mu}} \tag{2.1.15}$$

$$\alpha = \frac{2}{r_o} - \frac{v_o^2}{\mu} \tag{2.1.16}$$

$$p = 2r_o - \alpha r_o^2 - \sigma_o^2 \tag{2.1.17}$$

The deviation vector $\underline{\delta}(t)$ and $\underline{\nu}(t)$ are obtained by integrating the following differential equations:

$$\frac{d\underline{\delta}(t)}{dt} = \underline{\nu}(t) \tag{2.1.18}$$

$$\frac{d\underline{\nu}(t)}{dt} = -\frac{\mu}{r_{osc}^3(t)}[f(q)\underline{r}(t) + \underline{\delta}(t)] + \underline{a}_d(\underline{r}(t)) \tag{2.1.19}$$

subject to initial conditions $\underline{\delta}(t_o) = \underline{\nu}(t_o) = \underline{0}$ where

$$q = \frac{\underline{\delta} \cdot (\underline{\delta} - 2\underline{r})}{r^2} \tag{2.1.20}$$

and

$$f(q) = \frac{q(3 + 3q + q^2)}{1 + (1 + q)^{3/2}} \tag{2.1.21}$$

A recommended numerical integration technique, Nystrom's Method, exploits the fact that $\underline{a}_d$ is a function only of $\underline{r}$, the vector to be integrated.

For Encke's Method to be efficient, the first term on the right hand side of Eq. 2.1.19 must remain small, i.e., of the same order or less as the disturbing acceleration. To insure the efficiency, a new

osculating orbit is periodically defined from which $\underline{\delta}$ and $\underline{\nu}$ are calculated. When this rectification is done, the new osculating orbit is defined by the current values of $\underline{r}(t)$ and $\underline{v}(t)$ and the initial conditions for Equations 2.1.18 and 2.1.19 are again set equal to zero at the current time.

2.2. Error Covariance Matrix

The position and velocity vectors which are stored in the Apollo Guidance Computer (AGC) are estimates of their true values. Since these estimates will be in error, it is necessary as part of the maximum-likelihood filtering technique to maintain the statistics associated with these errors.

If $\underline{\epsilon}(t)$ is the three dimensional error in the position estimate and $\underline{\eta}(t)$ is the three dimensional error in the velocity vector, then the error in the estimate of the state vector is given by

$$\underline{e}(t) = \begin{bmatrix} \underline{\epsilon}(t) \\ \underline{\eta}(t) \end{bmatrix} \qquad (2.2.1)$$

When unbiased measurement data is processed to determine the maximum - likelihood estimate, the error in the estimate has a zero mean, i.e. $\overline{\underline{e}} = \underline{0}$ so that the 6 x 6 covariance matrix of estimation errors is defined by

$$E = \overline{\underline{e}\,\underline{e}^T} = \begin{bmatrix} \overline{\underline{\epsilon}\,\underline{\epsilon}^T} & \overline{\underline{\epsilon}\,\underline{\eta}^T} \\ \overline{\underline{\eta}\,\underline{\epsilon}^T} & \overline{\underline{\eta}\,\underline{\eta}^T} \end{bmatrix} \qquad (2.2.2)$$

and is also stored in the AGC.

A useful measure of the error in the position estimate is given by the rms position error. This error is determined by the square root of the trace of the upper left hand 3 x 3 partition of the covariance matrix and is given by

$$\text{rms position error} = \left[\text{tr}\ \overline{(\underline{\epsilon}_k \underline{\epsilon}_k^T)}\right]^{1/2} \qquad (2.2.3)$$

Similarly, the rms velocity error, a good measure of the error in the velocity estimate, is determined from the lower right hand corner of the covariance matrix according to

$$\text{rms velocity error} = \left[\text{tr}\ \overline{(\underline{\eta}_k \underline{\eta}_k^T)}\right]^{1/2} \qquad (2.2.4)$$

With the recursive formulation of the Kalman estimator, measurement date is processed as it is obtained. The covariance matrix is maintained in the AGC in the intervals between which measurements are taken and is updated as is the current estimate of the state vector when the measurement data is incorporated by this linear estimator.

The Kalman filter operates as follows. First, the old estimate is extrapolated to the current time, yielding the best estimate prior to the incorporation of measurement data. For coasting flight $E(t_{k-1})$ is extrapolated to the current time, t_k, by

$$E'(t_k) = \Phi(t_k, t_{k-1})\, E(t_{k-1})\, \Phi(t_k, t_{k-1})^T \qquad (2.2.5)$$

The prime ' to the upper right of $E(t_k)$ indicates the covariance matrix of estimation errors at t_k is that based on previous $k-1$ measurements and $\Phi(t_k, t_{k-1})$ is the 6×6 state transition matrix by which the state and certain statistical quantities are extrapolated in time from t_{k-1} to t_k. The transition matrix satisfies the first order matrix differential equation

$$\dot{\Phi}(t_k, t_{k-1}) = F(t)\,\Phi(t_k, t_{k-1}) \qquad (2.2.6)$$

subject to the initial condition

$$\Phi(t_0, t_0) = I$$

where I is the 6×6 identity matrix,

$$F(t) = \begin{bmatrix} 0 & I \\ G(t) & 0 \end{bmatrix} \qquad (2.2.7)$$

where

$$G(t) = \left\| \frac{\partial \underline{g}}{\partial \underline{r}} \right\|$$

The 3×3 matrix G(t) is the gradient of the gravitational field $\underline{g}$ with respect to the components of the position vector $\underline{r}$. For orbital navigation about a primary body, G(t) is given by

$$G(t) = \frac{\mu}{r^5(t)} [\, 3\,\underline{r}(t)\,\underline{r}(t)^T - r^2(t)\, I] \qquad (2.2.8)$$

An alternate method of extrapolating the covariance matrix rather than by first determining $\Phi(t_k, t_{k-1})$ and then substituting this matrix into Equation 2.2.5 is to integrate the first order differential equation for $E'(t_K)$

$$\dot{E}'(t_k) = F(t_k)\, E'(t_k) + E'(t_k)\, F(t_k)^T \qquad (2.2.9)$$

This is obtained by differentiating Equation 2.2.5 with respect to time and substituting Equation 2.2.6 in the resulting equation, the derivation of which is given in Appendix A.

Once the extrapolated covariance matrix is obtained, the measurement data is incorporated according to optimal estimation theory. As a result of the measurement incorporation, the statistics of the error covariance matrix are changed. A weighting vector $\underline{\omega}$ is determined which minimizes the mean squared error in the estimate. According to maximum-likelihood theory, the weighting vector is given by

$$\underline{\omega} = \frac{1}{a} E' \underline{b} \qquad (2.2.10)$$

where $\underline{b}$ is a 6 dimensional geometry vector associated with the measurement and

$$a = \underline{b}^T E' \underline{b} + \overline{\alpha^2} \qquad (2.2.11)$$

where $\overline{\alpha^2}$ is apriori variance of the measurement error. In terms of $E'(t_k)$ as well as Equations 2.2.10 and 2.2.11, the new value for the covariance matrix of estimation errors is determined according to

$$E(t_k) = E'(t_k) - \underline{\omega}\,\underline{b}^T E'(t_k) \tag{2.2.12}$$

or

$$\boxed{E(t_k) = (I - \underline{\omega}\,\underline{b}^T)\, E'(t_k)} \tag{2.2.13}$$

2.3 Measurement Incorporation

For flight paths which are close to a nominal one, $\delta\underline{x}$ may be expressed as a linearized deviation about the nominal state and is denoted by

$$\delta\underline{x} = \begin{bmatrix} \delta\underline{r} \\ \delta\underline{v} \end{bmatrix} \tag{2.3.1}$$

The estimate of the state vector is obtained by the operation of the optimum linear estimator on the state deviation vector. First, the previous state deviation estimate is extrapolated to the current time yielding its best value prior to the incorporation of new information. This is expressed by the following relationship

$$\delta\hat{\underline{x}}'(t_k) = \Phi(t_k, t_{k-1})\, \underline{\delta\hat{x}}(t_{k-1}) \tag{2.3.2}$$

where $\Phi(t_k, t_{k-1})$ is the state transition matrix. The best estimate of the measured quantity $\delta\hat{q}'$, is computed according to

$$\delta\hat{q}'(t_k) = \underline{b}^T \delta\hat{\underline{x}}'(t_k) \tag{2.3.3}$$

The difference between the actual measurement data $\delta\tilde{q}$ and the filter's prediction of what this value should be $\delta\hat{q}'$ is weighed statistically against $\delta\hat{\underline{x}}'$. This is accomplished through the use of a statistical weighting vector $\overline{\omega}$ defined by

$$\underline{\omega} = \frac{E'\underline{b}}{a} \tag{2.3.4}$$

where

$$a = \underline{b}^T E' \underline{b} + \overline{\alpha^2} \tag{2.3.5}$$

Making use of Equations 2.3.2 through 2.3.5, the updated state estimate at measurement time t_k is obtained from

$$\boxed{\delta\hat{\underline{x}}(t_k) = \delta\hat{\underline{x}}'(t_k) + \underline{\omega}(\delta\tilde{q}(t_k) - \delta\hat{q}'(t_k))} \tag{2.3.6}$$

Equation 2.3.6 is simplified by adding the estimate of the state deviation from the nominal path to the current state;

$$\underline{\hat{x}}_{nom}(t_k) = \underline{\hat{x}}(t_k) + \delta\underline{\hat{x}}(t_k) \tag{2.3.7}$$

so that a new nominal path is defined at every measurement time t_k. By adding $\delta\underline{\hat{x}}$ to the current estimate of the state, the spacecraft is assumed to be on the nominal trajectory which is redefined at each measurement time. The extrapolated deviation of the vehicle from the nominal path at time t_k is then zero since the spacecraft was on the nominal trajectory at time t_{k-1}. This is illustrated in Figure 2.1.

The equation for determining the state deviation estimate at t_k then reduces to

$$\delta\underline{\hat{x}}(t_k) = \underline{\omega}\,\delta\tilde{q}(t_k) \tag{2.3.8}$$

This is seen by substituting $\delta\underline{\hat{x}}'(t_k) = \underline{0}$ in Equation 2.3.2 and noting that $\delta\hat{q}'$ which is a function of $\delta\underline{\hat{x}}'(t_k)$ is also zero.

2.4 Design Philosophy of the Epoch State Filter

Current position and velocity of the spacecraft are the typical vector quantities which are estimated by a spacecraft computer doing recursive processing such as the AGC. These quantities vary continuously along the path. An estimate of the current state is obtained by integrating the equations governing the motion of the vehicle. In

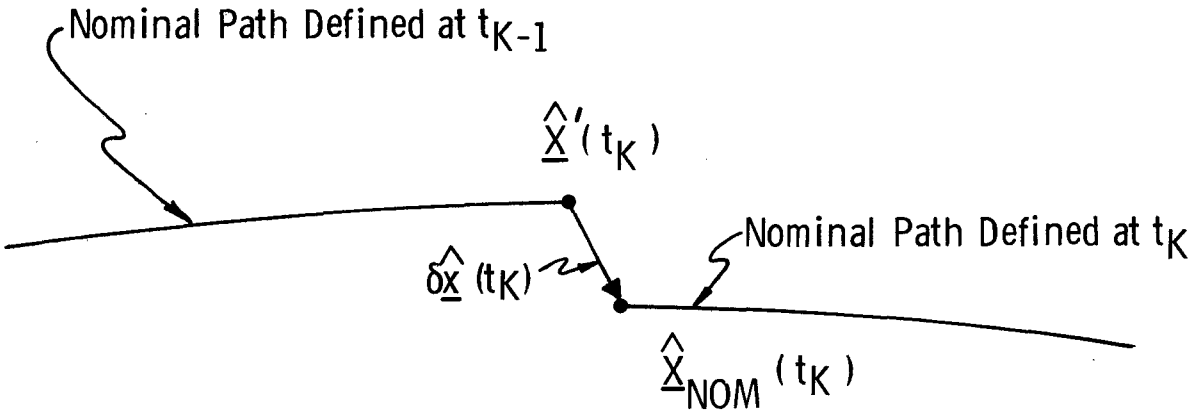

Figure 2.1 Effect of adding the expected deviation of the state $\delta\hat{\underline{x}}$ to the expected state $\hat{\underline{x}}$ at time t_K

the Apollo formulation of the navigational problem, current position and velocity along the path of the spacecraft are the quantities used in the integration of these equations. This is a convenient and intuitively correct choice of state variables since current position and velocity are the quantities to be estimated. Estimation of the state vector is then made by incorporating measurement data using Kalman gains in the space navigation filter. This current measurement information is used to update the current estimate of the position and velocity vectors.

The formulation of the navigational problem developed in this paper employs a related set of state variables, namely, the position and velocity of the spacecraft at some initial or epoch time which are adjusted in a manner such that a simple conic trajectory connects this point with the current position. This adjustment is made so that the extrapolated velocity also matches the current velocity at the current time. A scalar variational parameter is also used along with the above two vector quantities, as a means of extrapolating quantities from the epoch to the current state. This is the true anomoly difference, θ, the central angle between the current and the epoch position vectors and is considered the independent variable.

Because the epoch state is not accurately known initially, measurement data is incorporated using a Kalman filter to estimate these initial conditions. This is analogous to what is done in Apollo however, for that formulation of the navigation problem, measurement data is used to improve the current estimate of the state. When

sufficient new information is incorporated, the epoch state vector is brought up to the current time by solving Kepler's equation.

The main difference between the conventional and epoch formulation of the navigational problem is illustrated in Figure 2.2. In the conventional state filter, current position and velocity are used as state variables whereas for the epoch state filter, epoch position and velocity are used as state variables. These epoch quantities are integrated between measurements and then updated at the current time using current measurement data.

The epoch formulation of the navigation problem developed in this thesis makes use of the variable epoch form of the variational[2] equations. This means that the epoch time, t_o, is forced to vary in the intervals between measurements. The variable epoch form of these equations was used because of their relative simplicity when compared with the fixed epoch form, however, the navigational problem could just as well have been formulated using the fixed epoch form of the variational equations for which $\dot{t}_o = 0$. This feature is explained in Chapter III.

Rather than using the true anomaly difference θ as the independent variable, the generalized anomaly, x, may be treated as the scalar variational parameter. Solving a differential equation for x eliminates the necessity of solving Kepler's equation for this same variable in the same fashion as integrating the differential equation for θ eliminates obtaining Kepler's solution. Still another differential equation in terms of the epoch time, t_o, can be integrated instead

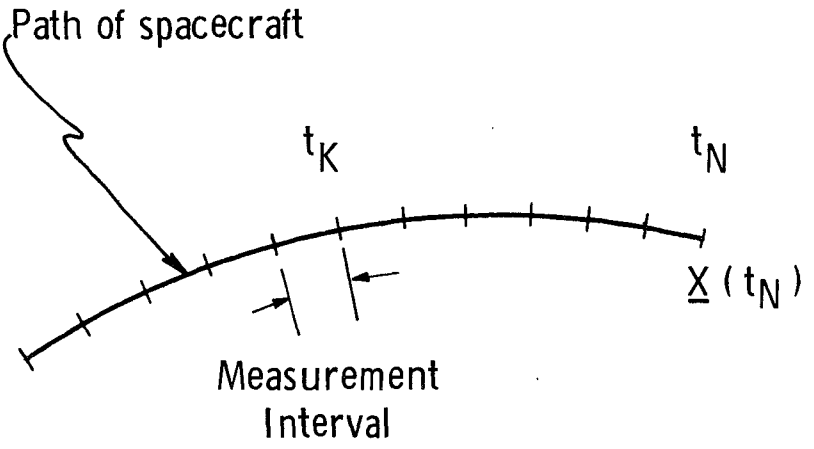

$\underline{X}_0(t_0), E_0(t_0)$

$\underline{X}_0(t_K), E_0(t_K)$

$\underline{X}_0(t_N), E_0(t_N)$

Epoch formulation of the Navigational Problem

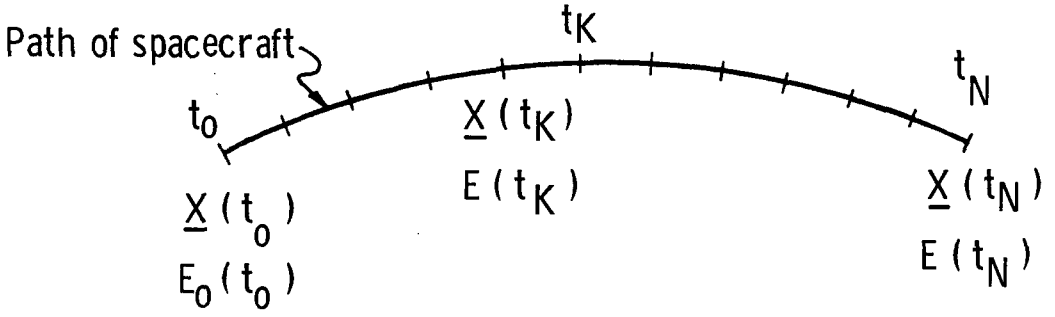

Figure 2.2 Conventional Formulation of the navigational problem.

of the two equations indicated above. However, solving this equation for t_o necessitates solving Kepler's equation for x.

Position and velocity were chosen as state variables for both the Apollo and the epoch formulations of the navigation problem for convenience, because this state is the quantity that is estimated by the filter. However, other variational parameters may be used to formulate estimates of the current state vector, such as the orbital elements. Equations for this formulation are developed in Reference 2.

CHAPTER III

THE EPOCH STATE FILTER

3.1 Derivation of the Epoch State Filter

Current position and velocity are the state variables used in the Apollo navigation filter and in the integration of the equations of motion of the spacecraft. The current state is estimated by measurement data which is incorporated to update the current state estimate directly.

For the Epoch State Filter (ESF), position and velocity of the vehicle at the epoch time are the state variables which are used in the integration of the equations of motion. This filter estimates the current state indirectly by first estimating the epoch state. Current measurement data is processed to update the epoch state estimate. The improved current state estimate is then obtained from the epoch state estimate by conic extrapolation.

The state equations of motion used for the ESF formulation are derived as variations of the epoch state, $\underline{r}_o$ and $\underline{v}_o$. An additional differential equation in terms of the independent scalar variable θ is also integrated. Theta, the true anomaly difference, is the angle between the epoch and current position vector as illustrated in Figure 3.1.

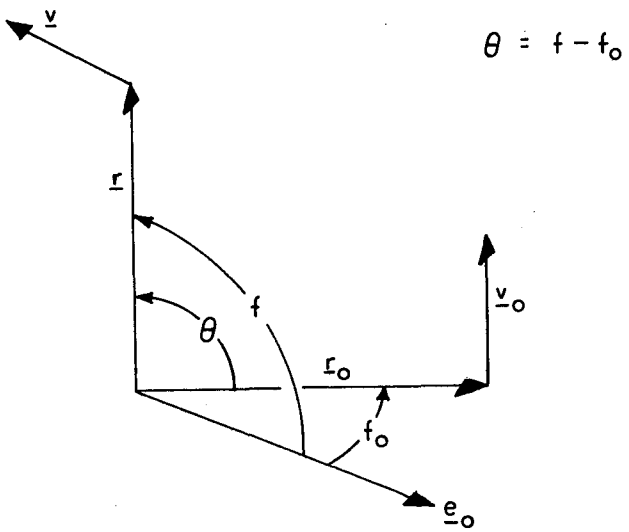

Figure 3.1 The True Anomaly Difference

These differential equations for $\dot{\underline{r}}_o$, $\dot{\underline{v}}_o$, and $\dot{\theta}$ (derived in Section 3.3) are integrated to propagate the estimate of the epoch state before the new information is introduced. Measurement data is then incorporated to estimate the epoch state deviation, $\delta \hat{\underline{x}}_o(t)$, from its nominal value at the current time. This is related to the estimate of the current state deviation $\delta \hat{\underline{x}}(t)$ by

$$\delta \hat{\underline{x}}_o = \Phi^{-1} \delta \hat{\underline{x}} \tag{3.1.1}$$

in terms of the state transition matrix $\Phi(t, t_o)$. The current state estimate, $\delta \hat{\underline{x}}$, determined by Equation 2.3.6 is rewritten here as

$$\delta \hat{\underline{x}} = \delta \hat{\underline{x}}' + \underline{\omega} (\delta \tilde{q} - \underline{b}^T \delta \hat{\underline{x}}') \tag{3.1.2}$$

replacing $\delta \hat{q}'$ by its equivalent $\underline{b}^T \delta \hat{\underline{x}}'$ where

$$\underline{\omega} = \frac{E' \underline{b}}{a} \tag{3.1.3}$$

The current covariance matrix of estimation errors, E', before the measurement is incorporated is related to the epoch covariance matrix by

$$E' = \Phi E_o' \Phi^T \tag{3.1.4}$$

Substituting Equations 3.1.2 through 3.1.4 into Equation 3.1.1 and bracketing significant terms yields

$$\delta\hat{\underline{x}}_o = [\Phi^{-1}\,\delta\hat{\underline{x}}'] + \Phi^{-1}\,\Phi E_o'\,([\Phi^T\underline{b}]/a)\,(\delta\tilde{q} - \underline{b}^T\,\delta\hat{\underline{x}}') \quad (3.1.5)$$

The product $\Phi^{-1}\,\Phi$ is the identity matrix so that the first term in brackets is just $\delta\hat{\underline{x}}_o$, i.e.

$$\Phi^{-1}\,\delta\hat{\underline{x}}' = \delta\hat{\underline{x}}_o' \quad (3.1.6)$$

and $\underline{b}_o$ is related to $\underline{b}$ according to

$$\underline{b}_o = \Phi^T\,\underline{b} \quad (3.1.7)$$

so the second term in brackets is $\underline{b}_o$. When Equations 3.1.6 and 3.1.7 are substituted into Equation 3.1.5 the resulting equation is

$$\delta\hat{\underline{x}}_o = \delta\hat{\underline{x}}_o' + [E_o'\,\underline{b}_o/a]\,(\delta\tilde{q} - \underline{b}^T\,\delta\hat{\underline{x}}') \quad (3.1.8)$$

The term in brackets can be defined as the epoch filter gain $\underline{\omega}_o$, where

$$\underline{\omega}_o = \frac{E_o'\,\underline{b}_o}{a} \quad (3.1.9)$$

Substituting Equation 3.1.9 into 3.1.8, post multiplying $\underline{b}^T$ in Equation 3.1.8 by the identity matrix $\Phi\Phi^{-1}$, and bracketing significant terms yields

$$\delta\hat{\underline{x}}_o = \delta\hat{\underline{x}}_o' + \underline{\omega}_o\,(\delta\tilde{q} - [\underline{b}^T\Phi]\,[\Phi^{-1}\,\delta\hat{\underline{x}}']) \quad (3.1.10)$$

But

$$\underline{b}^T \Phi = \underline{b}_o^T \tag{3.1.11}$$

and

$$\Phi^{-1} \delta \hat{\underline{x}}' = \delta \hat{\underline{x}}_o' \tag{3.1.12}$$

When Equations 3.1.11 and 3.1.12 are substituted into Equation 3.1.10 the resulting equation for the ESF is

$$\delta \hat{\underline{x}}_o = \delta \hat{\underline{x}}_o' + \underline{\omega}_o (\delta \tilde{q} - \underline{b}_o^T \delta \hat{\underline{x}}_o') \tag{3.1.13}$$

As is done in the Apollo navigation system, $\delta \hat{\underline{x}}_o'$ is added to the estimate of the total state vector so that the nominal path is redefined by the k^{th} measurement. Therefore, for the nominal path defined by the $(k-1)^{th}$ measurement, the extrapolated estimate of the deviation from the nominal trajectory is zero, i.e. $\delta \hat{\underline{x}}_o' (t_k) = \underline{0}$ as illustrated by Figure 3.2. Substituting $\delta \hat{\underline{x}}_o' = \underline{0}$ into Equation 3.1.13 yields

$$\delta \hat{\underline{x}}_o = \underline{\omega}_o \delta \tilde{q} \tag{3.1.14}$$

which is the ESF equation for incorporating scalar measurement data to update the estimate of the epoch state.

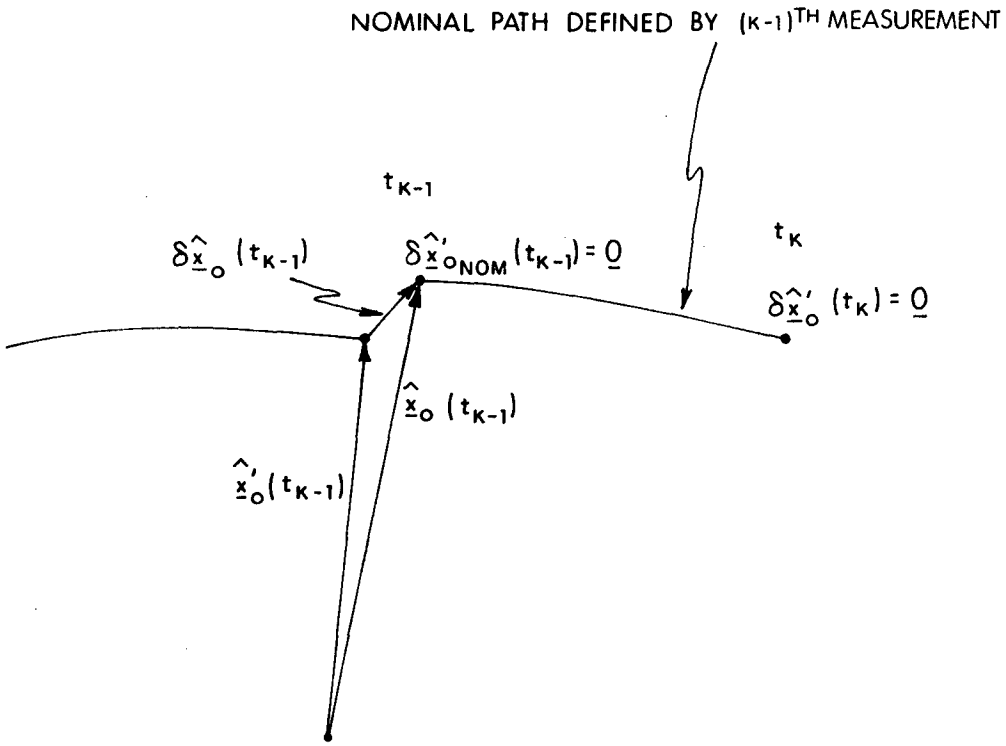

Figure 3.2 Redefinition of the Nominal Path

3.2 Derivation of the Error Covariance Matrix Used in the ESF

The equation for the epoch error covariance matrix E_o associated with the state deviation $\delta \underline{x}_o$ is obtained from the covariance matrix equation developed in Section 2.2

$$E_k = E_k' - \underline{\omega}\,\underline{b}^T E_k' \tag{3.2.1}$$

where the subscript k indicates the quantity at time t_k. Noting the relations between the epoch and current parameters

$$E_k' = \Phi_{k',0}\, E_o'\, \Phi_{k,0}^T \tag{3.2.2}$$

$$E_k = \Phi_{k',0}\, E_o\, \Phi_{k,0}^T \tag{3.2.2}$$

and substituting these into Equation 3.2.1 yields

$$\Phi E_o \Phi^T = \Phi E_o' \Phi^T - \Phi E_o' \Phi^T \frac{\underline{b}\,\underline{b}^T}{a} \Phi E_o \Phi^T \tag{3.2.4}$$

where $\underline{\omega}$ in Equation 3.2.1 has been replaced by

$$\underline{\omega} = \frac{E_k' \underline{b}}{a} \tag{3.2.5}$$

and the subscripts on Φ have been dropped for simplicity.

Premultiplying Equation 3.2.4 by Φ^{-1}, postmultiplying by Φ^{T-1} and grouping significant terms produces the following equation

$$E_o = E_o' - \frac{E_o' [\Phi^T \underline{b}]}{a} [\underline{b}^T \Phi] E_o' \qquad (3.2.6)$$

but

$$\underline{b}_o = \Phi^T \underline{b} \qquad (3.2.7)$$

so that

$$\underline{b}_o^T = \underline{b}^T \Phi \qquad (3.2.8)$$

The first term in brackets is then $\underline{b}_o$ and the second is $\underline{b}_o^T$. Rewriting Equation 3.2.6 making these substitutions yields

$$E_o = E_o' - \frac{E_o' \underline{b}_o}{a} \underline{b}_o^T E_o' \qquad (3.2.9)$$

by defining the new variable $\underline{\omega}_o$ as

$$\underline{\omega}_o = \frac{E_o' \underline{b}_o}{a} \qquad (3.2.10)$$

Equation (3.2.9) reduces to

$$\boxed{E_o = E_o' - \underline{\omega}_o \underline{b}_o^T E_o'} \qquad (3.2.11)$$

Equation 3.2.11 is of the same form as Equation 3.2.1 but the "k" subscripts of the latter equation have been replaced by "0" subscripts in the epoch form.

The "a" in Equation 3.2.10 is equivalent to the epoch quantity a_o as demonstrated by the derivation. Rewriting the equation for a

$$a = \underline{b}^T E_k' \underline{b} + \overline{\alpha^2} \qquad (3.2.12)$$

and substituting for $\underline{b}^T$ and $\underline{b}$ in terms of their epoch quantities, and bracketing significant terms yields

$$a = \underline{b}_o^T [\Phi_{k,o}^{-1} E_k' \Phi_{k,o}^{T-1}] \underline{b}_o + \overline{\alpha^2} \qquad (3.2.13)$$

The term in brackets is E_o' so that Equation 3.2.13 reduces to

$$a = \underline{b}_o^T E_o' \underline{b}_o + \overline{\alpha^2} \qquad (3.2.14)$$

which is the expression for a_o, hence

$$a_o = a \qquad (3.2.15)$$

3.3 Explanation of Assumptions Made to Integrate the ESF Equations

The position and velocity, $\underline{r}(t)$ and $\underline{v}(t)$ respectively, in the Apollo navigation filter are updated in real time and change continuously along the path. For the epoch state version of the navigation filter the initial position and velocity, $\underline{r}_o$ and $\underline{v}_o$, are updated at measurement times; however, between measurements these vectors remain constant. Similarly, the initial error vector, $\underline{e}_o$, is constant between measurements. Thus between measurements:

$$\underline{e}_o = \text{constant} \tag{3.3.1}$$

so the time derivative of the error vector is zero, i.e.

$$\dot{\underline{e}}_o = \underline{0} \tag{3.3.2}$$

also, since

$$E_o = \overline{\underline{e}_o \underline{e}_o^T} \tag{3.3.3}$$

the time derivate of the epoch covariance matrix is zero

$$\dot{E}_o = \overline{\dot{\underline{e}}_o \underline{e}_o^T} + \overline{\underline{e}_o \dot{\underline{e}}_o^T} \tag{3.3.4}$$

Therefore, between measurements

$$\dot{E}_o = 0 \tag{3.3.5}$$

Unlike the current error covariance matrix, E(t), which changes continuously along the path, the epoch covariance matrix, E_o, remains constant between measurements so that it does not have to be propagated. In the interval between the $(k-1)^{th}$ measurement and the k^{th} measurement, E_o remains constant or $E_o'(t_k) = E_o(t_k - 1)$ as illustrated graphically in Figure 3.3.

For ideal two body motion the above results may be applied exactly. Also, Φ, the transition matrix, may be calculated analytically for a conic path.

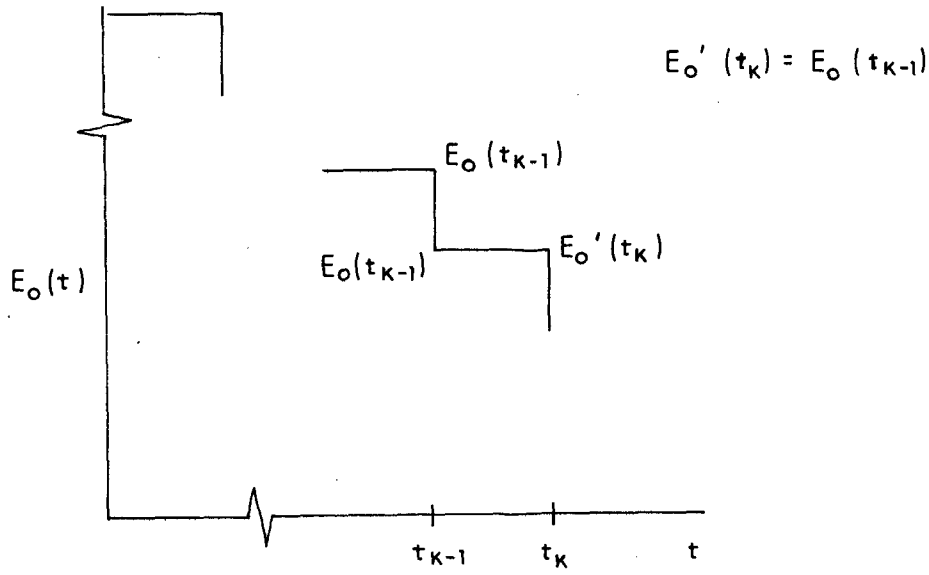

Figure 3.3 Graphical Illustration of the Components of E.

With a disturbing acceleration, $\underline{a}_d$, present, the concepts derived above still hold, i.e. the epoch state and epoch covariance matrix may remain constant within measurement intervals. But motion under the influence of a disturbing acceleration is not two body motion. The equation governing the motion of the spacecraft is then

$$\ddot{\underline{r}} + \frac{\mu}{r^3}\underline{r} = \underline{a}_d(\underline{r}) \qquad (3.3.6)$$

In order to use the two-body formulation of the navigational problem, the disturbing acceleration is considered to perturb $\underline{r}_o$ and $\underline{v}_o$ from their nominal two body values. Similarly, $\underline{\epsilon}_o$ and thus E_o are perturbed from their ideal two body values. However, because these change only slowly for non-ideal two body motion, the perturbations are ignored and E_o is not propagated between measurements. Proof that E_o for the actual path is close to E_o for the conic path and varies only slowly is given here, thus validifying the approximation that $\dot{E}_o = 0$ for the actual path. Remember that $\dot{E}_o = 0$ for the conic path is exact.

Let the "c" subscript on the state transition matrix Φ and the * superscript on the covariance matrix E denote the values of these quantities for the conic path. See Figure 3.4 for an illustration of the conic and actual path and their related quantities.

The differential equation for Φ as given in Section 2.2 is

$$\frac{d\Phi}{dt} = F\Phi \qquad (3.3.7)$$

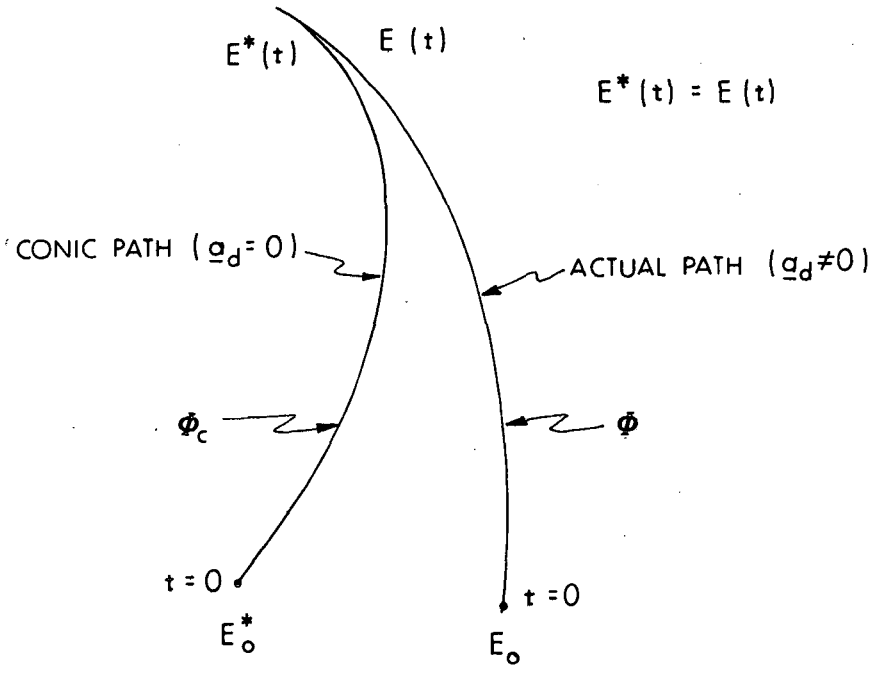

Figure 3.4 Illustration of Actual Path to Which the Conic Path of the Spacecraft is Matched

where

$$F = \begin{bmatrix} O & I \\ G & O \end{bmatrix} \tag{3.3.8}$$

For the conic path, the differential equation is

$$\frac{d\Phi_c}{dt} = F_c \Phi_c \tag{3.3.9}$$

The current covariance matrix E(t) in terms of the epoch covariance matrix for the actual path is given by

$$E(t) = \Phi E_o \Phi^T \tag{3.3.10}$$

but

$$E^*(t) = E(t) \tag{3.3.11}$$

so

$$\Phi_c E_o^* \Phi_c^T = \Phi E_o \Phi^T \tag{3.3.12}$$

Solving for E_o^* in Equation 3.3.12 and grouping significant terms yields

$$E_o^* = [\Phi_c^{-1} \Phi] E_o [\Phi^T \Phi_c^{T-1}] \tag{3.3.13}$$

Define the new variable Φ_T as

$$\Phi_T = \Phi_c^{-1} \Phi \tag{3.3.14}$$

so that Equation 3.3.13 expressed in terms of Φ_T is

$$E_o^* = \Phi_T E_o \Phi^T \tag{3.3.15}$$

Φ expressed in terms of Φ_T is

$$\Phi_c \Phi_T = \Phi \tag{3.3.16}$$

Taking the time derivative of 3.3.16 yields

$$\dot{\Phi}_c \Phi_T + \Phi_c \dot{\Phi}_T = \dot{\Phi} \tag{3.3.17}$$

Substituting Equation 3.3.9 for $\dot{\Phi}_c$ and 3.3.7 and 3.3.16 for $\dot{\Phi}$, Equation 3.3.17 becomes

$$F_c \Phi_c \Phi_T + \Phi_c \dot{\Phi}_T = F \Phi_c \Phi_T \tag{3.3.18}$$

Collecting like terms Equation 3.3.18 reduces to

$$\Phi_c \dot{\Phi}_T = (F - F_c) \Phi_c \Phi_T \tag{3.3.19}$$

Solving for $\dot{\Phi}_T$ yields

$$\dot{\Phi}_T = [\Phi_c^{-1} (F - F_c) \Phi_c] \Phi_T \tag{3.3.20}$$

But

$$\dot{\Phi}_T = F_T \Phi_T \tag{3.3.21}$$

so

$$F_T = \Phi_c^{-1} (F - F_c) \Phi_c \tag{3.3.22}$$

Rewritting $F - F_c$ in terms of its constituents

$$F - F_c = \begin{bmatrix} O & I \\ G & O \end{bmatrix} - \begin{bmatrix} O & I \\ G_c & O \end{bmatrix} \tag{3.3.23}$$

and simplifying replacing $(G - G_c)$ by G_{ad}, $F - F_c$ is given by

$$F - F_c = \begin{bmatrix} O & O \\ G_{ad} & O \end{bmatrix} \tag{3.3.24}$$

Defining $F - F_c$ as F_{ad} so that Equation 3.3.22 becomes

$$F_T = \Phi_c^{-1} F_{ad} \Phi_c \tag{3.3.25}$$

Equation 3.3.20 is then written as

$$\dot{\Phi}_T = \Phi_c^{-1} F_{ad} \Phi_c \Phi_T \tag{3.3.26}$$

By observing the components of Equation 3.3.26 it is seen that $\dot{\Phi}_T$ is small; also since initially $\Phi_T(t_o, t_o) = I$, Φ_T remains close to I, and from Equation 3.3.16 it is seen that

$$\Phi \cong \Phi_c \tag{3.3.27}$$

Also, since

$$E_o^* = \Phi_T E_o \Phi_T^T$$

and Φ_T is close to I

$$E_o \cong E_o^* \tag{3.3.28}$$

The assumption that $\dot{E}_o = O$ between measurements for non ideal two-body motion greatly simplifies calculations. The epoch state covariance matrix does not have to be propagated within measurement intervals. Also, because Φ is close to Φ_c, the transition matrix may be calculated agebraically, as in the case for ideal two-body motion, as opposed to integrating a differential equation for Φ.

Analytical calculation of the state transition matrix, Φ, is explained here. Consider the state vector $\underline{x}$ where

$$\underline{x} = \begin{bmatrix} \underline{r} \\ \underline{v} \end{bmatrix} \tag{3.3.29}$$

$\underline{r}$ and $\underline{v}$ are functions of initial position and velocity

$$\underline{r} = \underline{r}\,(\underline{r}_o, \underline{v}_o, t) \tag{3.3.30}$$

$$\underline{v} = \underline{v}\,(\underline{r}_o, \underline{v}_o, t) \tag{3.3.31}$$

and t is the independent variable upon which $\underline{r}_o$, $\underline{v}_o$ and thus $\underline{r}$ and $\underline{v}$ are dependent. Taking partial derivatives of $\underline{r}$ and $\underline{v}$ at time t_k yields

$$\delta \underline{r}_k = \frac{\partial \underline{r}}{\partial \underline{r}_o} \delta \underline{r}_o + \frac{\partial \underline{r}}{\partial \underline{v}_o} \delta \underline{v}_o \qquad (3.3.32)$$

$$\delta \underline{v}_k = \frac{\partial \underline{v}}{\partial \underline{r}_o} \delta \underline{r}_o + \frac{\partial \underline{v}}{\partial \underline{v}_o} \delta \underline{v}_o \qquad (3.3.33)$$

Expressing Equations 3.3.32 and 3.3.33 in matrix form results in

$$\begin{bmatrix} \delta \underline{r}_k \\ \delta \underline{v}_k \end{bmatrix} = \begin{bmatrix} \frac{\partial \underline{r}}{\partial \underline{r}_o} & \frac{\partial \underline{r}}{\partial \underline{v}_o} \\ \frac{\partial \underline{v}}{\partial \underline{r}_o} & \frac{\partial \underline{v}}{\partial \underline{v}_o} \end{bmatrix} \begin{bmatrix} \delta \underline{r}_o \\ \delta \underline{v}_o \end{bmatrix} \qquad (3.3.34)$$

Defining the 6 x 6 matrix of partial derivatives with respect to r_o and $\underline{v}_o$ as $\Phi(t_k, t_o)$ Equation 3.3.34 becomes

$$\delta \underline{x}_k = \Phi(t_k, t_o) \delta \underline{x}_o \qquad (3.3.35)$$

The partial derivatives of the state transition matrix as given in Reference 2 are written here

$$\frac{\partial \underline{r}}{\partial \underline{r}_o} = \overset{*}{V}(t_o)^T \qquad (3.3.36)$$

$$\frac{\partial \underline{v}}{\partial \underline{r}_o} = C(t)V^*(t_o)^T - R(t)^{T-1} \qquad (3.3.37)$$

$$\frac{\partial \underline{r}}{\partial \underline{v}_o} = R(t) = -R^*(t_o)^T \qquad (3.3.38)$$

$$\frac{\partial \underline{v}}{\partial \underline{v}_o} = V(t) \qquad (3.3.39)$$

where

$$C(t) = R^{T-1} V^T \qquad (3.3.40)$$

The R and V matrices are given by

$$R(t) = \frac{1}{\mu}\{[U_2(\underline{r} - \underline{r}_o) + c\,\underline{v}]\underline{v}_o^T - U_2(\underline{v} - \underline{v}_o)\underline{r}_o^T\} + G\,I \qquad (3.3.41)$$

$$V(t) = \frac{1}{r^3}(U_2\,\underline{r}\,\underline{r}_o^T - c\,\underline{r}\,\underline{v}_o^T) + \frac{r_o}{\mu}(\underline{v} - \underline{v}_o)(\underline{v} - \underline{v}_o)^T + G_t\,I \qquad (3.3.42)$$

where

$$\sqrt{\mu}\,c = 3U_5 - x\,U_4 - U_2\sqrt{\mu}(t - t_o) \qquad (3.3.43)$$

and x is obtained by solving Kepler's equation. The R^* and V^*

matrices obtained from Equations 3.3.41 and 3.3.42 by interchanging x and t by -x and -t as well as interchanging $\underline{r}$, $\underline{v}$ and $\underline{r}_o$, $\underline{v}_o$ are

$$R^*(t) = \frac{1}{\mu}\{[U_2(\underline{r}_o - \underline{r}) - c\underline{v}_o]\underline{v}^T - U_2(\underline{v}_o - \underline{v})\underline{r}^T\} - GI \qquad (3.3.44)$$

$$V^*(t) = \frac{1}{r_o^3}(U_2\underline{r}_o\underline{r}^T + c\underline{r}_o\underline{v}^T) + \frac{r}{\mu}(\underline{v}_o - \underline{v})(\underline{v}_o - \underline{v})^T + FI \qquad (3.3.45)$$

Because of the assumptions allowing for the analytical calculation of Φ, computer run time and computer storage space are conserved. This approximation is not without some loss of accuracy, however. The variation of parameters equations for $\underline{r}_o$ and $\underline{v}_o$ derived in section 3.4 are exact but the way they are used introduces some error in Φ. That is, the position and velocity of the spacecraft are matched with the position and velocity of a conic path yielding a conic epoch position and velocity that differ from the actual $\underline{r}_o$ and $\underline{v}_o$.

3.4 Derivation of the Variational Equations

The variational parameters for the epoch state filter are the epoch state variables $\underline{r}_o$ and $\underline{v}_o$, and the true anomoly difference θ. Derivation of the variational equations in terms of these parameters is presented here.

Current position and velocity vectors $\underline{r}$ and $\underline{v}$ can be expressed in terms of their values $\underline{r}_o$ and $\underline{v}_o$ at some epoch time t_o as follows

$$\begin{bmatrix} \underline{r}^T \\ \underline{v}^T \end{bmatrix} = \begin{bmatrix} F & G \\ F_t & G_t \end{bmatrix} \begin{bmatrix} \underline{r}_o^T \\ \underline{v}_o^T \end{bmatrix} \tag{3.4.1}$$

or

$$\begin{bmatrix} \underline{r}^T \\ \underline{v}^T \end{bmatrix} = \Psi \begin{bmatrix} \underline{r}_o^T \\ \underline{v}_o^T \end{bmatrix} \tag{3.4.2}$$

defining the matrix of scalar quantities F, G, F_t, G_t as Ψ where

$$F = 1 - \frac{U_2}{r_o} = \frac{1}{r_o}(r\,U_o - \sigma\,U_1) \tag{3.4.3}$$

$$\sqrt{\mu}\,G = r\,U_1 - \sigma\,U_2 \tag{3.4.4}$$

$$F_t = -\frac{\sqrt{\mu}}{r\,r_o}\,U_1 \tag{3.4.5}$$

$$G_t = 1 - \frac{U_2}{r} \tag{3.4.6}$$

and

$$\sigma = \frac{1}{\sqrt{\mu}}\,\underline{r} \cdot \underline{v} \tag{3.4.7}$$

The U functions used in this derivation are given in terms of θ as

$$U_o = 1 - \frac{\alpha\,r\,r_o}{p}(1 - \cos\theta) \tag{3.4.8}$$

$$U_1 = \frac{r}{\sqrt{p}} \sin\theta - \frac{r\sigma_o}{p}(1 - \cos\theta) \tag{3.4.9}$$

$$U_2 = \frac{r r_o}{p}(1 - \cos\theta) \tag{3.4.10}$$

$$U_3 = \sqrt{\mu}(t - t_o) - \frac{r r_o}{\sqrt{p}} \sin\theta \tag{3.4.11}$$

with

$$r = \frac{p}{1 + (\frac{p}{r_o} - 1)\cos\theta - \frac{h\sigma_o}{\sqrt{\mu} r_o}\sin\theta} \tag{3.4.12}$$

$$p = 2r_o - \alpha r_o^2 - \sigma_o^2 \tag{3.4.13}$$

$$\alpha = \frac{2}{r} - \frac{v^2}{\mu} \tag{3.4.14}$$

and

$$\sigma_o = \frac{1}{\sqrt{\mu}} \underline{r}_o \cdot \underline{v}_o \tag{3.4.15}$$

Equation 3.4.1 may be solved for $\underline{r}_o$ and $\underline{v}_o$ by premultiplying both sides of the equation by Ψ^{-1} thus obtaining

$$\begin{bmatrix} \underline{r}_o^T \\ \underline{v}_o^T \end{bmatrix} = \Psi^{-1} \begin{bmatrix} \underline{r}^T \\ \underline{v}^T \end{bmatrix} = \begin{bmatrix} G_t & -G \\ -F_t & F \end{bmatrix} \begin{bmatrix} \underline{r}^T \\ \underline{v}^T \end{bmatrix} \tag{3.4.16}$$

where the determinant of the matrix Ψ is unity. The perturbation derivatives of $\underline{r}_o$ and $\underline{v}_o$ may now be calculated from Equation 3.4.16 applying the formal rules for variation of the orbital elements. Briefly this means Equation 3.4.16 is to be differentiated according to the usual rules of differentiation but $\underline{r}$ is treated as a constant and the orbital elements as variables. The term $d\underline{v}/dt$ is replaced by $\underline{a}_d$ and dx/dt by $d\xi/dt$ where ξ represents the change in x arising solely from changes in the orbital elements due to $\underline{a}_d$.

Formal differentiation of Equation 3.4.16 yields

$$\begin{bmatrix} \frac{d\underline{r}_o^T}{dt} \\ \\ \frac{d\underline{v}_o^T}{dt} \end{bmatrix} = \frac{d\Psi^{-1}}{dt} \begin{bmatrix} \underline{r}^T \\ \\ \underline{v}^T \end{bmatrix} + \Psi^{-1} \begin{bmatrix} 0 \\ \\ \underline{a}_d \end{bmatrix} \qquad (3.4.17)$$

where $\frac{d\Psi^{-1}}{dt}$ is defined in terms of its components as

$$\frac{d\Psi^{-1}}{dt} = \begin{bmatrix} \frac{dG_t}{dt} & -\frac{dG}{dt} \\ \\ -\frac{dF_t}{dt} & \frac{dF}{dt} \end{bmatrix} \qquad (3.4.18)$$

The upper left-hand element of 3.4.18, $\frac{dG_t}{dt}$ is obtained by formally differentiating Equation 3.4.6. Thus,

$$\frac{dG_t}{dt} = -\frac{1}{r} \frac{dU_2(x;\alpha)}{dt} \qquad (3.4.19)$$

where $\frac{dU_2(x;\alpha)}{dt}$ is derived in Reference 2 using the formal rules for variation of the orbit elements and is written here as

$$\frac{dU_2}{dt} = U_1\left[\frac{d\xi}{dt} + (1/2)U_3\frac{d\alpha}{dt}\right] - (1/2)U_2^2\frac{d\alpha}{dt} \qquad (3.4.20)$$

The perturbation derivative for α, the reciprocal of the semimajor axis, is given by

$$\frac{d\alpha}{dt} = -\frac{2}{\mu}\underline{v}\cdot\underline{a}_d \qquad (3.4.21)$$

In order to express Equation 3.4.20 in terms of G_t and F_t, the first term on the right-hand side is multiplied and divided by $\sqrt{\mu}/r_o$ and $\frac{1}{\mu}U_2\underline{v}\cdot\underline{a}_d$ is added to and subtracted from the second term so that

$$\frac{dG_t}{dt} = \frac{r_o}{\sqrt{\mu}}\left(\frac{d\xi}{dt} + 1/2\frac{U_3}{\mu}\frac{d\alpha}{dt}\right)\left[-\frac{\sqrt{\mu}}{r_o}\frac{U_1}{r}\right] - \frac{1}{\mu r}U_2^2\underline{v}\cdot\underline{a}_d$$

$$+\frac{1}{\mu}U_2\underline{v}\cdot\underline{a}_d - \frac{1}{\mu}U_2\underline{v}\cdot\underline{a}_d \qquad (3.4.22)$$

The term in brackets is F_t and the third and fourth term simplify to $\frac{1}{\mu}U_2\underline{v}\cdot\underline{a}_d G_t$ so Equation 3.4.22 becomes

$$\frac{dG_t}{dt} = \frac{1}{\mu} U_2 \underline{v} \cdot \underline{a}_d G_t + \frac{r_o}{\sqrt{\mu}} \left(\frac{d\xi}{dt} + 1/2\, U_3 \frac{d\alpha}{dt}\right) F_t \qquad (3.4.23)$$

$$- \frac{1}{\mu} U_2 \underline{v} \cdot \underline{a}_d \qquad (3.4.23)$$

Similarly, differentiating the expressions for G, F_t and F the following Equations are obtained

$$- \frac{dG}{dt} = - \frac{U_2}{\mu} \underline{v} \cdot \underline{a}_d G - \frac{r_o}{\sqrt{\mu}} \left(\frac{d\xi}{dt} + 1/2\, U_3 \frac{d\alpha}{dt}\right) F \qquad (3.4.24)$$

$$+ \frac{1}{\mu} \underline{r} \cdot \underline{a}_d U_2$$

$$- \frac{dF_t}{dt} = \frac{\sqrt{\mu}}{r_o^2} \left(\frac{d\xi}{dt} + \frac{1}{2} U_3 \frac{d\alpha}{dt}\right) G_t - \frac{r}{\mu} (\underline{v}_o - \underline{v}) \underline{a}_d F_t \qquad (3.4.25)$$

$$\frac{dF}{dt} = - \frac{\sqrt{\mu}}{r_o^2} \left(\frac{d\xi}{dt} + 1/2\, U_3 \frac{d\alpha}{dt}\right) G + \frac{r}{\mu} (\underline{v}_o - \underline{v}) \cdot \underline{a}_d F \qquad (3.4.26)$$

$$- \frac{r}{\mu} (\underline{v}_o - \underline{v}) \cdot \underline{a}_d F$$

Details in the derivation of Equations 3.4.24 to 3.4.26 are given in Appendix C.

Equations 3.4.23 to 3.4.26 can be expressed in matrix form as a matrix multiplied by Ψ^{-1} plus another matrix, that is

$$\frac{d\Psi^{-1}}{dt} = \begin{bmatrix} \frac{1}{\mu} U_2 \underline{v}^T \underline{a}_d & -\frac{r_o}{\sqrt{\mu}} \left[\frac{d\xi}{dt} + (1/2) U_3 \frac{d\alpha}{dt} \right] \\ \frac{\sqrt{\mu}}{r_o^2} \left[\frac{d\xi}{dt} + (1/2) U_3 \frac{d\alpha}{dt} \right] & \frac{r}{\mu} (\underline{v}_o^T - \underline{v}^T) \underline{a}_d \end{bmatrix} \Psi^{-1}$$

$$+ \begin{bmatrix} -\frac{1}{\mu} U_2 \underline{v}^T \underline{a}_d & \frac{1}{\mu} U_2 \underline{r}^T \underline{a}_d \\ 0 & -\frac{r}{\mu} (\underline{v}_o^T - \underline{v}^T) \underline{a}_d \end{bmatrix} \qquad (3.4.29)$$

The variational equation for the epoch time, t_o, may be calculated from Kepler's equation

$$\sqrt{\mu} (t - t_o) = r_o U_1 + \sigma_o U_2 + U_3 = r_1 U_1 - \sigma U_2 + U_3 \qquad (3.4.28)$$

by formal differentiation, treating t as a constant and using the variational equations for the time derivatives of the U functions given in Reference 2. This equation is

$$\sqrt{\mu} \frac{dt_o}{dt} = - r_o \left[\frac{d\xi}{dt} + (1/2) U_3 \frac{d\alpha}{dt} \right] - \frac{1}{2} \sqrt{\mu}\, c \frac{d\alpha}{dt} + U_2 \frac{d\sigma}{dt} \qquad (3.4.29)$$

where c has been defined by

$$\sqrt{\mu}\, c = 3 U_5 - x U_4 - U_2 \sqrt{\mu} (t - t_o) \qquad (3.4.30)$$

If t_o varies so that $\frac{d\xi}{dt} + (1/2) U_3 \frac{d\alpha}{dt} = 0$, Equation 3.4.29 reduces to

$$\frac{dt_o}{dt} = -(1/2) c \frac{d\alpha}{dt} + \frac{U_2}{\sqrt{\mu}} \frac{d\sigma}{dt} \tag{3.4.31}$$

When $\frac{d\alpha}{dt}$ is replaced by Equation 3.4.21 and $\frac{d\sigma}{dt}$ by the following variational equation

$$\frac{d\sigma}{dt} = \frac{1}{\sqrt{\mu}} \underline{r} \cdot \underline{a}_d \tag{3.4.32}$$

the variational equation for the epoch time becomes

$$\frac{dt_o}{dt} = \frac{1}{\mu} (c \underline{v} + U_2 \underline{r}) \cdot \underline{a}_d \tag{3.4.33}$$

Getting back to $\frac{d\Psi^{-1}}{dt}$, when $\frac{d\xi}{dt} + (1/2) U_3 \frac{d\alpha}{dt} = 0$ is substituted into Equation 3.4.27, this matrix simplifies to

$$\frac{d\Psi^{-1}}{dt} = \begin{bmatrix} \frac{1}{\mu} U_2 \underline{v}^T \underline{a}_d & O \\ O & \frac{r}{\mu} (\underline{v}_o^T - \underline{v}^T) \underline{a}_d \end{bmatrix} \begin{bmatrix} G_t & -G \\ -F_t & F \end{bmatrix} + \begin{bmatrix} -\frac{1}{\mu} U_2 \underline{v}^T \underline{a}_d & \frac{1}{\mu} U_2 \underline{r}^T \underline{a}_d \\ O & -\frac{r}{\mu} (\underline{v}_o^T - \underline{v}^T) \underline{a}_d \end{bmatrix} \tag{3.4.34}$$

Taking components of Equation 3.4.17, the perturbation derivatives of $\underline{r}_o$ and $\underline{v}_o$ are expressed as

$$\frac{d\,\underline{r}_o^{\,T}}{dt} = \frac{dG_t}{dt}\,\underline{r}^T - \frac{dG}{dt}\,\underline{v}^T - G\underline{a}_d \tag{3.4.35}$$

$$\frac{d\,\underline{v}_o^{\,T}}{dt} = -\frac{dF_t}{dt}\,\underline{r}^T + \frac{d\dot{F}}{dt}\,\underline{v}^T + F\,\underline{a}_d \tag{3.4.36}$$

Multiplying out the matrices of Equation 3.4.34 produces

$$\frac{d\Psi^{-1}}{dt} = \begin{bmatrix} \frac{1}{\mu}\,U_2\,\underline{v}^T\,\underline{a}_d\,G_t & -\frac{1}{\mu}\,U_2\,\underline{v}^T\,\underline{a}_d\,G \\ -\frac{r}{\mu}\,(\underline{v}_o^{\,T} - \underline{v}^T)\,\underline{a}_d\,F_t & -\frac{r}{\mu}\,(\underline{v}_o^{\,T} - \underline{v}^T)\,\underline{a}_d\,F \end{bmatrix}$$

$$+ \begin{bmatrix} -\frac{1}{\mu}\,U_2\,\underline{v}^T\,\underline{a}_d & \frac{1}{\mu}\,U_2\,\underline{r}^T\,\underline{a}_d \\ O & -\frac{r}{\mu}\,(\underline{v}_o^{\,T} - \underline{v}^T)\,\underline{a}_d \end{bmatrix} \tag{3.4.37}$$

When the related components of $\frac{d\Psi^{-1}}{dt}$ from Equation 3.4.37 are substituted into Equation 3.4.35, the result is

$$\frac{d\,\underline{r}_o^{\,T}}{dt} = \frac{U_2}{\mu}\left[\underline{v}^T\,\underline{a}_d\,G_t\,\underline{r}^T - \underline{v}^T\,\underline{a}_d\,G\underline{v}^T - \underline{v}^T\,\underline{a}_d\,\underline{r}^T + \underline{r}^T\,\underline{a}_d\,\underline{v}^T\right] - G\,\underline{a}_d \tag{3.4.38}$$

Collecting like terms and making the substitution $\underline{r}_o^T = G_t \underline{r}^T - G\underline{v}^T$ produces the following equation

$$\frac{d\underline{r}_o^T}{dt} = \frac{U_2}{\mu}(\underline{v}^T \underline{a}_d \underline{r}_o^T - \underline{v}^T \underline{a}_d \underline{r}^T + \underline{r}^T \underline{a}_d \underline{v}^T) - G\underline{a}_d \qquad (3.4.39)$$

Finally, taking the transpose or Equation 3.4.39 and collecting like terms results in the variational equation for $\underline{r}_o$

$$\boxed{\frac{d\underline{r}_o}{dt} = \frac{U_2}{\mu}[(\underline{r}_o - \underline{r})\underline{v}^T + \underline{v}\,\underline{r}^T]\underline{a}_d - G\underline{a}_d} \qquad (3.4.40)$$

Similarly, when the related components of $\frac{d\Psi^{-1}}{dt}$ from Equation 3.4.37 are substituted into Equation 3.4.36 the result is

$$\frac{d\underline{v}_o^T}{dt} = \frac{\underline{r}}{\mu}[-(\underline{v}_o^T - \underline{v}^T)\underline{a}_d F_t \underline{r}^T + (\underline{v}_o^T - \underline{v}^T)\underline{a}_d F\,\underline{v}^T$$

$$- (\underline{v}_o^T - \underline{v}^T)\underline{a}_d \underline{v}^T] + F\underline{a}_d \qquad (3.4.41)$$

Making the substitution $\underline{v}_o^T = F_t \underline{r}^T + F\,\underline{v}^T$ in Equation 3.4.41 yields

$$\frac{d\underline{v}_o^T}{dt} = \frac{\underline{r}}{\mu}[(\underline{v}_o^T - \underline{v}^T)\underline{a}_d \underline{v}_o^T - (\underline{v}_o^T - \underline{v}^T)\underline{a}_d \underline{v}^T] + F\underline{a}_d \qquad (3.4.42)$$

Transposing Equation 3.4.42 results in the following variational equation for $\underline{v}_o$.

$$\frac{d\underline{v}_o^T}{dt} = \frac{r}{\mu}\,(\underline{v}_o - \underline{v})\,(\underline{v}_o - \underline{v})^T\,\underline{a}_d + F\,\underline{a}_d \qquad (3.4.43)$$

Using the following relation derived in Reference 2

$$\frac{d\xi}{dt} + (1/2)U_3\frac{d\alpha}{dt} = \frac{\sqrt{\mu}\,r_o}{h}\,\frac{d\delta}{dt} - \frac{\sqrt{\mu}}{r}\left(\frac{G}{h^2}\,\underline{h}\times\underline{r} + \frac{U_2}{\mu}\,\underline{r}\right)\cdot\underline{a}_d \qquad (3.4.44)$$

where G obtained form Equations 3.4.4, 3.4.9, and 3.4.10 is given by

$$G = \frac{r\,r_o}{h}\sin\theta \qquad (3.4.45)$$

and $\frac{d\delta}{dt}$ is determined according to

$$\frac{d\delta}{dt} = \frac{d\theta}{dt} - \frac{h}{r^2} \qquad (3.4.46)$$

δ being the variation in the true anomoly difference θ. Equation 3.4.47 is obtained when $\frac{d\xi}{dt} + (1/2)U_3\frac{d\alpha}{dt}$ is set equal to zero and substitutions 3.4.45 and 3.4.46 are made in Equation 3.4.44. Thus,

$$0 = \frac{\sqrt{\mu}\,r_o}{h}\left(\frac{d\theta}{dt} - \frac{h}{r^2}\right) - \frac{\sqrt{\mu}}{r}\left(\frac{r\,r_o}{h^3}\sin\theta\,\underline{h}\times\underline{r} + \frac{U_2}{\mu}\,\underline{r}\right)\cdot\underline{a}_d \qquad (3.4.47)$$

Solving for $\frac{d\theta}{dt}$ in the above equation results in

$$\frac{d\theta}{dt} = \frac{h}{r^2} + \frac{1}{h^2}\left[\sin\theta\,\underline{h}\times\underline{r} + \frac{h^3 U_2}{\mu\,r\,r_o}\,\underline{r}\right]\cdot\underline{a}_d \qquad (3.4.48)$$

Recalling Equation 3.4.10 for U_2 where

$$p = \frac{h^2}{\mu} \tag{3.4.49}$$

The second term in the brackets is

$$\frac{h^3 U_2}{\mu r r_o} \underline{r} = h(1 - \cos\theta)\underline{r} \tag{3.4.50}$$

Therefore, the variational equation for the independent variable θ is

$$\boxed{\frac{d\theta}{dt} = \frac{h}{r^2} + \frac{1}{h^2}\left[\sin\theta\, \underline{h} \times \underline{r} + h(1 - \cos\theta)\underline{r}\right] \cdot \underline{a}_d} \tag{3.4.51}$$

Equations 3.4.33, 3.4.40, 3.4.43, and 3.4.51 are the variable epoch form of the variational equations. This form of the variational equations was used in this thesis for simplicity, since the term $\frac{d\xi}{dt} + \frac{1}{2} U_3 \frac{d\alpha}{dt}$ was eliminated by forcing the epoch time, t_o, to vary according to: $\dot{t}_o = \frac{1}{\mu}(c\,\underline{v} + U_2\,\underline{r}) \cdot \underline{a}_d$. The variational equations for the fixed epoch case are obtained by setting $\dot{t}_o = 0$ in Equation 3 4.29.

3.5 Effect of a Measurement on the True Anomoly Difference θ

When a measurement is taken, current time is essentially stopped and the epoch time, t_o, remains fixed. Holding the epoch time constant during a measurement incorporation in the variable

epoch case does not introduce inconsistencies from the time-of-flight standpoint, since the state transition matrix relates variations in the state at the given "t_o" to state variations at the current time "t". However, since θ is the angle between the epoch and current position vectors and because measurement incorporation changes the estimate of these vectors by $\delta \hat{\underline{r}}_o$ and $\delta \hat{\underline{r}}$ respectively, the true anomoly difference may change by an amount $\Delta\theta$. This is illustrated in Figure 3.5. The epoch variation in the true anomoly difference is given by

$$\delta\theta_o = \frac{\underline{i}_{\theta_o} \cdot \delta \hat{\underline{r}}_o}{r_o} \qquad (3.5.1)$$

where $\underline{i}_{\theta_o}$ is the unit vector in the direction of the epoch change in θ and is normal to $\underline{r}_o$. Similarly, the current variation in the true anomoly difference is given by

$$\delta\theta = \frac{\underline{i}_{\theta} \cdot \delta \hat{\underline{r}}}{r} \qquad (3.5.2)$$

The total change in θ is the difference between the current and the epoch deviations, that is,

$$\Delta\theta = \delta\theta - \delta\theta_o \qquad (3.5.3)$$

Substituting Equations 3.5.1 and 3.5.2 into 3.5.3 produces

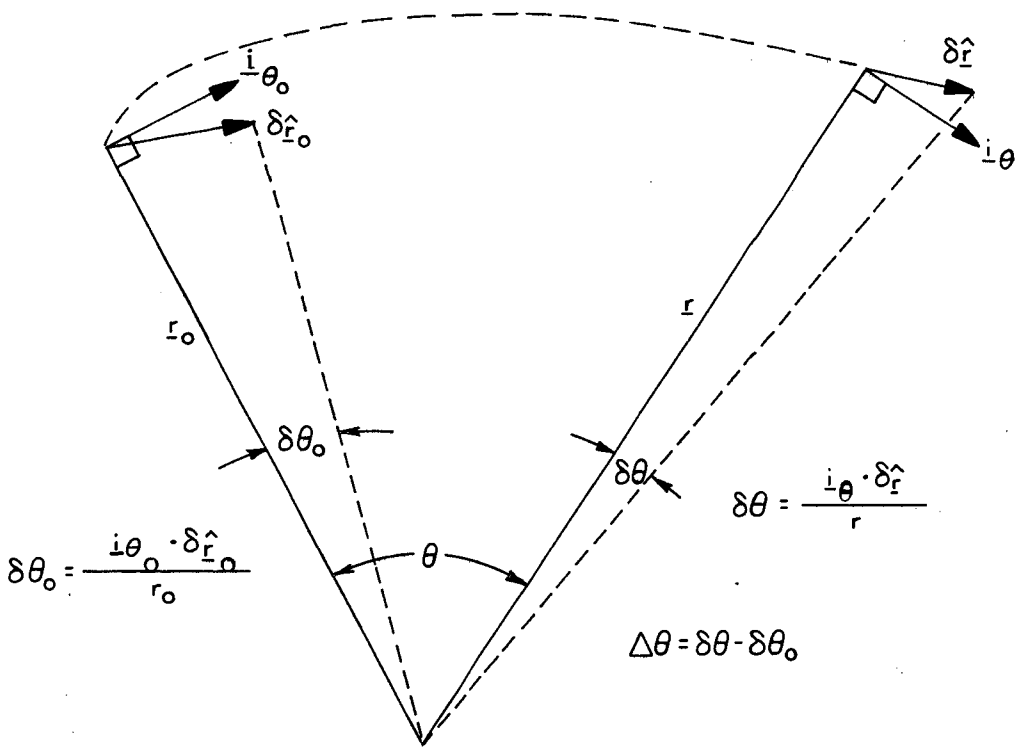

Figure 3.5 Geometric Illustration of the Total Change in the True Anomoly Difference

$$\Delta\theta = \frac{\underline{i}_\theta \cdot \delta\hat{\underline{r}}}{r} - \frac{\underline{i}_{\theta_o} \cdot \delta\hat{\underline{r}}_o}{r_o} \qquad (3.5.4)$$

Expressing Equation 3.5.4 in terms of the current and epoch state deviation vectors yields

$$\Delta\theta = \left[\frac{1}{r} \begin{pmatrix} \underline{i}_\theta \\ \underline{0} \end{pmatrix}^T \delta\hat{\underline{x}} - \frac{1}{r_o} \begin{pmatrix} \underline{i}_{\theta_o} \\ \underline{0} \end{pmatrix}^T \delta\hat{\underline{x}}_o \right] \qquad (3.5.5)$$

The estimate of the current state deviation vector $\delta\hat{\underline{x}}$ is determined from measurement data by

$$\delta\hat{\underline{x}} = \begin{bmatrix} \delta\hat{\underline{r}} \\ \\ \delta\hat{\underline{v}} \end{bmatrix} = \underline{\omega}\, \delta\tilde{q} \qquad (3.5.6)$$

Extrapolation of the epoch state deviation vector to the current time is accomplished by use of the state transition matrix according to

$$\delta\hat{\underline{x}} = \Phi(t, t_o)\, \delta\hat{\underline{x}}_o \qquad (3.5.7)$$

where $\delta\hat{\underline{x}}_o$ is determined from measurement data by

$$\delta\hat{\underline{x}}_o = \underline{\omega}_o\, \delta\tilde{q} \qquad (3.5.8)$$

Making these substitutions in Equation 3.5.5 and factoring out $\underline{\omega}_o\, \delta\tilde{q}$ results in the following Equation for the total change in the true anomoly difference:

$$\Delta\theta = \left[\frac{1}{r} \begin{pmatrix} \underline{i}_{\theta}^{T} \\ \underline{0} \end{pmatrix} \Phi(t, t_o) \qquad - \frac{1}{r_o} \begin{pmatrix} \underline{i}_{\theta_o}^{T} \\ \underline{0} \end{pmatrix} \right] \underline{\omega}_o \, \delta\tilde{q} \qquad (3.5.9)$$

3.6 Comparison of the Conventional and Epoch Formulations of the Navigational Problem

CONVENTIONAL FORMULATION	EPOCH FORMULATION
STATE VARIABLES AND VARIATIONAL EQUATIONS OF MOTION	
$\underline{r}(t),\ \underline{v}(t)$	$\underline{r}_o(t),\ \underline{v}_o(t)$
$\dot{\underline{\delta}} = \underline{\nu}$	$\dot{\underline{r}}_o = \frac{1}{\mu} U_2 \left[(\underline{r}_o - \underline{r})\,\underline{v}^T + \underline{v}\,\underline{r}^T \right] \underline{a}_d - G\,\underline{a}_d$
$\dot{\underline{\nu}} = -\frac{\mu}{r_{osc}^3} \left[f(q)\,\underline{r} + \underline{\delta} \right] + \underline{a}_d(\underline{r})$	$\dot{\underline{v}}_o = \frac{r}{\mu} (\underline{v}_o - \underline{v})\,(\underline{v}_o - \underline{v})^T\,\underline{a}_d + F\,\underline{a}_d$
where	$\dot{\theta} = \frac{h}{r^2} + \frac{1}{h^2} \left[\sin\theta\,\underline{h} \times \underline{r} + \underline{h}(1 - \cos\theta)\,\underline{r} \right] \cdot \underline{a}_d$
$q = \frac{\underline{\delta} \cdot (\underline{\delta} - 2\,\underline{r})}{r^2}$	for which the epoch time, t_o, is forced to vary according to
$f(q) = \frac{q(3 + 3q + q^2)}{1 + (1 + q)^{3/2}}$	$\dot{t}_o = \frac{1}{\mu} (c\,\underline{v} + U_2\,\underline{r}) \cdot \underline{a}_d$
	where
	$U_2 = \frac{r\,r_o}{p} (1 - \cos\theta)$

CONVENTIONAL FORMULATION

EPOCH FORMULATION

OPTIMUM LINEAR ESTIMATION EQUATIONS

$$\delta \underline{\hat{x}} = \delta \underline{\hat{x}}' + \underline{\omega} (\delta \tilde{q} - \underline{b}^T \delta \underline{\hat{x}}')$$

$$E = (I - \underline{\omega}\, \underline{b}^T) E'$$

where

$$\omega = \frac{E' \underline{b}}{a}$$

$$a = \underline{b}^T E' \underline{b} + \overline{\alpha_n^2}$$

$$\delta \underline{\hat{x}}_o = \delta \underline{\hat{x}}_o' + \underline{\omega}_o (\delta \tilde{q} - \underline{b}_o^T \delta \underline{\hat{x}}_o')$$

$$E_o = (I - \underline{\omega}_o \underline{b}_o^T) E_o'$$

where

$$\underline{\omega}_o = \frac{E_o' \underline{b}_o}{a_o}$$

$$a_o = \underline{b}_o^T E_o' \underline{b}_o + \overline{\alpha_n^2}$$

$$= \underline{b}^T E' \underline{b} + \overline{\alpha_n^2}$$

$$= a$$

$$\underline{b}_o = \Phi^T \underline{b}$$

3.7 Statistical Equations for Error Using the Epoch Formulation of the Navigational Problem

When the epoch formulation is used rather than the conventional formulation of the navigational problem, error is introduced because of the assumption that allows for the analytical calculation of the state transition matrix as opposed to integrating a differential equation. The statistical equations for this error are developed here. Let Φ_c denote the conic state transition matrix calculated for the epoch state filter. The current estimate of the state deviation vector for this filter is given by

$$\delta \underline{\hat{x}} = \underline{\omega}\, \delta \tilde{q} \tag{3.7.1}$$

where

$$\underline{\omega} = \frac{E' \underline{b}}{a} \tag{3.7.2}$$

and the estimate of the epoch state deviation vector is given by

$$\delta \underline{\hat{x}} = \underline{\omega}_o\, \delta \tilde{q} \tag{3.7.3}$$

where

$$\underline{\omega}_o = \frac{E_o' \underline{b}_o}{a} \tag{3.7.4}$$

The estimate of the current state deviation vector for the epoch state filter given in terms of epoch quantities is

$$\delta \underline{\hat{x}} = \Phi_c \, \delta \underline{\hat{x}}_o = \Phi_c \, \underline{\omega}_o \, \delta \tilde{q} \qquad (3.7.5)$$

Let the error vector, $\underline{e}_d$, incurred using the epoch formulation be the difference between the current state deviation vector of the conventional filter and that of the epoch state filter. This error is given by

$$\underline{e}_d = \underline{\omega} \, \delta \tilde{q} - \Phi \underline{\omega}_o \, \delta \tilde{q} \qquad (3.7.6)$$

Factoring out $\delta \tilde{q}$ and substituting equations 3.7.2 and 3.7.4 for $\underline{\omega}$ and $\underline{\omega}_o$ respectively yields

$$\underline{e}_d = \frac{1}{a} \left[E' \underline{b} - \Phi E_o' \underline{b}_o \right] \delta \tilde{q} \qquad (3.7.7)$$

Substituting for $\underline{b}_o$ in terms of $\underline{b}$ where

$$\underline{b}_o = \Phi^T \underline{b} \qquad (3.7.8)$$

and factoring out $\underline{b}$ results in

$$\underline{e}_d = \frac{1}{a} \left[E' - \Phi E_o' \Phi^T \right] \underline{b} \, \delta \tilde{q} \qquad (3.7.9)$$

The error covariance matrix, E_d, introduced by using the epoch as opposed to the conventional formulation of the navigational problem is

$$E_d = \overline{\underline{e}_d \underline{e}_d^T} \qquad (3.7.10)$$

$$E_d = \frac{\left[E' - \Phi E_o' \Phi^T\right] \underline{b}\, \overline{\delta \tilde{q}^2}\, \underline{b}^T \left[E' - \Phi E_o' \Phi^T\right]^T}{a^2} \qquad (3.7.11)$$

The total error vector, $\underline{e}_t$, the epoch solution of the navigational problem is the error inherent in the exact solution of the navigational problem, $\underline{e}_n$, plus the error incurred using the epoch formulation, $\underline{e}_d$. That is,

$$\underline{e}_t = \underline{e}_n + \underline{e}_d \qquad (3.7.12)$$

Solving for the total error covariance noting that $\underline{e}_n$ and $\underline{e}_d$ are uncorrelated yields

$$\overline{\underline{e}_t \underline{e}_t^T} = \overline{\underline{e}_n \underline{e}_n^T} + \overline{2\, \underline{e}_n \underline{e}_d} + \overline{\underline{e}_d \underline{e}_d^T} \qquad (3.7.13)$$

$$= \overline{\underline{e}_n \underline{e}_n^T} + \overline{\underline{e}_d \underline{e}_d^T} \qquad (3.7.4)$$

Since the first term on the right hand side of equation 3.7.14 is E_n, the error covariance matrix inherent in the exact solution of the navigational problem, and the second term on the right is just E_d, then the total error covariance matrix, E_t, is given by

$$E_t = E_n + E_d \qquad (3.7.15)$$

Thus, the total error in the epoch solution of the navigational problem is the sum of the error inherent in the exact solution plus the error

introduced by using the epoch as opposed to the conventional or exact formulation of the navigational problem.

The percentage of error introduced in the solution to the navigational problem by using the epoch state filter rather than the conventional state filter is obtained by comparing the estimated state vectors for both filters with the rms error in the estimate. For a particular solution, the percentage of error is given by the following:

$$\% \text{ error} = \frac{|\text{approximate solution} - \text{exact solution}|}{\text{exact solution}} \qquad (3.7.16)$$

The magnitude of the error between the position vector determined by the epoch state filter and the position vector determined by the Apollo navigation filter is given by $|\hat{\underline{r}}_{ESF} - \hat{\underline{r}}_{CSF}|$. A measure of the error in the position estimate of the exact or conventional solution to the navigational problem is given by the rms estimated position error. The percentage of actual error in the position estimate introduced by using the epoch rather than the conventional state filter is given by

$$\% \text{ actual error in position estimate} = \frac{|(\hat{\underline{r}}_{ESF} - \underline{r}_{TRUE}) - (\hat{\underline{r}}_{CSF} - \underline{r}_{TRUE})|}{(\text{rms position error})_{CSF}} \qquad (3.7.17)$$

Similarly, the percentage of error in the velocity estimate of the epoch state filter as compared with the conventional navigation filter is determined by

$$\% \text{ actual error in velocity estimate} = \frac{\left| (\hat{\underline{v}}_{ESF} - \underline{v}_{TRUE}) - (\hat{\underline{v}}_{CSF} - \underline{v}_{TRUE}) \right|}{(\text{rms velocity error})_{CSF}} \qquad (3.7.18)$$

When the percentage errors given by equations 3.7.17 and 3.7.18 are small, the ESF may be used in place of the CSF.

CHAPTER IV

COMPUTER SIMULATION RESULTS

4.1 Simulation Data

The purpose for computer simulating the ESF was to determine the error in this filtering technique as compared with both the true state and the error in the conventional navigation filter. A circular earth orbit with a 100 nautical mile altitude and a disturbing acceleration due to the J_2 term of the earth's gravitational potential was chosen for study. As a further demonstration of the characteristics of this filter, a circular orbit of radius equal to twice the equatorial radius of the earth was also studied. Finally, the ESF was simulated for the 100 nautical mile orbit with disturbing acceleration due to $10J_2$ to study the effects of larger disturbing accelerations.

Measurement data was incorporated at intervals of 10° around the orbit for 80 measurements, thus testing the filter for 800° or more than two revolutions. The measurement vector $\underline{b}$ was alternately chosen to be a unit vector in the x, y, and z directions respectively for sets of three measurements. This was done so as not to bias the problem in any one direction. The error in the measurement, α, was produced by a random number generator with a variance $\overline{\alpha^2}$ of 10^6 m^2.

The initial covariance matrix was chosen to be diagonal with an rms position error or 8.84×10^2 m and an rms velocity error of 8.65 m/sec. A diagonal matrix was used so as not to bias the estimation

problem, although for this simulation the initial covariance matrix is not critical provided, however, that it is large enough. The covariance matrix is gradually reduced by measurement incorporation regardless of its initial quantity.

For both the ESF and the CSF, maximum likelihood filtering techniques are employed. No approximations are made to extrapolate the error covariance matrix for the CSF as were made for the ESF so it might seem that the CSF is more accurate. However the CSF has extrapolation errors due to the equation $E = \Phi E' \Phi^T$. Since the ESF is an approximation to the CSF, a comparison of the performance of these filters was made. The results of this study are given for one Monte Carlo run rather than the average of many computer runs.

4.2 Integration Techniques

The integration techniques for both filters were compared on the IBM 360 model 75 computer. For the integration scheme of the ESF, epoch state variables are used to integrate the variational equations whereas for the CSF the current state variables are used. Several runs of the integration techniques for both filters were made with various integration step sizes. The results were compared with an exact solution of the equations of motion. This exact solution was obtained for a disturbing acceleration of $(-\mu/20)(\underline{r}/r^3)$ so that the equation of motion reduced to the following two-body equation:

$$\ddot{\underline{r}} + \frac{21}{20}\,\mu\,\frac{\underline{r}}{r^3} = \underline{0} \qquad (4.2.1)$$

Solution to this equation was obtained analytically.

Both filters were run for various integration step sizes. The error in significant figures between the states for both integration schemes and the exact state of the spacecraft was noted after one revolution for different integration step sizes. Also noted was the computer run time for both filters. Figure 4.1 illustrates the time, in seconds, for the computer runs of the integration techniques used in both filters with different integration step sizes for one revolution. From this figure it is seen that on the IBM 360 computer the integration scheme used in the ESF takes longer to run than that of the CSF for the same step size. However, reference to Figure 4.2 shows that the integration technique used in the ESF is more accurate for the same step size than that of the CSF. After one revolution, a 5 significant figure error in the estimate of the state as compared with the 12 significant figures of the solution was the accuracy chosen for the simulation. For this accuracy the errors in the Encke integration scheme did not degrade the solution and rectification was not required.

An error of 5 significant figures implied a 1° integration step size for the CSF and a 5° step size for the ESF as seen in Figure 4.2. When the step size was eliminated as a parameter from Figures 4.1 and 4.2 a plot of computer run time verses the error in the integration technique for both filters was made (Figure 4.3). The significance of this last plot is that when simulated on the IBM 360-75 computer the integration techniques of ESF takes longer to run for the same integration stap size than its counterpart, however, it is more accurate. It was originally thought that

the integration scheme for the ESF would be less accurate and more time consuming than that of the CSF but this is not the case. In any event, both integration schemes could be used for either filter.

4.3 Measurement Incorporation for the Simulation

Actual measurement data, δq, is incorporated by the filter to improve the estimate of the state. This data consists of the true measurement value given by $\underline{b}^T \delta \underline{x}_{TRUE}$ plus an error in the measurement, α, and is given in terms of its constituents as

$$\delta q = \underline{b}^T \delta \underline{x}_{TRUE} + \alpha \qquad (4.3.1)$$

For the CSF, the estimated and true position are determined by Encke's Method where $\hat{\underline{r}} = \underline{r}_{OSC} + \hat{\underline{\delta}}$ and $\underline{r}_{TRUE} = \underline{r}_{OCS} + \underline{\delta}_{TRUE}$. The position error vector is given by $\hat{\underline{r}} - \underline{r}_{TRUE}$ or $\hat{\underline{\delta}} - \underline{\delta}_{TRUE}$. Similarly, the true velocity error $\hat{\underline{v}} - \underline{v}_{TRUE}$ is given by $\hat{\underline{\nu}} - \underline{\nu}_{TRUE}$ so that the state deviation vector for the CSF is determined from

$$\delta \hat{\underline{x}} = \underline{\omega} (\delta q - \underline{b}^T \delta \hat{\underline{x}}') \qquad (4.3.2)$$

or

$$\delta \hat{\underline{x}} = \omega \left(\delta q - \underline{b} \cdot \left\{ \begin{bmatrix} \hat{\underline{\delta}}' \\ \hat{\underline{\nu}}' \end{bmatrix} - \begin{bmatrix} \underline{\delta}_{TRUE} \\ \underline{\nu}_{TRUE} \end{bmatrix} \right\} \right) \qquad (4.3.3)$$

For the ESF, the epoch state deviation vector is given by

$$\delta \hat{\underline{x}}_o = \underline{\omega}_o \left(\delta q - \underline{b}_o^T \, \delta \hat{\underline{x}}_o' \right) \tag{4.3.4}$$

or

$$\delta \hat{\underline{x}}_o = \underline{\omega}_o \left(\delta q - \underline{b}_o \cdot \left\{ \begin{bmatrix} \hat{\underline{r}}_o' \\ \hat{\underline{v}}_o' \end{bmatrix} - \begin{bmatrix} \underline{r}_{o_{TRUE}} \\ \underline{v}_{o_{TRUE}} \end{bmatrix} \right\} \right) \tag{4.3.5}$$

4.4 Measurement Incorporation for Zero Disturbing Acceleration

In order to demonstrate that the errors in the simulation study of the ESF are indeed the errors introduced because of measurement incorporation, the ESF was tested for a 100 nautical mile circular earth orbit with zero disturbing acceleration. The results of this simulation are given in Figures 4.4 to 4.11. For this case, the ESF and the exact solution to the navigational problem, the CSF, are essentially the same. The statement $\dot{\Phi} = 0$ between measurements is not an approximation for the ESF with zero disturbing acceleration since the motion of the spacecraft in its orbit is two-body.

In Figure 4.4 the magnitude of the difference between the estimated position of the ESF and the CSF, $|\hat{\underline{r}}_{ESF} - \hat{\underline{r}}_{CSF}|$, is plotted for 80 measurement intervals. This graph shows that both filters are close for the case of zero disturbing acceleration except for a slight random error which grows with time. At the eightieth measurement this error is only 1.46 meters. Figure 4.5 illustrates the magnitude of the difference between the estimated velocity of the ESF and the CSF, $|\hat{\underline{v}}_{ESF} - \hat{\underline{v}}_{CSF}|$ for 80 measurement intervals.

Figure 4.6 illustrates the fact that for zero disturbing acceleration both filters are comparable except for a small error. This random error has a maximum value of 1.44 meters for the case of Figure 4.6 and value of .55 meters after the eightieth measurement. Similarly, reference to Figure 4.7, a plot of the difference between the actual velocity error of both the ESF and the CSF $|\hat{\underline{v}}_{ESF} - \underline{v}_{TRUE}| - |\hat{\underline{v}}_{CSF} - \underline{v}_{TRUE}|$ for 80 measurement intervals, shows that both filters are comparable except for a slight random error which is .00182 m/sec at maximum. This is also the value of error after the eightieth measurement. To find the error in the ESF that is in excess of the error in the CSF at the eightieth measurement, the difference between the actual position vectors of the ESF and the CSF, .55 meters, is compared with the expected rms position error of the exact or CSF solution, 523 meters as seen in Figure 4.8. The percentage of error in the position estimate using the epoch formulation of the navigational problem instead of the conventional formulation is approximately .11% for the case of zero disturbing acceleration. Likewise, the error between the actual velocity errors of the ESF and the CSF, .00182 m/sec, is compared with the expected velocity error of the CSF solution, .55 m/sec as seen in Figure 4.9. The result is that a .33% error exists in the velocity estimate of the epoch state filter in excess of the error in the velocity estimate of the CSF.

In Figures 4.10 and 4.11 the expected rms position error and the rms velocity error at the epoch are given for the case of a 100 nautical mile circular earth orbit with zero disturbing acceleration. The rms position error starts out at its initial value, 8.84×10^2 meters, and

then decreases steadily to a value of 445 meters after 80 measurement intervals. Similarly, the rms velocity error decreases from its initial value of 8.65 m/sec to .52 m sec with measurement incorporation. Reference to Figures 4.10 and 4.11 shows that the rms velocity error at the epoch decreases faster with measurement incroporation than the rms position error of the epoch. The fact that these last two graphs are for the epoch covariance matrix is made clear by noting that between measurement intervals, the rms position errors are constant. This is in agreement with the fact that $\dot{E}_o = 0$ between measurements.

Between measurements, the errors in the current estimate of the state of the spacecraft grow with time. These errors are then reduced with the incorporation of new data as is seen in Figures 4.8 and 4.9. However, the errors in the estimate of the epoch state can only be reduced. They do not grow with time but are constant within measurement intervals, and the incorporation of new information acts to only decrease the error in the estimate of the epoch state (Figures 4.10 and 4.11)

4.5 Disturbing Acceleration Due to J_2 Term

The ESF was tested for a 100 nautical mile circular earth orbit with a disturbing acceleration due to the J_2 term. The results of this test were compared with similar results for the CSF. For this case, the magnitude of the estimated position deviation vector, $|\delta \underline{\hat{r}}|$, is given for both filters after 80 measurement intervals in

Figure 4.12. Reference to this figure shows that the magnitude of the position deviation is approximately the same for the ESF and the CSF until the thirty-seventh measurement and after that differs only slightly. The same is true of the velocity deviation $|\delta\hat{\underline{v}}|$ (Figure 4.13). The differences exhibited in these figures may be attributed to the random type of measurement data for the simulation. When the filter has been operating for a while and reducing the error in the estimate with measurement incorporation, the estimate of the state is more accurate. Since the estimate of the state is more reliable, the required state deviation is lessened. This is seen in Figures 4.12 and 4.13.

As time increases, the difference between the position deviation vectors for the ESF and the CSF grows (Figure 4.14) and is due to the difference between the filter gains. However, this difference is small, having a maximum value of about 48 meters and a value of about 2 meters at the eightieth measurement interval. Similarly, the difference between the velocity deviation vectors of the ESF and the CSF (Figure 4.15) has a maximum value of about .06 m/sec and a value of about .003 m/sec after the eightieth measurement interval.

Figures 4.12 to 4.15 are plots of the state deviation vector and illustrate the effect of each measurement incorporation on the filter. These figures show what is to be added to the estimate of the state because of the incorporation of new data. The accumulated effect of measurement incorporation on the ESF as compared with the CSF is given in Figures 4.16 and 4.17 for the estimated position

and velocity respectively. Again, the irregularity in these plots is due to the random type of measurement data. The significance of Figure 4.16 is that the estimated position difference between the ESF and the CSF remains nearly zero for ten measurements and then grows to about 40 meters after the eightieth measurement. Similarly, the estimated velocity difference (Figure 4.17) remains nearly zero for ten measurements and grows to .065 m/sec after the eightieth measurement.

The errors given in Figures 4.16 and 4.17 are for the difference between the estimates of the ESF and the CSF with no indication of the true state. At times, the estimate of the state as given by the epoch formulation of the navigational problem may be more correctly aligned with the true state than that of the CSF. This is because the ESF does not have the extrapolation errors of the CSF due to the equation $E = \Phi E_o \Phi^T$. Also, the approximation that $\dot{E}_o = \dot{\Phi} = 0$ between measurements for the ESF is nearly exact.

A more significant test of the epoch formulation of the navigational problem is obtained by comparing the actual errors for the ESF and the CSF. The actual error in the ESF is the difference between the estimated state for this filter and the true state, $|\hat{\underline{r}}_{ESF} - \underline{r}_{TRUE}|$, and is given in Figure 4.18. This is easily obtained since for the simulation the true orbit of the spacecraft is known. The actual error in the position estimate of the ESF has a maximum value of about 1800 meters and reduces to 523 meters after eightly measurement incorporations. The same is true for the actual position error of the CSF, $|\hat{\underline{r}}_{CSF} - \underline{r}_{TRUE}|$, as seen in Figure 4.19. When the

results of Figure 4.19 are subtracted from those of Figure 4.18, the difference between the actual position error of the ESF and the CSF results (Figure 4.20). This last graph is probably the most significant of the simulation. What it implies is that both filters are comparable. When the actual error difference is positive, the ESF has more error in the estimate of the position vector and the CSF is the more correct. Conversely, when the actual error difference is negative the ESF is more correct. After the eightieth measurement, the actual error difference has a magnitude of 16 meters. As compared with the corresponding rms estimated position error which has a value of 523 meters as seen in Figure 4.21, the percentage of error introduced by using the epoch formulation of the navigational problem is approximately 3.1%. This is the percentage of error due to the ESF in excess of the error inherent in the conventional solution to the navigational problem and is small for all practical purposes. Figures 4.22 and 4.23 are graphs of the actual velocity error for the ESF and the CSF respectively. As seen in these figures the actual error in the estimation of the velocity has a maximum value of about 3 m/sec and is reduced to about .2 m/sec after the eightieth measurement. More significantly the difference between Figures 4.22 and 4.23 as given by Figure 4.24 shows again that both filters are comparable. The ESF is more accurate than the CSF and vice versa. Initially, the actual error difference in the velocity estimates for both filters has a value of zero. After the eightieth measurement this error increases somewhat randomly to a magnitude of .048 m/sec. When this last value is compared with the corresponding rms velocity error which the percentage of error using the ESF to estimate the

velocity vector is approximately 8.7%. Again for all practical purposes this error is small.

One of the reasons that the ESF is an accurate estimator of the current state is evidenced by the change in the epoch state from its true initial value for eighty measurement intervals. In Figure 4.26 the epoch position change, $|\hat{\underline{r}}_o(t) - \hat{\underline{r}}_o(t_o)|$, is seen to be 390 meters at maximum and 170 meters after the eightieth measurement. The maximum value, $|\hat{\underline{v}}_o(t) - \hat{\underline{v}}_o(t_o)|$, is 2.5 m/sec and the change after the eightieth measurement is .55 m/sec as seen in Figure 4.27. Both the true epoch position and velocity change are small enough to insure the accuracy of this formulation of the navigational problem.

To insure that the errors in the simulation were not due to the integration technique, the osculating orbit was rectified every 180° for the 100 nautical mile circular earth orbit with a disturbing acceleration due to the J_2 term. As illustrated in Figures 4.28 to 4.31, rectification produced no observable change in the estimate of the state since the errors in the integration technique are small enough so as not to degrade the solution.

Results of another Monte Carlo run for the 100 nautical mile circular earth orbit with a disturbing acceleration due to the J_2 term are given in Figures 4.32 to 4.47. These graphs especially Figures 4.44 and 4.47 confirm the result of the previous Monte Carlo run, in particular that the ESF and the CSF are comparable for this orbit and disturbing acceleration.

The error in the approximation that $\dot{\Phi} = 0$ between measurements for the ESF decreases with the disturbing acceleration which is a

function of $1/r^4$. Because of this, the accuracy of the filter increases as the spacecraft travels farther into space away from the disturbing influence of the earth. To illustrate this characteristic of the filter, the ESF was simulated for a circular earth orbit with a radius equal to twice the equatorial radius of the earth. The results of this simulation are given in Figures 4.48 to 4.53.

As seen in Figure 4.48, the difference between the position estimates of the ESF and the CSF is considerably less for this orbit than for the 100 nautical mile orbit. After the eightieth measurement, the position difference for this larger orbit has a value of 11 meters as compared with 40 meters for the 100 nautical mile orbit. The difference between the actual position error of both filters (Figure 4.49) varies randomly having a magnitude of only 4.2 meters after the eightieth measurement as compared with 16 meters for the 100 nautical mile orbit. The rms position error for the circular orbit of radius $r = 2r_E$ (Figure 4.50) has a value of 500 meters after the eightieth measurement. Comparing the difference between the actual position errors with this value results in a .84% error. This is the extra percentage of error introduced by using the ESF to extimate the state of the spacecraft. A .84% error is a considerable reduction when compared with the 3.4% error for the 100 nautical mile orbit. After the eightieth measurement, the difference between the velocity estimates of the ESF and CSF (Figure 4.51) has a value of .0048 m/sec for the orbit of radius $r = 2r_E$ as compared with .048 m/sec for the 100 nautical mile orbit. The difference between the actual velocity errors (Figure 4.52) varies randomly having a magnitude of

.0048 m/sec for the 100 mile orbit. When the difference between the actual velocity errors after the eightieth measurement is compared with the corresponding rms velocity error which is .2 m/sec as seen in Figure 4.53, the percentage of error introduced by using the ESF for the circular earth orbit of radius $r = 2r_E$ is 2.4%. This percentage of error is considerably less than the 8% error in the velocity estimate for the 100 nautical mile orbit. These results demonstrate that the accuracy of the ESF increases for higher orbits becuase the relative accuracy of the approximations increase.

4.6 Disturbing Acceleration Due to 10 J_2

It would be interesting to apply the ESF to the re-entry navigational problem. However, for this problem the spacecraft is subject to large values of disturbing acceleration. To see if the epoch formulation of the navigation problem works properly for disturbing accelerations due to terms larger than J_2, the ESF was simulated for a 100 nautical mile circular earth orbit with a disturbing acceleration due to 10 J_2. Results of this simulation are presented in Figures 4.54 to 4.69.

In the first of these graphs, Figure 4.54, the magnitude of the position deviation for the ESF and CSF is seen to be the same for both filters until the eighth measurement. Although the difference there if only slight, it becomes more pronounced as time goes on and the error in the approximation for the ESF increases. This same result is seen for the magnitude of the velocity deviation (Figure 4.55). The difference between the position deviation for the ESF and CSF is given in Figure 4.56. In this case, $|\delta\hat{r}_{ESF} - \delta\hat{r}_{CSF}|$ has a

maximum value of 490 meters as compared with 48 meters for the case of a disturbing acceleration due to J_2, and a value of 30 meters after the eightieth measurement as compared with 2 meters for the J_2 case. The velocity deviation (Figure 4.57) has a maximum value of .58 m/sec for the 10 J_2 case as compared with .06 m/sec for the J_2 case and a value of .50 m/sec after the eightieth measurement for the 10 J_2 case as compared with .003 m/sec for the J_2 case. This considerable difference is due to the error in the simplifications of the ESF which is large for the case of a greater disturbing acceleration. The difference becomes more pronounced as time goes on and the errors of the filter diverge.

Similarly, the difference between the position estimates for the ESF and the CSF (Figure 4.58) has a maximum value of 400 meters for the 10 J_2 case as compared with 43 meters for the J_2 case and a value after the eightieth measurement of 275 meters for the 10 J_2 case as compared with 40 meters for the J_2 case. The difference between the velocity estimates, $|\hat{\underline{v}}_{ESF} - \hat{\underline{v}}_{CSF}|$, (Figure 4.59) has a maximum value of .51 m/sec for the 10 J_2 case as compared with .065 m/sec for J_2 case and a value of .35 m/sec after the eightieth measurement as compared with .050 m/sec for the J_2 case.

The actual error for the ESF with a disturbing acceleration due to 10 J_2 as seen in Figure 4.60 has a maximum value of about 1770 meters and a value of 470 meters after the eightieth measurement. The actual error for the CSF (Figure 4.61) has a maximum value of about 1770 meters and a value of 650 meters after the eightieth measurement.

Again, the difference between the actual errors for both the ESF and the CSF varies randomly (Figure 4.62) implying that the ESF and the CSF are comparable. That is, the ESF is more accurate in estimating the spacecraft's position vector just as often as the CSF. The difference here is that after the eightieth measurement, the difference between the actual position errors has a value of about 180 meters. When this is compared with 500 meters for the rms position error (Figure 4.63), a 36% error is determined. This is considerably larger than the 3.2% error for the case of a disturbing acceleration due to the simple J_2 term. However, not only is the ESF working for the case of a larger disturbing acceleration but it is comparable to the CSF in estimating the position of the spacecraft.

The same is true for the percentage of error in the velocity estimate for the ESF. Although there is a 60% error in the velocity estimate of the ESF, the ESF and the CSF are comparable as seen in Figure 4.66.

One of the reasons that the ESF approximately works for the case of a disturbing acceleration due to 10 J_2 is evidenced by reference to Figures 4.68 and 4.69. The magnitude of the difference between the estimated and true epoch position vectors $|\hat{\underline{r}}_o(t) - \underline{r}_o(t_o)|$ has a maximum value of 400 meters and a value of 250 meters after the eightieth measurement. Reference to Figure 4.69 shows that the magnitude of the difference between the estimated and true epoch velocity vectors has a maximum value of 2.5 m/sec and a value of .55 m/sec after the eightieth measurement.

The ESF was simulated for the case of a 100 nautical mile orbit with a disturbing acceleration due to 100 J_2. However, for this case, the ESF worked properly for a little over a fourth of a revolution. After that the errors in the approximation that $\dot{\Phi} = 0$ for the ESF significantly degraded the solution and the ESF did not work.

Included in this thesis are the computer programs written in the MAC language for the simulation of the ESF and the CSF.

4.7 Computation Time on AGC

The relative execution time for the various operations differs from computer to computer. The run time solutions given previously for the integration techniques of both filters on the IBM 360 computer are not necessarily the same for the Apollo computer. To compare the computation time for the epoch and the conventional state filters on a spacecraft computer such as the Apollo Guidance Computer, (AGC) the explicit computational algorithms for both solutions to the navigational problem are given here. However, only an approximation to the actual computation time for each of these solutions is determined according to the total number of various arithmetic and branching operations. Using the information presented here, a comparison of both filters for computers other than the AGC may be easily made.

The equations used in the computer subroutines for the ESF and the CSF were described in previous sections of this thesis. In the following paragraphs, the sequence of computations for both solutions of one navigation cycle are given precisely:

EPOCH STATE FILTER

Input

$\underline{b}$: measurement vector

$\delta\tilde{q}$: measurement data

τ: initial epoch time

$\underline{r}_o$: initial epoch position

$\underline{v}_o$: initial epoch velocity

θ: initial true anomaly difference

E_o: initial epoch covariance matrix

μ: earth gravitational constant

$\overline{\alpha^2}$: measurement variance

J_2: disturbing acceleration term

Initialization of Loop

$$\underline{i}_{r_o} = \frac{\underline{r}_o}{|\underline{r}_o|}$$

$$\underline{i}_r = \underline{i}_{r_o}$$

$$\sqrt{\mu} = \text{SQRT}(\mu)$$

$$i = 1$$

Iterative Loop

1) $\underline{i}_\theta = \underline{i}_z \times \underline{i}_r$

2) $\underline{i}_{\theta_o} = \underline{i}_z \times \underline{i}_{r_o}$

3) $\Delta\theta = \frac{1}{r}(\underline{i}_\theta \cdot \delta\hat{\underline{r}}) - \frac{1}{r_o}(\underline{i}_{\theta_o} \cdot \delta\hat{\underline{r}}_o)$

4) $\theta = \theta + \Delta\theta$

5) $\underline{r}_o = \underline{r}_o + \delta\underline{r}_o$

6) Set $\ell = 1$

7) Set k = 0

8) Call DIFEQ to integrate $\dot{\theta}$, $\dot{\underline{r}}_o$, $\dot{\underline{v}}_o$ with the following iterative loop

8a) Cos θ = cos (θ)

8b) Sin θ = sin (θ)

8c) $r_o = |\underline{r}_o|$

8d) $v_o = |\underline{v}_o|$

8e) $\sigma_o = \frac{1}{\sqrt{\mu}}\,\underline{r}_o \cdot \underline{v}_o$

8f) $\alpha = \frac{2}{r_o} - \frac{v_o^2}{\mu}$

8g) $p = 2r_o - \alpha r_o^2 - \sigma_o^2$

8h) $h = \sqrt{up}$

8i) $r = \dfrac{p}{1 + (\frac{p}{r_o} - 1)\cos\theta - \frac{h\sigma_o}{\sqrt{\mu}\,r_o}\sin\theta}$

8j) $U_1 = \frac{r}{\sqrt{p}}\sin\theta - \frac{r\sigma_o}{p}(1 - \cos\theta)$

8k) $U_2 = \frac{r\,r_o}{p}(1 - \cos\theta)$

8ℓ) $F = 1 - \frac{U_2}{r_o}$

8m) $F_t = \frac{-\sqrt{\mu}}{r\, r_o} U_1$

8n) $G = \frac{1}{\sqrt{\mu}} (r_o U_1 + \sigma_o U_2)$

8o) $G_t = 1 - \frac{U_2}{r}$

8p) $\underline{r} = F \underline{r}_o + G \underline{v}_o$

8q) $r = |\underline{r}|$

8r) $\underline{i}_r = \frac{\underline{r}}{r}$

8s) $\cos \phi = \underline{i}_r \cdot \underline{i}_z$

8t) $\underline{v} = F_t \underline{r}_o + G_t \underline{v}_o$

8u) $\underline{h} = \underline{r} \times \underline{v}$

8v) $\underline{a}_d = -1.5 \frac{\mu}{r^2} J_2 \left(\frac{r_E}{r}\right)^2 \left[\{1 - 5(\cos \phi)^2\} \underline{i}_r + 2 \cos \phi \, \underline{i}_z \right]$

8w) $\frac{d\theta}{dt} = \frac{h}{r^2} + \frac{1}{h^2} \left[\sin \theta \, \underline{h} \times \underline{r} + h (1 - \cos \theta) \underline{r} \right] \cdot \underline{a}_d$

8x) $\frac{d \underline{r}_o}{dt} = \frac{1}{\mu} U_2 \left[(\underline{r}_o - \underline{r}) \underline{v}^T + \underline{v} \, \underline{r}^T \right] \underline{a}_d - G \underline{a}_d$

8y) $\frac{d \underline{v}_o}{dt} = \left[\frac{\underline{r}}{\mu} (\underline{v}_o - \underline{v}) \right] (\underline{v}_o - \underline{v})^T \underline{a}_d + F \underline{a}_d$

8z) Set $k = k + 1$

8Ω) If $k < 4$, Go to 8a

9) Set $\ell = \ell + 1$

10) If $\ell < 3$, Go to 8a

11) $1/\alpha = \frac{1}{\alpha}$

12) $r_o = |\underline{r}_o|$

**13) Solve Kepler's equation for x

14) $U_3 = (1/\alpha)\,[x - U_1]$

15) $\sqrt{\mu}\,(t - \tau) = r_o\,U_1 + \sigma_o\,U_2 + U_3$

16) $U_4 = (1/\alpha)\,[\frac{x^2}{2} - U_2]$

17) $U_5 = (1/\alpha)\,[\frac{x^3}{6} - U_3]$

18) $c = \frac{1}{\sqrt{\mu}}\,[3\,U_5 - x\,U_4 - U_2\sqrt{u}\,(t-\tau)]$

19) $R(t) = \frac{1}{\mu}\,\{[U_2\,(\underline{r} - \underline{r}_o) + c\,\underline{v}]\;\underline{v}_o^{\,T} - [U_2\,(\underline{v} - \underline{v}_o)]\,\underline{r}_o^{\,T}\} + G\,I$

20) $V(t) = \frac{1}{r^3}\,[(U_2\,\underline{r})\,\underline{r}_o^{\,T} - (c\,\underline{r})\,\underline{v}_o^{\,T}] + [\frac{r_o}{\mu}\,(\underline{v} - \underline{v}_o)]\,(\underline{v} - \underline{v}_o)^T + G_t\,I$

21) $V^*(t_o) = \frac{1}{r_o^3}\,[(U_2\,\underline{r}_o)\,\underline{r}^T + (c\,\underline{r}_o)\,\underline{v}^T] + [\frac{r}{\mu}\,(\underline{v}_o - \underline{v})]\,(\underline{v}_o - \underline{v})^T + F\,I$

22) $R^{T-1} = (R^T)^{-1}$

23) $C(t) = R^{T-1}\,V^T$

24) $\frac{\partial\,\underline{r}}{\partial\,\underline{r}_o} = V^*(t_o)^T$

25) $\frac{\partial\,\underline{v}}{\partial\,\underline{r}_o} = C(t)\;V^*(t_o)^T - R(t)^{T-1}$

26) $\Phi(t,\,t_o) = \begin{pmatrix} V^*(t_o)^T & R(t) \\ C(t)\;V^*(t_o)^T - R(t)^{T-1} & V(t) \end{pmatrix}$

27) $\underline{b}_o = \Phi^T \underline{b}$

28) $a_o = \underline{b}_o \cdot (E_o' \underline{b}_o) + \overline{\alpha^2}$

29) $\underline{\omega}_o = \frac{1}{a_o} E_o' \underline{b}_o$

30) $E_o = E_o' - \underline{\omega}_o \underline{b}_o^T E_o'$

31) $\delta \hat{\underline{x}}_o = \underline{\omega}_o \delta q$

32) Divide $\delta \hat{x}_o$ into $\delta \hat{\underline{r}}_o$ and $\delta \hat{\underline{v}}_o$ components

ie, $\delta \hat{r}_o = \delta \hat{x}_o \ldots, \quad \delta \hat{v}_o = \delta \hat{x}_3 \ldots$

33) $\delta \hat{\underline{x}} = \Phi \delta \hat{\underline{x}}_o$

34) Divide $\delta \hat{\underline{x}}$ into $\underline{\delta} \hat{r}$ and $\delta \underline{\hat{v}}$ components

35) Set i = i + 1

36) Go to 1

CURRENT STATE FILTER

Input

$\underline{b}$:	measurement vector
$\delta \tilde{q}$:	measurement data
τ:	initial time
$\underline{r}_o$:	initial position
$\underline{v}_o$:	initial velocity
$E(t_o)$:	initial covariance matrix

μ: earth gravitational constant

$\overline{\alpha^2}$: measurement variance

J_2: disturbing acceleration term

Initialization of Loop

$$r_o = |\underline{r}_o|$$

$$v_o = |\underline{v}_o|$$

$$\alpha = \frac{2}{r_o} - \frac{v_o^2}{\mu}$$

$$1/\alpha = \frac{1}{\alpha}$$

$$\sigma_o = \frac{1}{\sqrt{\mu}} (\underline{r}_o \cdot \underline{v}_o)$$

$$\sqrt{\mu} = \text{SQRT}(\mu)$$

Set upper left-hand 3 x 3 corner and lower right-hand 3 x 3 corner elements of F equal to zero

Set i = 1

Iterative Loop:

1) Set off diagonal terms of Φ equal to zero

2) Set diagonal terms of Φ equal to one

3) $\underline{\delta} = \underline{\delta} + \delta\underline{r}$

4) $\underline{\nu} = \underline{\nu} + \delta\underline{v}$

5) set $\ell = 1$

6) Set k = 0

7) Call DIFEQ to integrate $\underline{\dot{\delta}}$, $\underline{\dot{\nu}}$ with the following iterative loop

7a) Determine x by solving Kepler's equation

7b) $U_2(x; \alpha) = (1/\alpha)\left[1 - U_0(x; \alpha)\right]$

7c) $r = r_o U_o + \sigma_o U_1 + U_2$

7d) $F = 1 - \dfrac{U_2}{r_o}$

7e) $G = \dfrac{1}{\sqrt{\mu}}\left(r_o U_1 + \sigma_o U_2\right)$

7f) $F_t = \dfrac{-\sqrt{\mu}}{r r_o} U_1$

7g) $G_t = 1 - \dfrac{U_2}{r}$

7h) $\underline{r}_{osc} = F \underline{r}_o + G \underline{v}_o$

7i) $\underline{v}_{osc} = F_t \underline{r}_o + G_t \underline{v}_o$

7j) $r_{osc} = |\underline{r}_{osc}|$

7k) $\underline{r} = \underline{r}_{osc} + \underline{\delta}$

7l) $\underline{r} = |\underline{r}|$

7m) $\underline{i}_r = \dfrac{\underline{r}}{r}$

7n) $\cos \phi = \underline{i}_r \cdot \underline{i}_z$

7o) $q = \dfrac{(\underline{\delta} - 2\underline{r}) \cdot \underline{\delta}}{r^2}$

7p) $$f(q) = q\frac{3 + 3Q + q^2}{1 + (1 + q)^{3/2}}$$

7q) $$\underline{a}_d = -1.5\frac{\mu}{r^2} J_2 \left(\frac{r_E}{r}\right)^2 \left[\{1 - 5(\cos\phi)^2\}\underline{i}_r + 2\cos\phi\,\underline{i}_z\right]$$

7r) $$G(t) = \frac{\mu}{r^5}\left[(3\,\underline{r})\underline{r}^T - r^2 I\right]$$

7s) Set lower left-hand 3 x 3 corner elements of F equal to their respective elements of G(t) i.e. $F_{18} = G_o$, $F_{19} = G_1 \ldots$

7t) $$\frac{d\underline{\delta}}{dt} = \underline{\nu}$$

7u) $$\frac{d\underline{\nu}}{dt} = \frac{-\mu}{r_{osc}^3}(f(q)\,\underline{r} + \underline{\delta}) + \underline{a}_d$$

7v) $$\frac{d\Phi}{dt} = F\,\Phi$$

7w) Set k = k + 1

7x) If k < 4, Go to 7a

8) Set $\ell = \ell + 1$

9) If $\ell < 11$, Go to 7a

10) $$E = \Phi E' \Phi^T$$

11) $$a = \underline{b} \cdot (E'\,\underline{b}) + \overline{\alpha^2}$$

12) $$\underline{\omega} = \frac{1}{a} E'\,\underline{b}$$

13) $$E = E' - \underline{\omega}\,\underline{b}^T E'$$

14) $$\delta\underline{\hat{x}} = \underline{\omega}\,\delta q$$

15) Divide $\delta\underline{\hat{x}}$ into $\delta\underline{\hat{r}}$ and $\delta\underline{\hat{v}}$ components i.e.,

$\delta\hat{r}_o = \delta\hat{x}_o \ldots$, $\delta\hat{v}_o = \delta\hat{x}_3 \ldots$

16) Set i = i + 1

17) Go to 1

Iterative Solution of Kepler's Equation for x

KE1 Set j = 0

KE2 $$x_o = \frac{\sqrt{\mu}(t-\tau)}{r_o}\left\{1 - \frac{\sigma_o}{2r_o^2}\sqrt{\mu}(t-\tau) + \frac{1}{6r_o^4}\left[3\sigma_o^2 - r_o(1-\alpha r_o)\right]\right.$$

$$\left.\left[\sqrt{\mu}(t-\tau)\right]^2 + \ldots\right\}$$

KE3 $$U_o(x_n;\alpha) = \left[1 - \frac{\alpha x_n^2}{2!} + \frac{(\alpha x_n^2)^2}{4!} - \ldots\right]$$

KE4 $$U_1(x_n;\alpha) = x_n\left[1 - \frac{\alpha x_n^2}{3!} + \frac{(\alpha x_n^2)^2}{5!} - \ldots\right]$$

KE5 $$U_3(x_n;\alpha) = (1/\alpha)\left[x_n - U_1(x_n;\alpha)\right]$$

KE6 $$\sqrt{\mu}(t_n - \tau) = r_o U_1(x_n;\alpha) + \sigma_o U_2(x_n;\alpha) + U_3(x_n;\alpha)$$

KE7 $$r_n = r_o U_o(x_n;\alpha) + \sigma_o U_1(x_n;\alpha) + U_2(x_n;\alpha)$$

KE8 $$x_{n+1} = x_n - \frac{\sqrt{\mu}\, t_n - \sqrt{\mu}\, t}{r_n}$$

KE9 $$x_n = x_{n+1}$$

KE10 $$j = j + 1$$

KE11 If $j < 4$, Go to KE3

These equations are given in Reference 3

DIFEQ (Common to both techniques)

Given the differential equation:

$$dy/dt = f(t, y)$$

where y is the dependent variable, t is the independent variable and Δt is the increment, the value of y at $t = t + \Delta t$ can be obtained from the following process:

DQ1 Set $y = y_o$ and $t = t_o$ (i.e., their initial values)

DQ2 Set $\Delta t = h$

DQ3 Evaluate $dy/dt = f(t_o, y_o)$

DQ4 Evaluate $k_1 = hf(t_o, y_o)$

DQ5 Set $t = t_o + (h/2)$ and $y = y_o + (k_1/2)$

DQ6 Evaluate $dy/dt = f(t_o + (h/2), y_o + (k_1/2))$

DQ7 Evaluate $k_2 = hf(t_o + (h/2), y_o + (k_1/2))$

DQ8 Set $y = y_o + (k_2/2)$

DQ9 Evaluate $dy/dt = f(x_o + (h/2), t_o + (k_2/2))$

DQ10 Evaluate $k_3 = hf(t_o + (h/2), y_o + (k_2/2))$

DQ11 Set $t = t_o + h$ and $y = y_o + k_3$

DQ12 Evaluate $dy/dt = f(t_o + h, y_o + k_3)$

DQ13 Evaluate $k_4 = hf(t_o + h, y_o + k_3)$

DQ14 Evaluate $k = (k_1 + 2k_2 + 2k_3 + k_4)/6$

DQ15 Set $y = y_o + k$

y at this point contains the desired result

These equations are given in Reference 9.

Since the time consumed for the input and initialization of the loop is a small part of the total computation time for both algorithms, these parts are ignored in the following calculations. Table I contains a list of some operations common to both filter algorithms and the number of functions involved in these operations. The number of various arithmetic and branching operations required by each line of the iteration loops for the ESF and the CSF algorithms are given in Tables II and III. The parameter "i" represents the number of iterations performed over the whole iterative loop. Parameters "ℓ" and "k" represent iterations performed over the extrapolation of the state. The maximum value of "ℓ" is 2 for the ESF and 10 for the CSF and the maximum "value of "k" is 4 for both filters. "j" represents iterations performed over the solution to Kepler's equation and has a maximum value of 4 for both filters.

It is pointed out that in formulating the algorithms, little attempt has been made to organize the computation so as to minimize the overall execution time on the AGC. Tables II and III and subsequent tables derived from these, represent a reasonable count of the number of various operations required to execute the algorithms for both filters. In Tables II and III computation has been divided into three sections: (A) extrapolation of the state, (B) extrapolation of the covariance matrix, and (C) update of the estimates. The computation time for the first and third of these sections should be

approximately the same for both filters. However, if the method of extrapolating the state for the ESF is too time consuming, then this method can be replaced by that used in the CSF with a slight modification. The big savings for the ESF comes in the extrapolation of the covariance matrix. Isolation of the computation time for this section emphasizes this savings.

The total number of various arithmetic and branching operations required for each of the algorithmic divisions described previously i.e., (A) extrapolation of the state, (B) extrapolation of the covariance matrix, and (C) update of the estimate, are presented in Tables IV and V for the ESF and the CSF respectively, after one complete execution.

The relative time required for a single execution of each of these operations on the AGC execution of each of these operations on the AGC is summarixed in Table VI. The information is adopted from the Users Guide to the Block II AGC/LGC Interpreter, Reference 11.

The total number of "add times" required by one complete execution of the ESF and CSF algorithms is given in Table VII in "i" iterations. Finally a rough estimate of the overall computation time for the AGC required by the ESF and CSF algorithms is given in Table VIII for the algorithmic divisions previously described and their total. These tables give the results of converting the information for "our case" in Tables IV and V into actual computation time in seconds. The results given in Table VIII were expected,

and in particular those of Section B. Even if the integration scheme for the ESF, Section A, were more time consuming than that of the CSF, the latter method could be substituted in its place. However, there is a considerable savings in the execution time for the ESF because of the assumption that $\dot{\Phi} = 0$ between measurements. This savings is evidenced by Section B of Table VIII. The assumption allows for Φ to be calculated analytically rather than by integrating a differential equation. When Φ is calculated by integrating a differential equation using the MAC subroutine DIFEQ[9], the integration is carried out in four steps to yield Φ for 1° increments. All of the equations used in determining the differential equation for $\dot{\Phi}$ are sequenced on four times to determine Φ for the 1° increment. To calculate Φ at 10° measurement intervals, the equations for $\dot{\Phi}$ are cycled forty times. Using the assumption $\dot{E} = 0$ between measurements for the ESF, Φ is calculated only once for the 10° measurement intervals and need not be computed along the path.

Operation	Add	Multiply	Divide	SQRT	Initialize
(3x3) Matrix Transpose*					6
(3x3) Matrix Inverse	14	27	9		6
(3x3) (3x3) Matrix Matrix Multiplication	18	27			
(3x3) (3x1) Matrix Vector Multiplication	6	9			
(3x1) (1x3) Vector Vector Multiplication		9			
(6x6) (6x6) Matrix Matrix Multiplication	180	216			
(6x6) (6x1) Matrix Vector Multiplication	30	36			
(6x1) (1x6) Vector Matrix Multiplication		36			
(3x1) Vector Cross Product	3	6			
(3x1) Vector Dot Product	2	3			
(6x1) Vector Dot Product	5	6			
Magnitude (3x3) Vector	2	3		1	

*The transpose of a (3x3) matrix is considered as 6 initializations since only the off-diagonal elements change locations

TABLE I

Functions Used in Some Operations Common to Both Filter Algorithms

TABLE II (ESF)

Line	Section	Add Subtract	Multiply	Divide	SQRT	Trans. Function	If (Branch)	Initialize
1	C	3i	6i					
2	C	3i	6i					
3	C	5i	6i	2i				
4	C	1i						
5	C	3i						
6	A							1i
7	A							1i
*8	A	718i	1248i	220i	40i	16i	8i	18i
9	A	1ℓi						
10	A						1ℓi	
11	B			1i				
12	B	2i	3i		1i			
**13	B	33i	30i	5i		9i	4i	5i
14	B	1i	1i					

TABLE II (Contd.)

Line	Section	Add Subtract	Multiply	Divide	SQRT	Trans. Function	If (Branch)	Initialize
15	B	2i	2i					
16	B	1i	2i	1i				
17	B	1i	3i	1i				
18	B	2i	4i					
19	B	27i	45i					
20	B	33i	56i	2i				
21	B	33i	56i	2i				
22	B	14i	27i	9i				12i
23	B	18i	27i					6i
24	B							6i
25	B	27i	27i					
26	B							36i
27	B	30i	36i					30i
28	B	36i	42i					
29	B	30i	36i	6i				

TABLE II (Contd.)

Line	Section	Add Subtract	Multiply	Divide	SQRT	Trans. Function	If (Branch)	Initialize
30	B	66i	72i					
31	C		6i					
32	C							6i
33	C	30i	36i					
34	C							6i
35	C	1i						
36	C						1i	
*DIFEQ for $\dot{\underline{r}}_o$, $\dot{\underline{v}}_o$ and $\dot{\theta}$								
DQ1	A							8ℓi
DQ2	A							1ℓi
DQ3	A	77ℓi	149ℓi	22ℓi	5ℓi	2ℓi	1ℓi	
DQ4	A		7ℓi					
DQ5	A	8ℓi		8ℓi				
DQ6	A	77ℓi	149ℓi	22ℓi	5ℓi	2ℓi	1ℓi	

TABLE II (Contd.)

Line	Section	Add Subtract	Multiply	Divide	SQRT	Trans. Function	If (Branch)	Initialize
DQ7	A		7ℓi					
DQ8	A	7ℓi		7ℓi				
DQ9	A	77ℓi	149ℓi	22ℓi	5ℓi	2ℓi	1ℓi	
DQ10	A		7ℓi					
DQ11	A	8ℓi						
DQ12	A	77ℓi	149ℓi	22ℓi	5ℓi	2ℓi	1ℓi	
DQ13	A		7ℓi					
DQ14	A	21ℓ		7ℓi				
DQ15	A	7ℓi						
DIFEQ loop used to evaluate DQ3, DQ6, DQ9, and DQ12								
8a	A					1kℓi		
b	A					1kℓi		
c	A	2kℓi	3kℓi		1kℓi			
d	A	2kℓi	3kℓi		1kℓi			
e	A	2kℓi	3kℓi	1kℓi				
f	A	1kℓi	1kℓi	2kℓi				

TABLE II (contd.)

Line	Section	Add Subtract	Multiply	Divide	SQRT	Trans Function	If (Branch)	Initialize
g	A	2kℓi	4kℓi					
h	A		1kℓi		1kℓi			
i	A	3kℓi	4kℓi	3kℓi				
j	A	2kℓi	3kℓi	2kℓi	1kℓi			
k	A	1kℓi	2kℓi	1kℓi				
l	A	1kℓi		1kℓi				
m	A		3kℓi	1kℓi				
n	A	1kℓi	2kℓi	1kℓi				
o	A	1kℓi		1kℓi				
p	A	3kℓi	6kℓi					
q	A	2kℓi	3kℓi		1kℓi			
r	A			3kℓi				
s	A	2kℓi	3kℓi					
t	A	3kℓi	6kℓi					
u	A	3kℓi	6kℓi					
v	A	4kℓi	18kℓi	2kℓi				

TABLE II completed

Line	Section	Add Subtract	Multiply	Divide	SQRT	Trans. Function	If (Branch)	Initialize
w	A	10kℓi	18kℓi	2kℓi				
x	A	16kℓi	36kℓi	1kℓi				
y	A	15kℓi	24kℓi	1kℓi				
z	A	1kℓi						
Ω	A						1kℓi	
**Solution to Kepler's equation used to determine 13								
KE1	B							1i
KE2	B	1i	2i	1i		1i		
KE3	B					1ji		
KE4	B					1ji		
KE5	B	1ji	1ji					
KE6	B	2ji	2ji					
KE7	B	2ji	2ji					
KE8	B	2ji	2ji	1ji				
KE9	B							1ji
KE10	B	1ji						
KE11	B						1ji	

TABLE III (CSF)

Line	Section	Add Subtract	Multiply	Divide	SQRT	Trans. Function	If (Branch)	Initialize
1	C							30i
2	C							6i
3	C	3i						
4	C	3i						
5	A							1ℓi
6	A							1ℓi
*7	A	3,400i	4,160i	860i	120i		200i	400i
7	B	10,080i	11,480i	1120i				720i
8	B	1ℓi						
9	B						1ℓi	
10	B	360i	432i					36i
11	B	36i	42i					
12	B	30i	36i	6i				
13	B	66i	72i					
14	C		6i					
15	C							6i

TABLE III (CSF) (Contd.)

Line	Section	Add Subtract	Multiply	Divide	SQRT	Trans. Function	If (Branch)	Initialize
16	C	1i						
17	C						1i	
*DIFEQ for $\underline{\dot{\delta}}$, $\underline{\dot{\nu}}$ and $\dot{\Phi}$								
DQ1	A							7ℓi
	B							36ℓi
DQ2	A							1ℓi
DQ3	A	74ℓi	98ℓi	17ℓi	3ℓi		5ℓi	8ℓi
	B	189ℓi	251ℓi	1ℓi				9ℓi
DQ4	A		6ℓi					
	B		36ℓi					
DQ5	A	7ℓi		6ℓi				
	B	36ℓi		36ℓi				
DQ6	A	74ℓi	98ℓi	17ℓi	3ℓi		5ℓi	8ℓi
	B	189ℓi	251ℓi	1ℓi				9ℓi

TABLE III (Contd.)

Line	Section	Add Subtract	Multiply	Divide	SQRT	Trans. Function	If (Branch)	Initialize
DQ7	A		6ℓi					
	B		36ℓi					
DQ8	A	6ℓi		6ℓi				
	B	36ℓi		36ℓi				
DQ9	A	74ℓi	98ℓi	17ℓi	3ℓi		5ℓi	8ℓi
	B	189ℓi	251ℓi	1ℓi				9ℓi
DQ10	A		6ℓi					
	B		36ℓi					
DQ11	A	7ℓi						
	B	36ℓi						
DQ12	A	74ℓi	98ℓi	17ℓi	3ℓi		5ℓi	8ℓi
	B	189ℓi	251ℓi	1ℓi				9ℓi
DQ13	A		6ℓi					
	B		36ℓi					
DQ14	A	18ℓi		6ℓi				
	B	108ℓi		36ℓi				

TABLE III (Contd.)

Line	Section	Add Subtract	Multiply	Divide	SQRT	Trans. Function	If (Branch)	Initialize
DQ15	A	6ℓi						
	B	36ℓi						
DIFEQ loop used to evaluate DQ3, DQ6, DQ9, DQ12								
**7a	A	33kℓi	30kℓi	5kℓi		9kℓi	4kℓi	5kℓi
b	A	1kℓi	1kℓi					
c	A	2kℓi	2kℓi					
d	A	1kℓi		1kℓi				
e	A	1kℓi	2kℓi	1kℓi				
f	A		3kℓi	1kℓi				
g	A	1kℓi		1kℓi				
h	A	3kℓi	6kℓi					
i	A	3kℓi	6kℓi					
j	A	2kℓi	3kℓi		1kℓi			
k	A	3kℓi						
l	A	2kℓi	3kℓi		1kℓi			

TABLE III (Contd.)

Line	Section	Add Subtract	Multiply	Divide	SQRT	Trans. Function	If (Branch)	Initialize
m	A			3kℓi				
n	A	2kℓi	3kℓi					
o	A	5kℓi	7kℓi	1kℓi				
p	A	4kℓi	5kℓi	1kℓi	1kℓi			
q	A	4kℓi	18kℓi	2kℓi				
r	B	9kℓi	35kℓi	1kℓi				
s	B							9kℓi
t	A							3kℓi
u	A	6kℓi	9kℓi	1kℓi				
v	B	180kℓi	216kℓi					
w	A	1kℓi						
x	A						1kℓi	
**Solution to Kepler's equation used to determine 7a								
KE1	A							1kℓi
KE2	A	1kℓi	2kℓi	1kℓi		1kℓi		

TABLE III(Contd.)

Line	Section	Add Subtract	Multiply	Divide	SQRT	Trans. Function	If (Branch)	Initialize
KE3	A					1jkℓi		
KE4	A					1jkℓi		
KE5	A	1jkℓi	1jkℓi					
KE6	A	2jkℓi	2jkℓi					
KE7	A	2jkℓi	2jkℓi					
KE8	A	2jkℓi	2jkℓi	1jkℓi				
KE9	A							1jkℓi
KE10	A	1jkℓi						
KE11	A						1jkℓi	

Section of ESF	Add Subtract	Multiply	Divide	SQRT	Trans. Function	If (Branch)	Initialize
A	720i	1248i	220i	40i	16i	10i	20i
B	356i	469i	27i	1i	9i	4i	95i
C	46i	60i	2i			1i	12i

TABLE IV

Total Number of Operations Required by One Complete Execution of the ESF Algorithm in "i" Iterations

Section of CSF	Add Subtract	Multiply	Divide	SQRT	Trans. Function	If (Branch)	Initialize
A	3400i	4160i	860i	120i		200i	420i
B	10, 582i	12, 062i	1, 126i			10i	756i
C	7i	6i				1i	42i

TABLE V

Total Number of Operations Required by One Complete Execution of the CSF Algorithm in "i" Iterations

Operation	Relative Execution Time*
Addition	1
Subtraction	1
Multiplication	2
Division	4
Square Root	3
Transcendental Function	9
If (Branch)	1
Initialize	2

*Approximate "add - times" where one add-time = .66 milliseconds

TABLE VI

Relative Execution Time of Operations on the AGC

	A	B	C	Total
ESF	4,410i	1,680i	199i	6,289i
CSF	19,800i	40,812i	113i	60,725i

TABLE VII

Total Number of "Add Times" Required by One Complete Execution of the ESF and CSF Algorithms in "i" Iterations

	A(sec)	B(sec)	C(sec)	Total
ESF	2.91i	1.11i	.13i	4.15i
CSF	13.1i	26.9i	.1i	40.1i

TABLE VIII

Estimate of Total Computation Time for the AGC Required by One Complete Execution of the ESF and CSF Algorithms in "i" Iterations

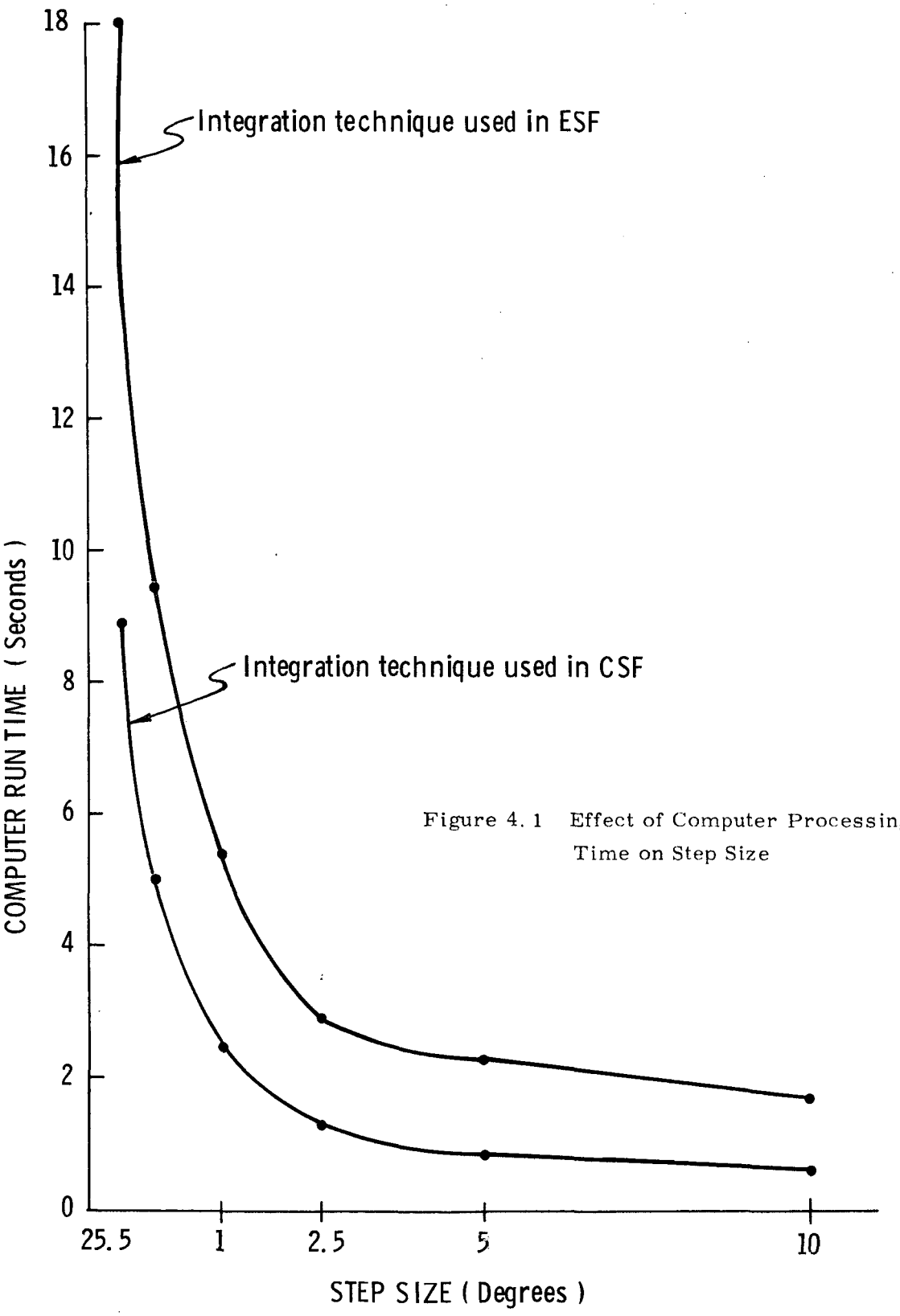

Figure 4.1 Effect of Computer Processing Time on Step Size

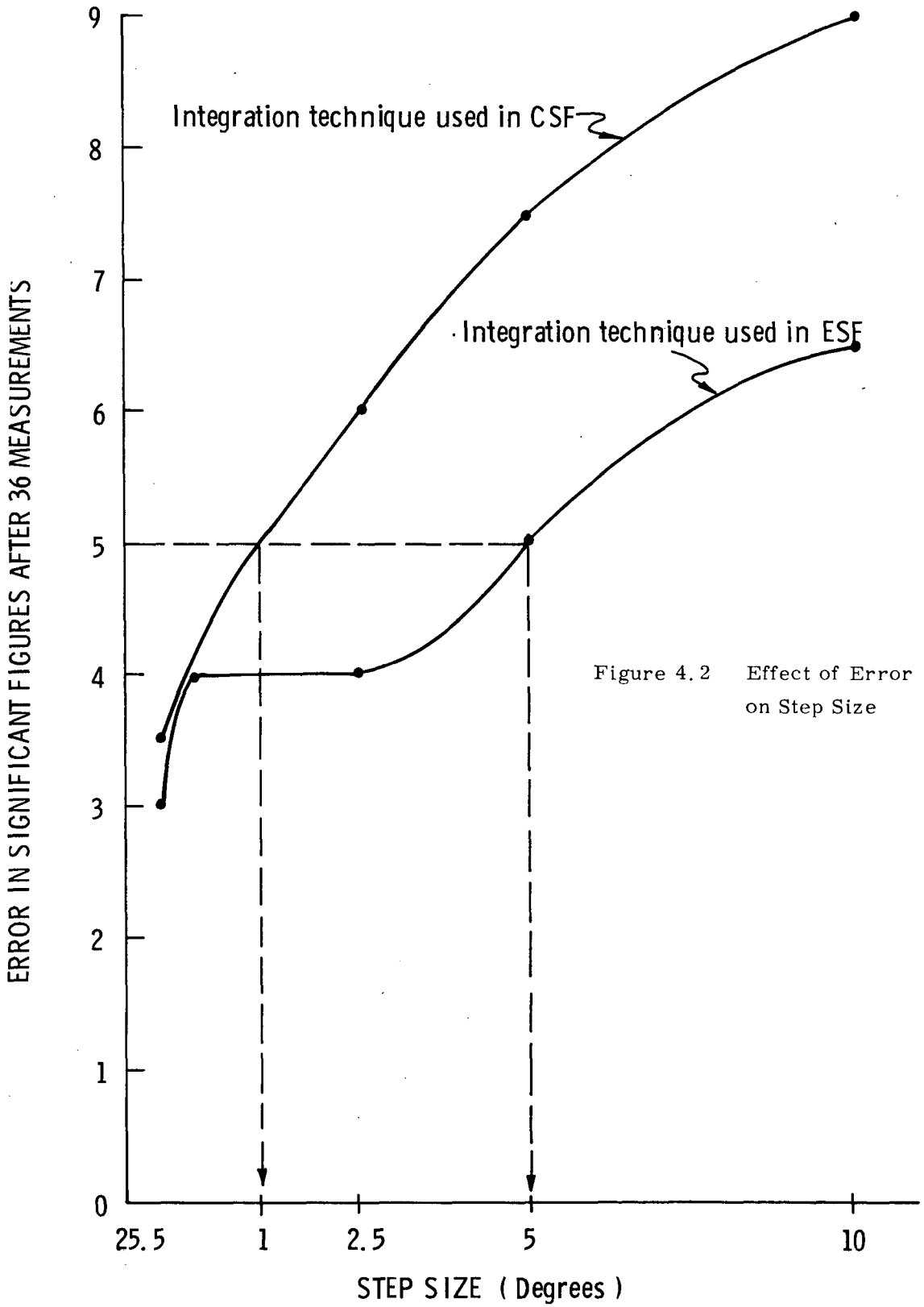

Figure 4.2 Effect of Error on Step Size

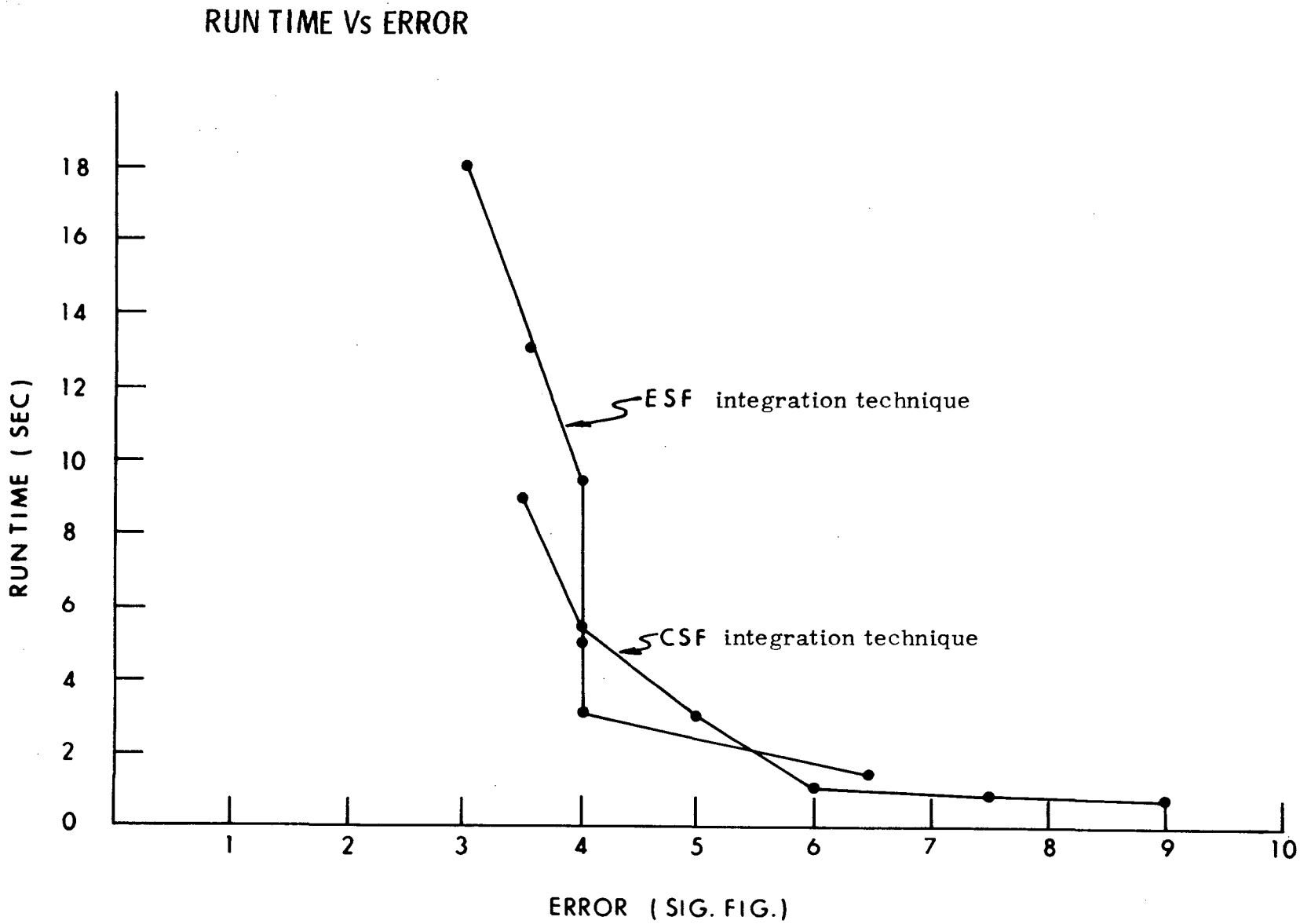

Figure 4.3 Effect of Computer Run Time on Integration Error

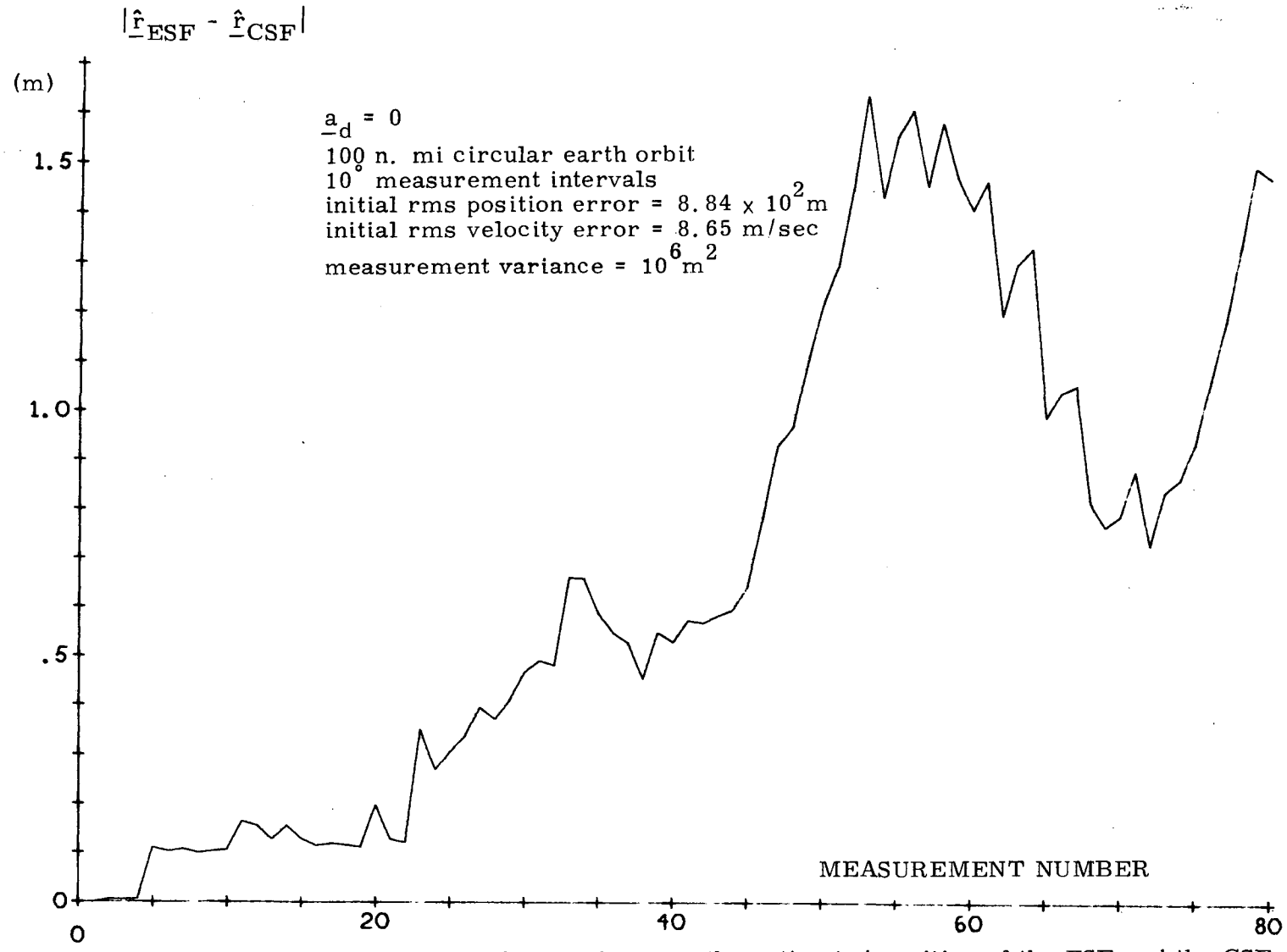

Figure 4.4 Magnitude of the difference between the estimated position of the ESF and the CSF for one Monte Carlo run

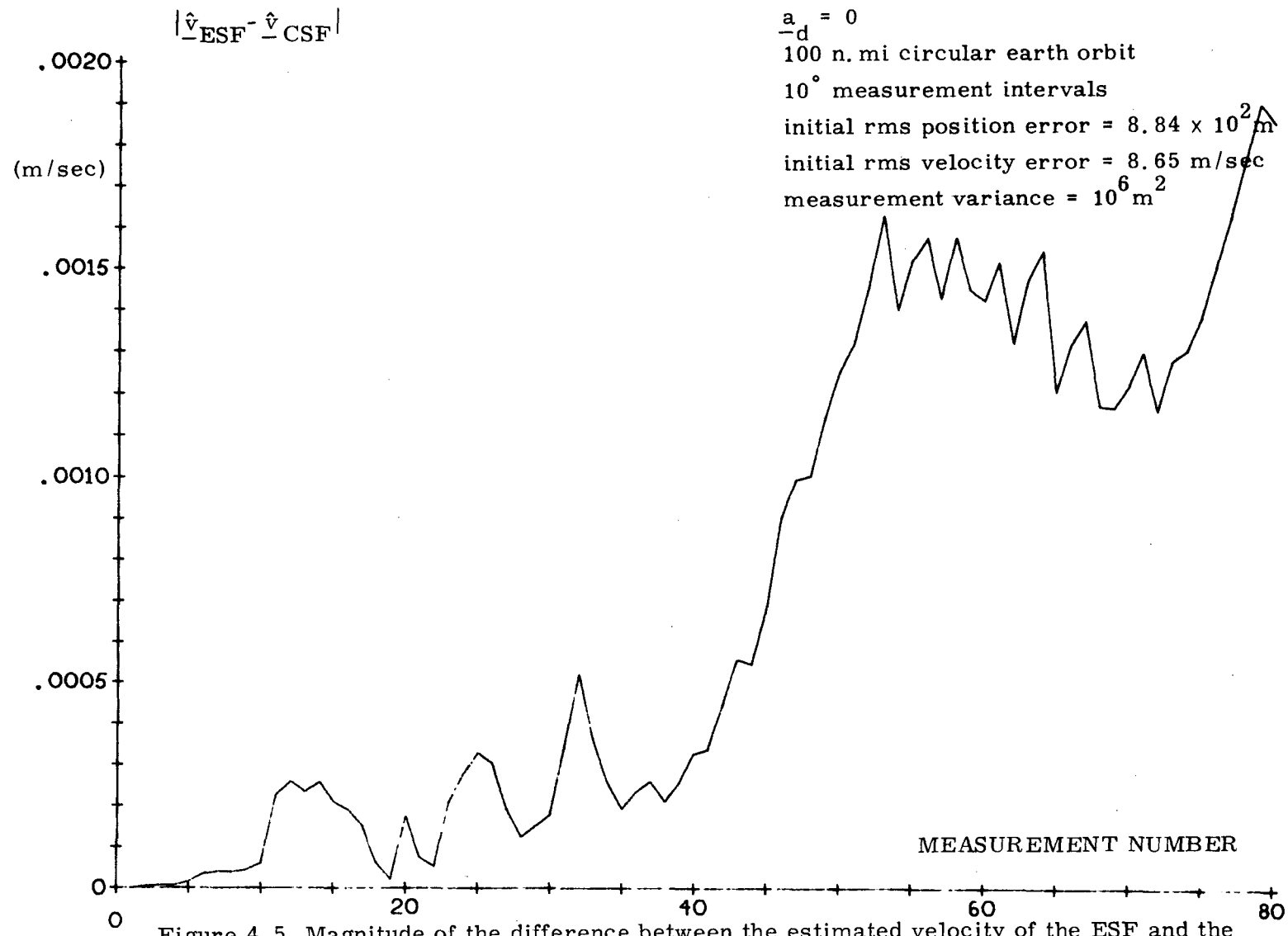

Figure 4.5 Magnitude of the difference between the estimated velocity of the ESF and the CSF for one Monte Carlo run.

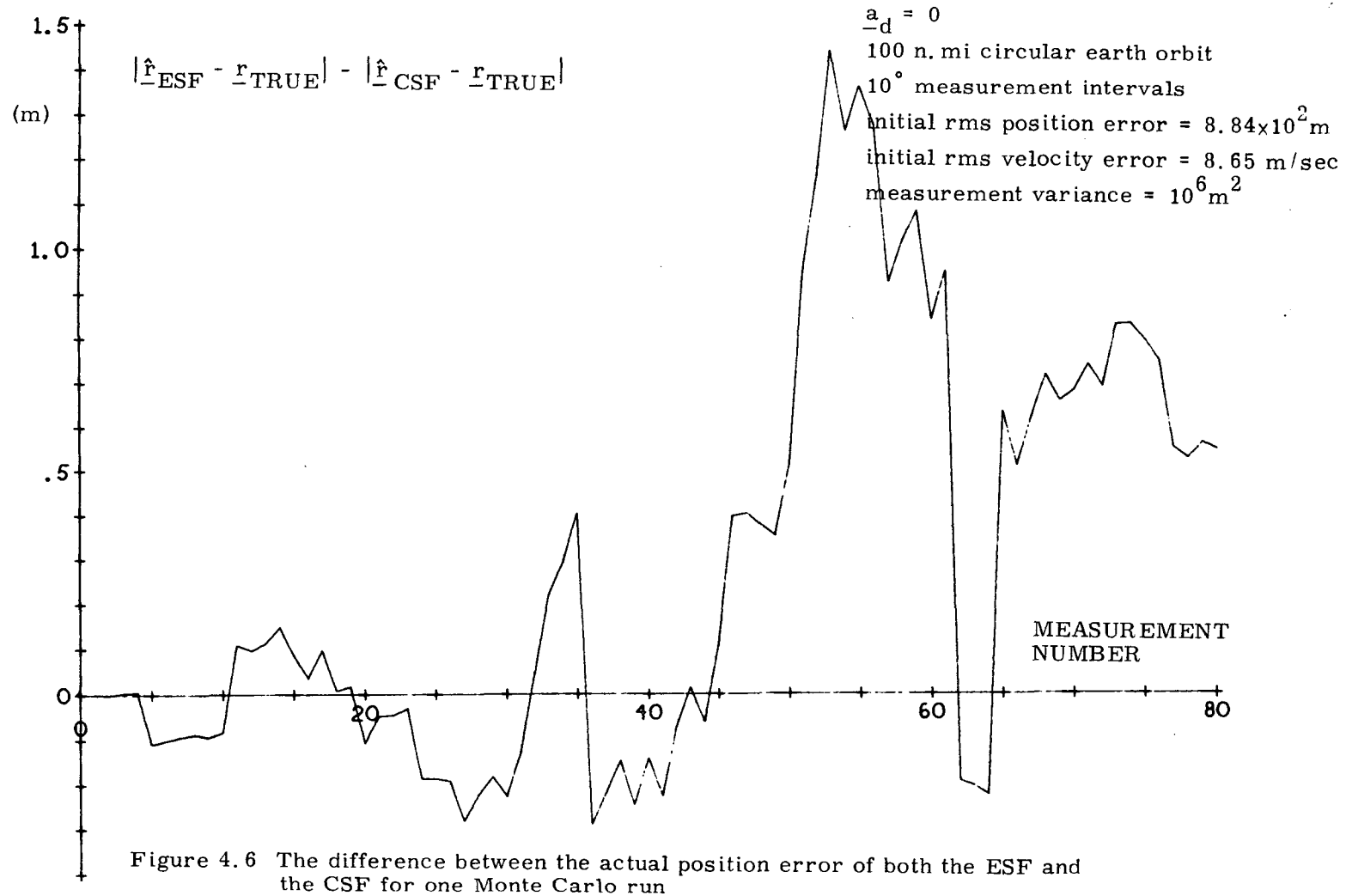

Figure 4.6 The difference between the actual position error of both the ESF and the CSF for one Monte Carlo run

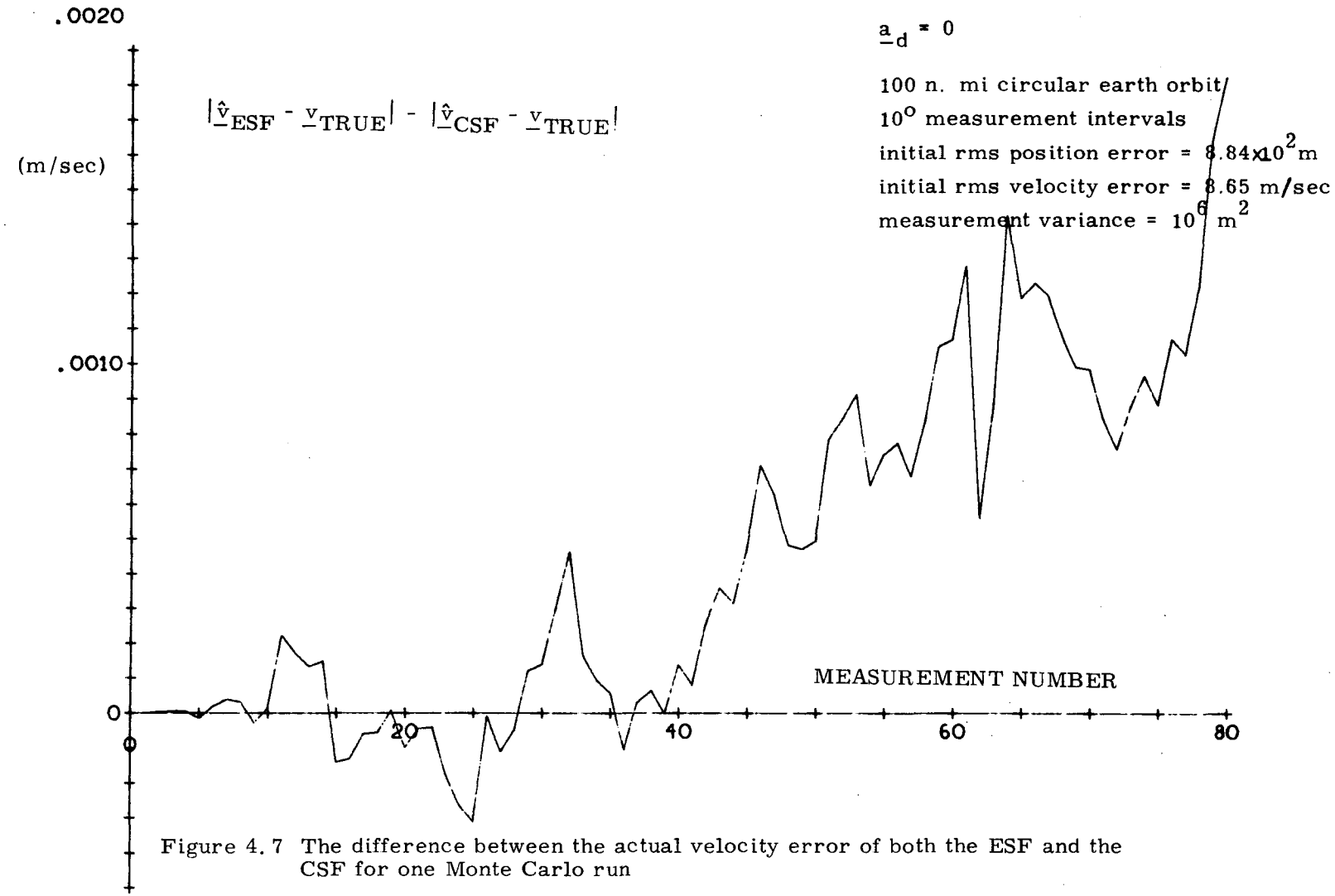

Figure 4.7 The difference between the actual velocity error of both the ESF and the CSF for one Monte Carlo run

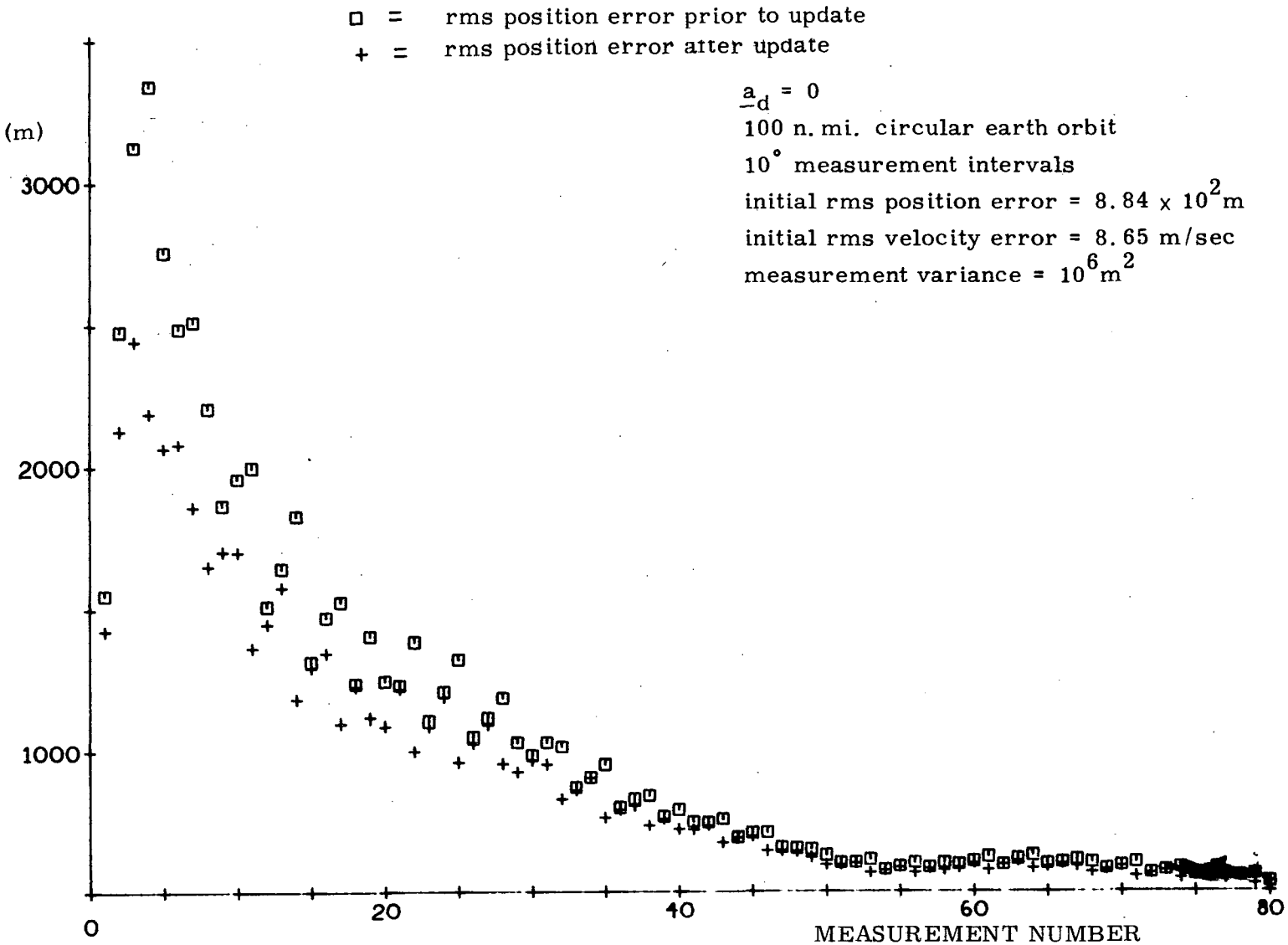

Figure 4.8 RMS estimated current position error for one Monte Carlo run

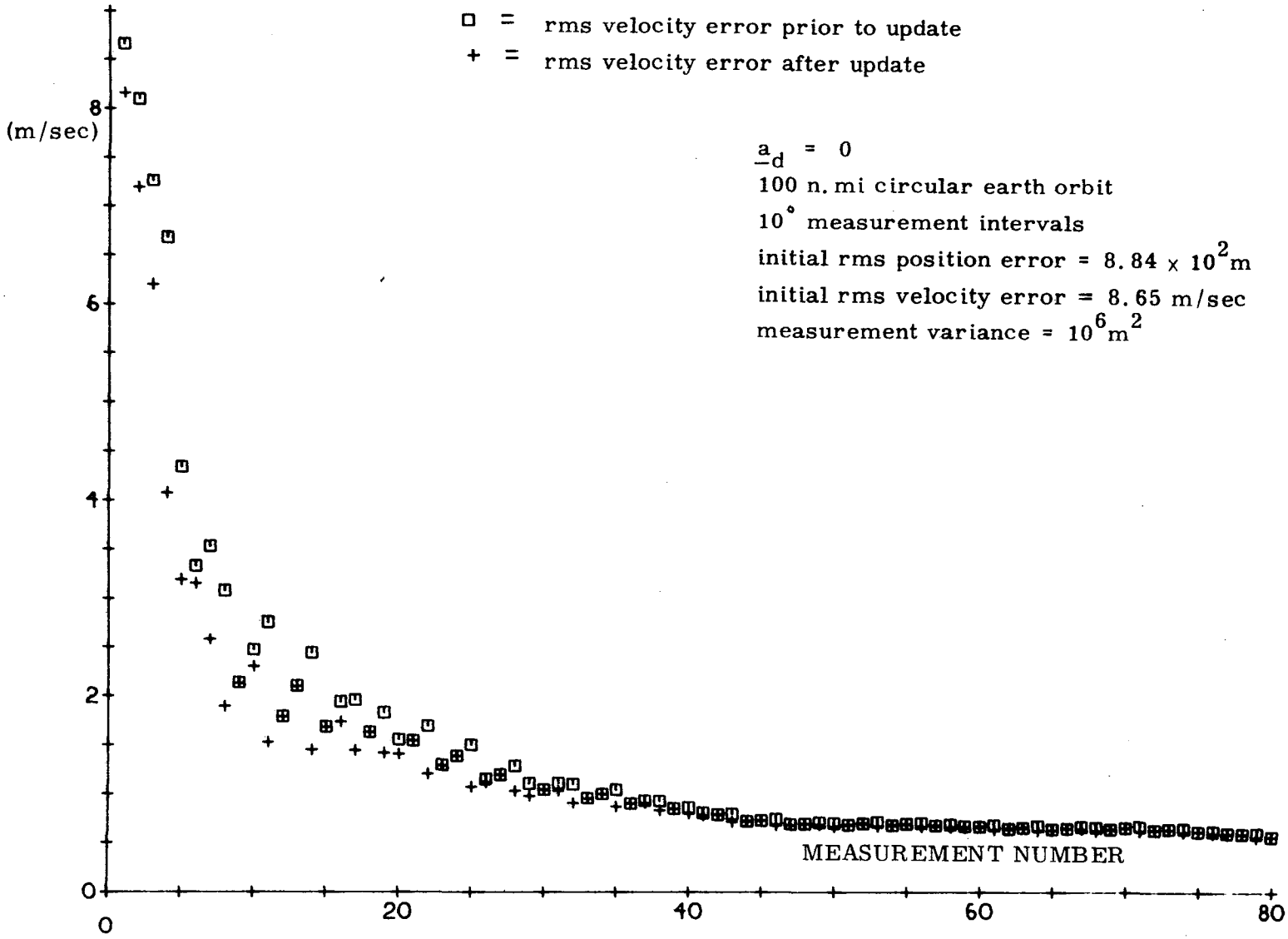

Figure 4.9 RMS estimated current velocity deviation error for one Monte Carlo run

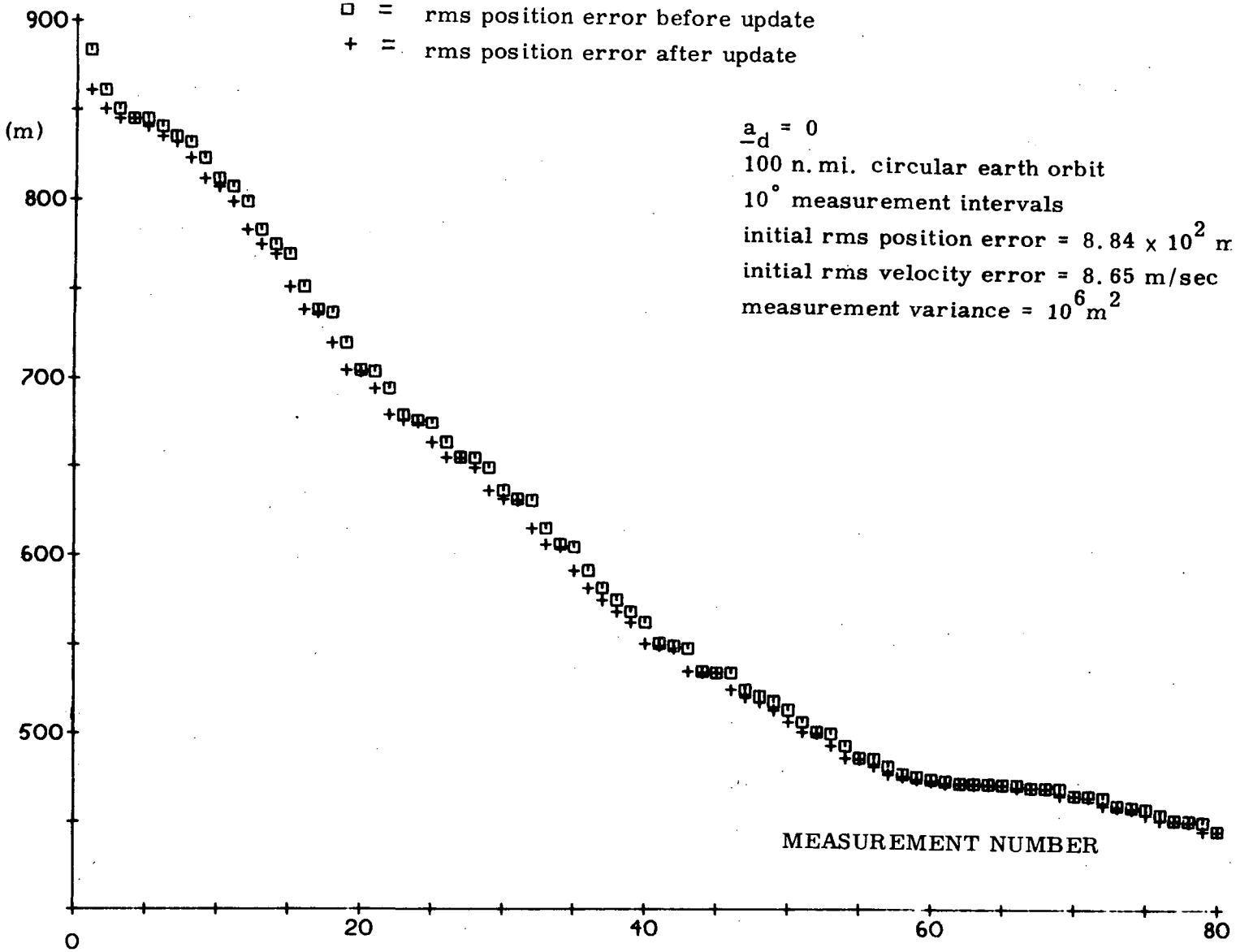

Figure 4.10 RMS estimated position error at the epoch for one Monte Carlo run

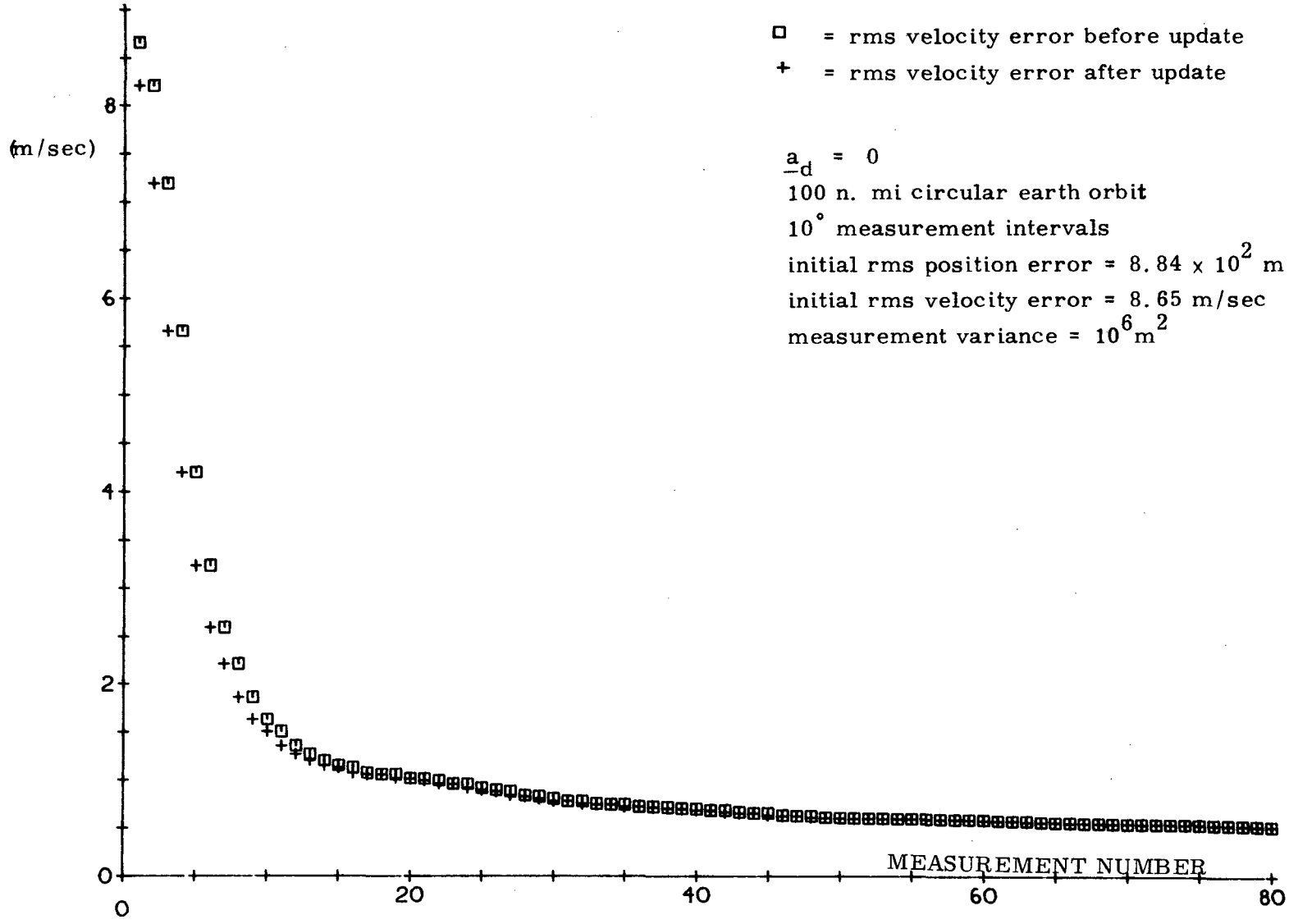

Figure 4.11 RMS estimated velocity error at the epoch for one Monte Carlo run

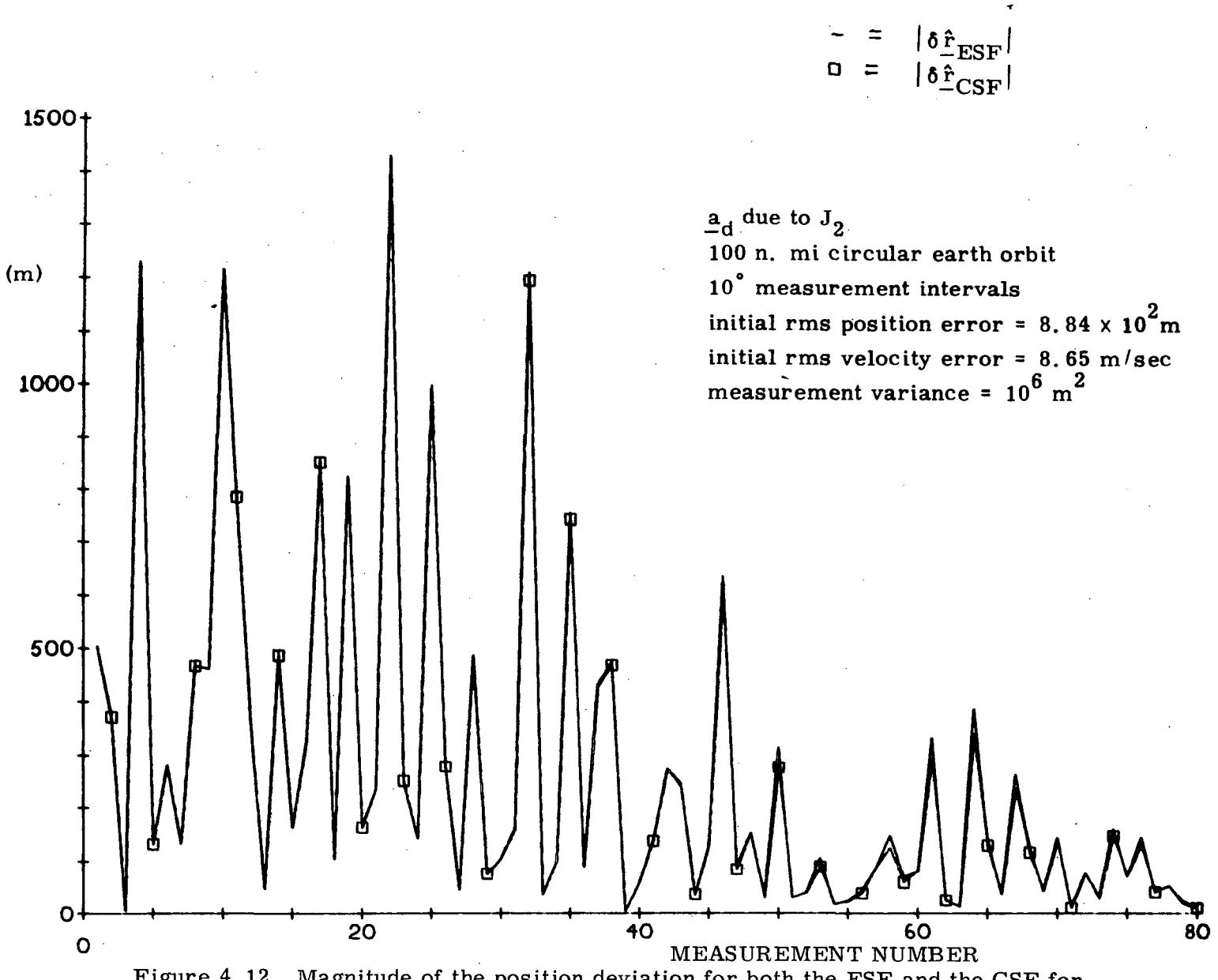

Figure 4.12 Magnitude of the position deviation for both the ESF and the CSF for one Monte Carlo run

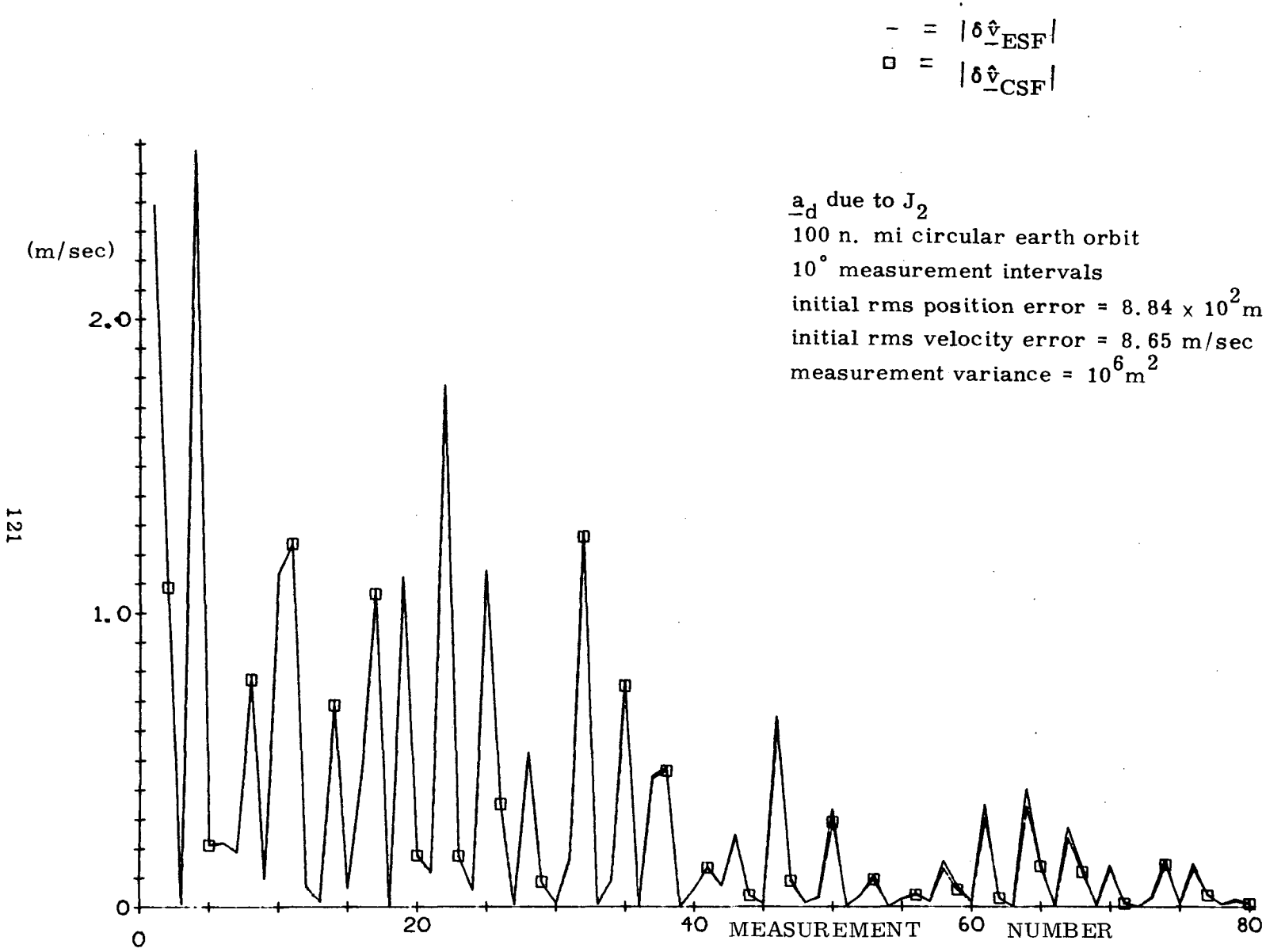

Figure 4.13 Magnitude of the velocity deviation for both the ESF and the CSF for one Monte Carlo run

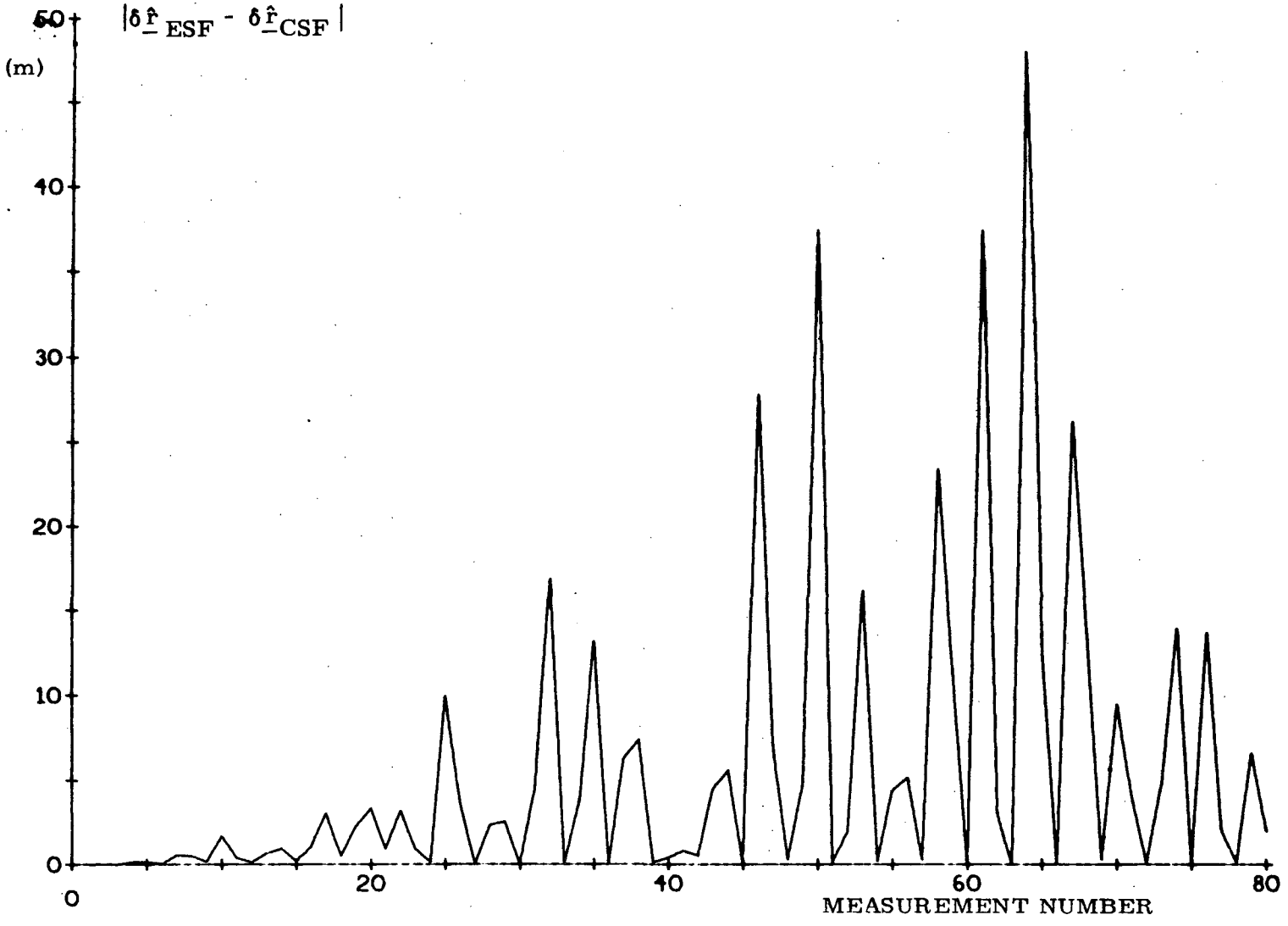

Figure 4.14 Magnitude of the difference between the estimated position deviation of the ESF and the CSF for one Monte Carlo run

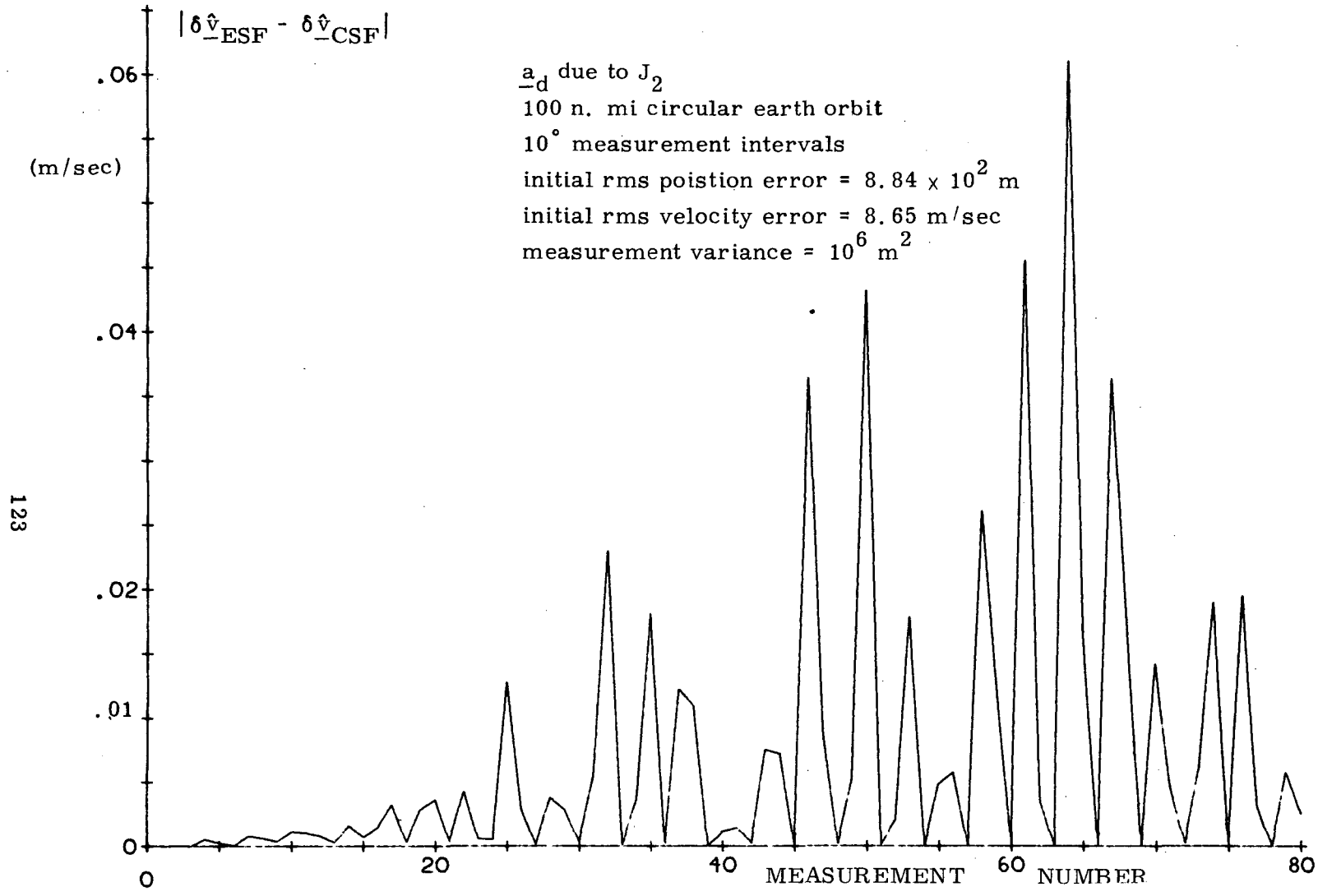

Figure 4.15 Magnitude of the difference between the estimated velocity deviation of the ESF and the CSF for one Monte Carlo run

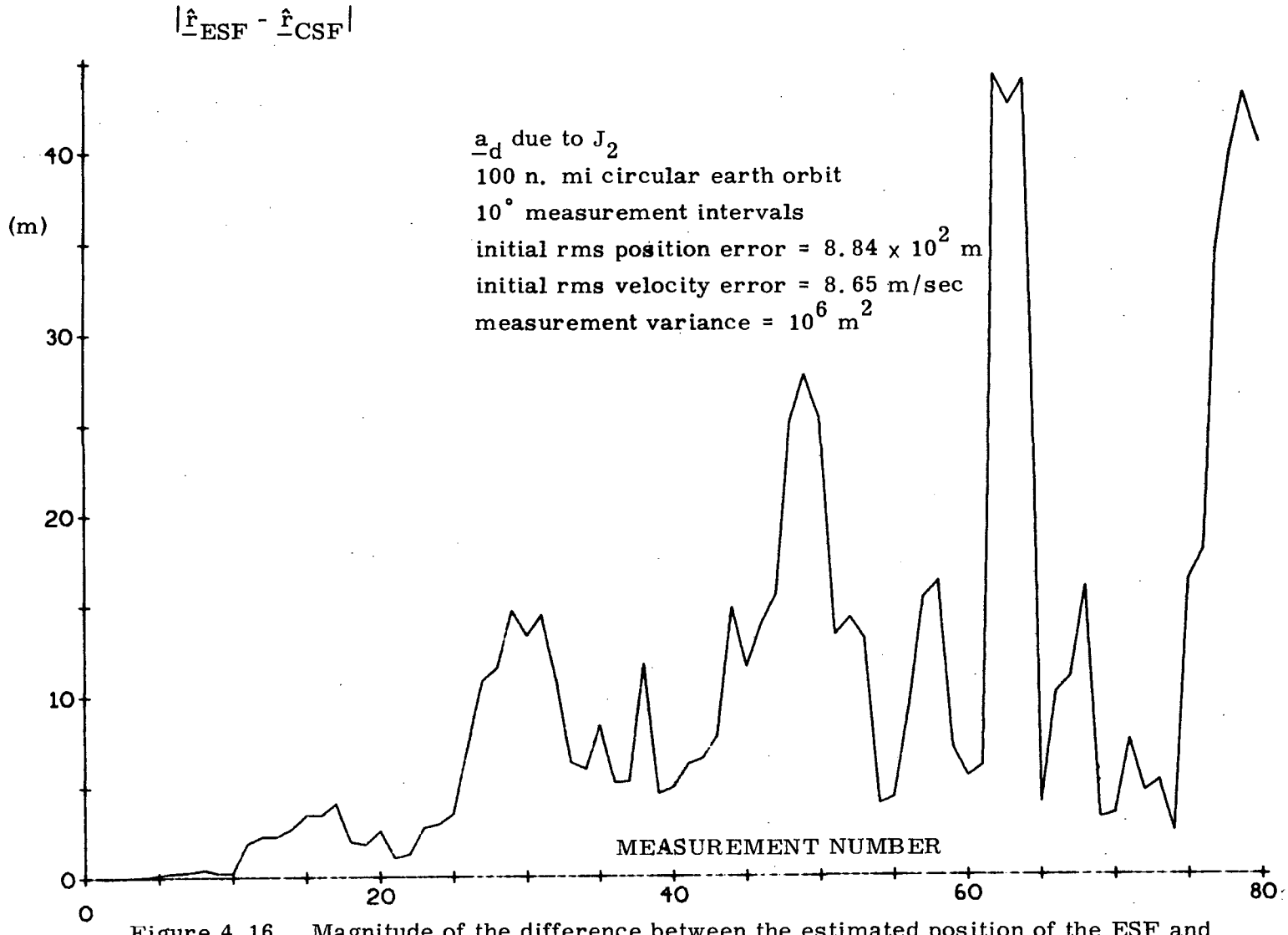

Figure 4.16 Magnitude of the difference between the estimated position of the ESF and the CSF for one Monte Carlo run

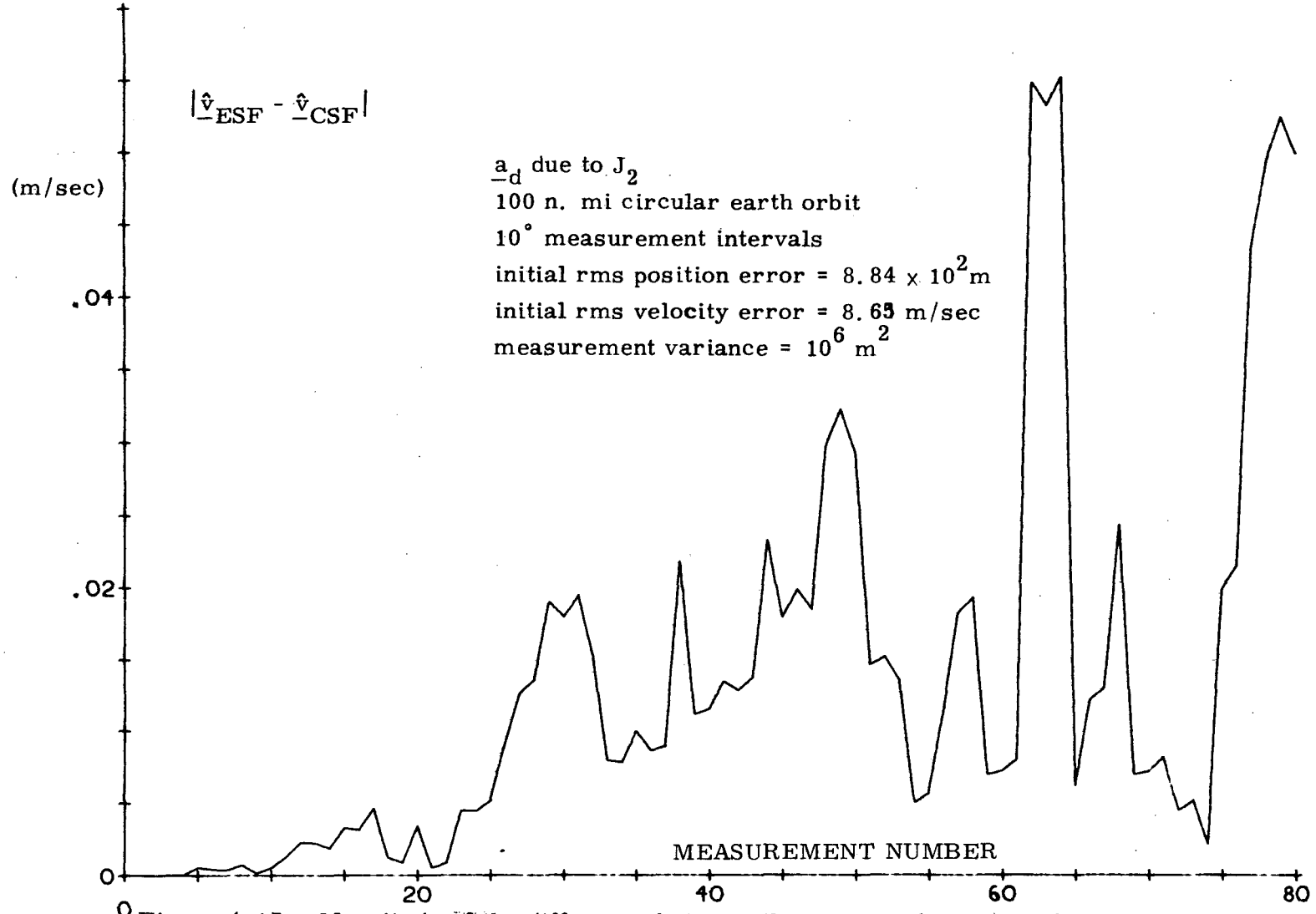

Figure 4.17 Magnitude of the difference between the estimated velocity of the ESF and the CSF for one Monte Carlo run

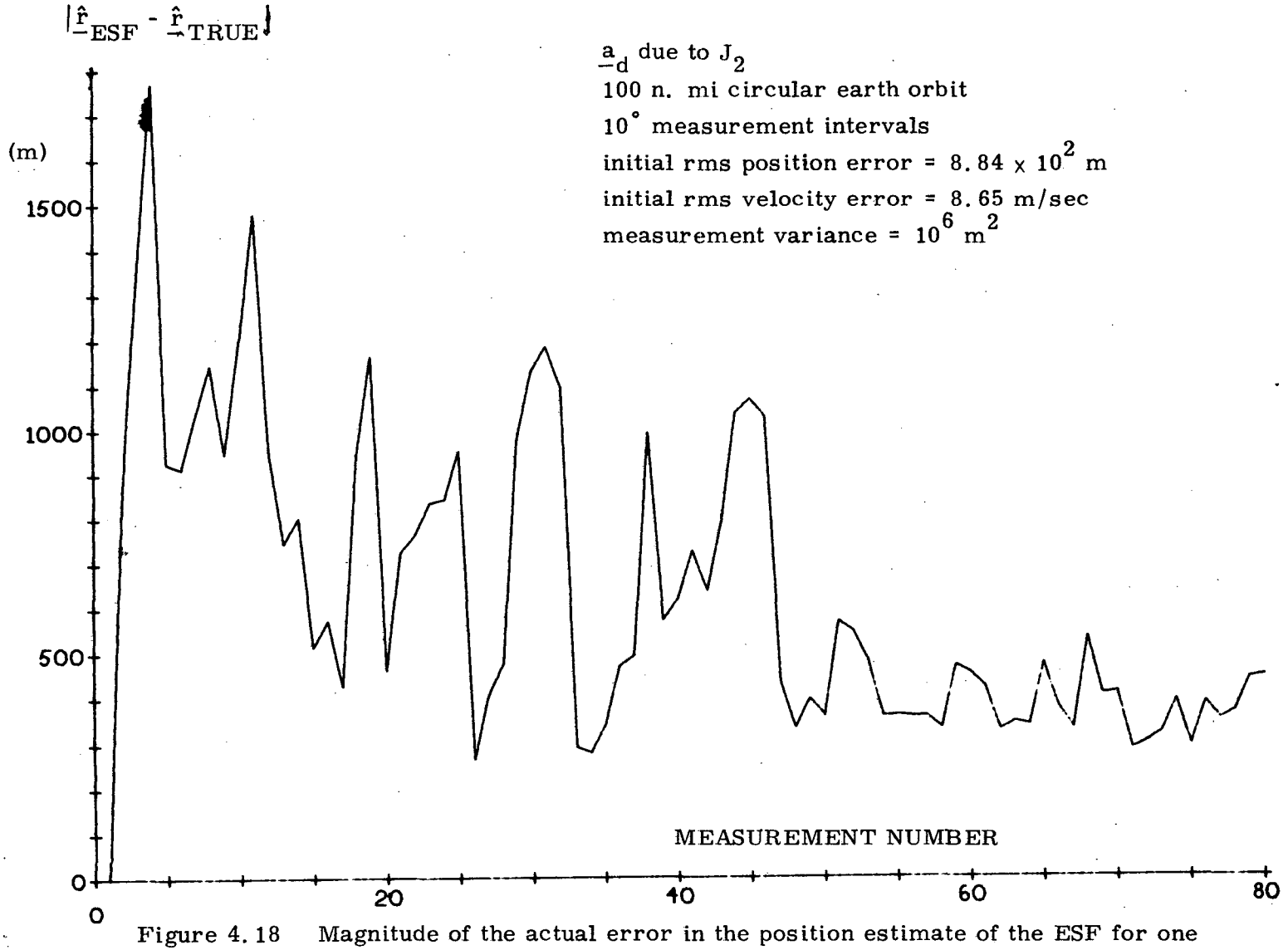

Figure 4.18 Magnitude of the actual error in the position estimate of the ESF for one Monte Carlo run

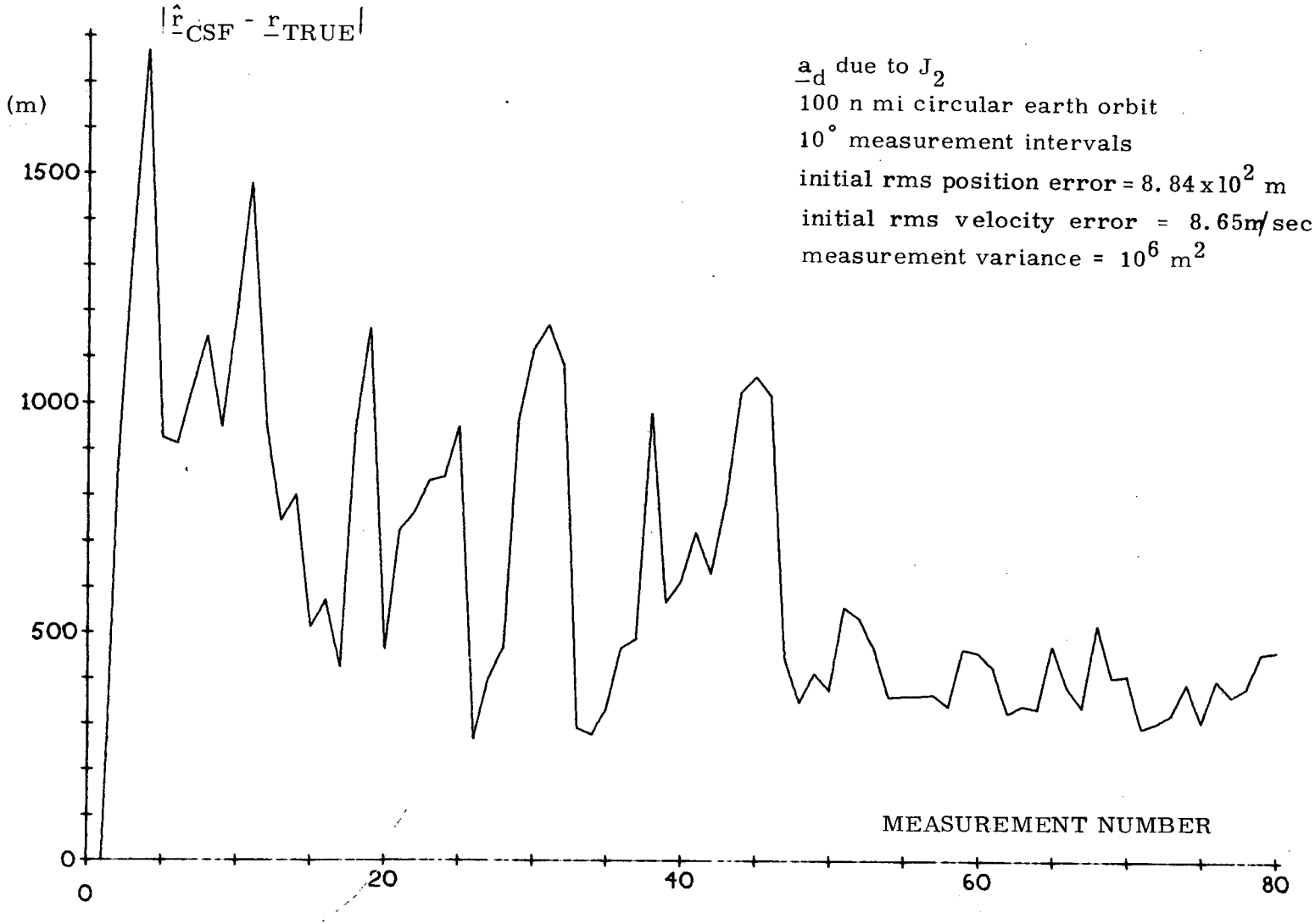

Figure 4.19 Magnitude of the Actual Position Error of the CSF for one Monte Carlo Run.

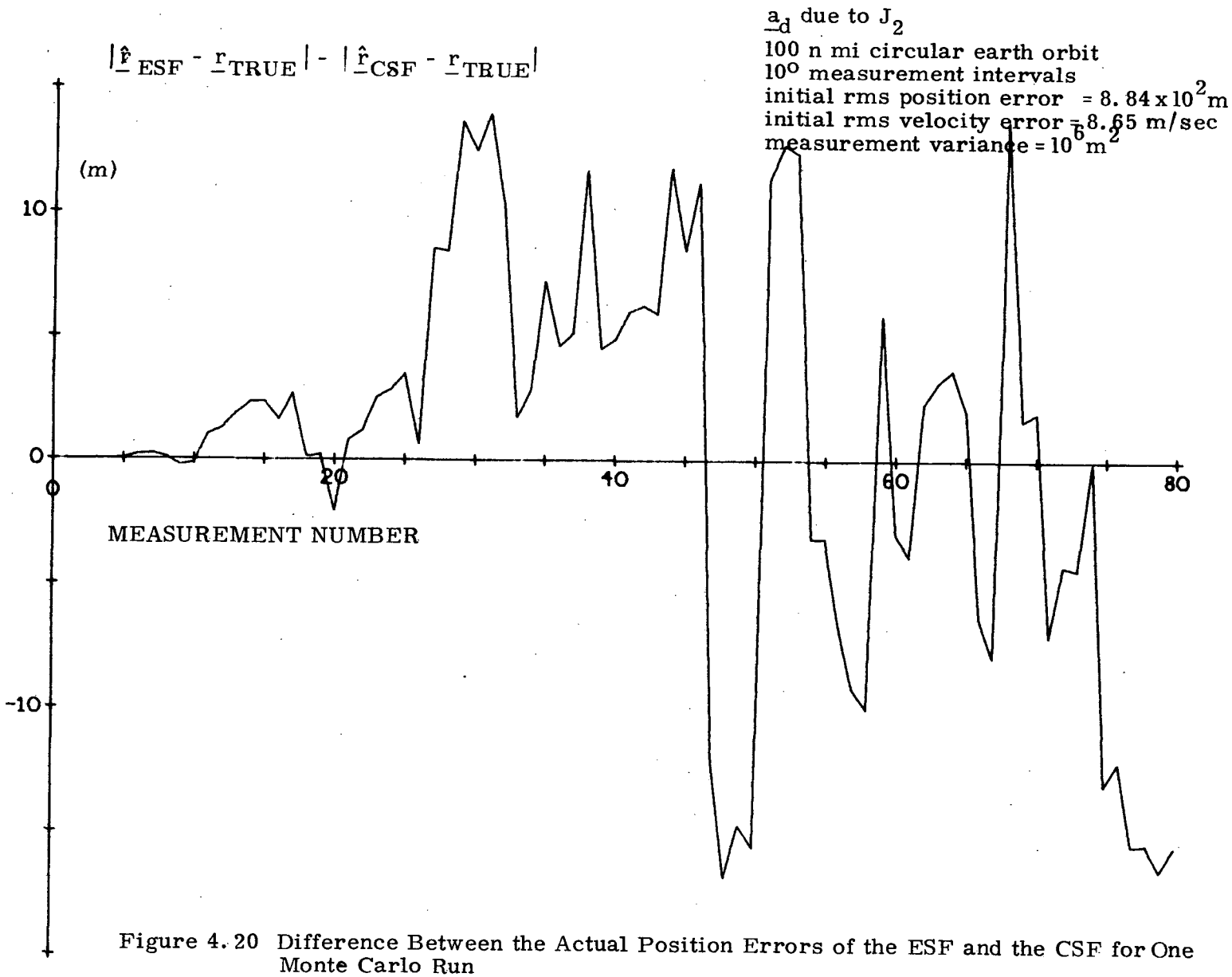

Figure 4.20 Difference Between the Actual Position Errors of the ESF and the CSF for One Monte Carlo Run

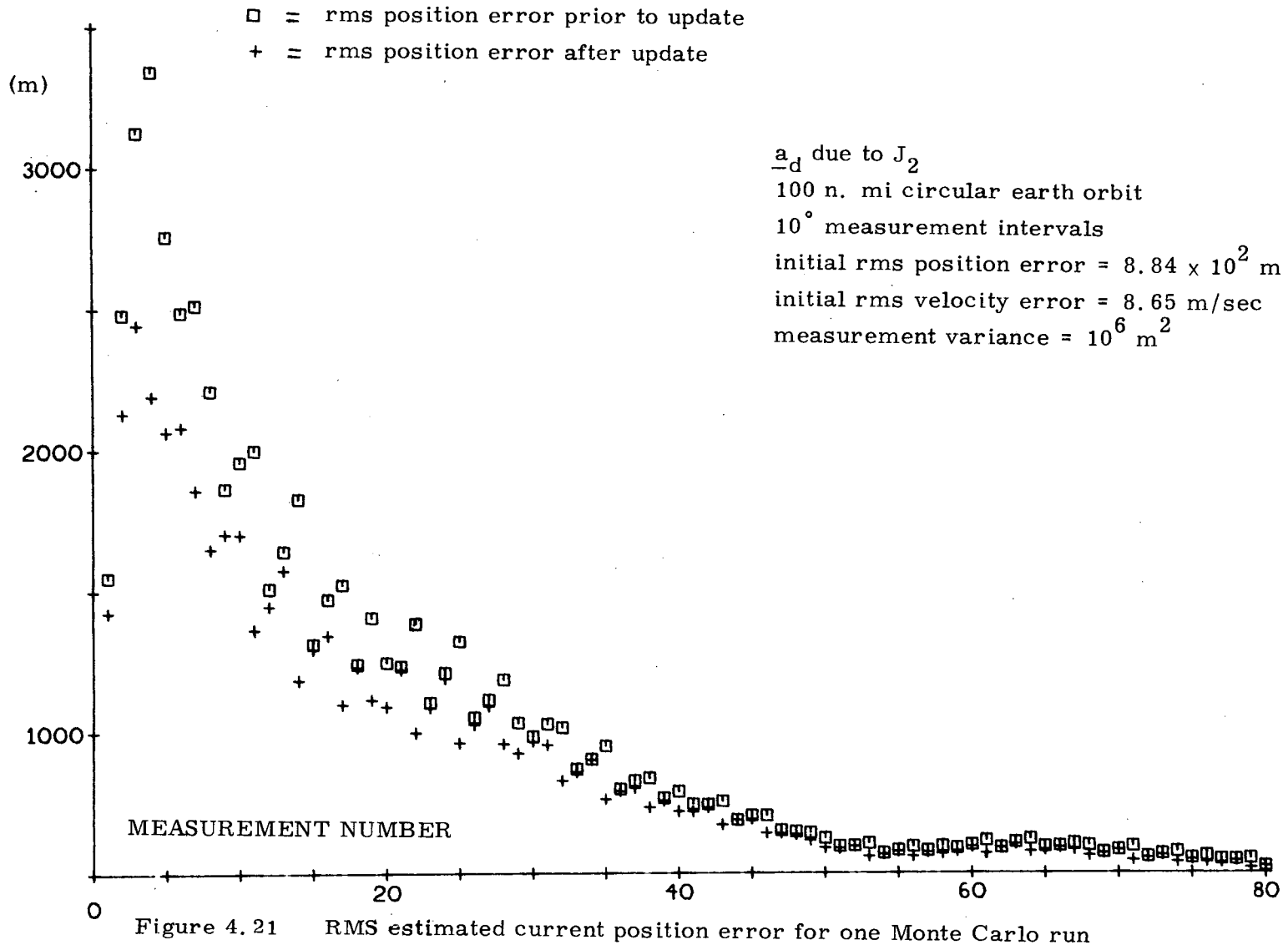

Figure 4.21 RMS estimated current position error for one Monte Carlo run

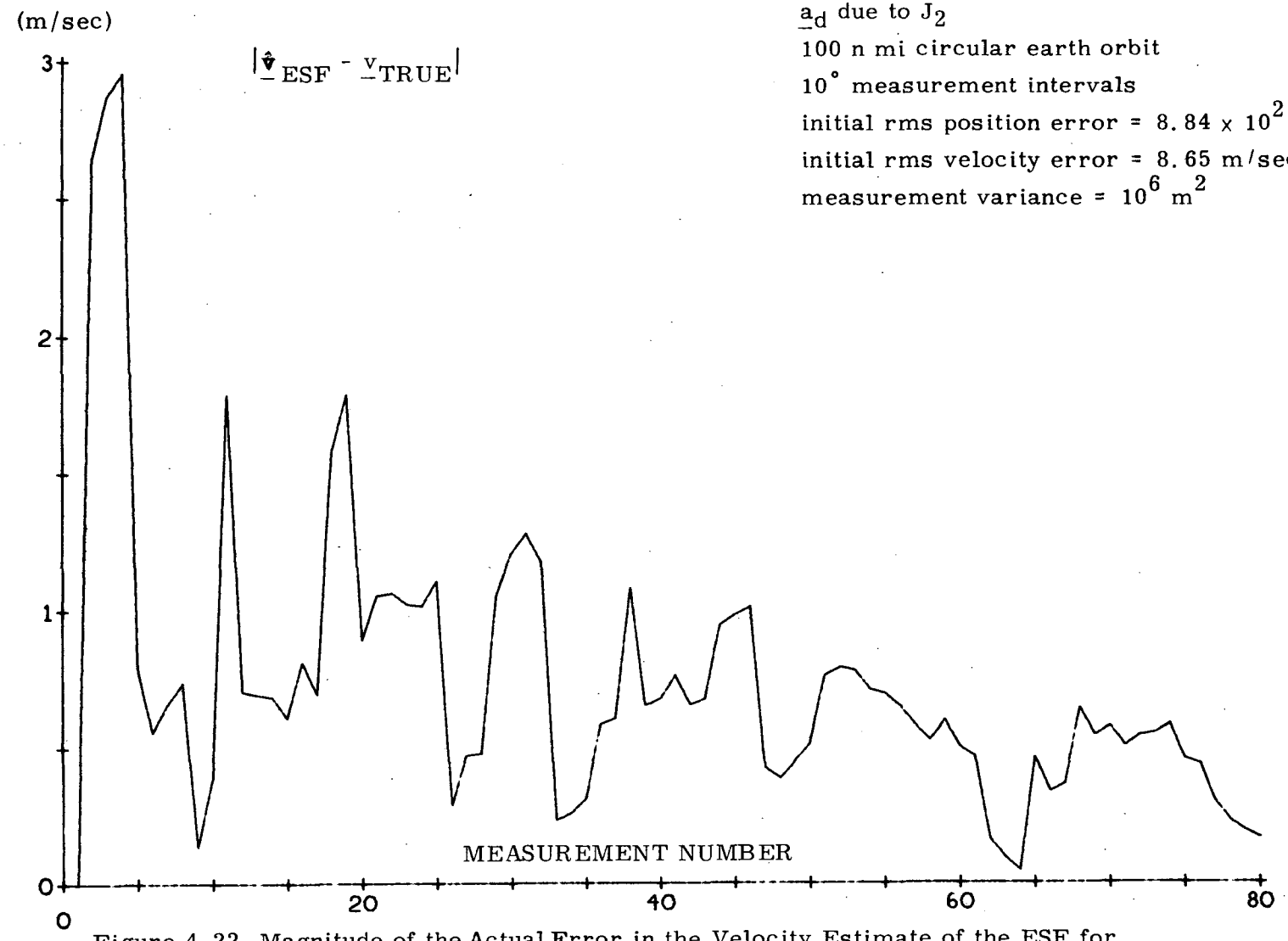

Figure 4.22 Magnitude of the Actual Error in the Velocity Estimate of the ESF for One Monte Carlo Run

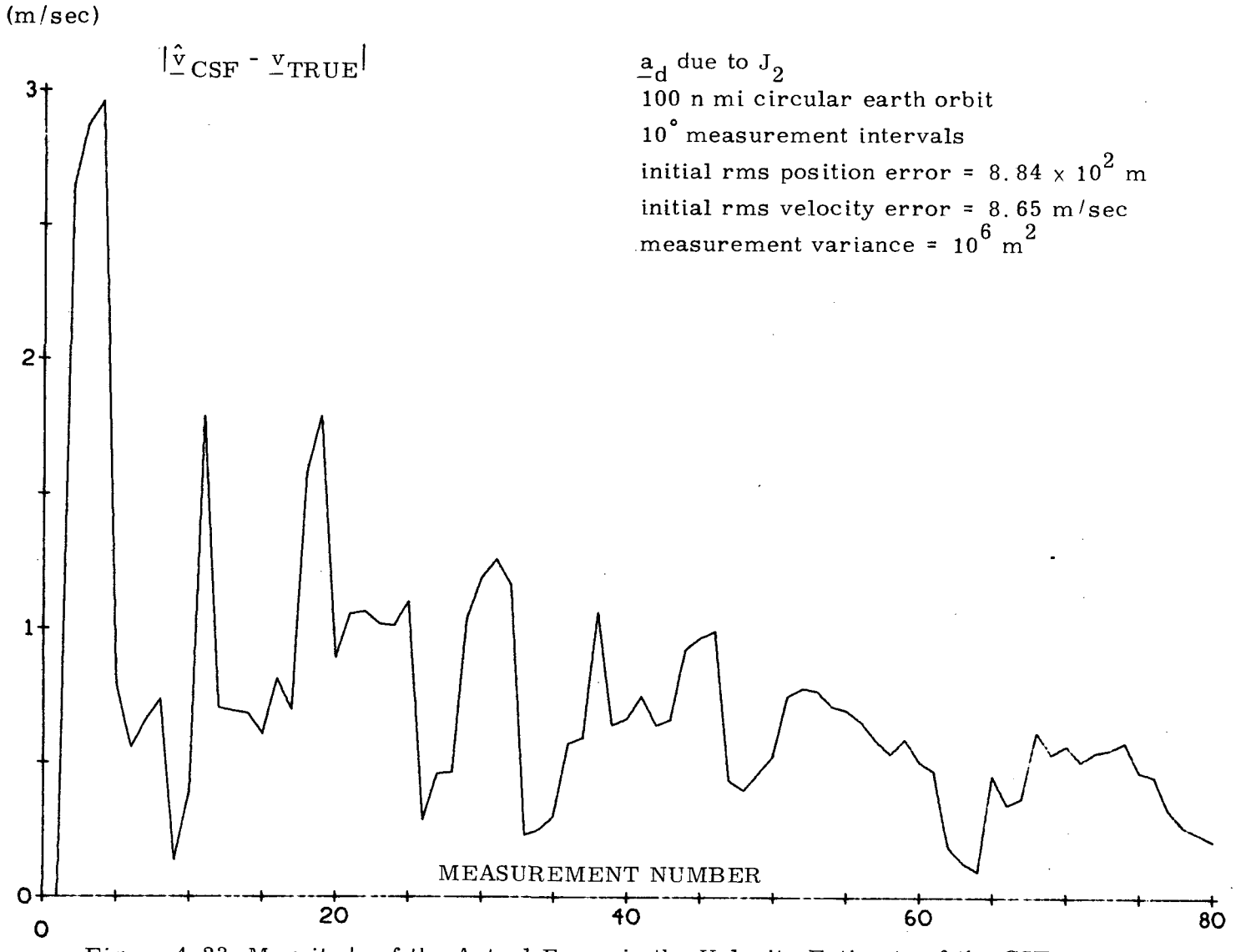

Figure 4.23 Magnitude of the Actual Error in the Velocity Estimate of the CSF for One Monte Carlo Run

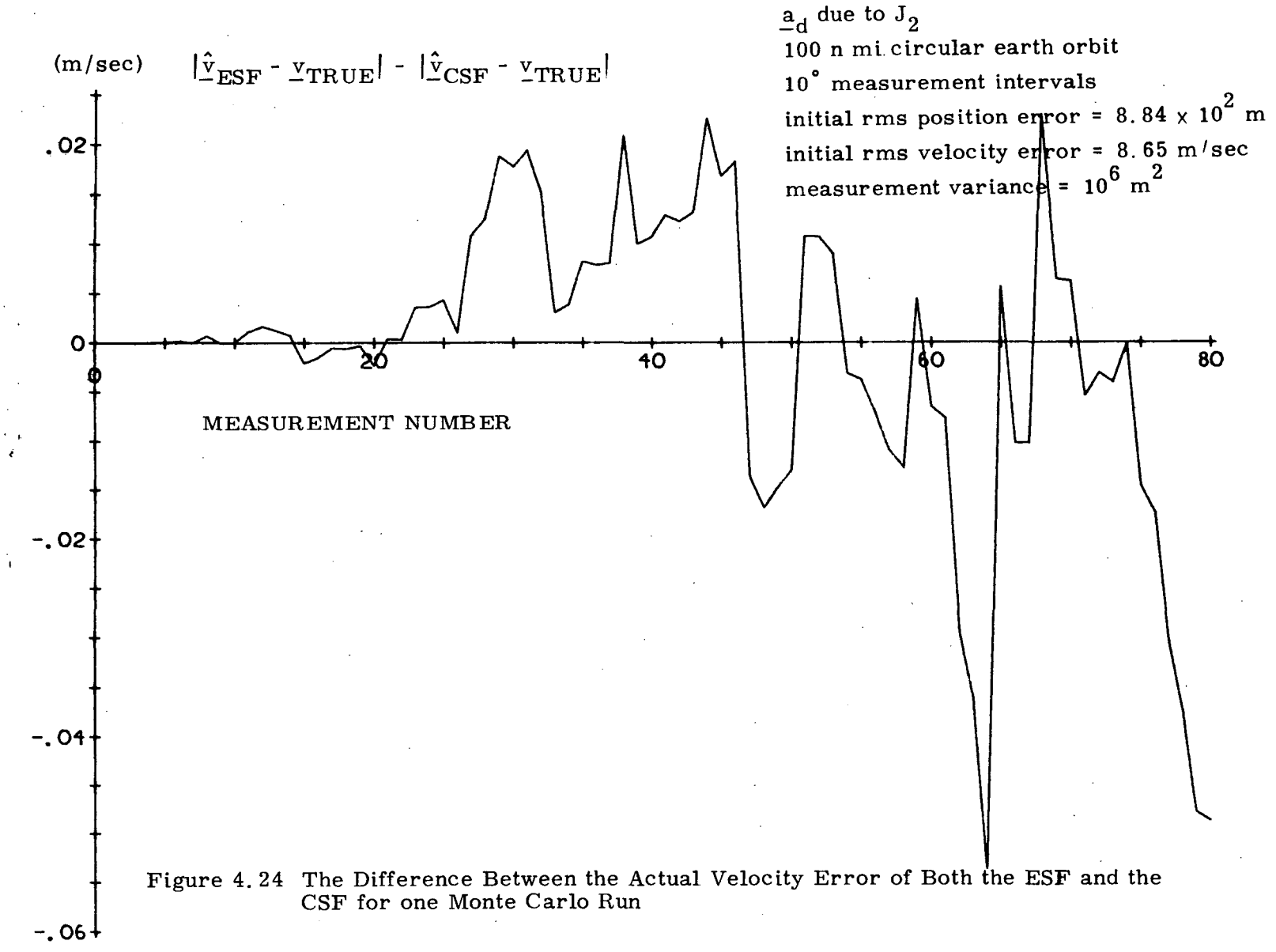

Figure 4.24 The Difference Between the Actual Velocity Error of Both the ESF and the CSF for one Monte Carlo Run

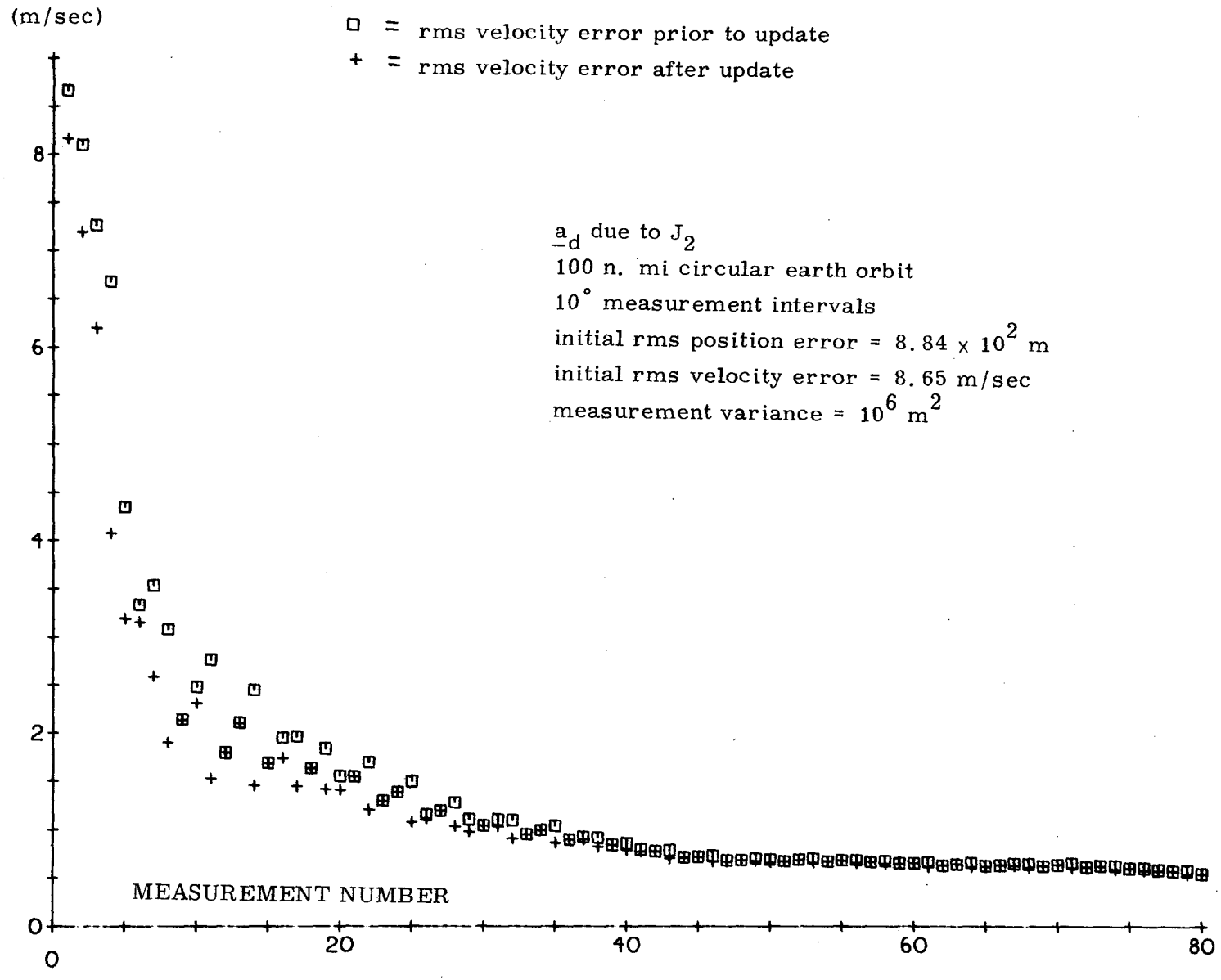

Figure 4.25 RMS estimated current velocity error for one Monte Carlo run

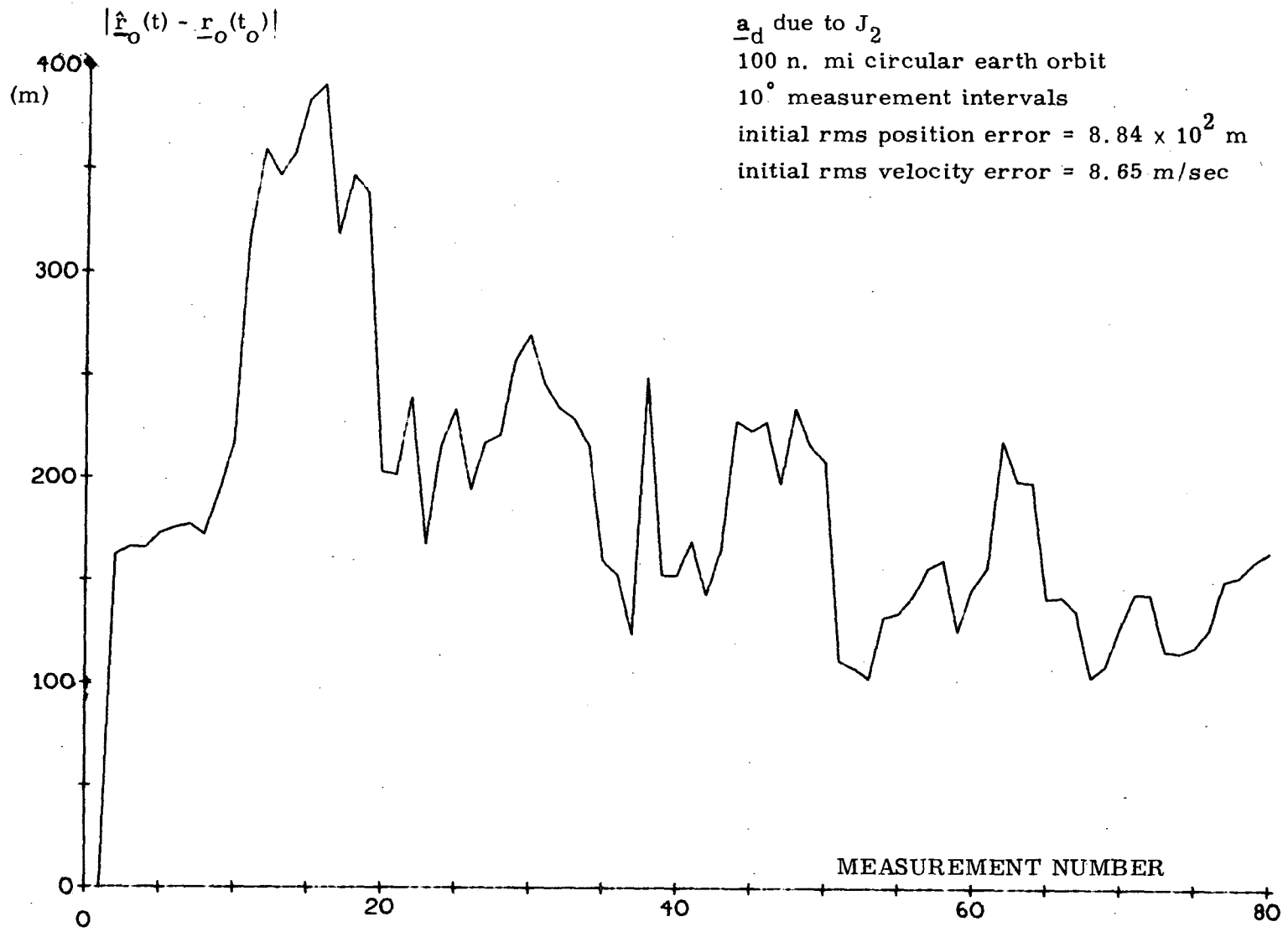

Figure 4.26 Magnitude of the change in the epoch position from its true initial value for one Monte Carlo run

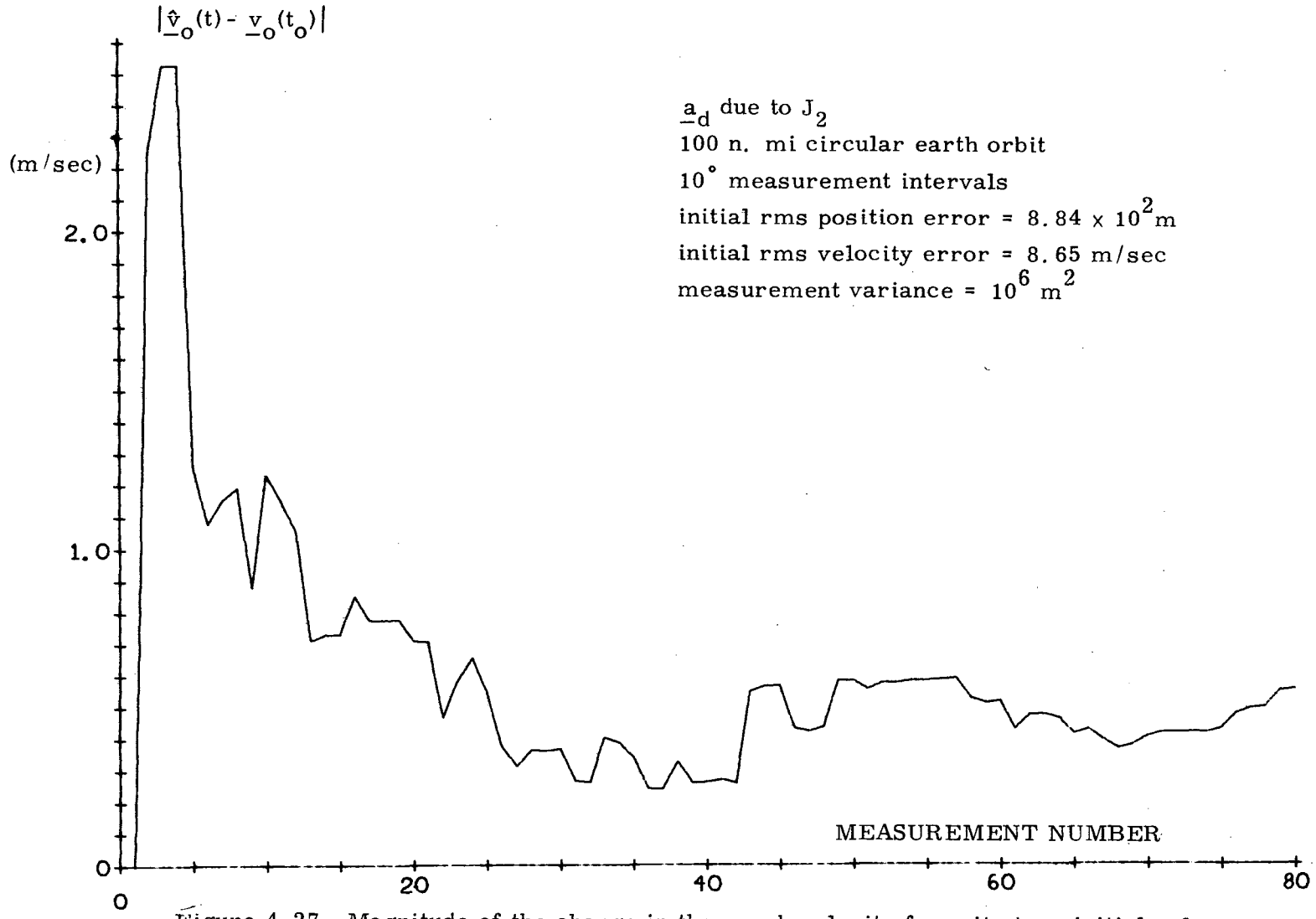

Figure 4.27 Magnitude of the change in the epoch velocity from its true initial value for one Monte Carlo run

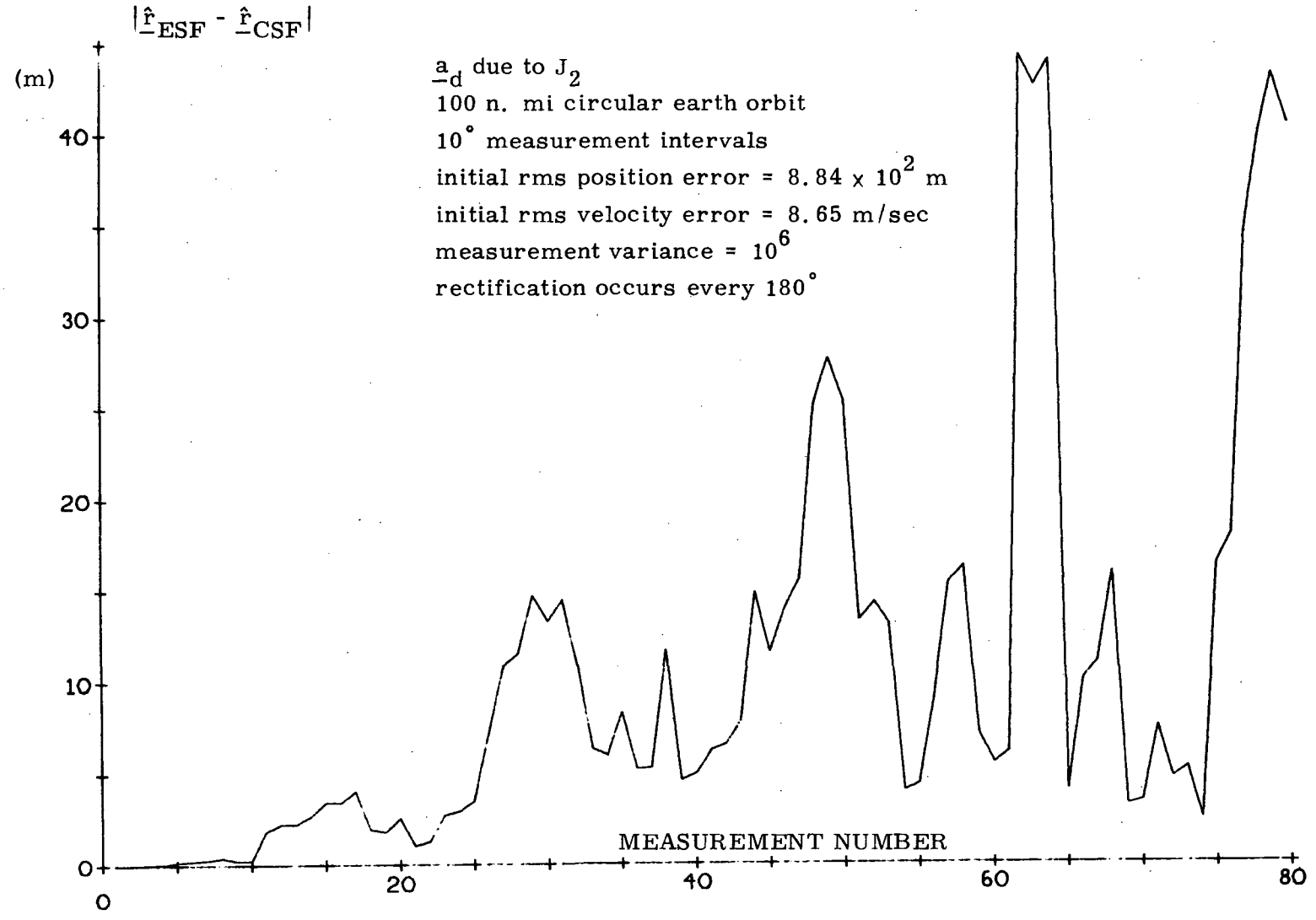

Figure 4.28 Magnitude of the difference between the estimated position of the ESF and the CSF for one Monte Carlo run

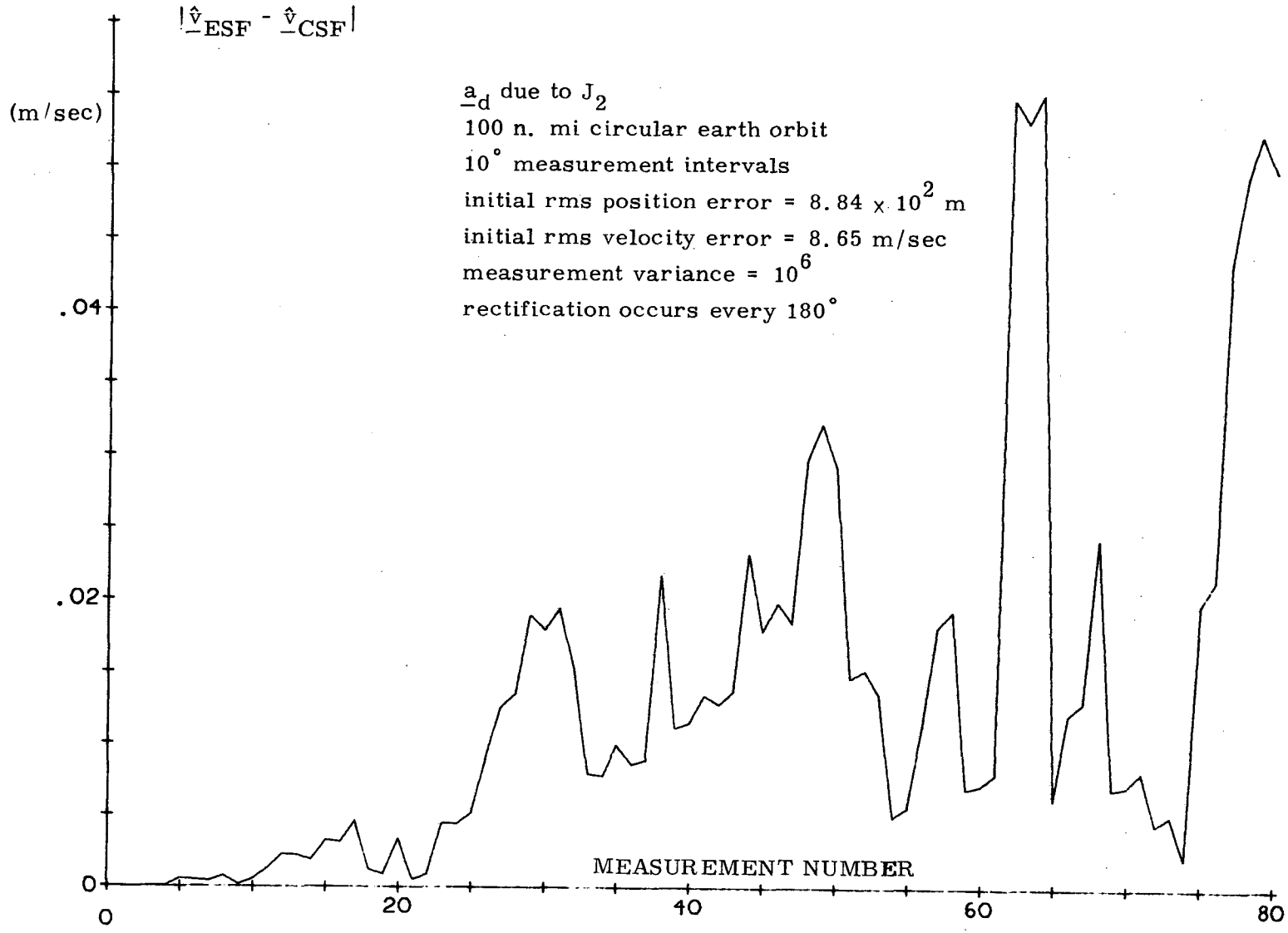

Figure 4.29 Magnitude of the difference between the estimated velocity of the ESF and the CSF for one Monte Carlo run

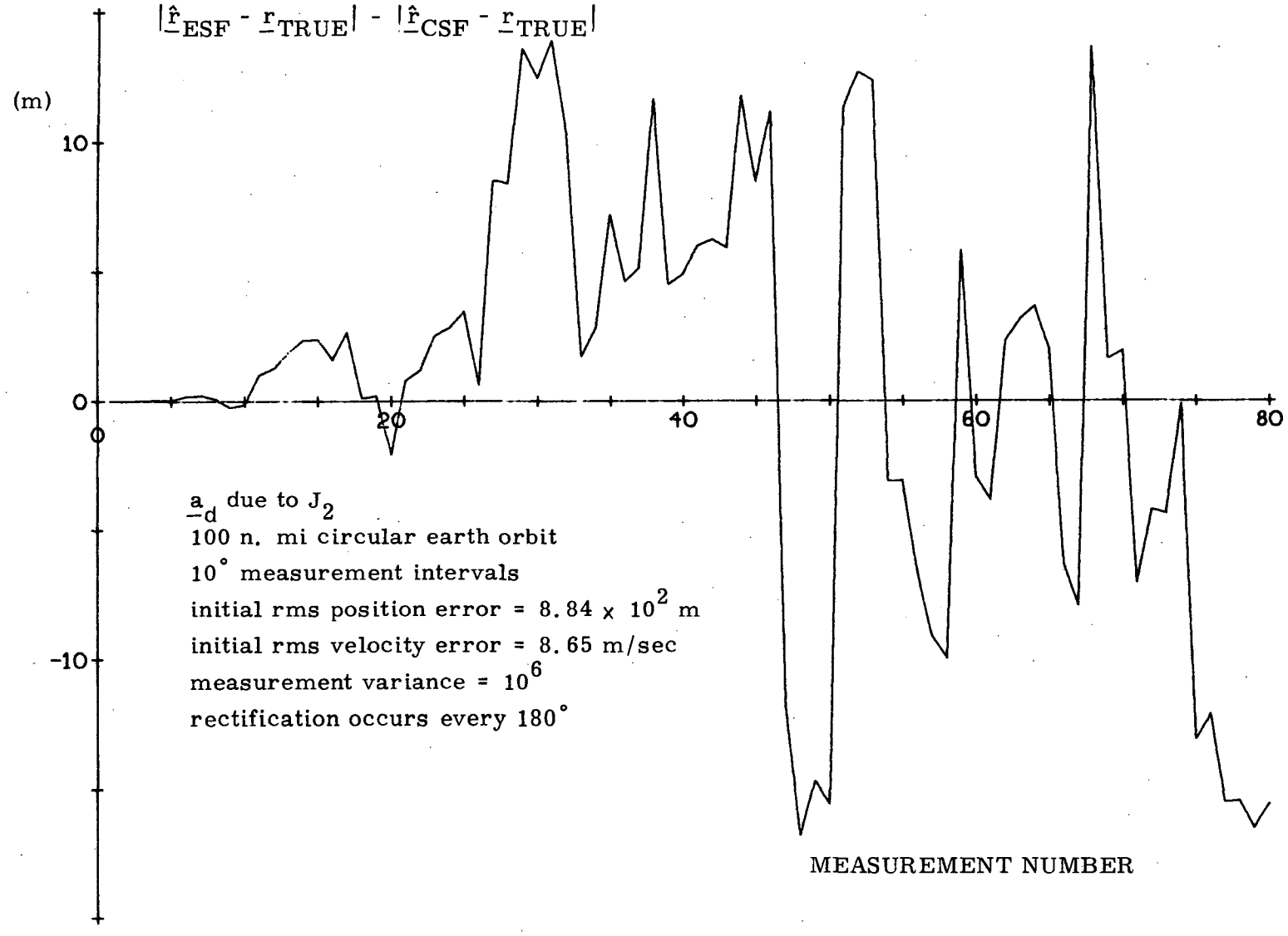

Figure 4.30 The difference between the actual position error of both the ESF and the CSF for one Monte Carlo run

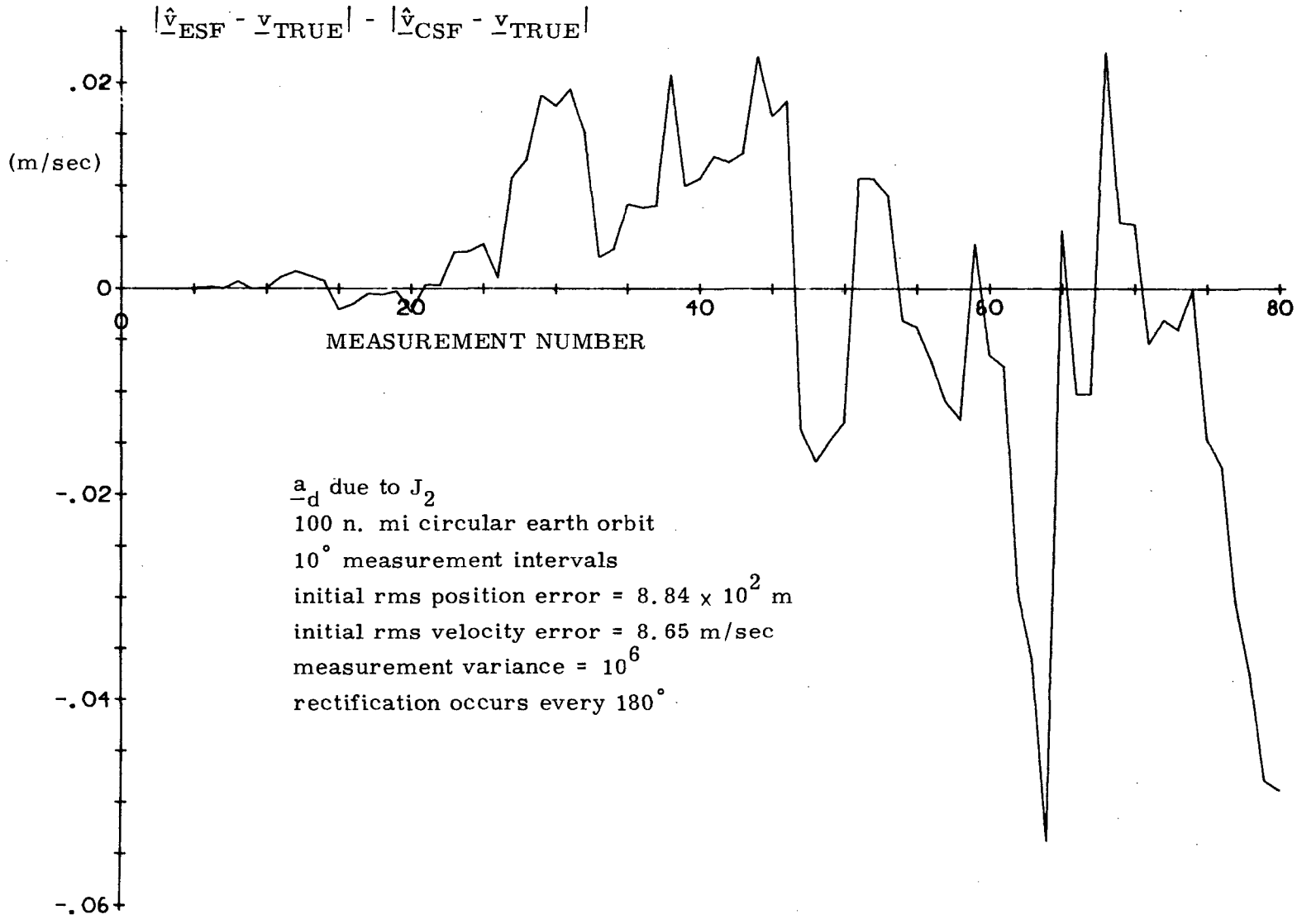

Figure 4.31 The difference between the actual velocity error of both the ESF and the CSF for one Monte Carlo run

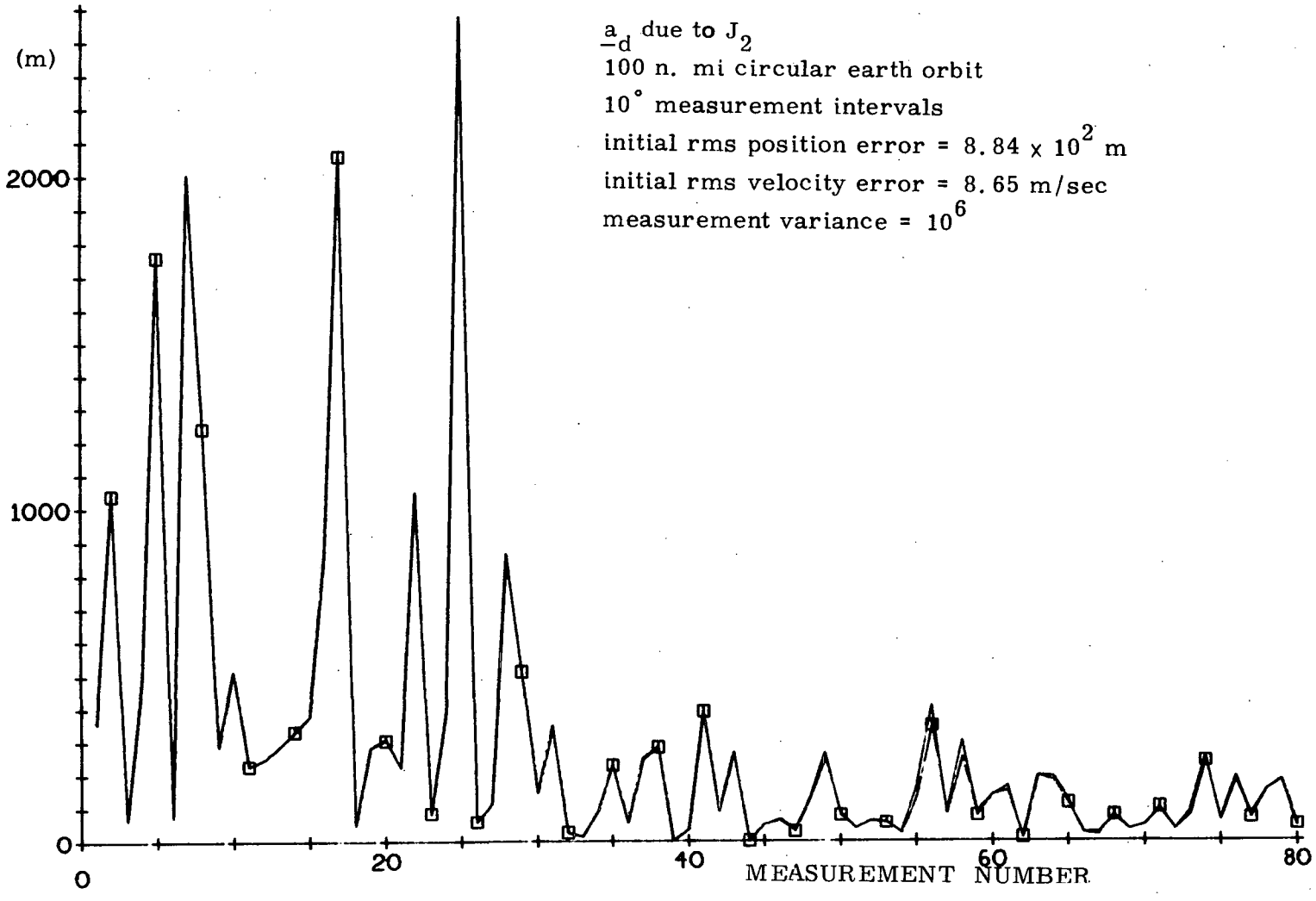

Figure 4.32 Magnitude of the position deviation for both the ESF and the CSF for a different Monte Carlo run

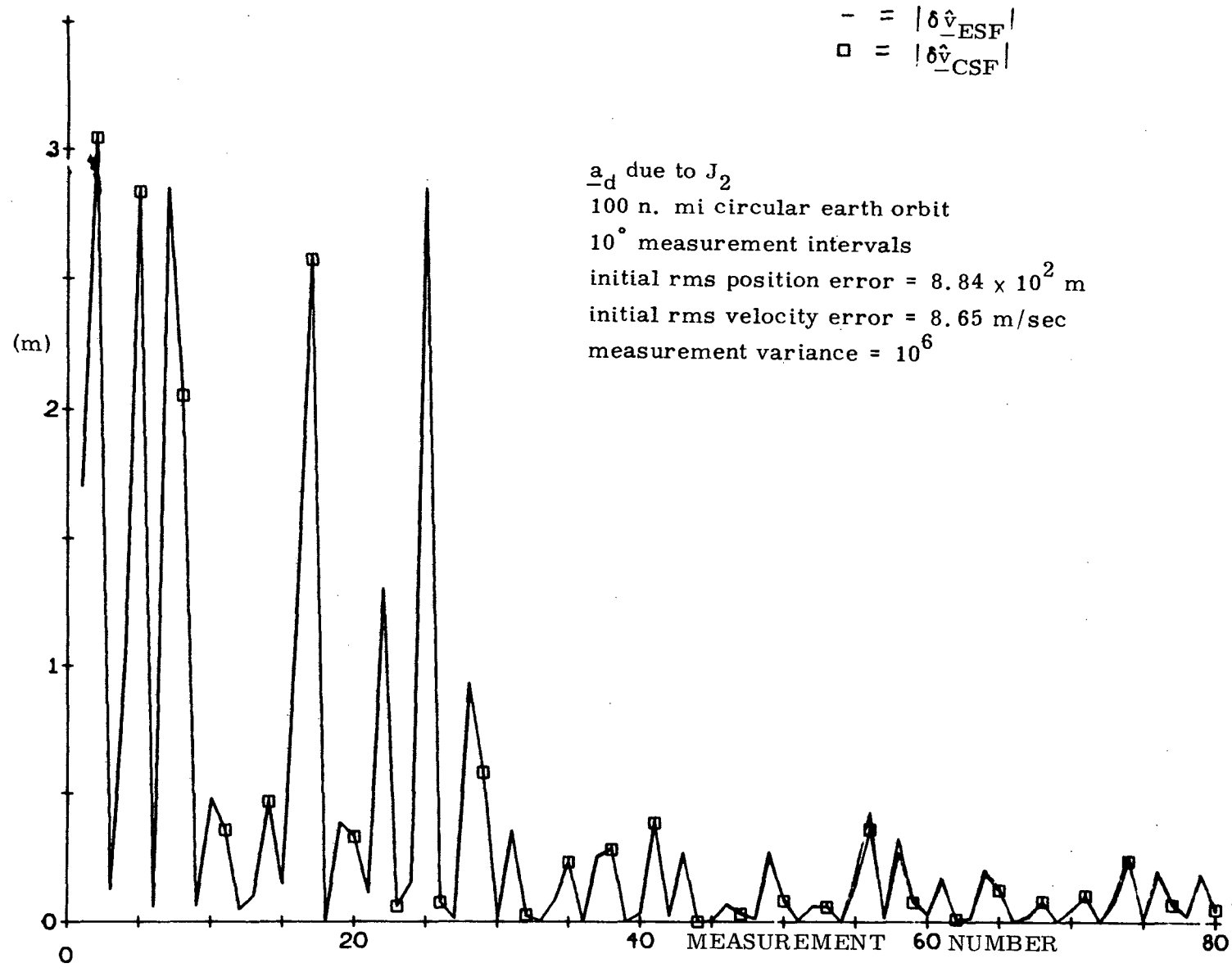

Figure 4.33 Magnitude of the velocity deviation for both the ESF and the CSF for a different Monte Carlo run

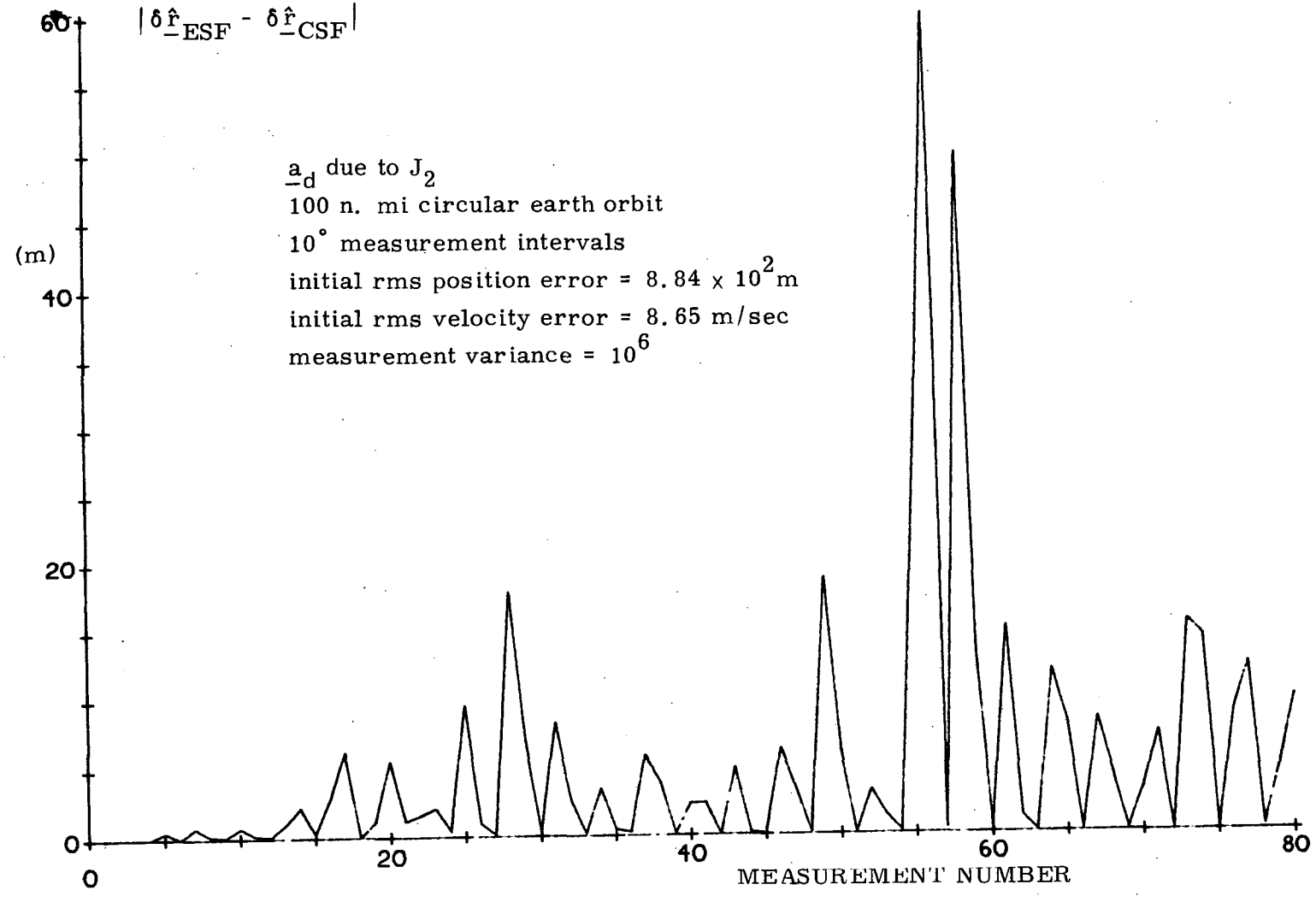

Figure 4.34 Magnitude of the difference between the estimated position deviation of the ESF and the CSF for a different Monte Carlo run

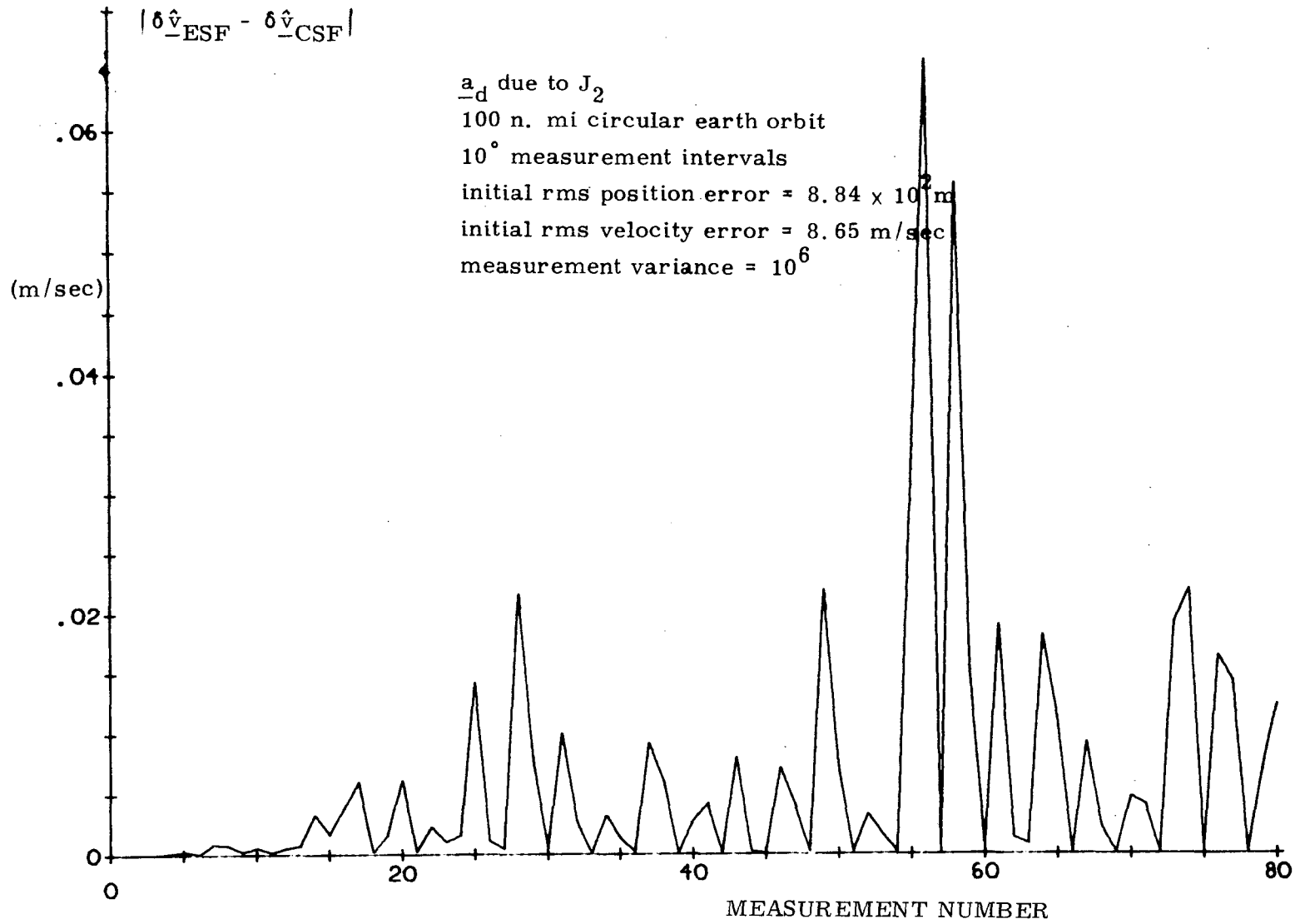

Figure 4.35 Magnitude of the difference between the estimated velocity deviation of the ESF and the CSF for a different Monte Carlo run

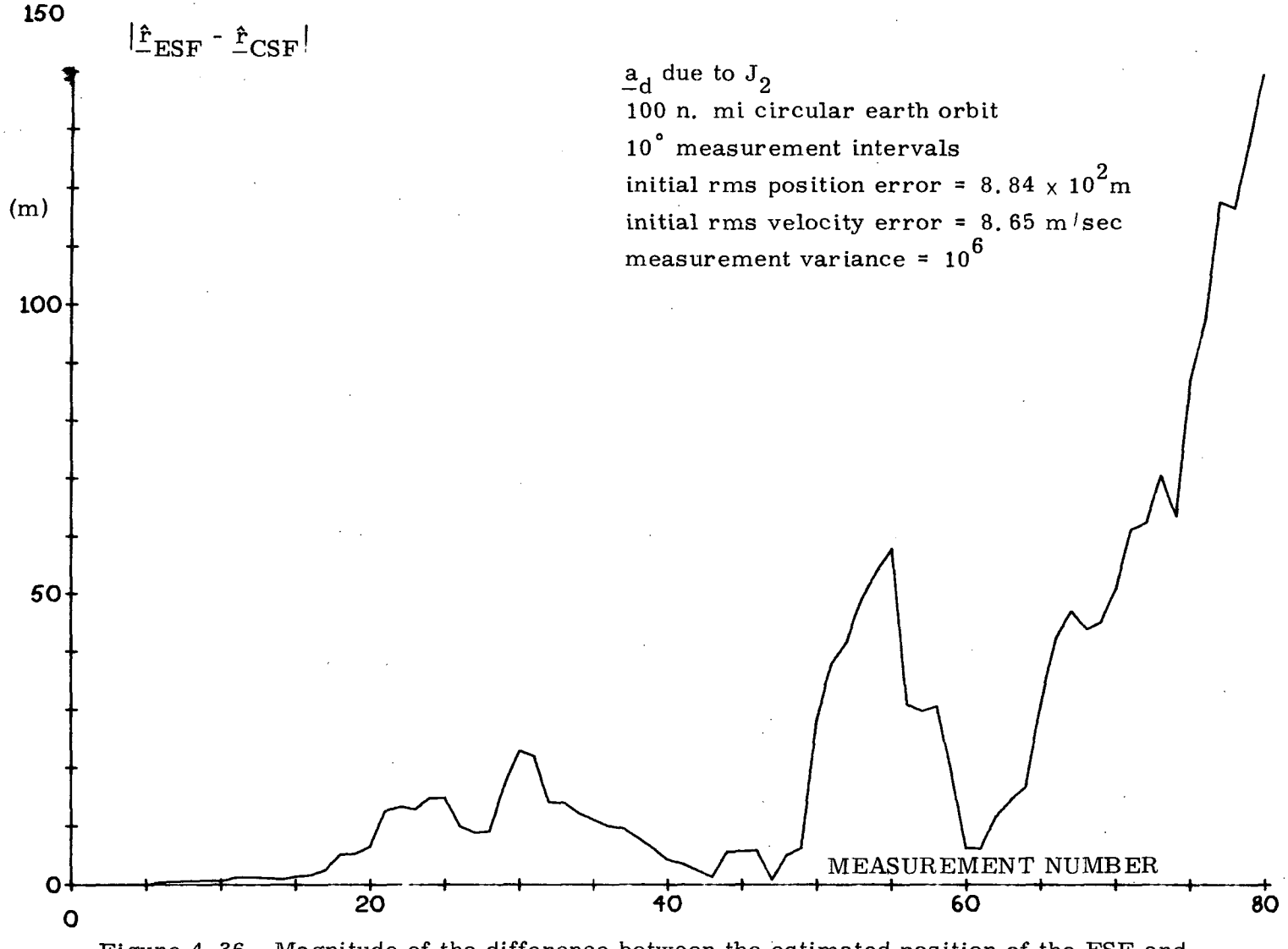

Figure 4.36 Magnitude of the difference between the estimated position of the ESF and the CSF for a different Monte Carlo run

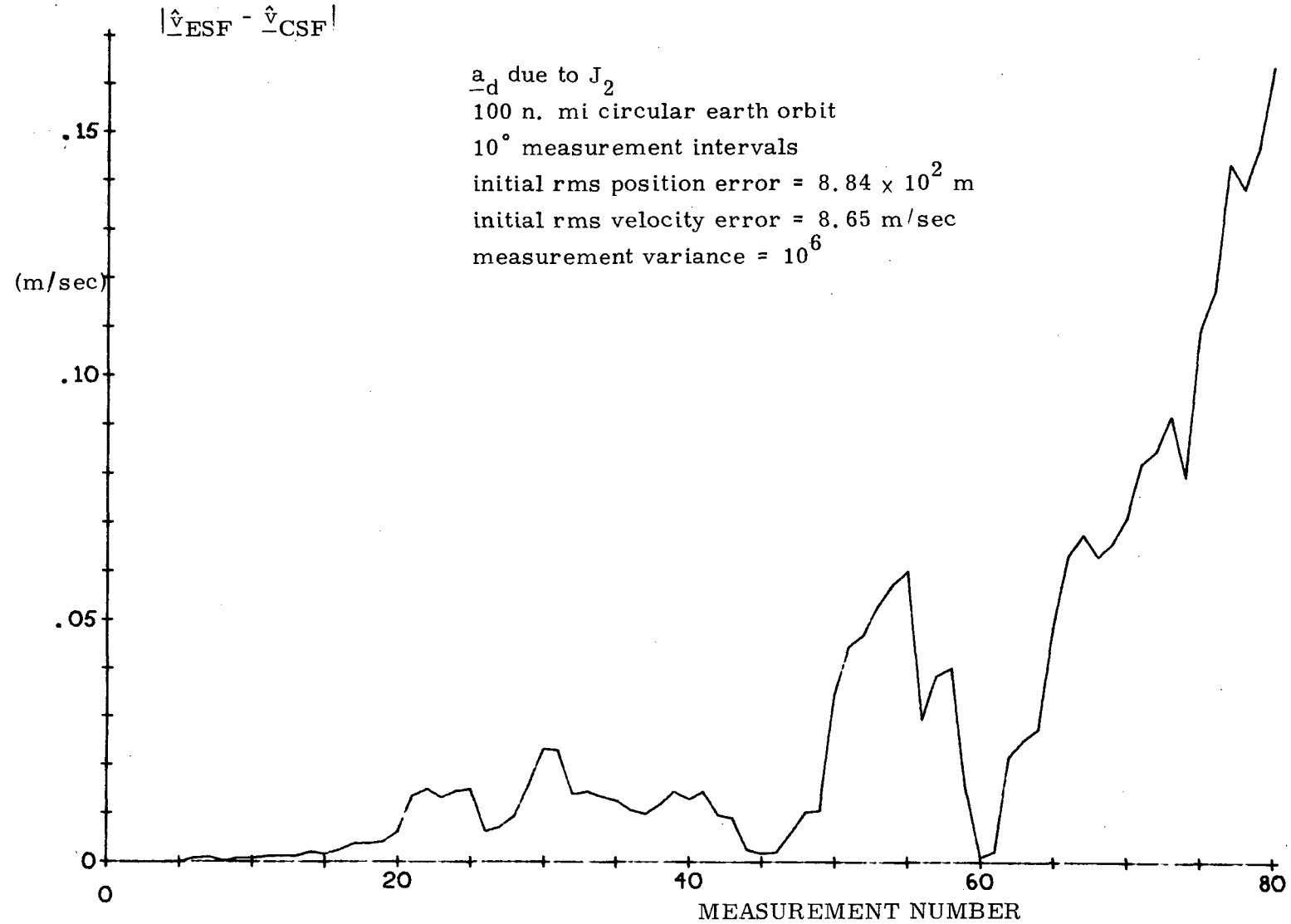

Figure 4.37 Magnitude of the difference between the estimated velocity of the ESF and the CSF for a different Monte Carlo run

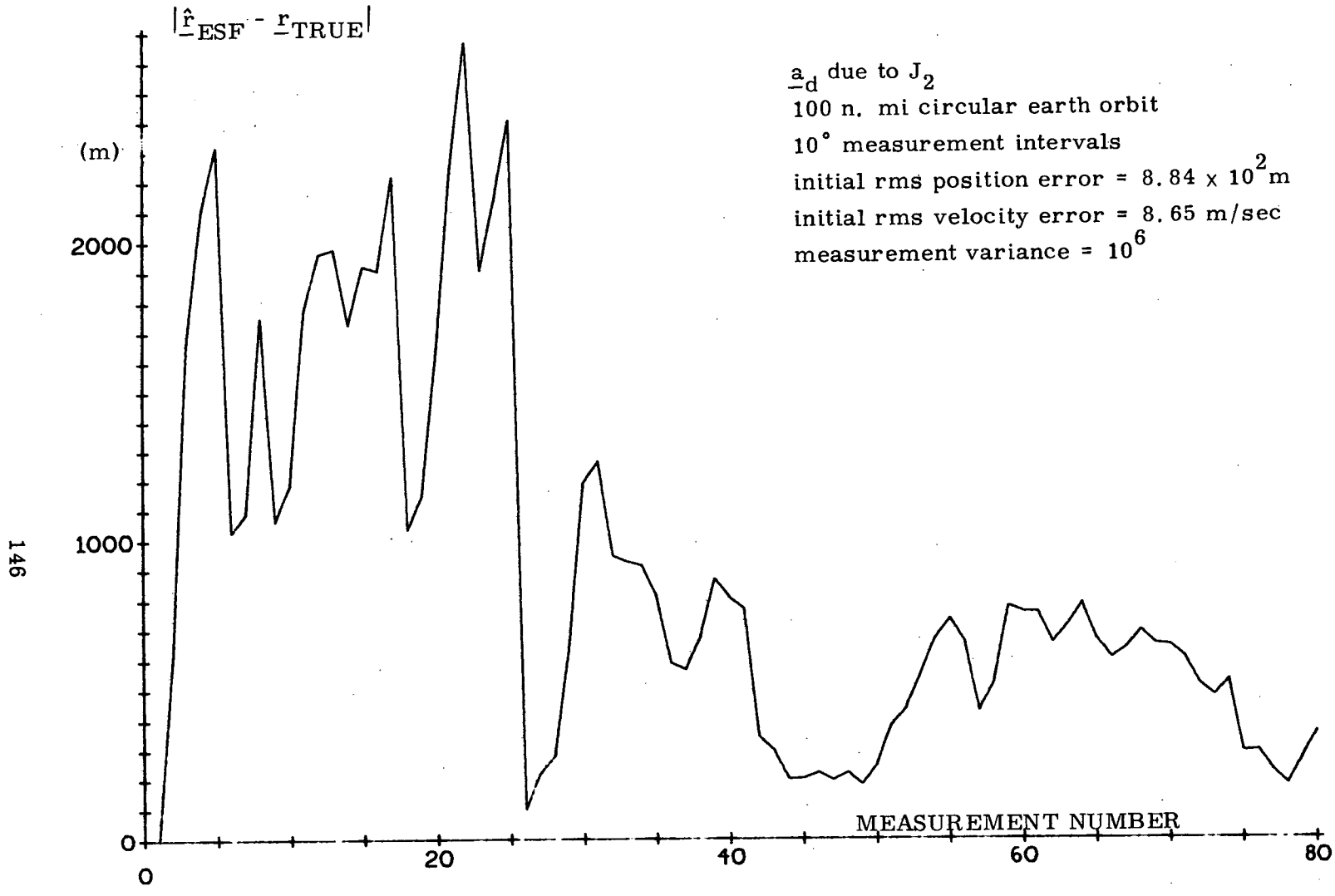

Figure 4.38 Magnitude of the actual error in the position estimate of the ESF for a different Monte Carlo run

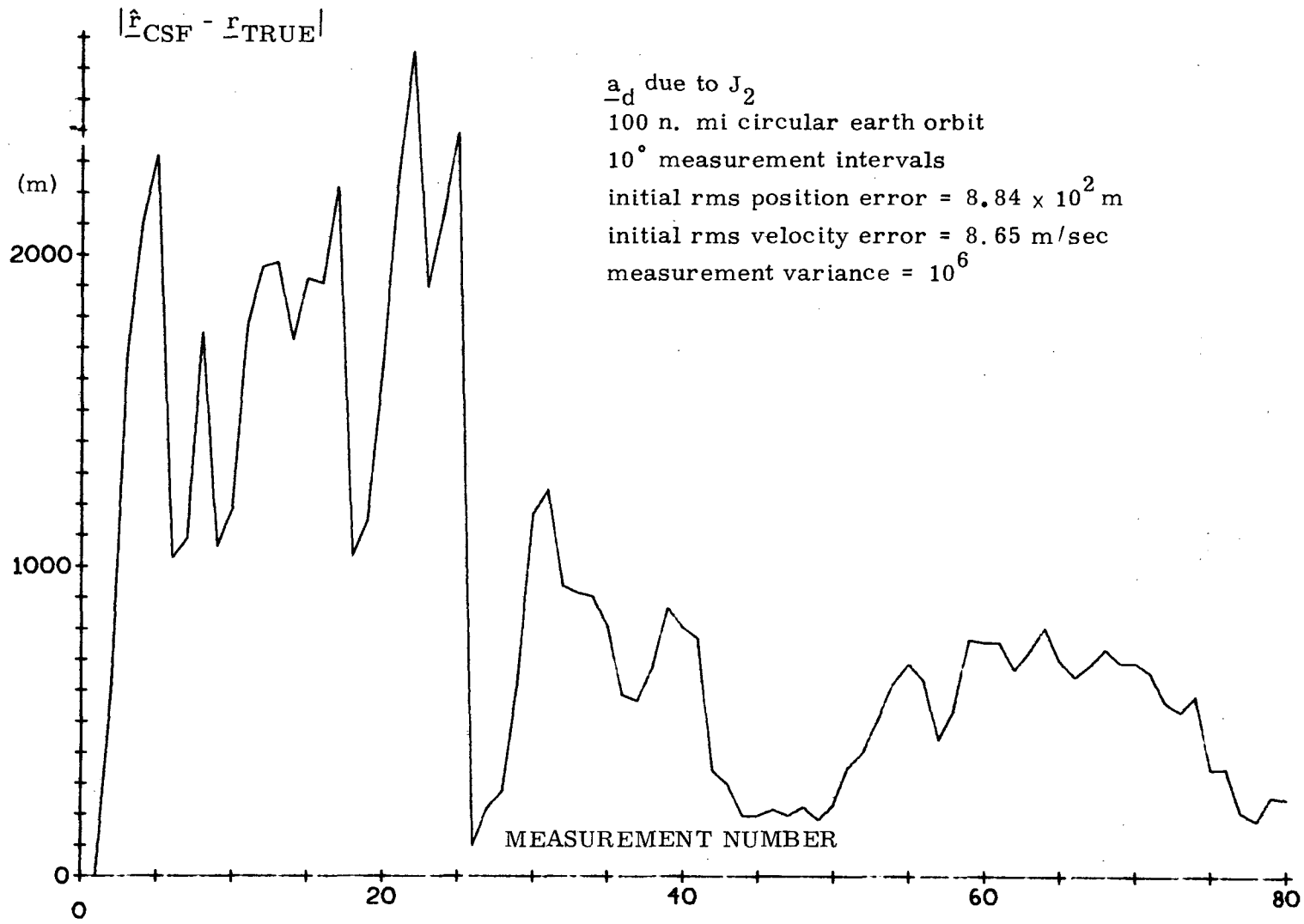

Figure 4.39 Magnitude of the actual error in the position error of the CSF for a different Monte Carlo run

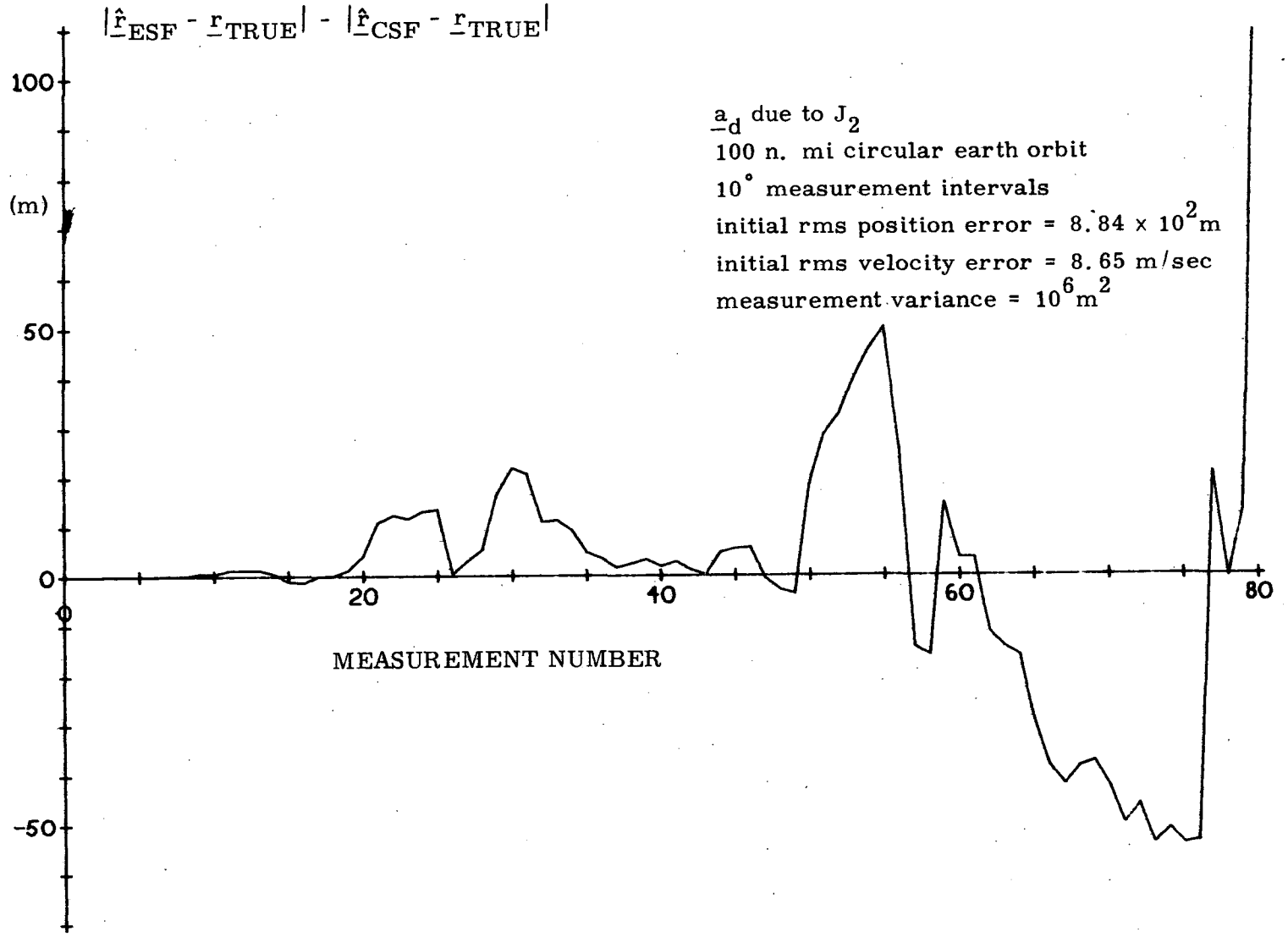

Figure 4.40 The difference between the actual position errors of both the ESF and the CSF for a different Monte Carlo run

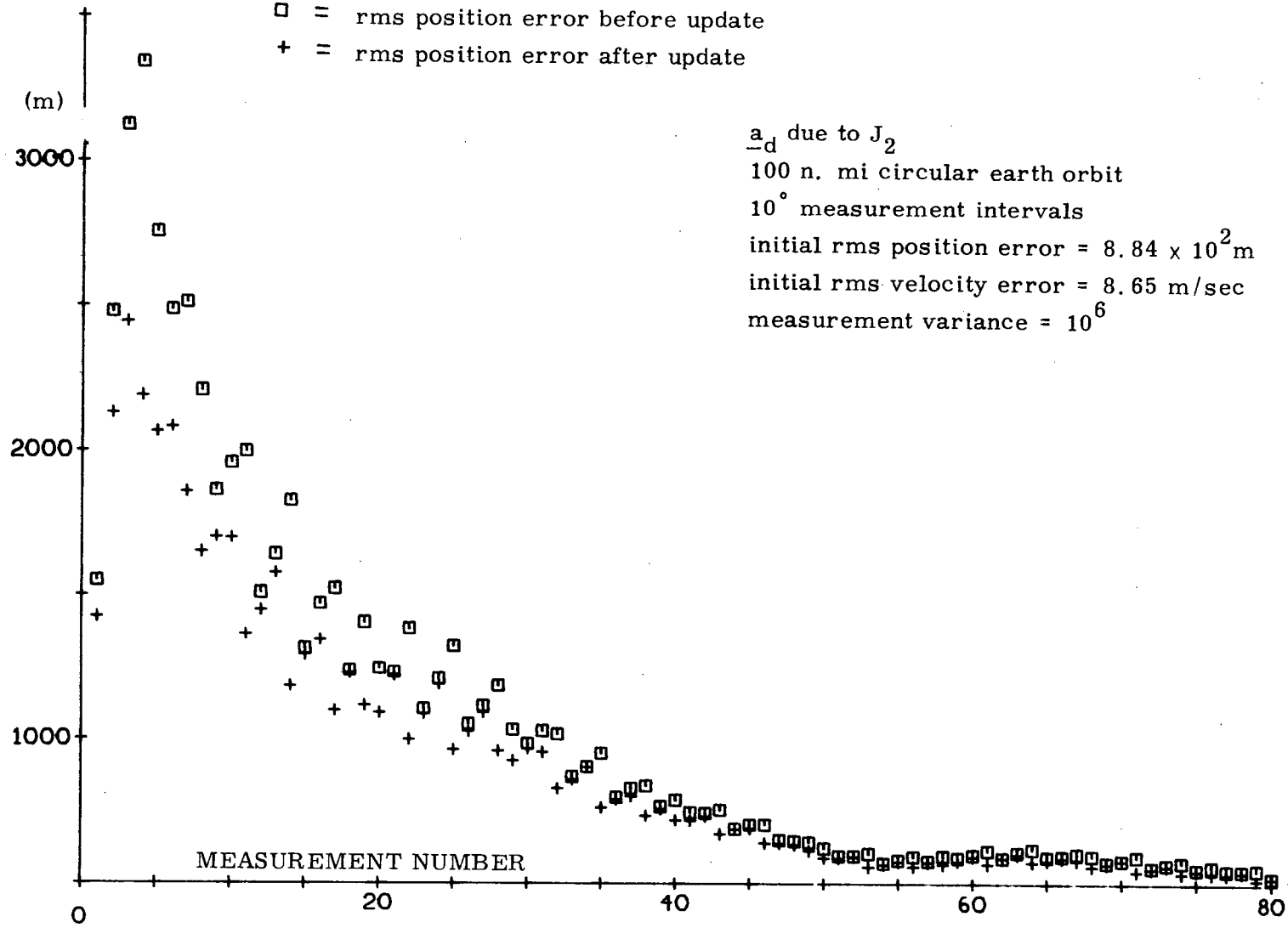

Figure 4.41 RMS estimated current position error for a different Monte Carlo run

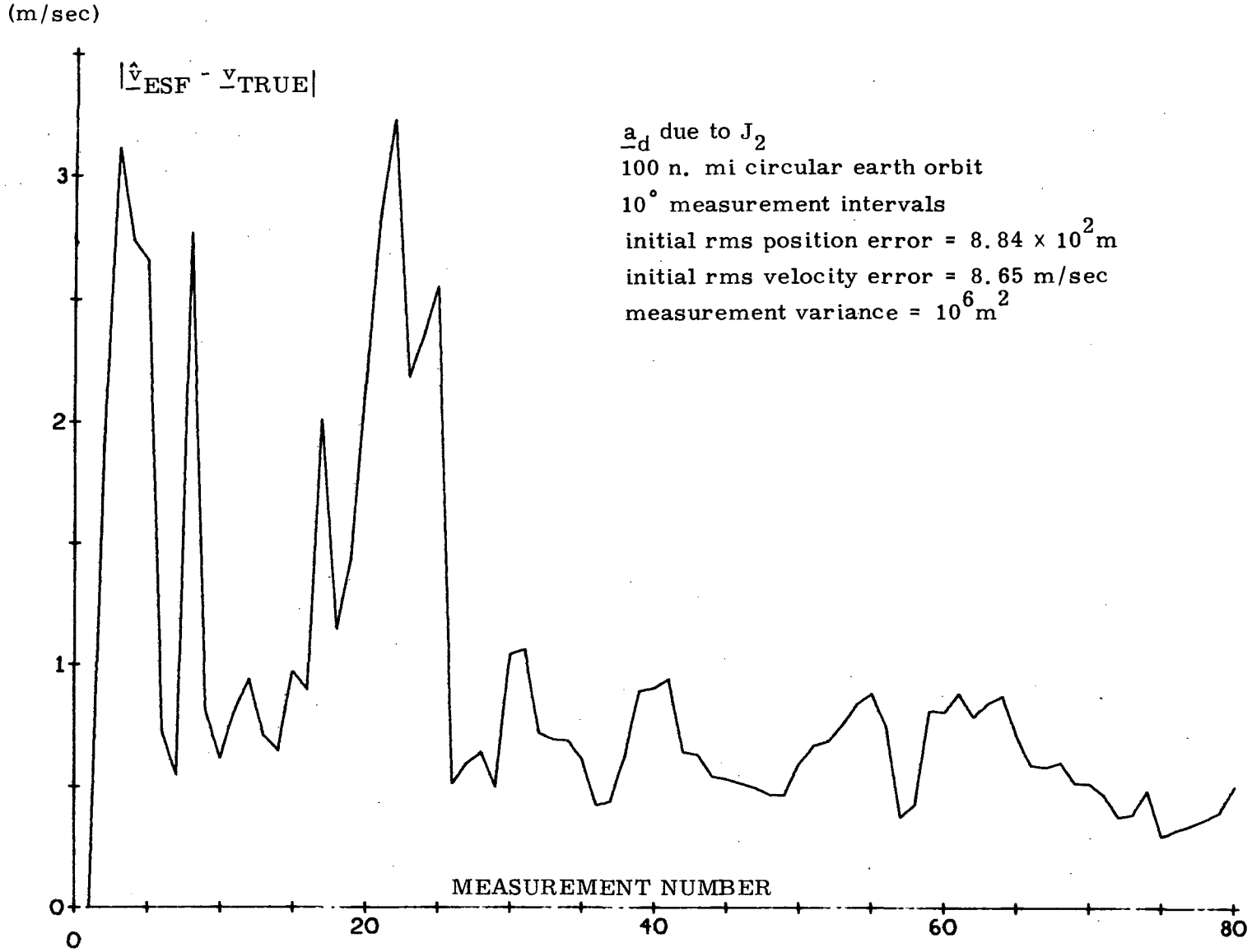

Figure 4.42 Magnitude of the actual error in the velocity estimate of the ESF for a different Monte Carlo run

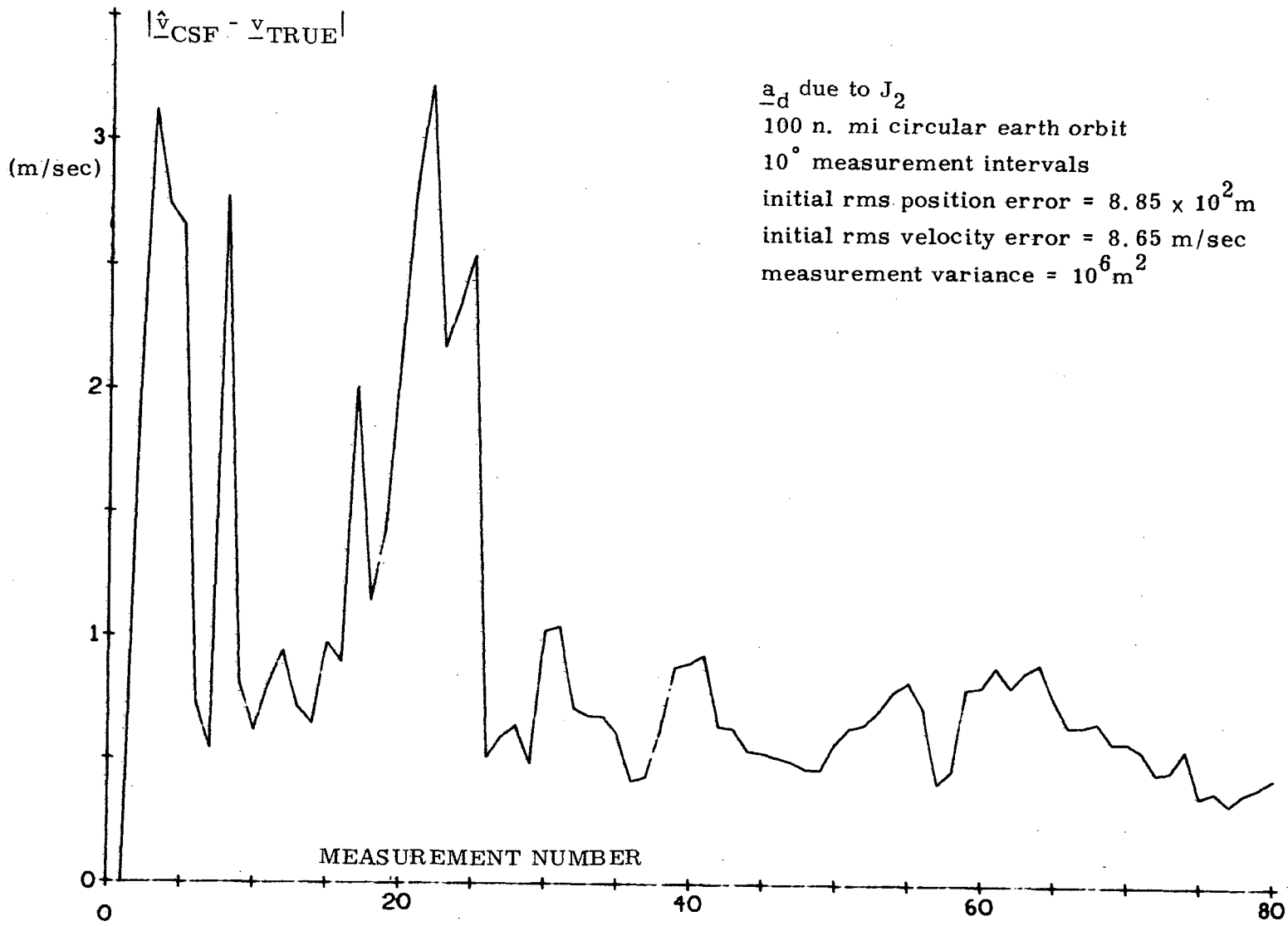

Figure 4.43 Magnitude of the actual error in the velocity estimate of the CSF for a different Monte Carlo run

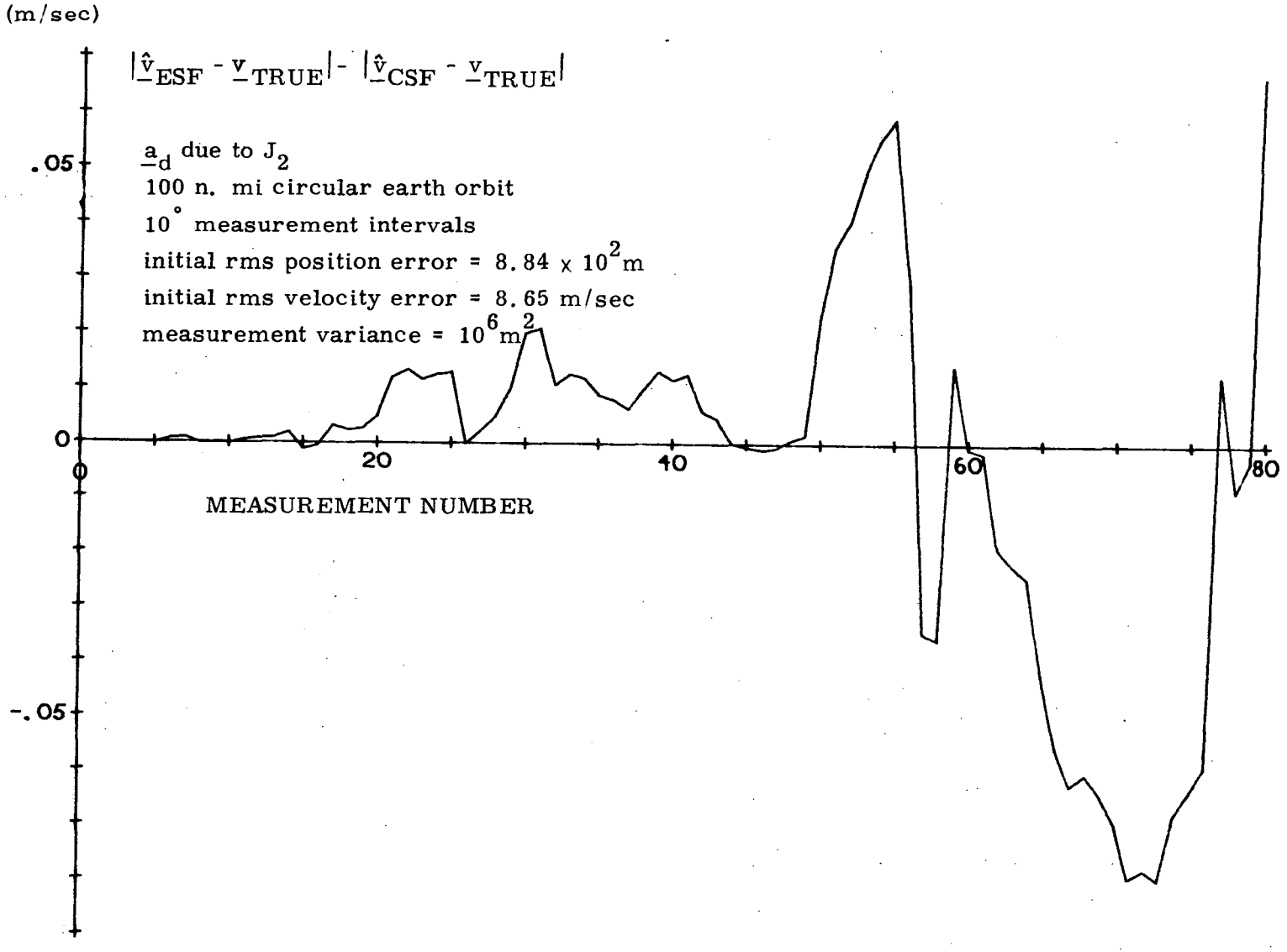

Figure 4.44 The difference between the actual velocity error of both the ESF and the CSF for a different Monte Carlo run

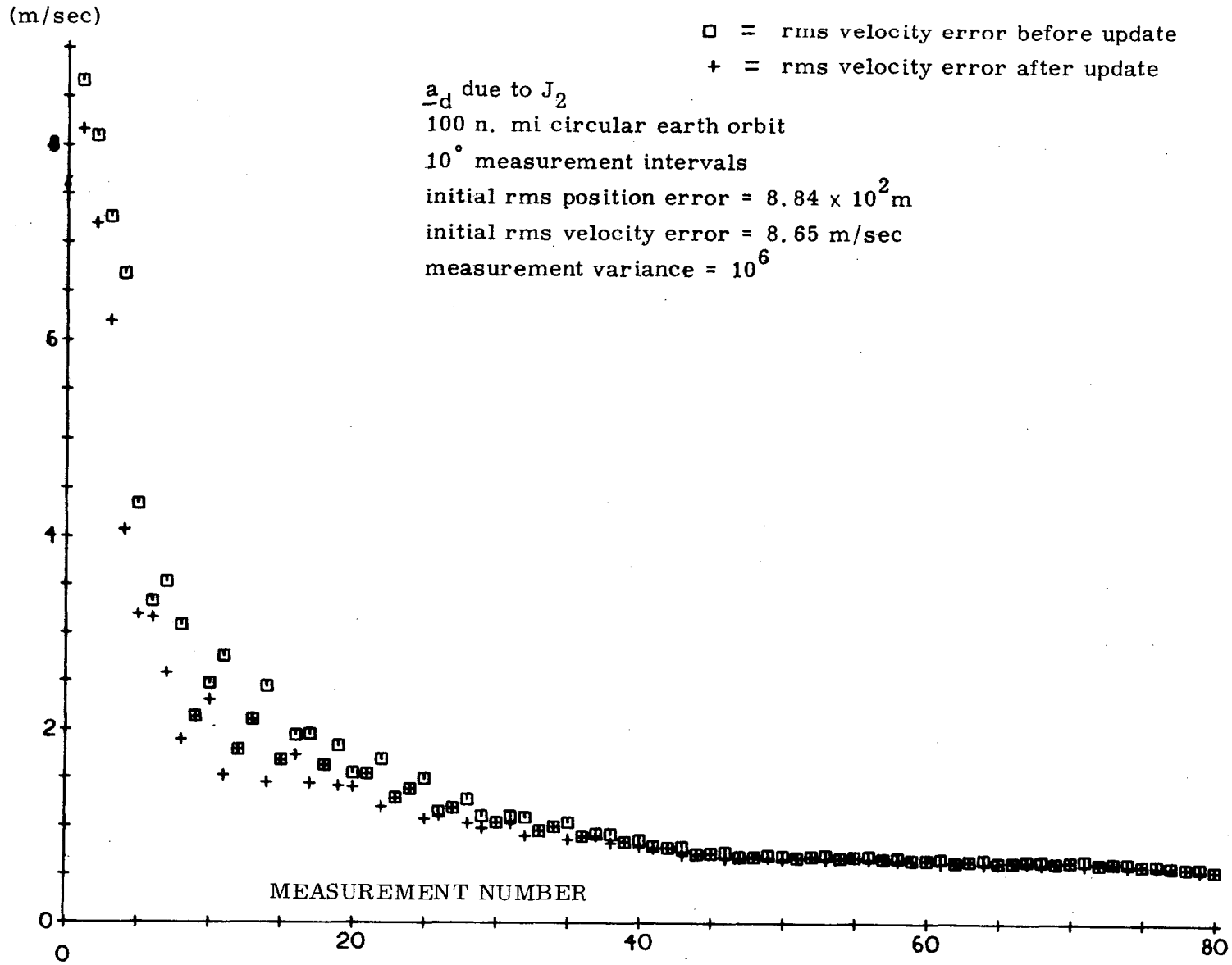

Figure 4.45 RMS estimated current velocity error for a different Monte Carlo run

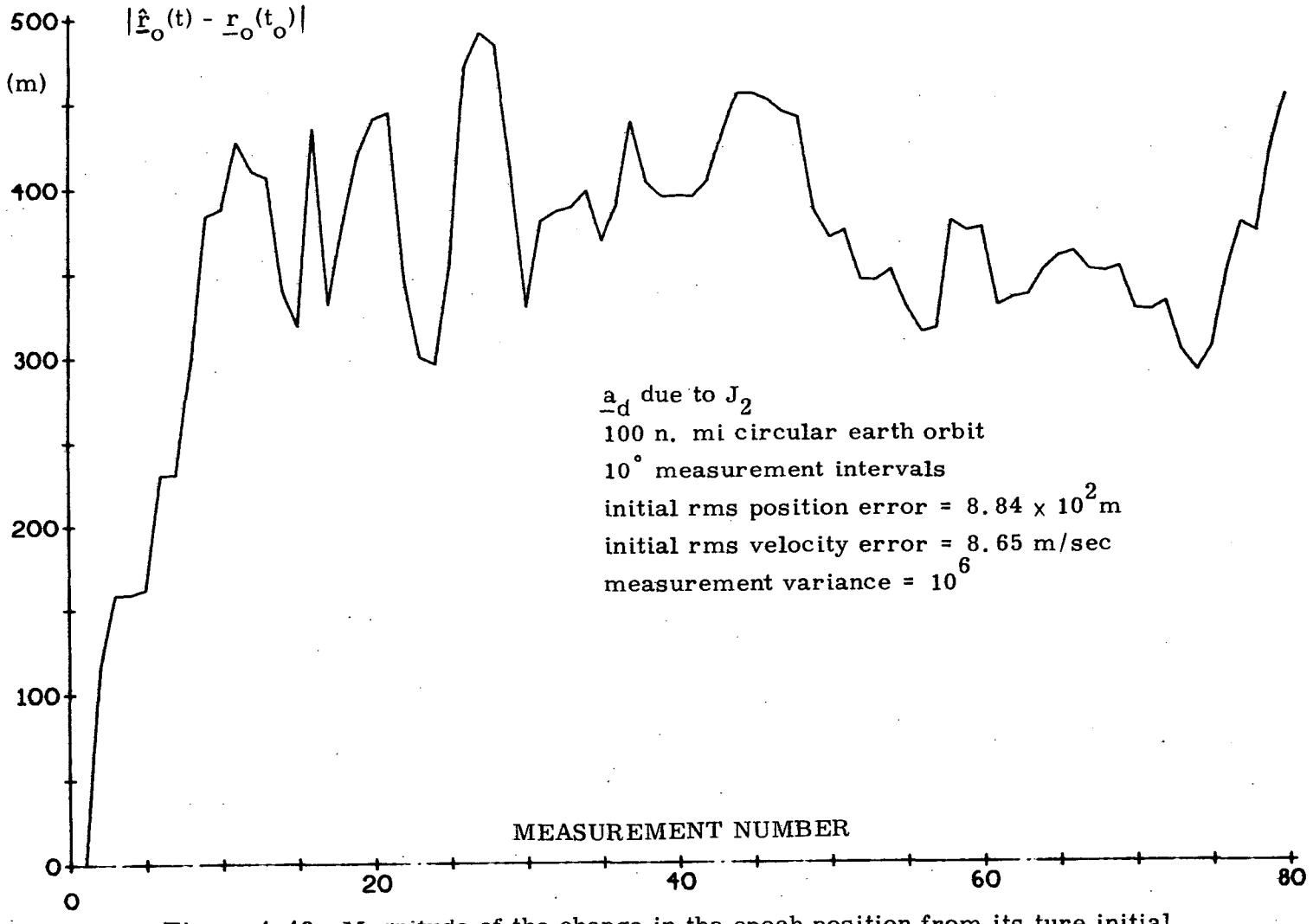

Figure 4.46 Magnitude of the change in the epoch position from its ture initial value for a different Monte Carlo run

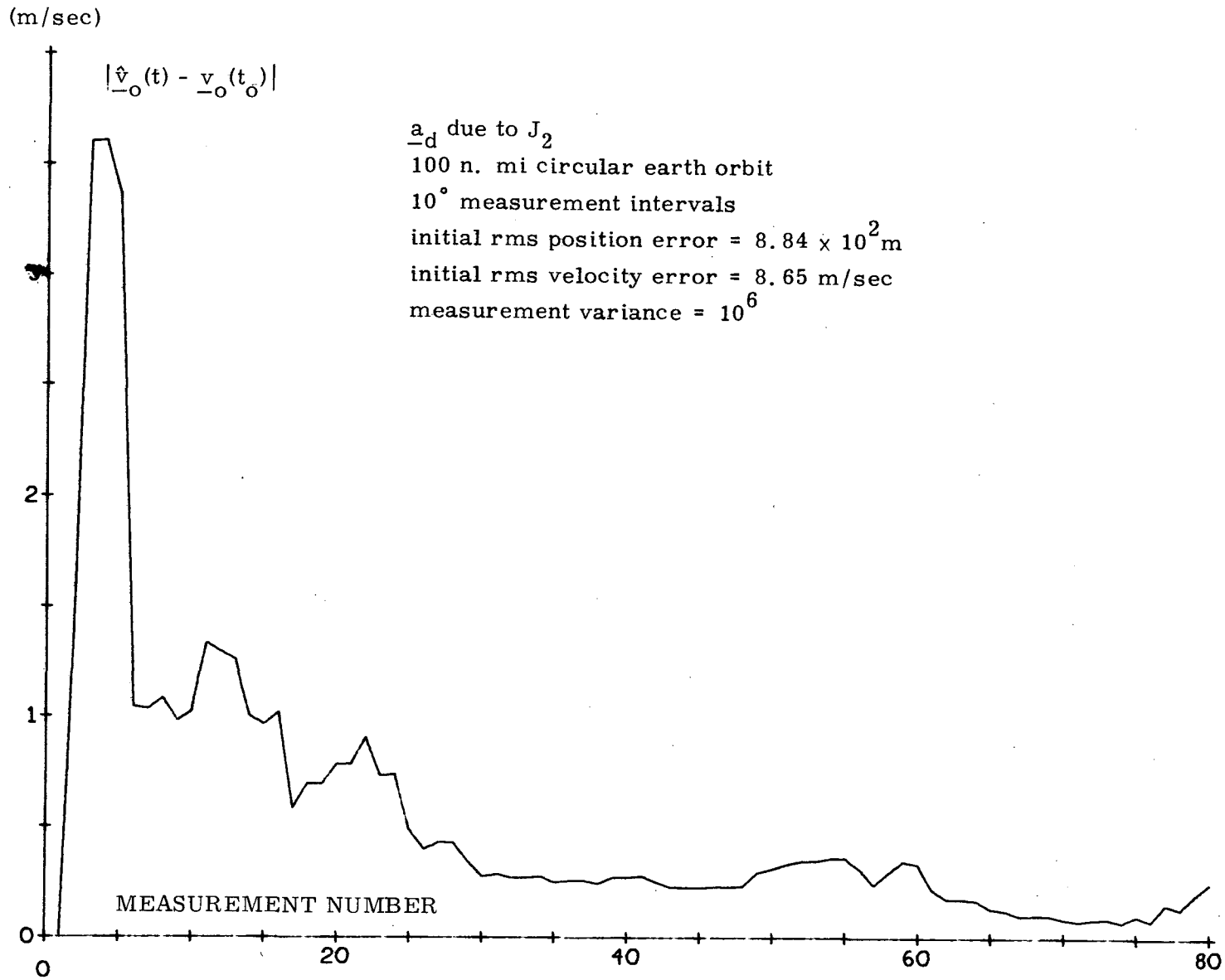

Figure 4.47 Magnitude of the change in the epoch velocity from its ture initial value for a different Monte Carlo run

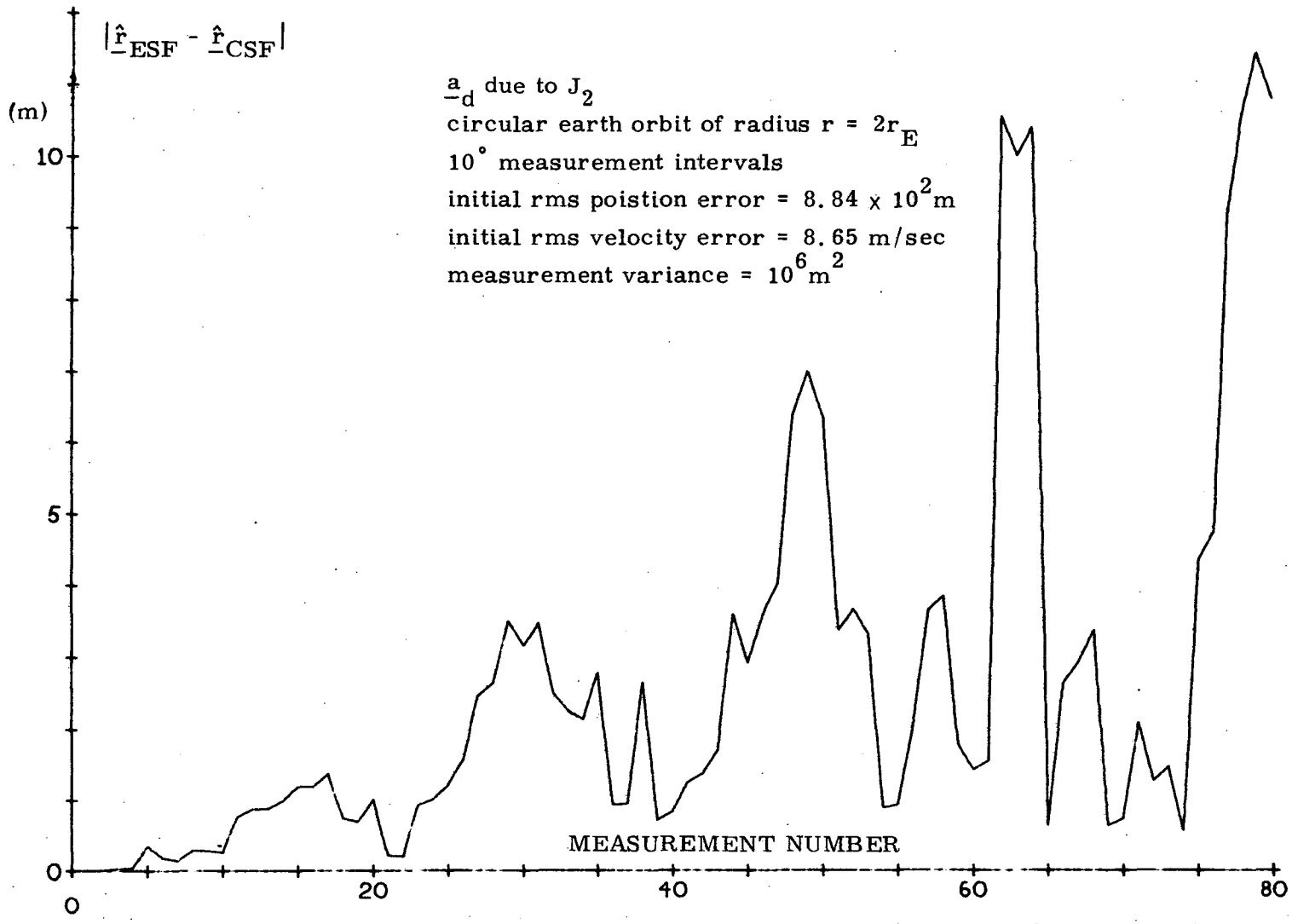

Figure 4.48 Magnitude of the difference between the estimated position of the ESF and the CSF for one Monte Carlo run

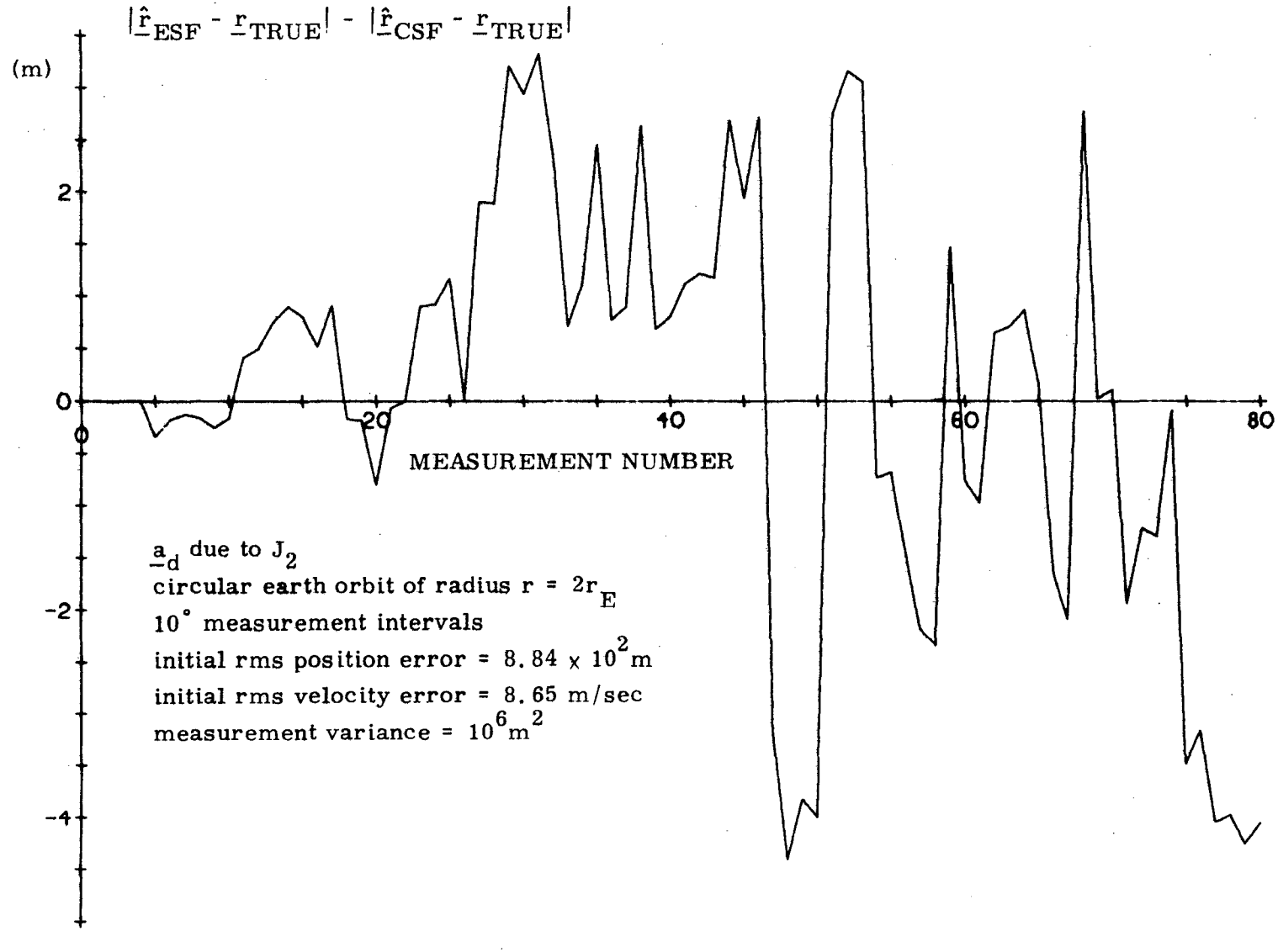

Fig. 4.49 The difference between the actual position error of both the ESF and the CSF one Monte Carlo run

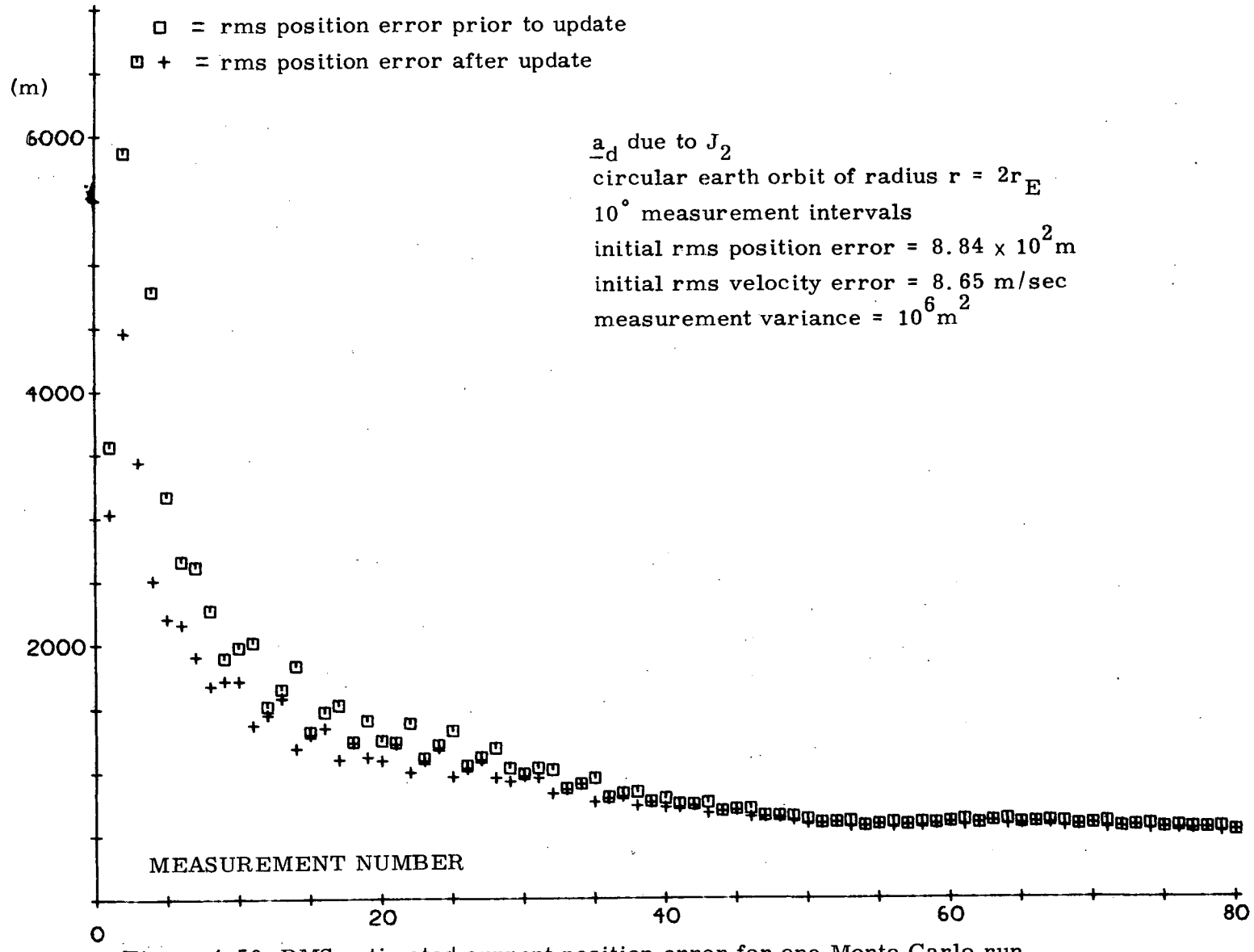

Figure 4.50 RMS estimated current position error for one Monte Carlo run

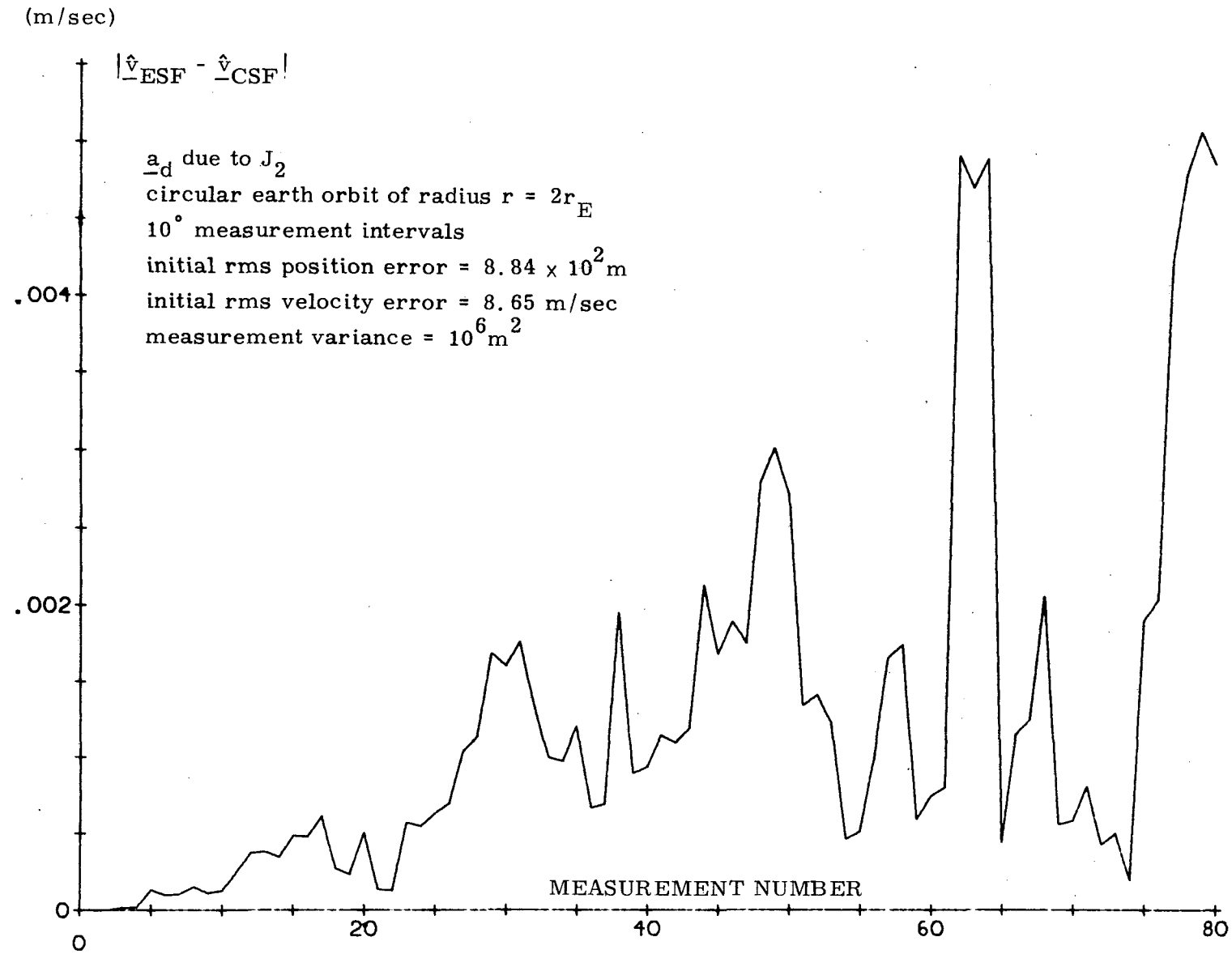

Figure 4.51 Magnitude of the difference between the estimated velocity of the ESF and the CSF for one Monte Carlo run

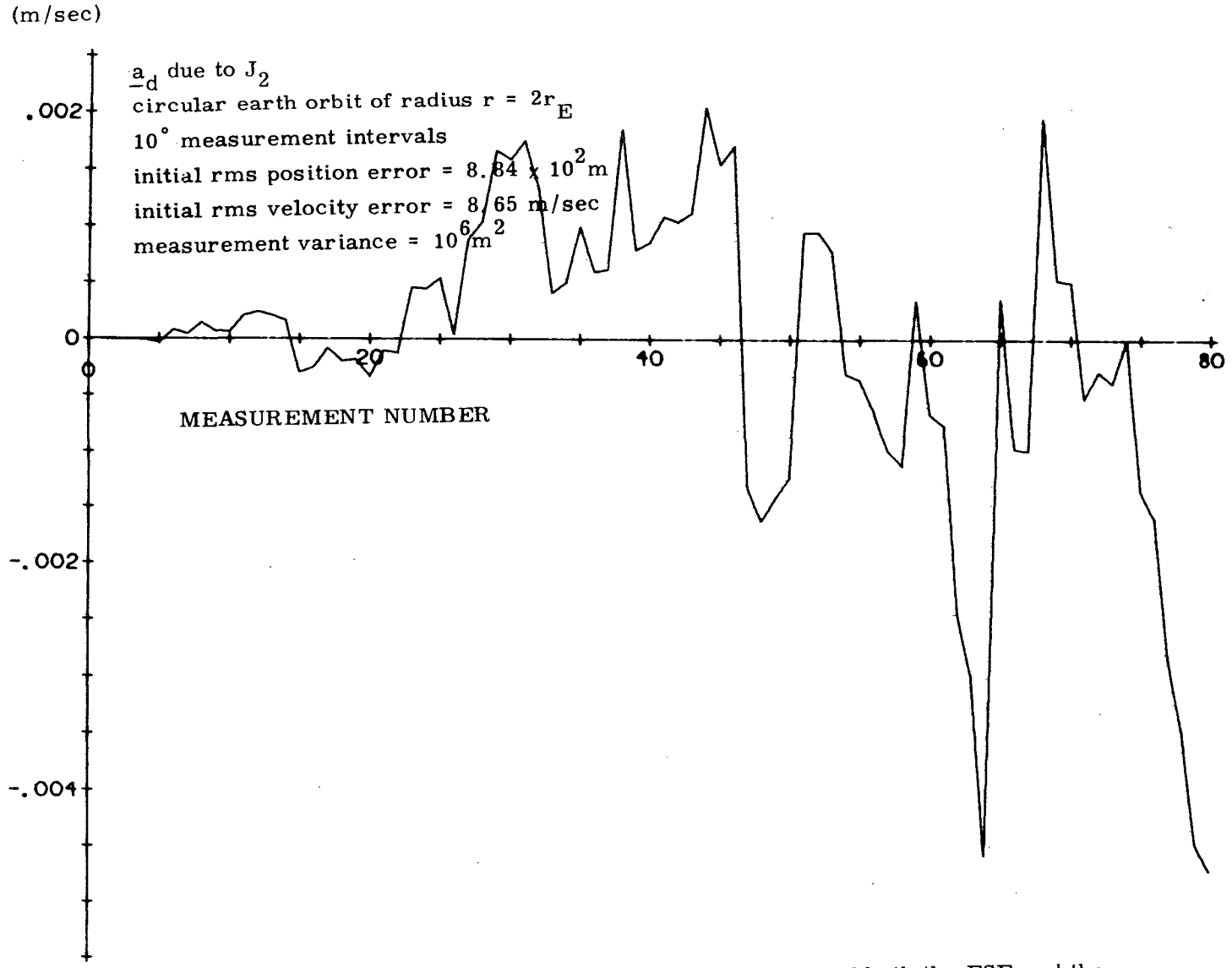

Figure 4.52 The difference between the actual velocity error of both the ESF and the CSF for one Monte Carlo run

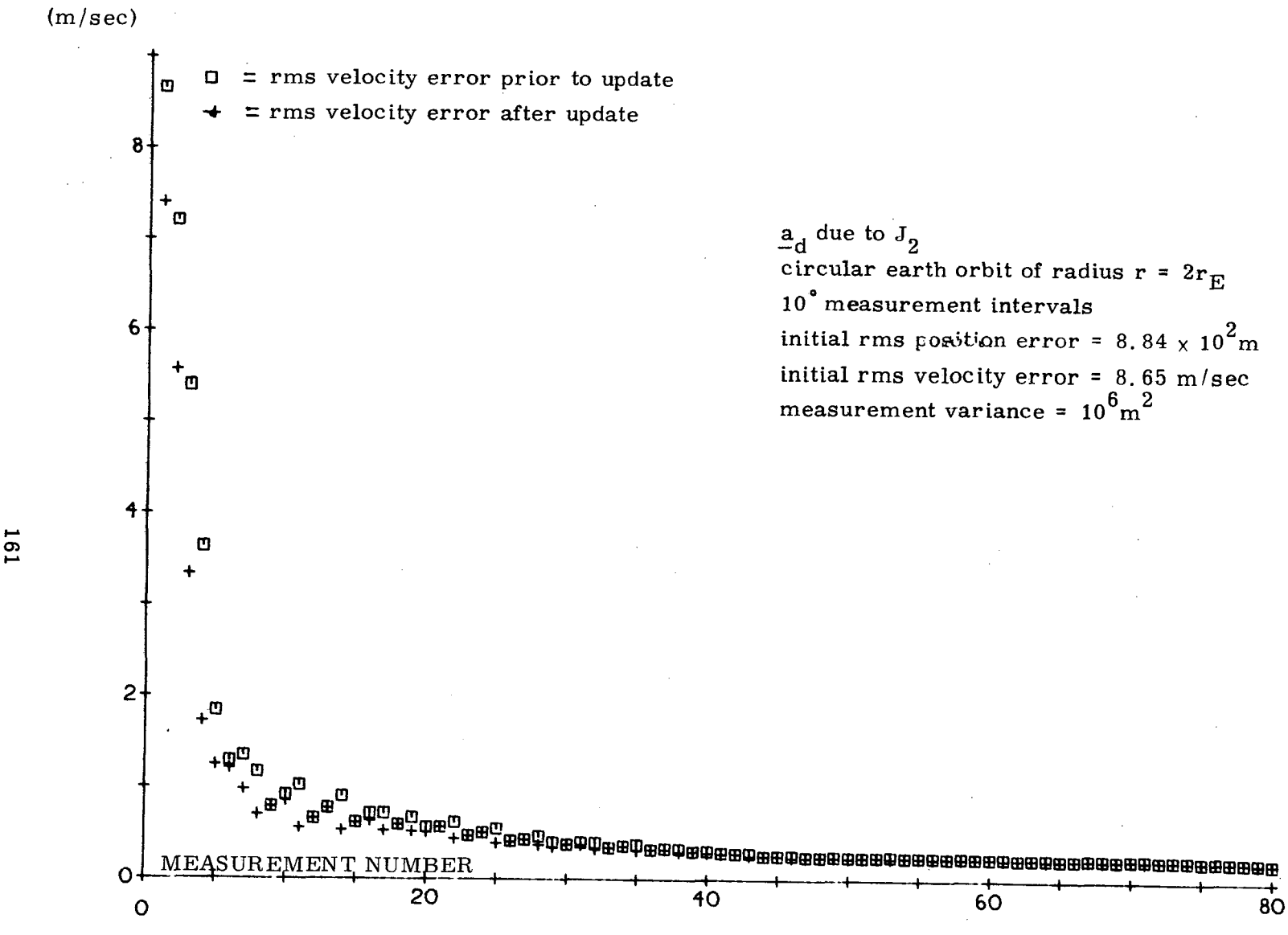

Figure 4.53 RMS estimated current velocity deviation error for one Monte Carlo run

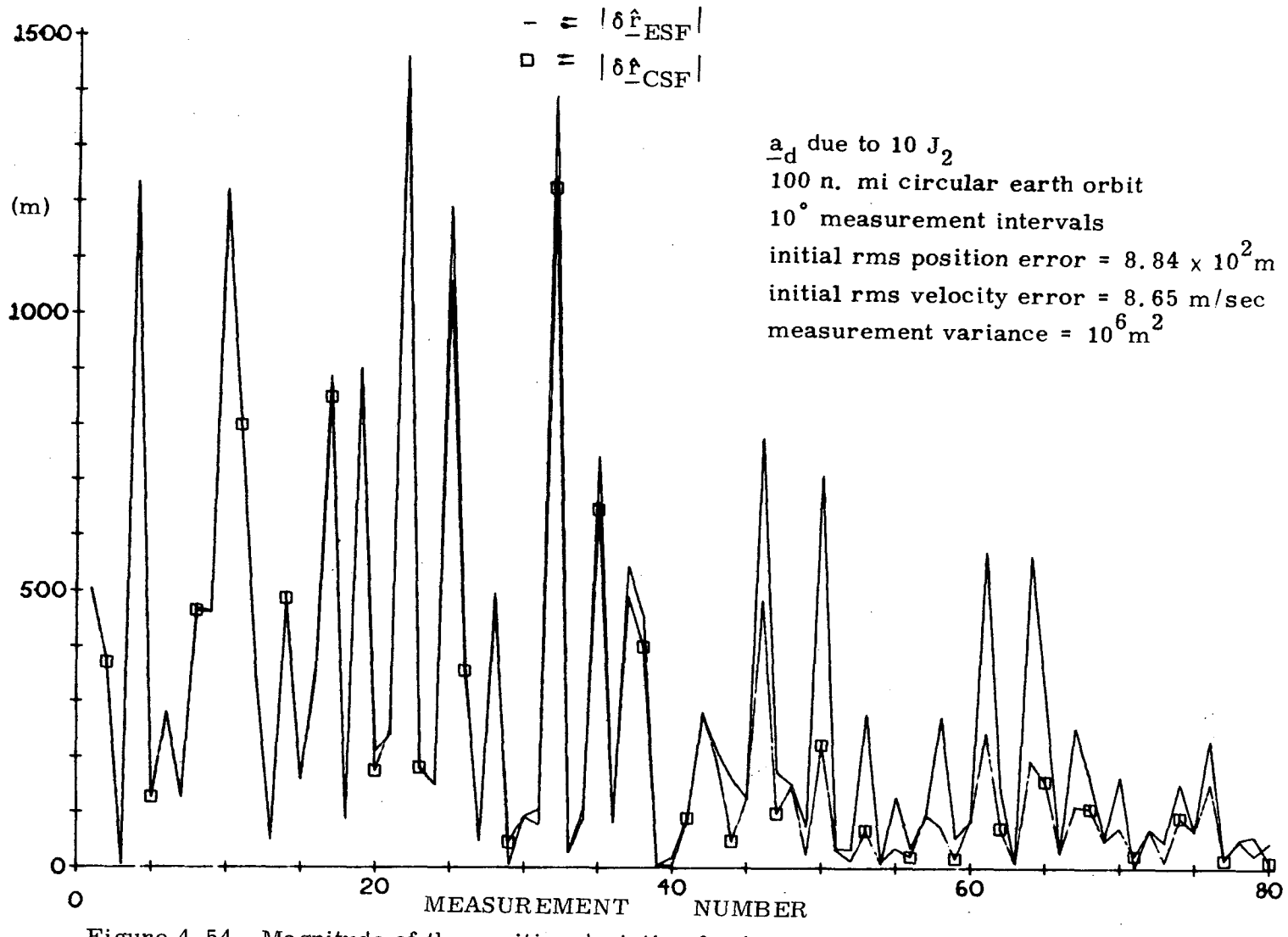

Figure 4.54 Magnitude of the position deviation for both the ESF and the CSF for one Monte Carlo run

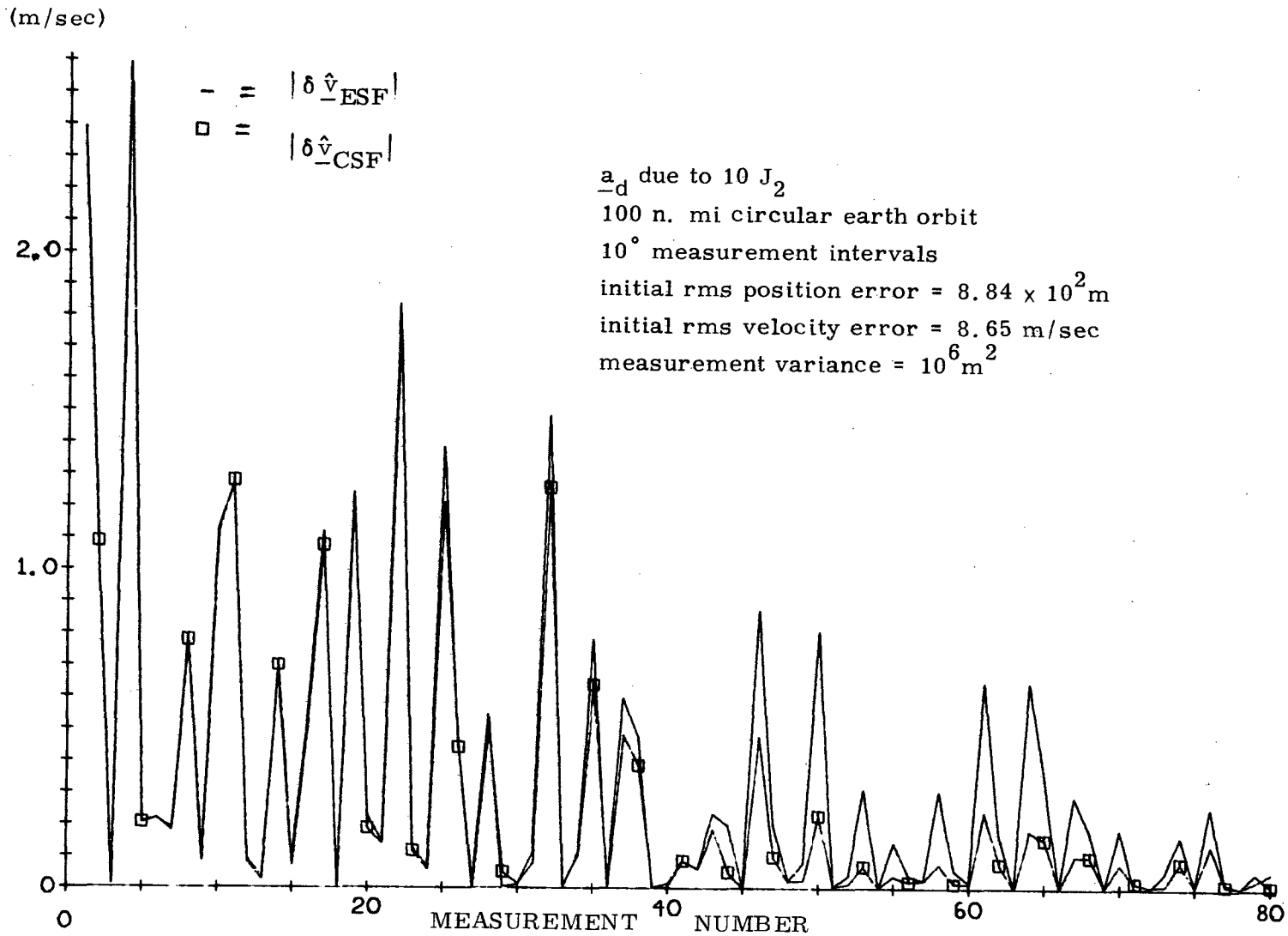

Figure 4.55 Magnitude of the velocity deviation for both the ESF and the CSF for one Monte Carlo run

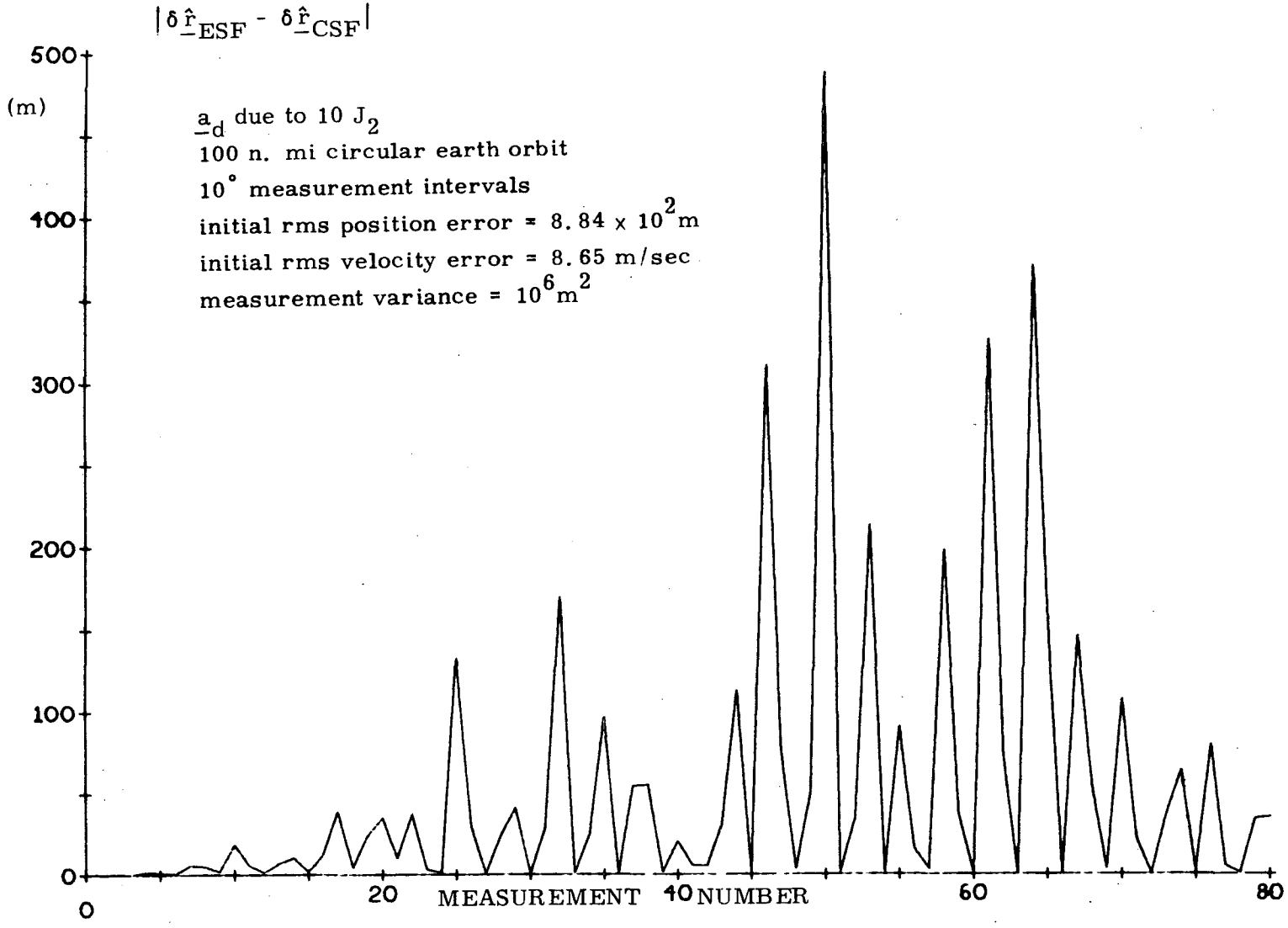

Figure 4.56 Magnitude of the difference between the estimated position deviation of the ESF and the CSF for one Monte Carlo run

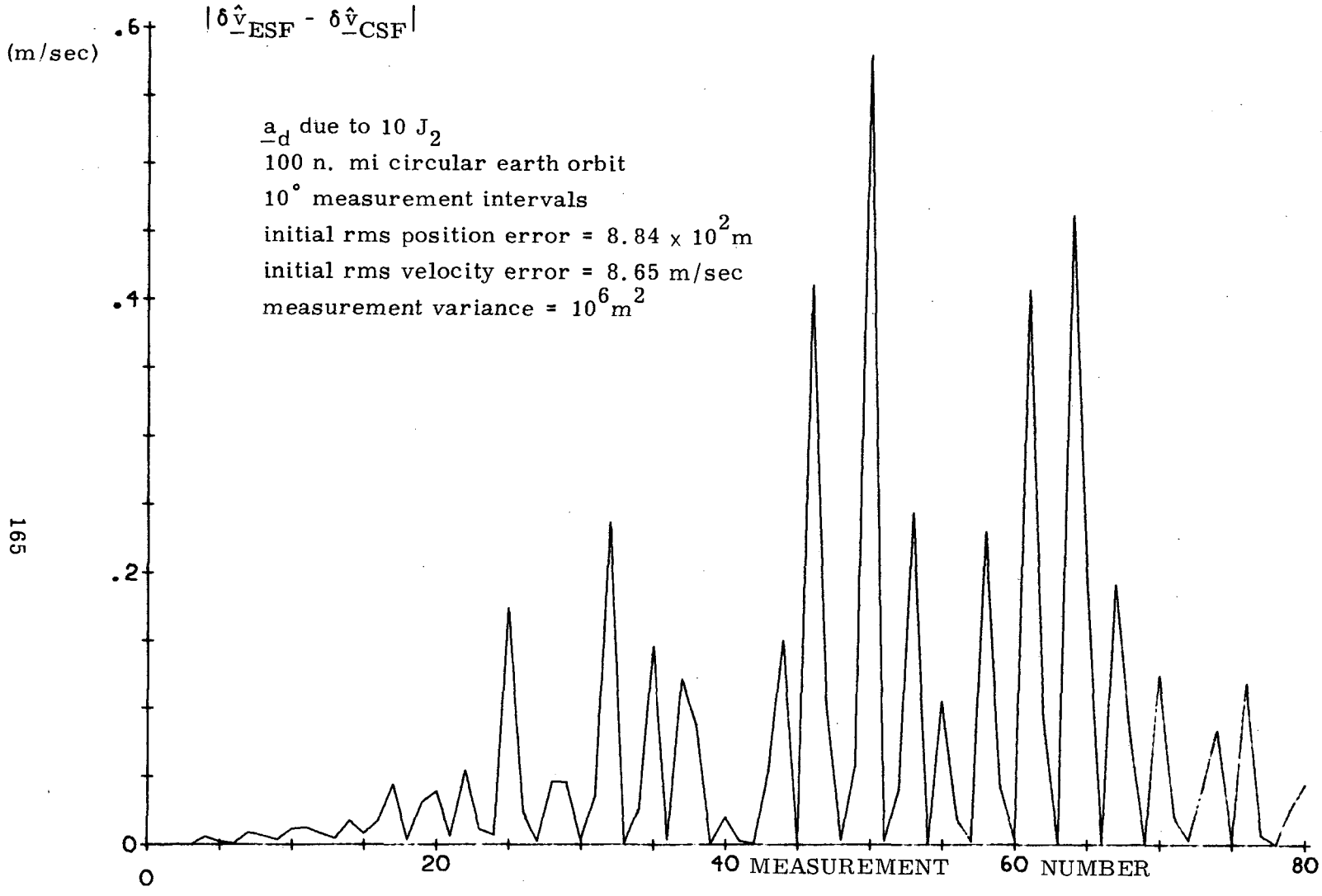

Figure 4.57 Magnitude of the difference between the estimated velocity deviation of the ESF and the CSF for one Monte Carlo run

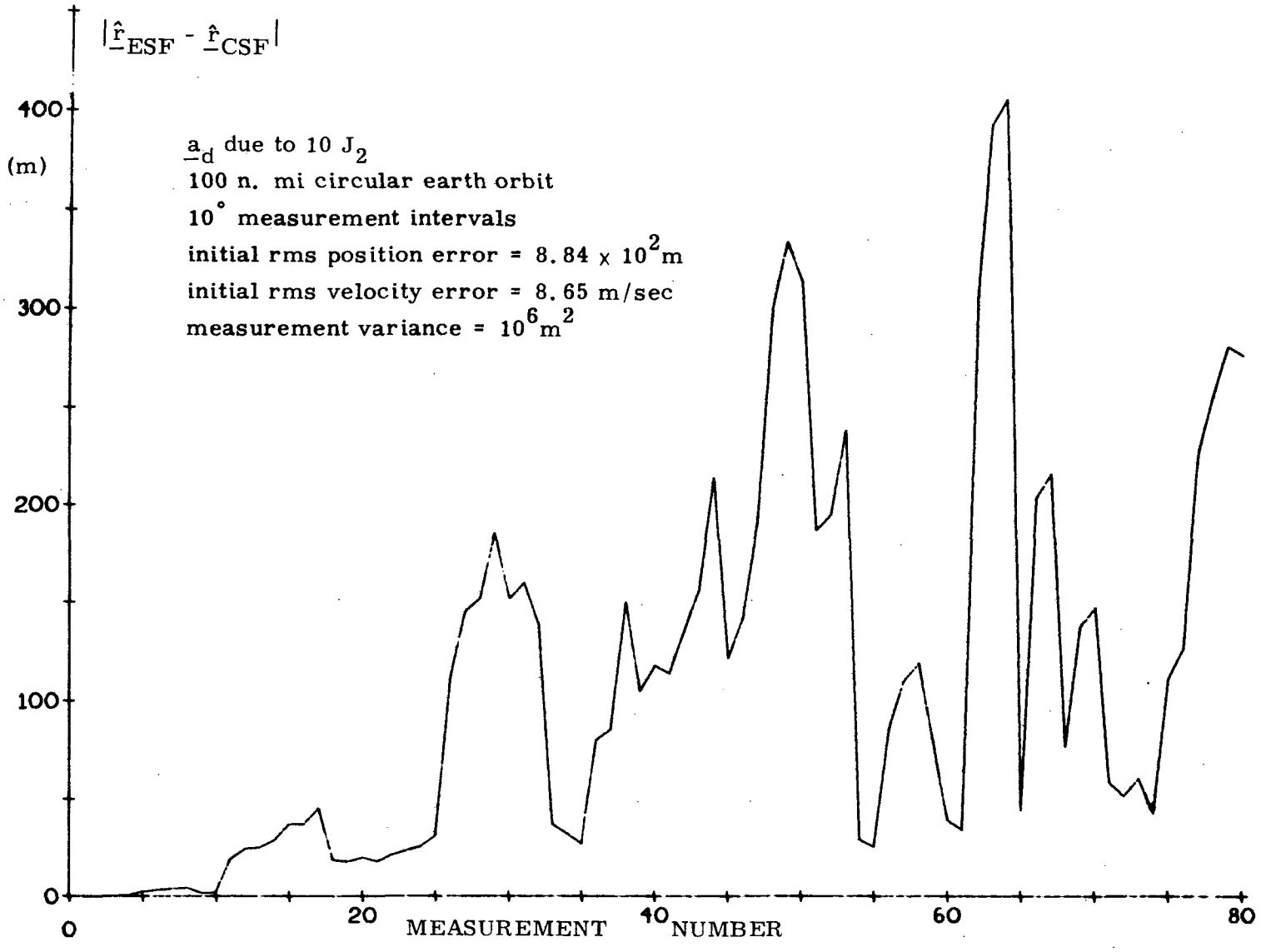

Figure 4.58 Magnitude of the difference between the estimated position of the ESF and the CSF for one Monte Carlo run

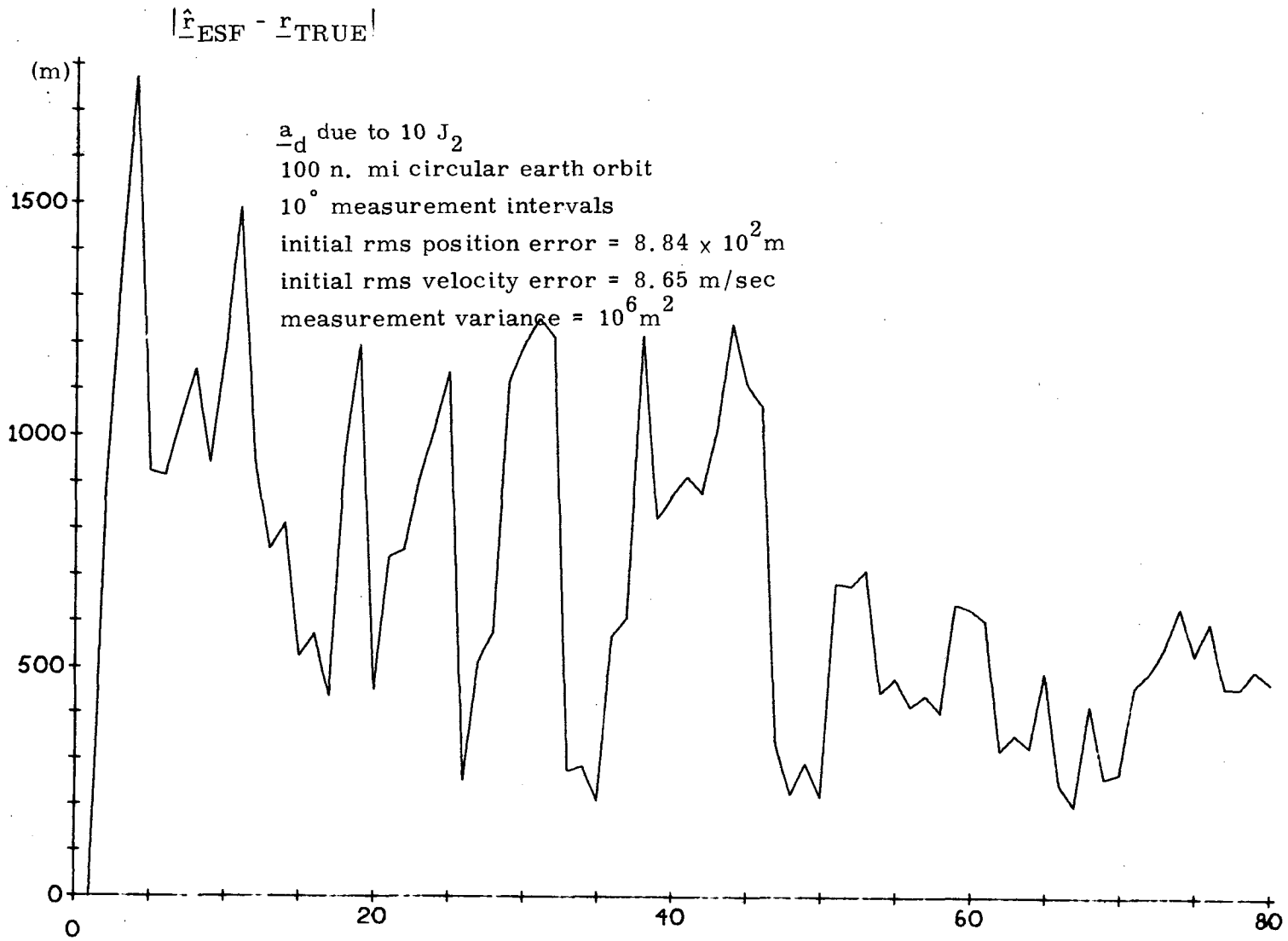

Figure 4.59 Magnitude of the actual error in the position estimate of the ESF for one Monte Carlo run

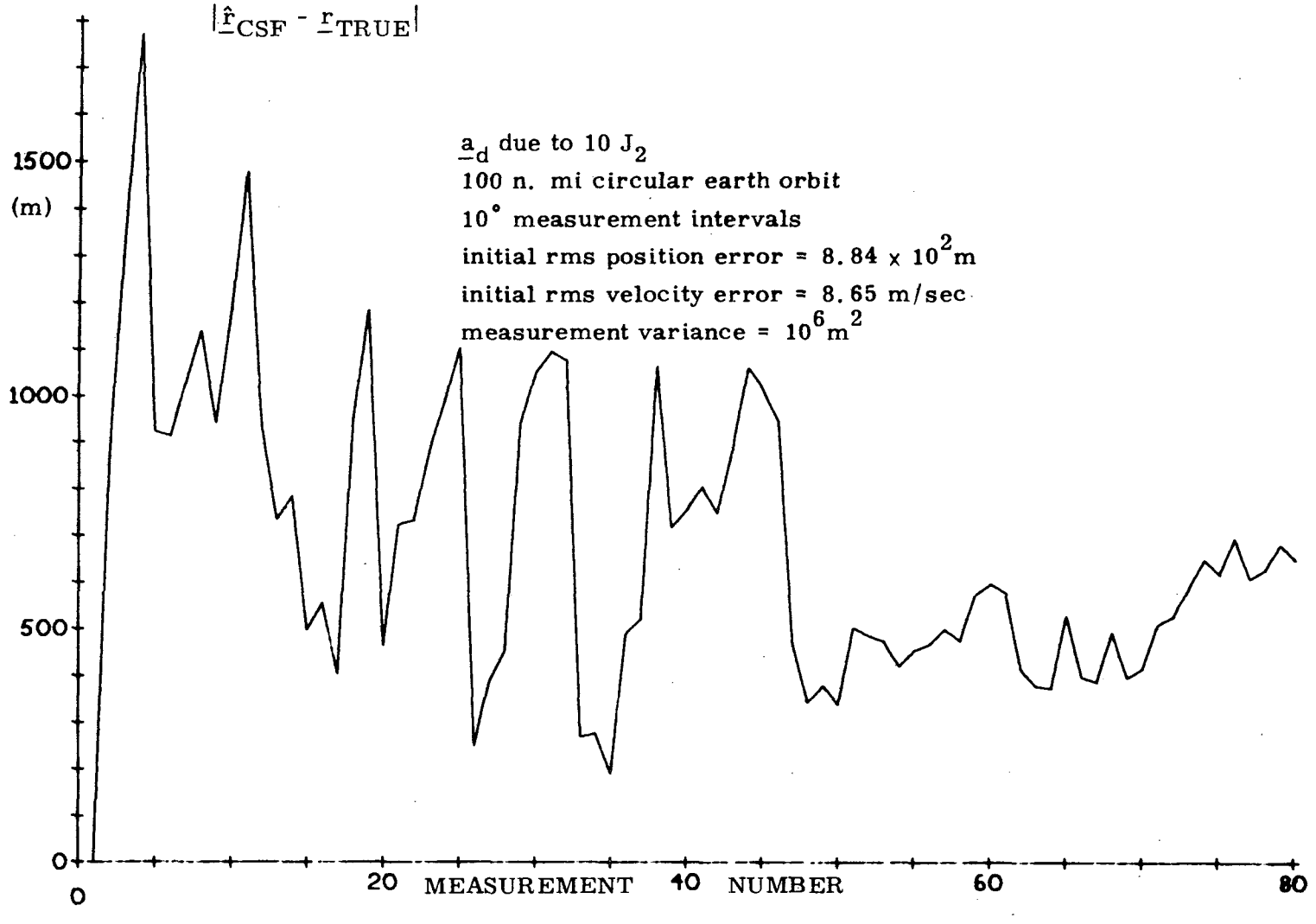

Figure 4.60 Magnitude of the actual error in the position error of the CSF for one Monte Carlo run

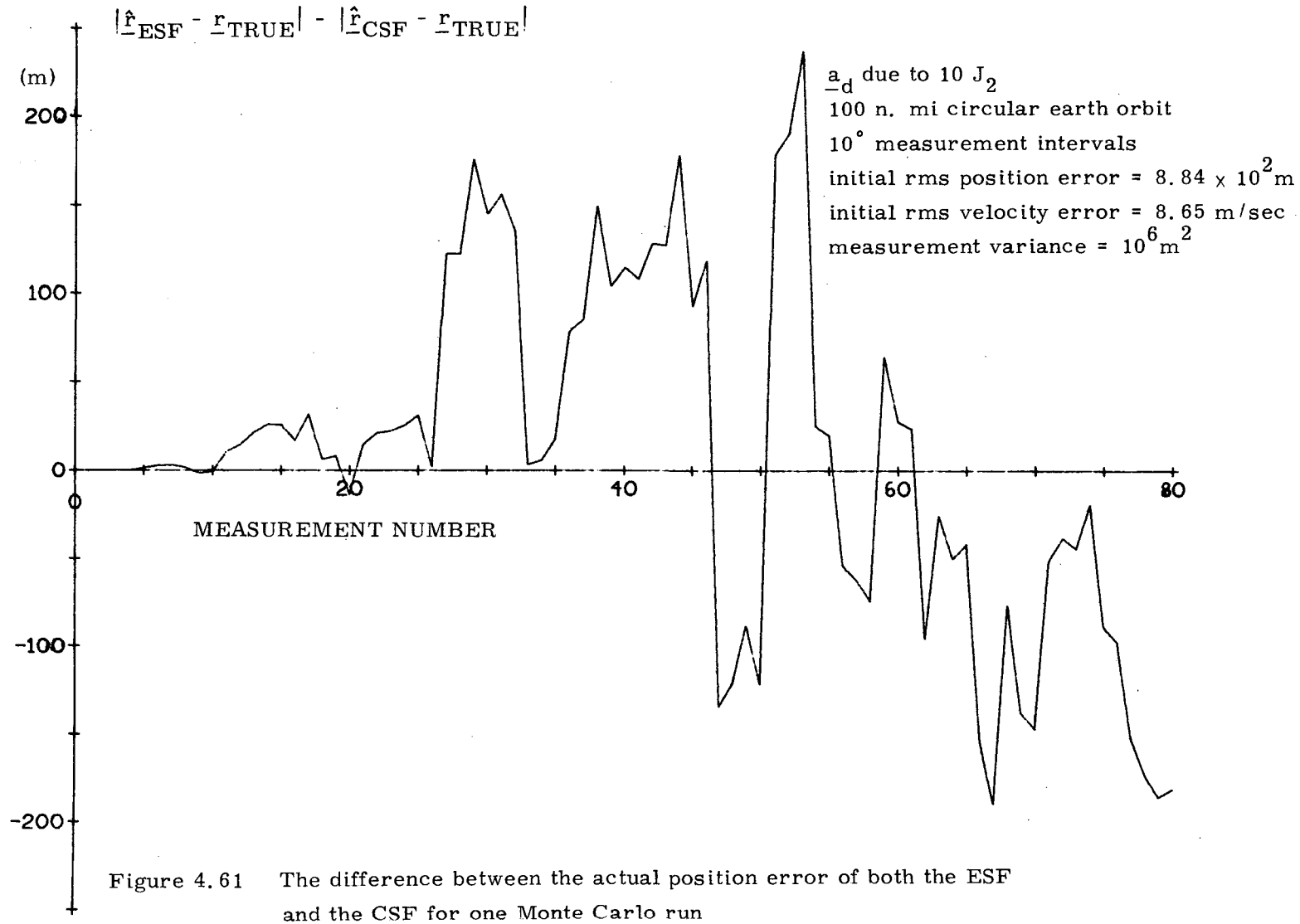

Figure 4.61 The difference between the actual position error of both the ESF and the CSF for one Monte Carlo run

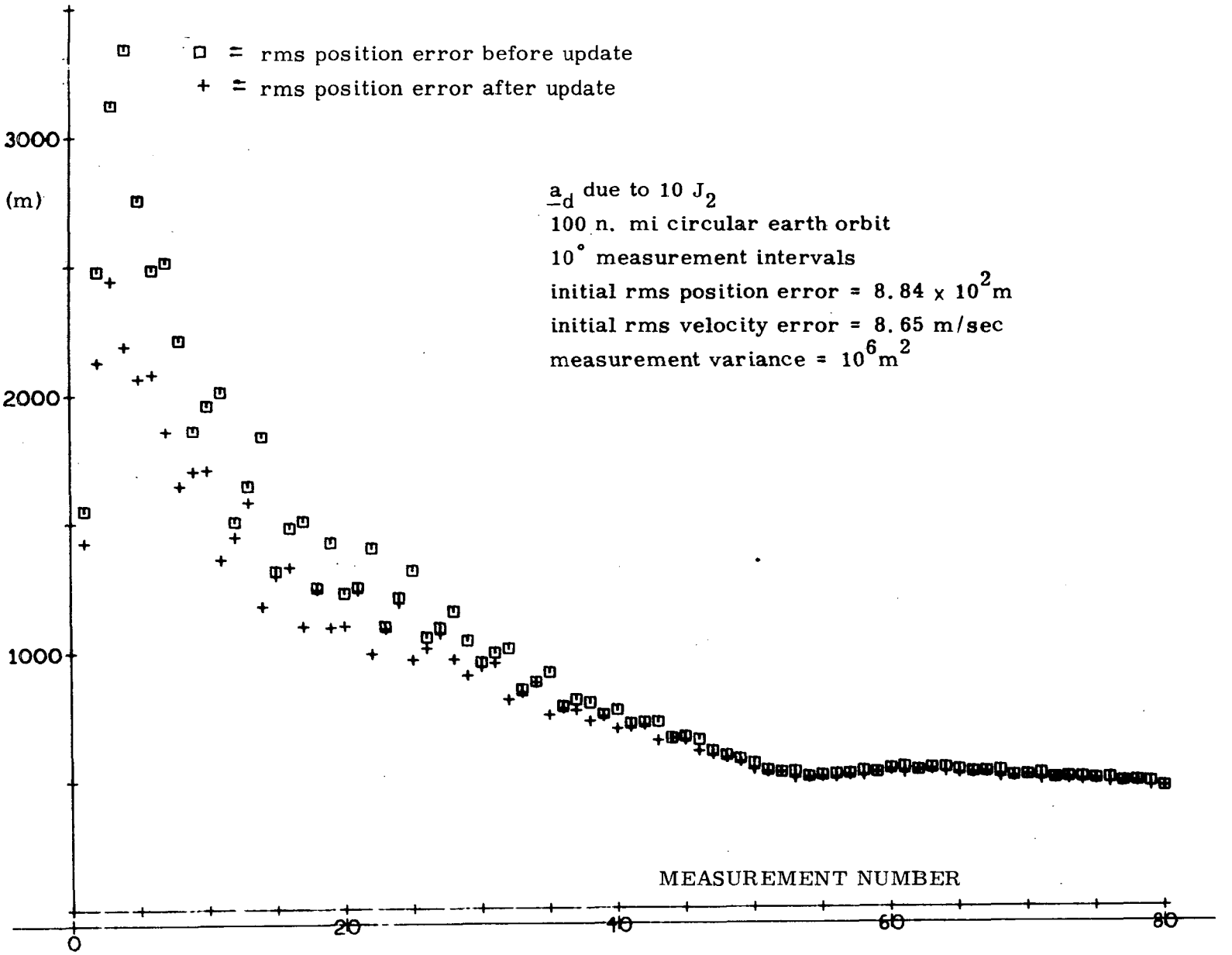

Figure 4.62 RMS estimated current position error for one Monte Carlo run

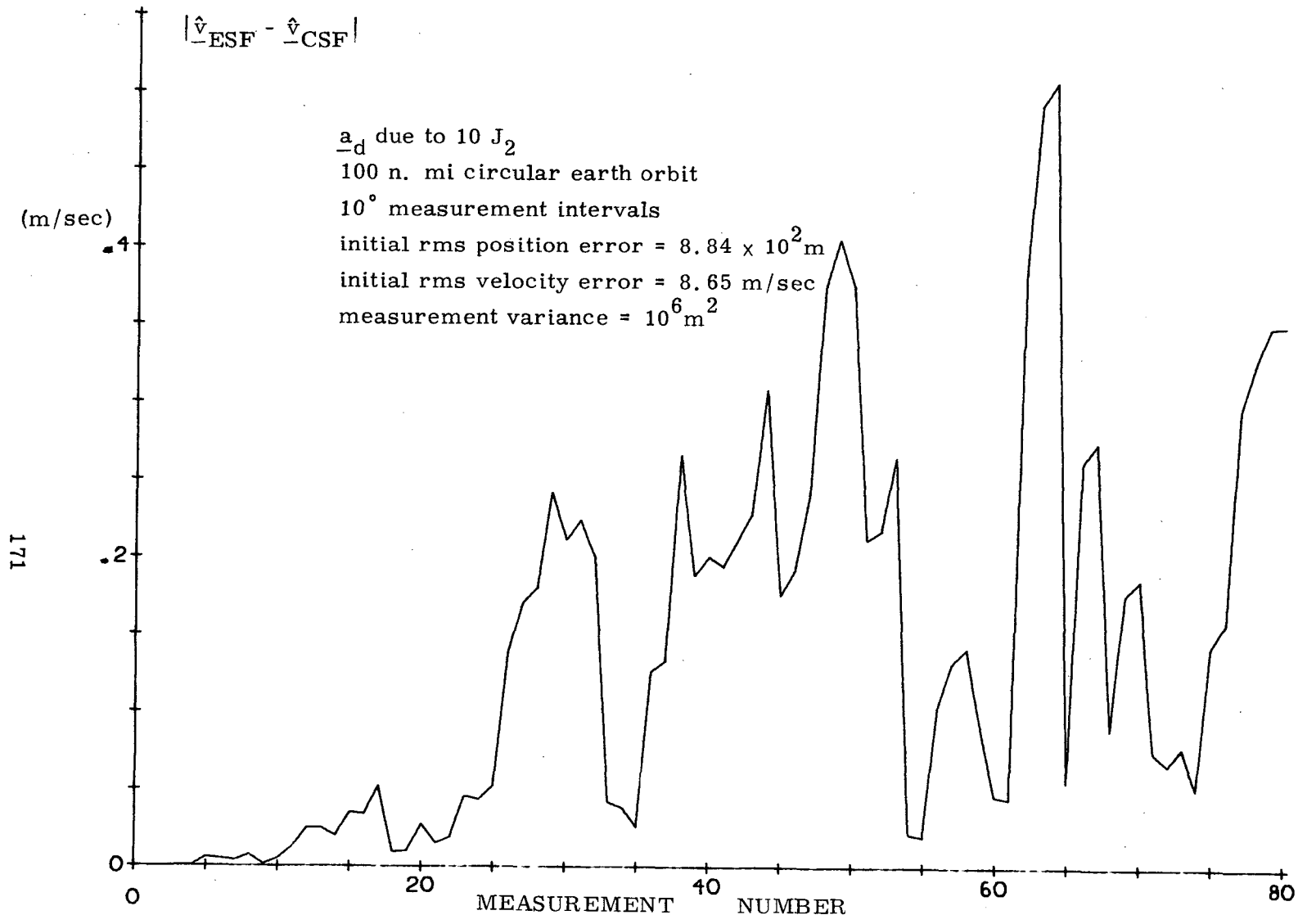

Figure 4.63 Magnitude of the difference between the estimated velocity of the ESF and the CSF for one Monte Carlo run

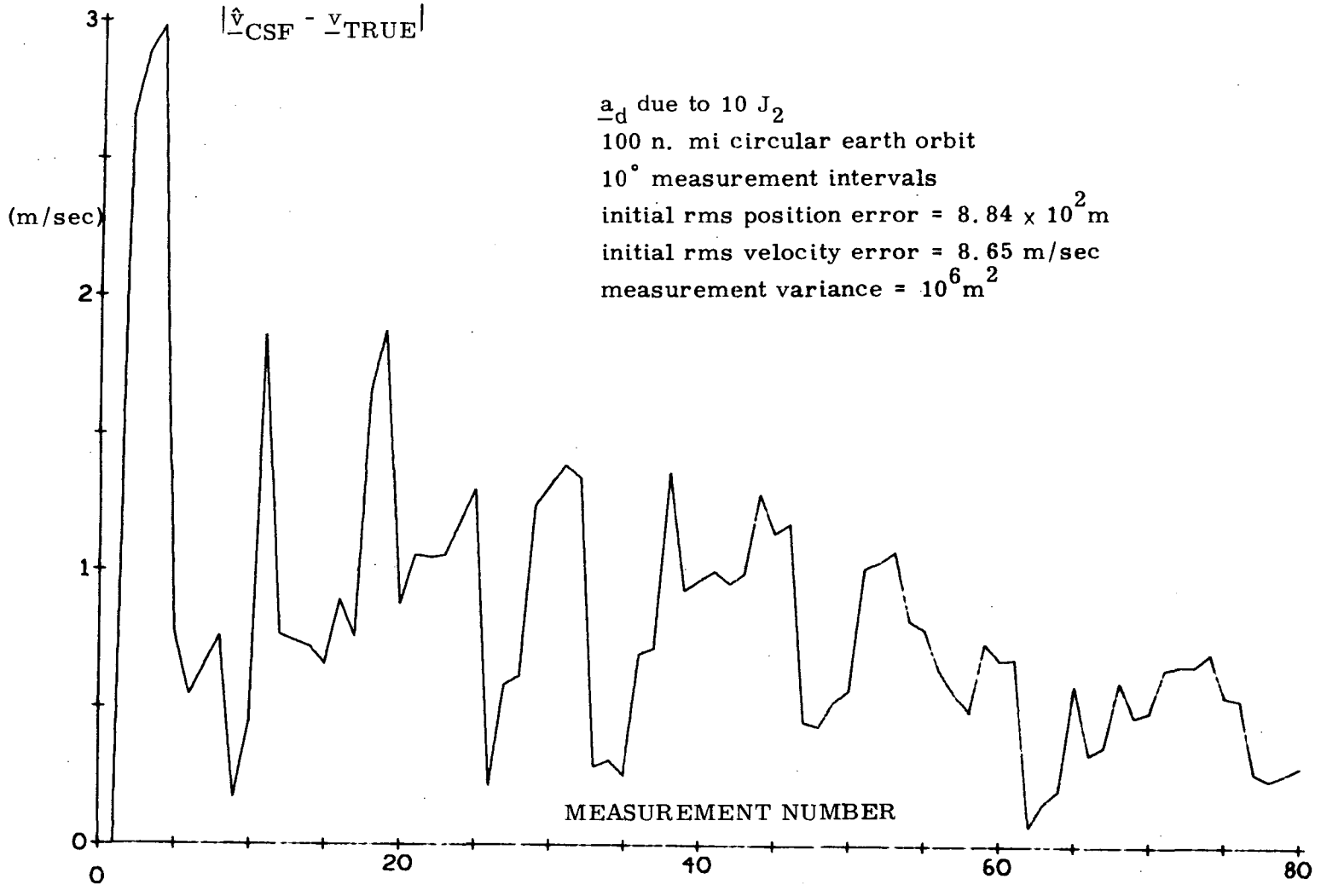

Figure 4.64 Magnitude of the actual error in the velocity estimate of the ESF for one Monte Carlo run

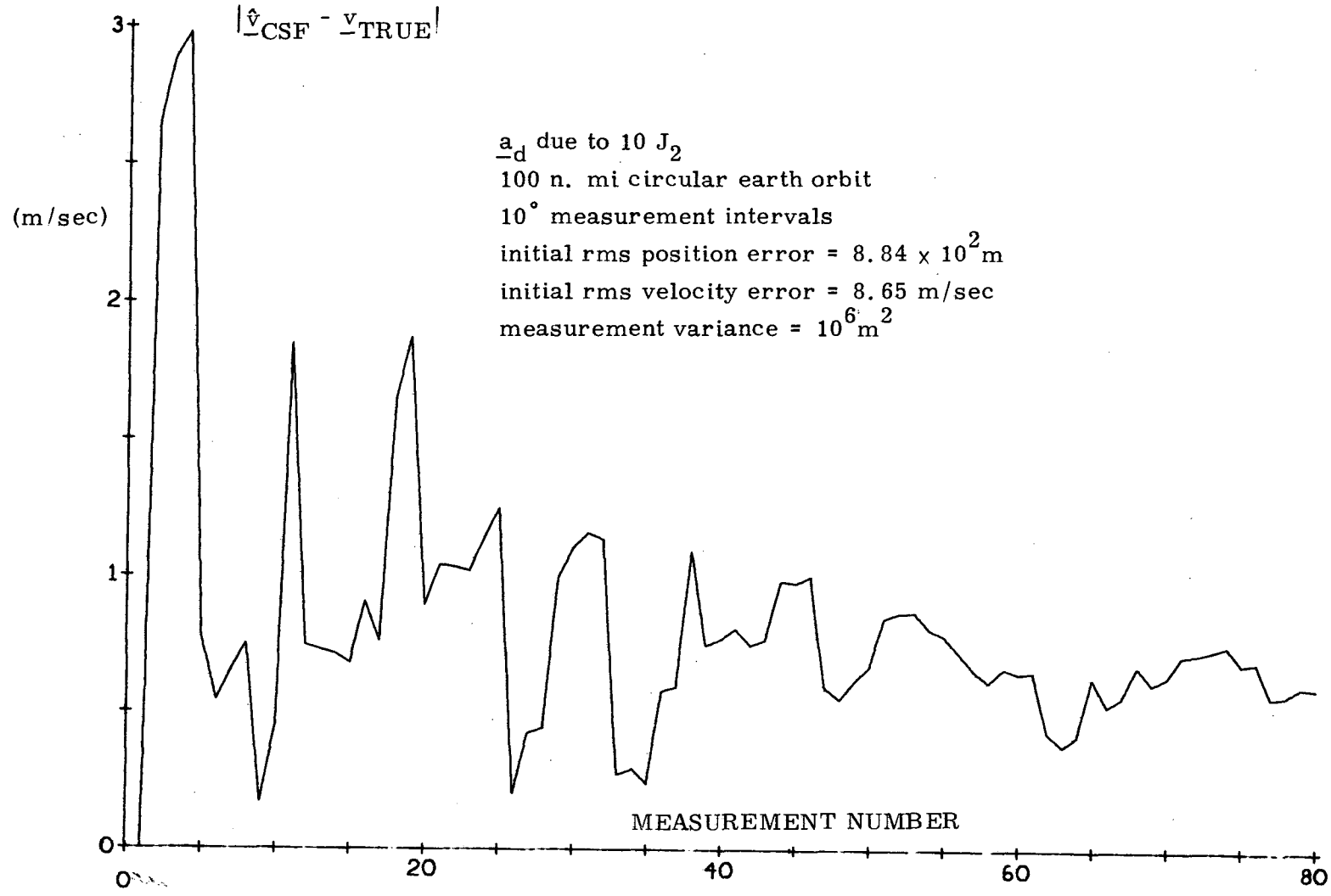

Figure 4.65 Magnitude of the actual error in the velocity estimate of the CSF for one Monte Carlo run

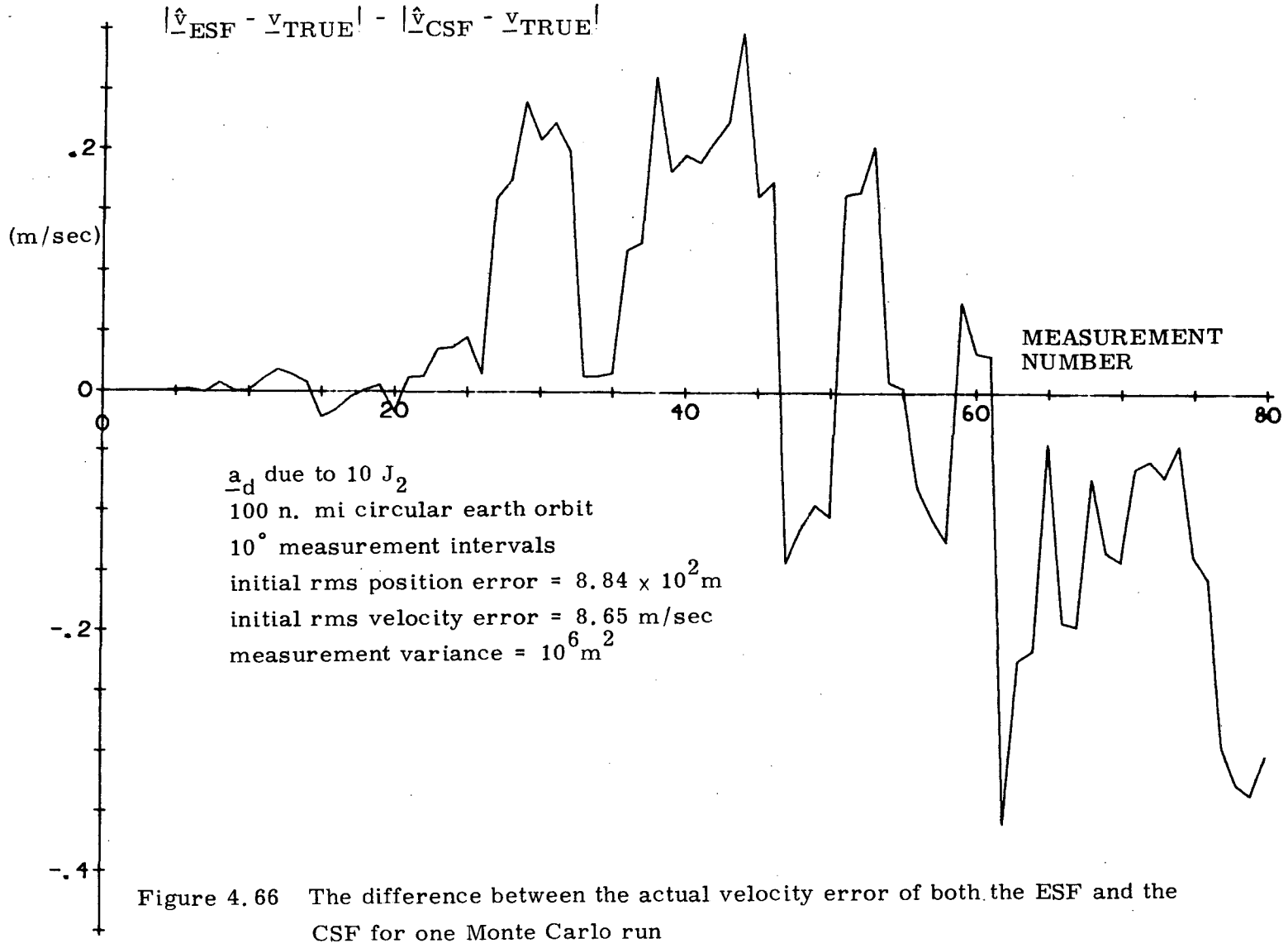

Figure 4.66 The difference between the actual velocity error of both the ESF and the CSF for one Monte Carlo run

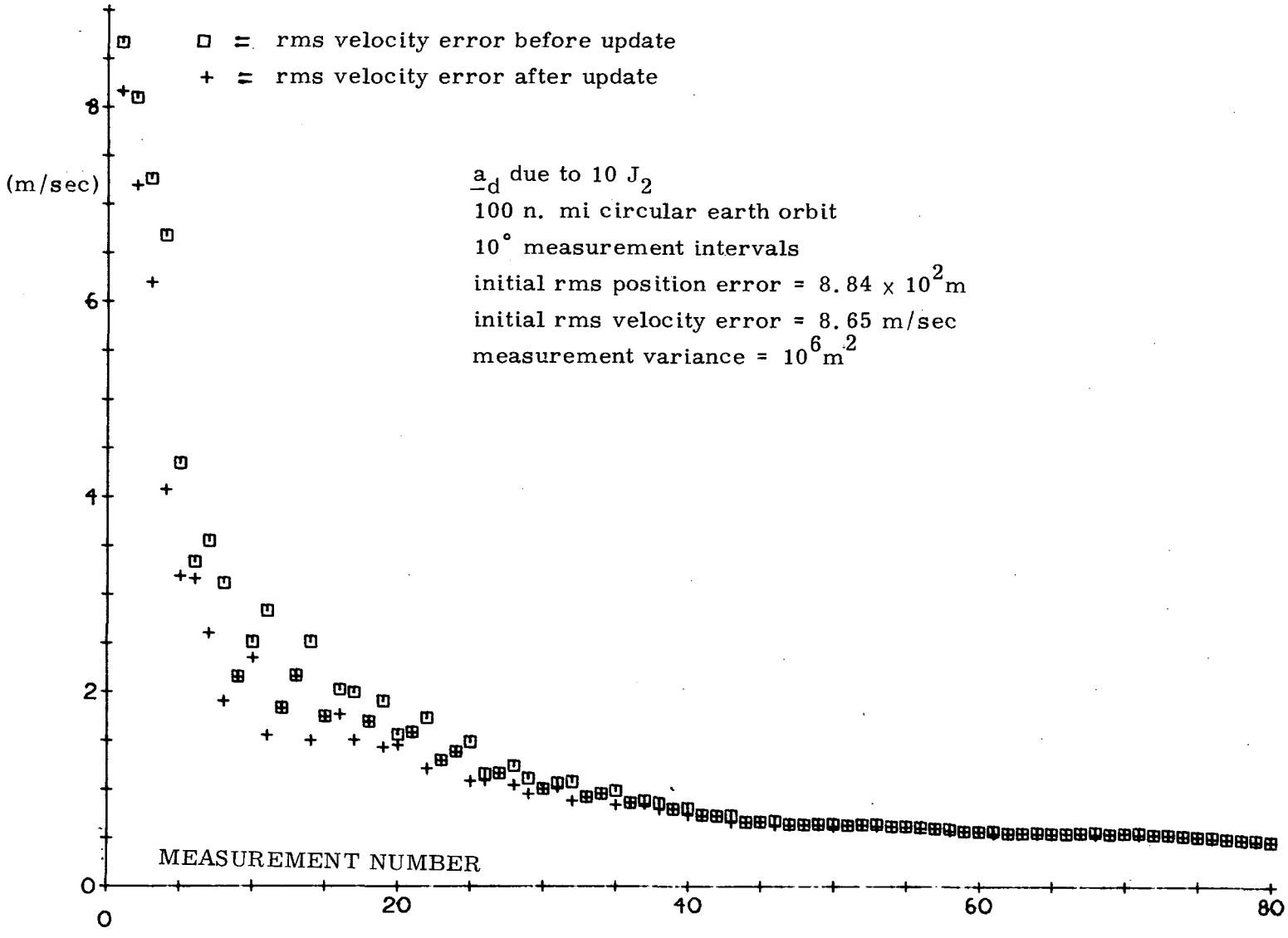

Figure 4.67 RMS estimated current velocity error for one Monte Carlo run

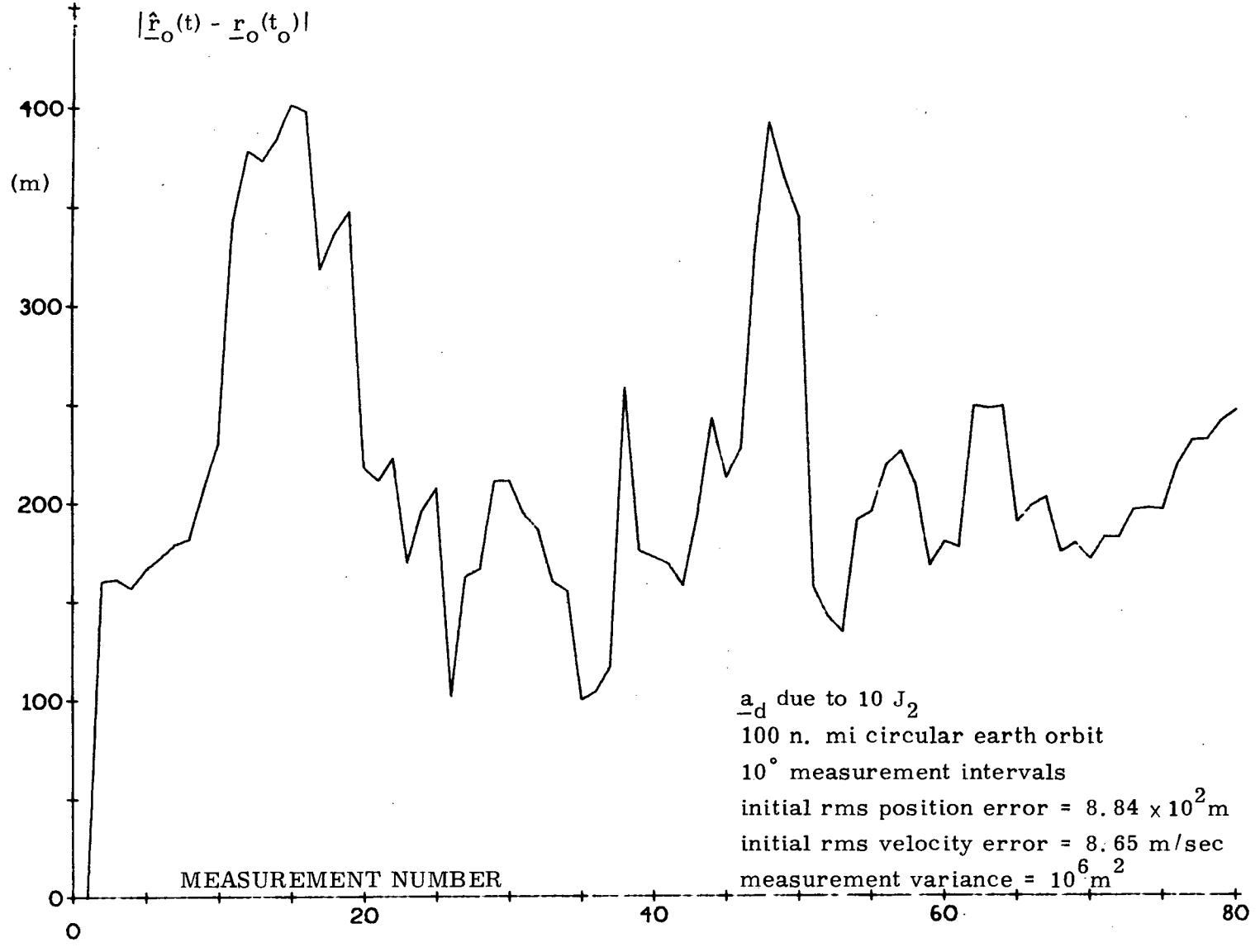

Figure 4.68 Magnitude of the change in epoch position from its true initial value for one Monte Carlo run

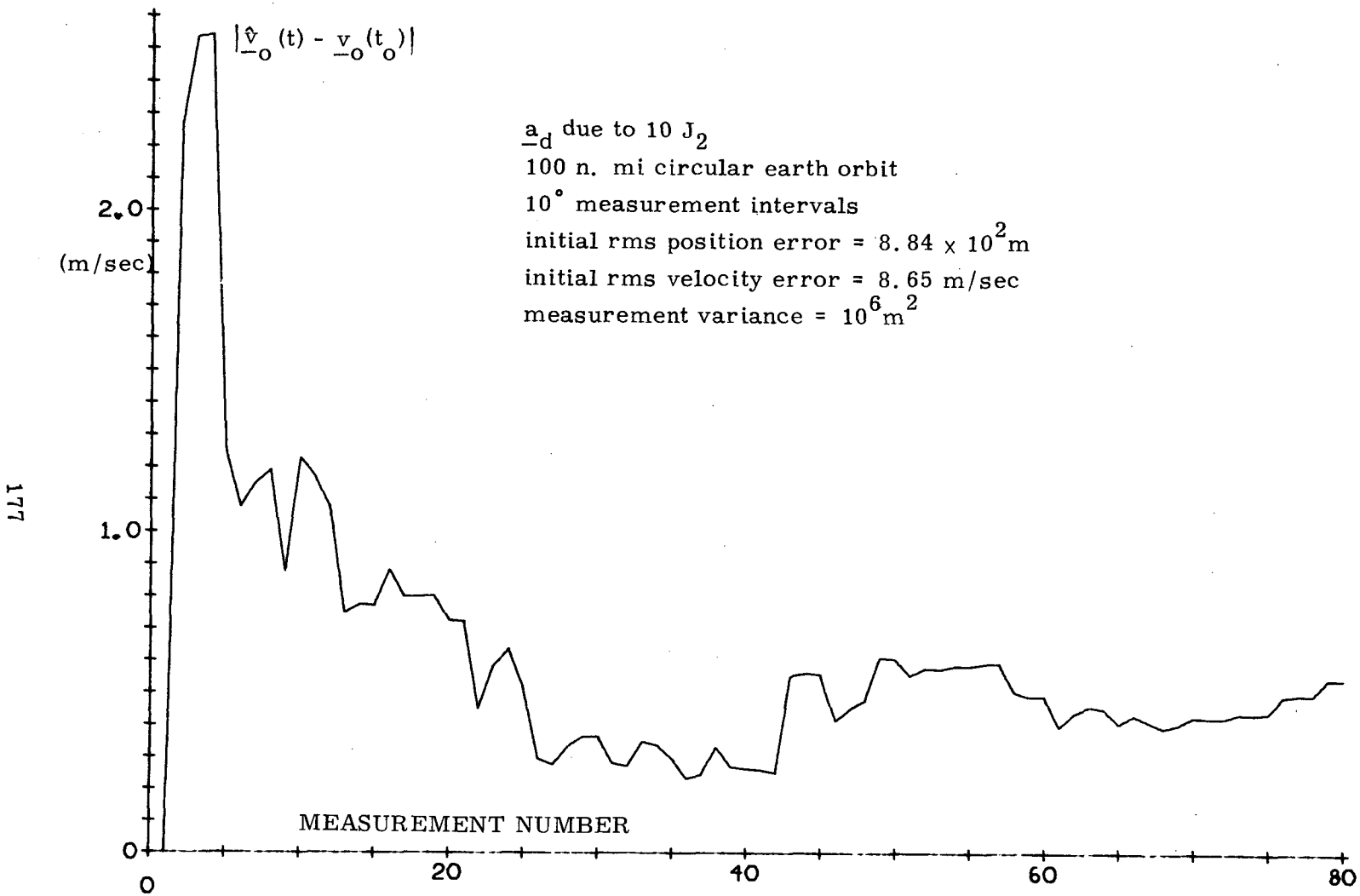

Figure 4.69 Magnitude of the change in the epoch velocity from its true initial value for one Monte Carlo run

CHAPTER V

CONCLUSIONS

From the computer simulation results of Chapter IV it is seen that the epoch state filter produces the estimated state of the spacecraft with nearly the same accuracy as the current state filter, but with a considerable savings in computational time. The inaccuracy in the ESF, incurred because of the assumption that allows for the analytical calculation of the state transition matrix, is small for a 100 nautical mile circular earth orbit with a disturbing acceleration due to as much as $10\,J_2$. At times in the orbit, the ESF is even shown to be more accurate than the CSF.

Computer simulation results were for low earth orbits where the effect of the disturbing acceleration due to the J_2 term is greatest, thus contributing to the largest possible inaccuracy for the ESF. This inaccuracy decreases as the spacecraft's altitude increases away from the influence of disturbing bodies. It was further demonstrated that disturbing accelerations due to as much as $10\,J_2$ were tolerable. The fact that for a larger circular earth orbit with radius twice the equatorial radius of the earth, the errors in the estimate of the state of the spacecraft are decreased considerably is consistent with this trend.

The savings in computation time for the ESF on the AGC is a substantial improvement over the conventional solution to the

navigational problem. This savings is due largely to the analytical extrapolation of the state transition matrix as opposed to the numerical integration of a matrix differential equation. Also, the integration technique for the ESF, which was thought to be more time consuming than that of the CSF, proved to be comparable on an IBM 360 Model 75 computer and faster on the AGC.

The results of the study indicate that the epoch state filter is an economical filter which may be used to estimate the same quantities as the Apollo navigation filter.

APPENDIX A

DIFFERENTIAL EQUATION FOR THE EXTRAPOLATED COVARIANCE MATRIX

$$E'(t_k) = \Phi(t_k, t_{k-1})\, E(t_{k-1})\, \Phi^T(t_k, t_{k-1}) \tag{A.1}$$

$$\dot{\Phi}(t_k, t_{k-1}) = F(t_k)\, \Phi(t_k, t_{k-1}) \tag{A.2}$$

$$\dot{\Phi}^T(t_k, t_{k-1}) = \Phi^T(t_k, t_{k-1})\, F(t_k)^T \tag{A.3}$$

Differentiating A.1 with respect to time yields

$$\dot{E}'(t_k) = \dot{\Phi}(t_k, t_{k-1})\, E(t_{k-1})\, \Phi^T(t_k, t_{k-1}) + \Phi(t_k, t_{k-1})\, E(t_{k-1})\, \dot{\Phi}^T(t_k, t_{k-1}) \tag{A.4}$$

Substituting Equations A.2 and A.3 in A.4

$$\dot{E}'(t_k) = F(t_k)\left[\Phi(t_k, t_{k-1})\, E(t_{k-1})\, \Phi^T(t_k, t_{k-1})\right] + \left[\Phi(t_k, t_{k-1})\, E(t_{k-1})\, \Phi^T(t_k, t_{k-1})\right] F(t_k)^T \tag{A.5}$$

Noticing that the terms in brackets are $E'(t_k)$ Equation A.5 reduces to

$$\dot{E}'(t_k) = F(t_k)\, E'(t_k) + E'(t_k)\, F(t_k)^T \tag{A.6}$$

APPENDIX B

VARIATIONS OF THE EPOCH FORMULATION

Rather than using θ as the independent variable and solving the following differential equation

$$\boxed{\frac{d\theta}{dt} = \frac{h}{r^2} + \frac{1}{h^2}\left[\sin\theta\,\underline{h}\times\underline{r} + h\,(1-\cos\theta)\,\underline{r}\right]\cdot\underline{a}_d} \tag{B.1}$$

The generalized anomoly, x, may be used instead. The differential equation to be integrated is then

$$\boxed{\frac{dx}{dt} = \frac{\sqrt{\mu}}{r} + \frac{U_3(x;\alpha)}{\mu}\,\underline{v}\cdot\underline{a}_d} \tag{B.2}$$

where $U_3(x;\alpha)$ is the transcendental function

$$U_n(x;\alpha) = x^n\left(\frac{1}{n!} - \frac{\alpha x^2}{(n+2)!} + \frac{(\alpha x^2)^2}{(n+4)!} - \ldots\right) \tag{B.3}$$

and α is obtained from the following equation

$$\alpha = \frac{2}{r} - \frac{v^2}{\mu} \tag{B.4}$$

as given in References 1 and 2. Integrating Equation B.2 for x eliminates the need to solve Kepler's equation. This is also the case when θ is used as the independent variable since Kepler's equation can be solved

for either x or θ. The U functions used in solving Kepler's equation can be expressed in terms of either x or θ, i.e., $U = U(x; \alpha)$ or $U = U(\theta; \alpha)$. Still another variational parameter which may be used is the variable epoch time, t_o, and the equation to be integrated is

$$\frac{dt_o}{dt} = \frac{1}{\mu} (c \underline{v} + U_2 \underline{r}) \cdot \underline{a}_d \tag{B.5}$$

where c is defined by

$$\sqrt{\mu}\, c = 3 U_5 - x U_4 - U_2 \sqrt{\mu}\, (t - t_o) \tag{B.6}$$

where U_2, U_4, and U_5 are transendental functions of order 2, 4, and 5 respectively and t is the current time. Use of the differential equation for t_o necessitates solving Kepler's equation

$$\sqrt{\mu}\, (t - t_o) = r_o\, U_1(x; \alpha) + \sigma_o\, U_2(x; \alpha) + U_3(x; \alpha) \tag{B.7}$$

for x. In Equation B.7, σ_o is given by

$$\sigma_o = \frac{1}{\sqrt{\mu}} \underline{r}_o \cdot \underline{v}_o \tag{B.8}$$

APPENDIX C

DERIVATION OF THE VARIATIONAL EQUATIONS FOR -G, $-F_t$, AND F

The equation for -G in terms of the U functions is given as

$$-G = -\frac{r}{\sqrt{\mu}} U_1 + \frac{\sigma}{\sqrt{\mu}} U_2 \tag{C.1}$$

Differentiating this equation according to the formal rules of differentiation given in Section 3.4 results in

$$\frac{-dG}{dt} = -\frac{r}{\sqrt{\mu}} \frac{dU_1}{dt} + \frac{1}{\sqrt{\mu}} \frac{d\sigma}{dt} U_2 + \frac{\sigma}{\sqrt{\mu}} \frac{dU_2}{dt} \tag{C.2}$$

where the variational equations for the transcendental functions are given by

$$\frac{dU_1}{dt} = U_o \left(\frac{d\xi}{dt} + \frac{1}{2} U_3 \frac{d\alpha}{dt} \right) - \frac{1}{2} U_1 U_2 \frac{d\alpha}{dt} \tag{C.3}$$

$$\frac{dU_2}{dt} = U_1 \left(\frac{d\xi}{dt} + \frac{1}{2} U_3 \frac{d\alpha}{dt} \right) - \frac{1}{2} U_2^2 \frac{d\alpha}{dt} \tag{C.4}$$

and that of α by

$$\frac{d\alpha}{dt} = -\frac{2}{\mu} \underline{v} \cdot \underline{a}_d \tag{C.5}$$

Substituting Equations C. 3 to C. 5 into Equation C. 2 and collecting terms yields

$$-\frac{dG}{dt} = -\frac{r_o}{\sqrt{\mu}}\left(\frac{d\xi}{dt} + \frac{1}{2} U_3 \frac{d\alpha}{dt}\right)\left[\frac{1}{r_o}(r U_o - \sigma U_1)\right]$$
$$-\frac{U_2}{\mu} \underline{v} \cdot \underline{a}_d \left[\frac{r}{\sqrt{\mu}} U_1 - \frac{\sigma}{\sqrt{\mu}} U_2\right] + \frac{1}{\mu} \underline{r} \cdot \underline{a}_d U_2 \qquad (C.6)$$

The first term in brackets is F and the second bracketed term is G. Making these substitutions in Equation C. 6 results in the following variational equation for - G

$$-\frac{dG}{dt} = -\frac{U_2}{\mu} \underline{v} \cdot \underline{a}_d G - \frac{r_o}{\sqrt{\mu}}\left(\frac{d\xi}{dt} + \frac{1}{2} U_3 \frac{d\alpha}{dt}\right) F + \frac{1}{\mu} \underline{r} \cdot \underline{a}_d U_2 \qquad (C.7)$$

Similarly, differentiating the equation for F_t where

$$-F_t = \frac{\sqrt{\mu}}{r} \frac{U_1}{r_o} \qquad (C.8)$$

yields

$$-\frac{dF_t}{dt} = \frac{\sqrt{\mu}}{r r_o} \frac{dU_1}{dt} - \frac{\sqrt{\mu}}{r r_o^2} U_1 \frac{dr_o}{dt} \qquad (C.9)$$

Upon substituting Equation C. 3 for $\frac{dU_1}{dt}$ and C. 5 for $\frac{d\alpha}{dt}$ and

$$\frac{dr_o}{dt} = -\sigma_o\left(\frac{d\xi}{dt} + \frac{1}{2} U_3 \frac{d\alpha}{dt}\right) - \frac{1}{2}(r + r_o) U_2 \frac{d\alpha}{dt} - U_1 \frac{d\sigma}{dt} \qquad (C.10)$$

where

$$\frac{d\sigma}{dt} = \frac{1}{\sqrt{\mu}} \underline{r} \cdot \underline{a}_d \tag{C.11}$$

Into Equation C. 9, the resulting equation is

$$-\frac{dF_t}{dt} = \frac{\sqrt{\mu}}{r r_o}\left[U_o\left(\frac{d\xi}{dt} + \frac{1}{2} U_3 \frac{d\alpha}{dt}\right) + \frac{U_1 U_2}{\mu} \underline{v} \cdot \underline{a}_d\right]$$

$$-\frac{\sqrt{\mu}}{r r_o^2} U_1\left[-\sigma_o\left(\frac{d\xi}{dt} + \frac{1}{2} U_3 \frac{d\alpha}{dt}\right) + \frac{U_2}{\mu}(r + r_o)\underline{v} \cdot \underline{a}_d\right.$$

$$\left.-\frac{U_1}{\sqrt{\mu}} \underline{r} \cdot \underline{a}_d\right] \tag{C.12}$$

Collecting terms and simplifying Equation C. 12 produces

$$-\frac{dF_t}{dt} = \frac{\sqrt{\mu}}{r_o^2}\left(\frac{d\xi}{dt} + \frac{1}{2} U_3 \frac{d\alpha}{dt}\right)\left[\frac{1}{r}(r_o U_o + \sigma_o U_1)\right] +$$

$$+\frac{U_1 U_2}{r r_o}\frac{1}{\sqrt{\mu}} \underline{v} \cdot \underline{a}_d - \frac{U_1 U_2}{r_o^2}\frac{1}{\sqrt{\mu}} \underline{v} \cdot \underline{a}_d - \frac{U_1 U_2}{r r_o}\frac{1}{\sqrt{\mu}} \underline{v} \cdot \underline{a}_d +$$

$$+\frac{U_1^2}{r r_o^2} \underline{r} \cdot \underline{a}_d \tag{C.13}$$

The second and fourth terms on the right-hand side of Equation C. 13 cancel and the term in brackets is G_t. Making these changes and collecting related terms results in

$$-\frac{dF_t}{dt} = \frac{\sqrt{\mu}}{r_o^2}\left(\frac{d\xi}{dt} + \frac{1}{2}U_3\frac{d\alpha}{dt}\right)G_t + \frac{U_1}{\sqrt{\mu}r_o}\left(-\frac{U_2}{r_o}\underline{v}\cdot\underline{a}_d + \underline{v}\cdot\underline{a}_d\right.$$

$$\left. - \underline{v}\cdot\underline{a}_d + \frac{U_1\sqrt{\mu}}{r\,r_o}\underline{r}\cdot\underline{a}_d\right) \qquad (C.14)$$

where $\underline{v}\cdot\underline{a}_d$ has been added to and subtracted from the second term in parantheses. Collecting terms within the second set of parentheses results in $-\underline{v}\cdot\underline{a}_d + (-F_t\underline{r}\cdot\underline{a}_d + F\underline{v}\cdot\underline{a}_d)$ which is equal to $(\underline{v}_o - \underline{v})\underline{a}_d$. Thus, the variational equation for $-F_t$ is

$$-\frac{dF_t}{dt} = \frac{\sqrt{\mu}}{r_o^2}\left(\frac{d\xi}{dt} + \frac{1}{2}U_3\frac{d\alpha}{dt}\right)G_t - \frac{r}{\mu}(\underline{v}_o - \underline{v})\cdot\underline{a}_d F_t \qquad (C.15)$$

Finally, the equation for F is

$$F = 1 - \frac{U_2}{r_o} \qquad (C.16)$$

Differentiating this equation as was done previously for $-G$ and F_t yields

$$\frac{dF}{dt} = -\frac{1}{r_o}\frac{dU_2}{dt} + \frac{U_2}{r_o^2}\frac{dr_o}{dt} \qquad (C.17)$$

Substituting for $\frac{dU_2}{dt}$, $\frac{dr_o}{dt}$, $\frac{d\alpha}{dt}$, and $\frac{d\sigma}{dt}$ with equations C.4, C.10, C.5, and C.11 respectively results in

$$\frac{dF}{dt} = -\frac{1}{r_o^2}\left(\frac{d\xi}{dt} + \frac{1}{2}U_3\frac{d\alpha}{dt}\right)\left[r_o U_1 + \sigma_o U_2\right] - \frac{U_2^2}{\mu r_o}\,\underline{v}\cdot\underline{a}_d$$

$$+\frac{U_2^2 r}{\mu r_o^2}\,\underline{v}\cdot\underline{a}_d + \frac{U_2^2}{\mu r_o}\,\underline{v}\cdot\underline{a}_d - \frac{U_1 U_2}{r_o^2}\,\frac{\underline{r}\cdot\underline{a}_d}{\sqrt{\mu}} \qquad \text{(C. 18)}$$

Cancelling the second and fourth terms on the right-hand side of Equation C. 18, replacing the term in brackets by $\sqrt{\mu}\,G$, and collecting related terms yields

$$\frac{dF}{dt} = -\frac{1}{r_o}\left(\frac{d\xi}{dt} + \frac{1}{2}U_3\frac{d\alpha}{dt}\right)\sqrt{\mu}\,G - \frac{r U_2}{\mu r_o}\left(\frac{U_1\sqrt{\mu}}{r_o r}\,\underline{r}\cdot\underline{a}_d\right.$$

$$\left. -\frac{U_2}{r_o}\,\underline{v}\cdot\underline{a}_d + \underline{v}\cdot\underline{a}_d - \underline{v}\cdot\underline{a}_d\right) \qquad \text{(C. 19)}$$

where $\underline{v}\cdot\underline{a}_d$ has been added to and subtracted from the term in the second set of parentheses. But this term is just $\frac{r}{\mu}(\underline{v}_o - \underline{v})\,\underline{a}_d$ so that the variational equation for F is

$$\frac{dF}{dt} = -\frac{\sqrt{\mu}}{r_o^2}\left(\frac{d\xi}{dt} + \frac{1}{2}U_3\frac{d\alpha}{dt}\right)G + \frac{r}{\mu}(\underline{v}_o - \underline{v})\cdot\underline{a}_d\,F$$

$$-\frac{r}{\mu}(\underline{v}_o - \underline{v})\cdot\underline{a}_d\,F \qquad \text{(C. 20)}$$

REFERENCES

1. Battin, R. H., Astronautical Guidance, McGraw-Hill, Inc., New York, 1964.

2. Battin, R. H., and Fraser, D. C., Space Guidance and Navigation, AIAA Professional Study Series, Santa Barbara, California, August, 1970.

3. Battin, R. H., and Fraser, D. C., Notebook for Space Guidance and Navigation, AIAA Professional Study Series, Santa Barbara, California, August, 1970.

4. "Guidance System Operations Plan to Manned CM Earth Orbital and Lunar Missions Using Program Collossus 2C (Comanche 67)," M. I. T. Instrumentation Laboratory, Cambridge, Massachusetts, July 1969.

5. Battin, R. H., "Variation of Parameters," Chapter II of First Quarterly Progress Report, M. I. T., Instrumentation Laboratory, Cambridge, Massachusetts, May 19, 1970.

6. Croopnick, S. R., "The Epoch State Filter," Chapter IV of Fourth Quarterly Progress Report, M. I. T. Instrumentation Laboratory, Cambridge, Massachusetts, April 30, 1971.

7. Croopnick, S. R., "The Epoch State Filter", Chapter IV of First Quarterly Progress Report, M. I. T. Instrumentation Laboratory, Cambridge, Massachusetts, August 30, 1971.

8. Robertson, W. M., "The Deyst-Pines Solution to Lambert's Problem," Report DLMC-71-2, M.I.T. Draper Laboratory, Cambridge, Massachusetts, March 1971.

9. Users Guide to Mac - 360, M.I.T. Instrumentation Laboratory, Cambridge, Massachusetts, March 1971.

10. Phillips, R., REPCONICS, "Space Guidance Analysis Memo #9-70 (Revision1) M.I.T. Instrumentation Laboratory, Cambridge, Massachusetts, January 20, 1971.

11. Muntz, C.A., Users Guide to the Block II AGC/LGC Interpreter, R-489, M.I.T. Instrumentation Lab, Cambridge, Massachusetts, April 1965.

EPOCH STATE FILTER

```
M                INDEX I,J

M                DIMENSION(E,6X6),(B,6X3),(PHI,6X6),(W,6),(BD,6),(DXE,6),

M                (DQ,80),(DXOE,6),(PHI1,6X6),(PHI2,6X6),(PHI3,6X6),(DVTN,6)

M       BEGIN    DO TO 2 FOR I = 0(1)79

M           2    DQ   = RNDMN(1000)
S                   I

E                *
M                E = 0

M                DO TO 3 FOR I = 0(7)14

M           3    E   = 260100
S                  I

M                DO TO 4 FOR I = 21(7)35

M           4    E   = 25
S                  I

E                *
M                B = 0

M                DO TO 6 FOR I = 0(4)8

M           6    B   = 1
S                  I

M                1P5PI = 1.5 PI

M                3PI = 3 PI

E                                  6
M                ALPHA = 1.0 10

E                                     15
M                MU = .3986012 10

M                RMU = SQRT( MU )

M                RR = 6563365

M                R = RR

M                VC = SQRT( MU / RR )

E                                          3
M                PDOSC = 2 PI SQRT(RR   / MU)

M                DT = PDOSC / 72

M                RE = 6378165
```

```
M                J2 = .0010823

M                J = 0

M                T = 0

M                THETA = 0

M                THETAI = 0

E                 -
M                IZ = (0, 0, 1)

E                -
M                RO = (RR, 0, 0)

E                -     -
M                ROI = RO

E                -           -
M                IRO = UNIT( RO )

M                RO = RR

E                -   -
M                R = RO

E                -    -
M                IR = IRO

E                -
M                VO = (0, VC, 0)

E                -     -
M                VOI = VO

E                -
M                DROE = (0, 0, 0)

E                -     -
M                DRE = DROE

E                -      -
M                DVOE = DROE

M                DO TO 16 FOR I = 1(1)80

E                -     -  -
M                ITH = IZ*IR

E                -      -  -
M                ITHO = IZ*IRO

E                              -   -       -    -
M                DELTH = ( ITH.DRE/R - ITHO.DROE/RO )

M                THETA = THETA + DELTH
```

$$\overline{\mathrm{AD}} = \left(-\mathrm{MU}/\mathrm{R}^2 \right) 1.5\ \mathrm{J2}\ \left(\mathrm{RE}/\mathrm{R} \right)^2 \left(\left(1 - 5\ \mathrm{CPHI}^2 \right) \overline{\mathrm{IR}} + 2\ \mathrm{CPHI}\ \overline{\mathrm{IZ}} \right)$$

$$\mathrm{CTHETAI} = \mathrm{COS}(\mathrm{THETAI})$$

$$\mathrm{STHETAI} = \mathrm{SIN}(\mathrm{THETAI})$$

$$\mathrm{ROI} = \mathrm{ABVAL}\left(\overline{\mathrm{ROI}} \right)$$

$$\mathrm{VOI} = \mathrm{ABVAL}\left(\overline{\mathrm{VOI}} \right)$$

Reproduced from best available copy.

$$\mathrm{SIGMAOI} = \overline{\mathrm{ROI}}.\overline{\mathrm{VOI}}\ /\ \mathrm{RMU}$$

$$\mathrm{ALFAI} = (2\ /\ \mathrm{ROI}) - \left(\mathrm{VOI}^2\ /\ \mathrm{MU} \right)$$

$$\mathrm{IP} = 2\ \mathrm{ROI} - \mathrm{ALFAI}\ \mathrm{ROI}^2 - \mathrm{SIGMAOI}^2$$

$$\mathrm{HI} = \mathrm{SQRT}(\mathrm{MU}\ \mathrm{IP})$$

$$\mathrm{RI} = \mathrm{IP}/\ (1 + (\mathrm{IP}/\mathrm{ROI} - 1)\ \mathrm{CTHETAI} - \mathrm{HI}\ \mathrm{SIGMAOI}\ \mathrm{STHETAI}/\ \mathrm{ROI}\ \mathrm{RMU})$$

$$\mathrm{FI} = 1 - \mathrm{RI}\ (1 - \mathrm{CTHETAI})/\ \mathrm{IP}$$

$$\mathrm{FTI} = \mathrm{RMU}\ \mathrm{SIGMAOI}\ (1 - \mathrm{CTHETAI})/\ \mathrm{ROI}\ \mathrm{IP} - \mathrm{MU}\ \mathrm{STHETAI}\ /\ \mathrm{ROI}\ \mathrm{HI}$$

$$\mathrm{GI} = \mathrm{RI}\ \mathrm{ROI}\ \mathrm{STHETAI}\ /\ \mathrm{HI}$$

$$\mathrm{GTI} = 1 - \mathrm{ROI}\ (1 - \mathrm{CTHETAI})\ /\ \mathrm{IP}$$

$$\overline{\mathrm{RI}} = \mathrm{FI}\ \overline{\mathrm{ROI}} + \mathrm{GI}\ \overline{\mathrm{VOI}}$$

$$\overline{\mathrm{IRI}} = \mathrm{UNIT}\left(\overline{\mathrm{RI}} \right)$$

$$\mathrm{CPHII} = \overline{\mathrm{IRI}}.\overline{\mathrm{IZ}}$$

$$\overline{\mathrm{VI}} = \mathrm{FTI}\ \overline{\mathrm{ROI}} + \mathrm{GTI}\ \overline{\mathrm{VOI}}$$

$$\overline{\mathrm{HI}} = \overline{\mathrm{RI}} * \overline{\mathrm{VI}}$$

$$\overline{\mathrm{ADI}} = \left(\left(-\mathrm{MU}/\mathrm{RI}^2 \right) 1.5\ \mathrm{J2}\ (\mathrm{RE}/\mathrm{RI})^2 \left(\left(1 - 5\ \mathrm{CPHII}^2 \right) \overline{\mathrm{IRI}} + 2\ \mathrm{CPHII}\ \overline{\mathrm{IZ}} \right) \right)$$

```
E                  _    _    _
M                  RO = RO + DROE

E                  _    _    _
M                  VO = VO + DVOE

M                  DO TO 13 FOR L = 1(1)2

M                  DO TO 13 FOR K = 0(1)3

M                  CTHETA = COS(THETA)

M                  STHETA = SIN(THETA)

E                             _
M                  RO = ABVAL( RO )

E                             _
M                  VO = ABVAL( VO )

E                        _  _
M                  SIGMAO = RO.VO / RMU

E                                      2
M                  ALFA = (2 / RO) - (VO  / MU)

E                                 2          2
M                  P = 2 RO - ALFA RO  - SIGMAO

M                  H = SQRT( MU P )

M                  R = P / (1 + (P/RO -1) CTHETA - H SIGMAO STHETA / RO RMU)

M                  F = 1 - R (1 - CTHETA)/ P

M                  FT = RMU SIGMAO (1 - CTHETA)/ RO P  - MU STHETA / RO H

M                  G = R RO STHETA / H

M                  GT = 1 - RO (1 - CTHETA) / P

E                  _     _     _
M                  R =  F RO +  G VO

E                   _          _
M                  IR = UNIT( R )

E                        _  _
M                  CPHI = IR.IZ

E                  _     _     _
M                  V = FT RO + GT VO

E                  _   _ _
M                  H = R*V
```

```
E
M               DTHETA/DT = H / R**2 + ( STHETA H*R + H (1 - CTHETA) R ).AD / H**2

E
M               DRO/DT = (R RO/ (MU P)) (1- CTHETA) ((RO- R) V + V R) AD - G AD

E
M               DVO/DT = (R / MU) (VO - V) (VO - V) AD  + F AD

E
M               DTHETAI/DT =(HI/RI**2 + (STHETAI HI*RI + HI (1 - CTHETAI) RI).

E
M               ADI / HI**2 )

E
M               DROI/DT =((RI ROI/ (MU IP)) (1 - CTHETAI) ((ROI - RI) VI + VI

E
M               RI) ADI - GI ADI)

E
M               DVOI/DT = (RI / MU) (VOI - VI) (VOI - VI) ADI + FI ADI

E
M         13    DIFEQ T,DT,DTHETA/DT,DRO/DT,DVO/DT,DTHETAI/DT,DROI/DT,DVOI/DT

E
M               ROCNG = ABVAL( RO - ROI)

E
M               VOCNG = ABVAL( VO - VOI )

E
M               RO = ABVAL( RO )

E
M               IRO = UNIT( RO )

M               IF THETA <= 1P5PI, GO TO 14

M               IF THETA GOREQ 3PI, GO TO 12

E
M               CALL KWK.CONICS, 4, 0, RO, VO, 1P5PI, MU

E
M               RESUME TF1, R1, V1, THETA1, SLR, COGA, SMA, PERIOD, R1, SOLNTAG

E
M               CALL KWK.CONICS, 4, 0, R1, V1, ( THETA - 1P5PI ), MU

E
M               RESUME TF2, R, V, THETA2, SLR, COGA, SMA, PERIOD, R, SOLNTAG
```

```
F                                    - -
M                CALL REP.CONICS, 3, 0, R0, V0, TF1, MU, 0

F                          - -
M                RESUME TF1.R1.V1,THETA1,SLR,COGA,SMA,PERIOD,R1,SOLNTAG,ANOMOLY,

F                 *
M                PHI1

F                                    - -
M                CALL REP.CONICS, 3, 0, R1, V1, TF2, MU, 0

F                          - -
M                RESUME TF2.R.V,THETA2,SLR,COGA,SMA,PERIOD,R,SOLNTAG,ANOMOLY,

F                 *
M                PHI2

F                 *      *     *
M                PHI = PHI2 PHI1

M                GO TO 15

F                                    - -
M           12   CALL KWK.CONICS, 4, 0, R0, V0, 1P5PI, MU

F                          - -
M                RESUME TF1, R1, V1, THETA1, SLR, COGA, SMA, PERIOD, R1, SOLNTAG

F                                    - -
M                CALL KWK.CONICS, 4, 0, R1, V1, 1P5PI, MU

F                          - -
M                RESUME TF2, R2, V2, THETA2, SLR, COGA, SMA, PERIOD, R2, SOLNTAG

F                                    - -
M                CALL KWK.CONICS, 4, 0, R2, V2, (THETA - 3PI), MU

F                          - -
M                RESUME TF3, R, V, THETA3, SLR, COGA, SMA, PERIOD, R, SOLNTAG

F                                    - -
M                CALL REP.CONICS, 3, 0, R0, V0, TF1, MU, 0

F                          - -
M                RESUME TF1,R1.V1,THETA1,SLR,COGA,SMA,PERIOD,R1,SOLNTAG,ANOMOLY,

F                 *
M                PHI1

F                                    - -
M                CALL REP.CONICS, 3, 0, R1, V1, TF2, MU, 0

F                          - -
M                RESUME TF2,R2.V2,THETA2,SLR,COGA,SMA,PERIOD,R2,SOLNTAG,ANOMOLY,
```

```
F                *
M               PHI2

E                                  _   _
M               CALL REP.CONICS, 3, 0, R2, V2, TF3, MU, 0

F                     _ _
M               RESUME TF3,R,V,THETA3,SLR,COGA,SMA,PERIOD,R,SOLNTAG,ANOMOLY,

F                *
M               PHI3

F                *      *     *     *
M               PHI = PHI3 PHI2 PHI1

M               GO TO 15

E                                  _   _
M          14   CALL KWK.CONICS, 4, 0, R0, V0, THETA, MU

E                     _ _
M               RESUME TF, R, V, THETA2, SLR, COGA, SMA, PERIOD, R, SOLNTAG

E                                  _   _
M               CALL REP.CONICS, 3, 0, R0, V0, TF, MU, 0

E                     _ _                                                  *
M               RESUME TF,R,V,THETA2,SLR,COGA,SMA,PERIOD,R,SOLNTAG,ANOMOLY,PHI

E               -      * T -C
M          15   B0 = PHI   B
S                     ,I

F               -           -
M               IR = UNIT( R )

E                    -    * -
M               A0 = B0.( E B0) + ALPHA

E               -    * -
M               W = E B0 / A0

E               *    *    - -  *
M               E = E - W B0 E

M               DVTN   = R0    - R0I
S                    0       0       0

M               DVTN   = R0    - R0I
S                    1       1       1

M               DVTN   = R0    - R0I
S                    2       2       2

M               DVTN   = V0    - V0I
S                    3       0       0
```

```
M                   DVTN   = VO   - VOI
S                      4       1       1

M                   DVTN   = VO   - VOI
S                      5       2       2

E                   -      -                -   -
M                   DXOE = W ( DO     - RO.DVTN )
S                                I-1

M                   DROE   = DXOE
S                      0         0

M                   DROE   = DXOE
S                      1         1

M                   DROE   = DXOE
S                      2         2

M                   DVOE   = DXOE
S                      0         3

M                   DVOE   = DXOE
S                      1         4

M                   DVOE   = DXOE
S                      2         5

E                   -      *   -
M                   DXE = PHI DXOE

M                   DRE    = DXE
S                      0         0

M                   DRE    = DXE
S                      1         1

M                   DRE    = DXE
S                      2         2

M                   DVE    = DXE
S                      0         3

M                   DVE    = DXE
S                      1         4

M                   DVE    = DXE
S                      2         5

M                   J = J + 1

M              16   IF J > 2, J = 0

M                   START AT BEGIN
```

CONVENTIONAL STATE FILTER

```
M                INDEX I, J, Z
M                DIMENSION(F,6X6),(B,6X3),(W,6),(P,6X6),(ID,6X6),(PHI,6X6),
M                (DQ,80),(DXE,6),(DVTN,6)
M       BEGIN    DO TO 2 FOR I = 0(1)79
M           2    DQ  = RNDMN(1000)
S                  I
E                *
M                E = 0
M                DO TO 3 FOR I = 0(7)14
M           3    E  = 260100
S                 I
M                DO TO 4 FOR I = 21(7)35
M           4    E  = 25
S                 I
F                *
M                ID = 0
M                DO TO 5 FOR I = 0(7)35
M           5    ID  = 1
S                  I
E                *
M                B = 0
M                DO TO 6 FOR I = 0(4)8
M           6    B  = 1
S                 I
E                *
M                P = 0
M                P  = 1
S                 3
M                P  = 1
S                 10
M                P  = 1
S                 17
M                J2 = .0010823
E                                    6
M                ALPHA = 1.0 10
```

Reproduced from best available copy.

```
M                RE = 6378165

E                                  15
M                MU = .3986012 10

M                RR = 6563365

E                                     3
M                PDOSC = 2 PI SQRT(RR  / MU)

M                DT = PDOSC / 360

M                VC = SQRT( MU / RR )

M                T1 = 0

M                J = 0

E                 -
M                IZ = (0, 0, 1)

E                 -
M                NU = (0, 0, 0)

E                   -     -
M                DELTA = NU

E                   -     -
M                DELAD = NU

E                 -       -
M                NUAD = NU

E                 -
M                RO = (RR, 0, 0)

E                 -
M                VO = (0, VC, 0)

E                 -
M                DRE = (0, 0, 0)

E                 -     -
M                DVE = DRE

M                DO TO 18 FOR I = 1(1)80

E                 *
M                PHI = 0

M                DO TO 11 FOR Z = 0(7)35

M           11   PHI   = 1
S                   Z
```

Reproduced from best available copy.

```
E                 -        -       -
M                 DELTA = DELTA + DRE

E                 -      -      -
M                 NU = NU + DVE

M                 DO TO 16 FOR L = 1(1)10

M                 DO TO 16 FOR K = 0(1)3

M                 ANGLE = 2 PI T1 / PDOSC

E                 -
M                 ROSC1 = ( RR COS(ANGLE), RR SIN(ANGLE), 0 )

E                 -   -          -
M                 R = ROSC1  +  DELTA

E                  -         -
M                 IR = UNIT( R )

E                            -
M                 R = ABVAL( R )

E                         -  -
M                 CPHI = IR.IZ

E                           -       -     -           2
M                 Q = (( DELTA - 2 R ).DELTA ) / R

E                                     2                   1.5
M                 FQ = Q ( 3 + 3 Q + Q ) / ( 1 + ( 1 + Q )    )

E                 -            2                   2                 2    -          -
M                 AD = ( -MU/R  ) 1.5 J2 ( RE/R )  ((1 - 5 CPHI ) IR + 2 CPHI IZ)

E                 *            5       - -       2    *
M                 G = ( MU / R  ) ( 3 R R  - R  IDMATRIX )

M                 F    = G
S                  18     0

M                 F    = G
S                  19     1

M                 F    = G
S                  20     2

M                 F    = G
S                  24     3

M                 F    = G
S                  25     4

M                 F    = G
S                  26     5
```

$$F_{30} = G_{6}$$

$$F_{31} = G_{7}$$

$$F_{32} = G_{8}$$

$$\overline{RT} = \overline{ROSCT} + \overline{DELAD}$$

$$\overline{IRT} = UNIT(\overline{RT})$$

$$RT = ABVAL(\overline{RT})$$

$$TCPHI = \overline{IRT}.\overline{IZ}$$

$$QT = ((\overline{DELAD} - 2\ \overline{RT}).\overline{DELAD}) / RT^{2}$$

$$FQT = QT\ (3 + 3\ QT + QT^{2}) / (1 + (1 + QT)^{1.5})$$

$$\overline{ADT} = (-MU/RT^{2})\ 1.5\ J2\ (RE/RT)^{2}\ ((1-5\ TCPHI^{2})\ \overline{IRT} + 2\ TCPHI\ \overline{IZ})$$

$$D\overline{DELTA}/DT = \overline{NU}$$

$$D\overline{NU}/DT = (-MU / RR^{3}) (FQ\ \overline{R} + \overline{DELTA}) + \overline{AD}$$

$$D\overline{DELAD}/DT = \overline{NUAD}$$

$$D\overline{NUAD}/DT = (-MU/RR^{3}) (FQT\ \overline{RT} + \overline{DELAD}) + \overline{ADT}$$

$$D\overset{*}{PHI}/DT = \overset{*}{F}\ \overset{*}{PHI}$$

16 $$DIFEQ\ T1,\ DT.\ D\overline{DELTA}/DT,\ D\overline{NU}/DT,\ D\overline{DELAD}/DT,\ D\overline{NUAD}/DT,\ D\overset{*}{PHI}/DT$$

$$\overline{VOSC} = (-VC\ SIN(ANGLE),\ VC\ COS(ANGLE),\ 0)$$

$$\overline{VT} = \overline{VOSC} + \overline{NUAD}$$

$$\overline{V} = \overline{VOSC} + \overline{NU}$$

```
E                   *     *   *   * T
M                   E = PHI F PHI

E                        -C   * -C
M                   A = B .( E B ) + ALPHA
S                         J      J

E                   -     * -C
M                   W = E B   / A
S                         J

E                   *       *      - -C    *    *      - -C   T          - -
M                   E = ( ID - W B    ) E ( ID - W B    )   + ALPHA W W
S                             J                  J

M                   DVTN   = DELTA   - DELAD
S                        0          0          0

M                   DVTN   = DELTA   - DELAD
S                        1          1          1

M                   DVTN   = DELTA   - DELAD
S                        2          2          2

M                   DVTN   = NU    - NUAD
S                        3        0          0

M                   DVTN   = NU    - NUAD
S                        4        1          1

M                   DVTN   = NU    - NUAD
S                        5        2          2

E                   -       -                -C -
M                   DXE = W ( DQ       - B .DVTN )
S                               I-1      J

M                   DRE   = DXE
S                        0        0

M                   DRE   = DXE
S                        1        1

M                   DRE   = DXE
S                        2        2

M                   DVE   = DXE
S                        0        3

M                   DVE   = DXE
S                        1        4

M                   DVE   = DXE
S                        2        5

M                   J = J + 1
```

```
M          18    IF J > 2, J = 0
M                CALL JWH.GRAPH(SUBR),1,2,0,1,5,80,1,0,21,2660,0
M                START AT BEGIN
```